INFORMATION TO USERS

This manuscript has been reproduced from the microfilm master. UMI films the text directly from the original or copy submitted. Thus, some thesis and dissertation copies are in typewriter face, while others may be from any type of computer printer.

The quality of this reproduction is dependent upon the quality of the copy submitted. Broken or indistinct print, colored or poor quality illustrations and photographs, print bleedthrough, substandard margins, and improper alignment can adversely affect reproduction.

In the unlikely event that the author did not send UMI a complete manuscript and there are missing pages, these will be noted. Also, if unauthorized copyright material had to be removed, a note will indicate the deletion.

Oversize materials (e.g., maps, drawings, charts) are reproduced by sectioning the original, beginning at the upper left-hand corner and continuing from left to right in equal sections with small overlaps.

ProQuest Information and Learning
300 North Zeeb Road, Ann Arbor, MI 48106-1346 USA
800-521-0600

DEVELOPMENT OF A VERTICAL TDR PROBE TO MEASURE THE WATER CONTENT PROFILE WITH DEPTH IN PEAT COLUMNS

BY
XIAOYANG ZHANG

A Thesis presented to
the Faculty of Graduate Studies and Research
in partial fulfillment of the requirements
for the degree of
Master of Applied Science*
Department of Civil and Environmental Engineering
Carleton University
Ottawa, Ontario
Canada

JANUARY 28, 2005

*The Master of Applied Science program is a joint program with the University of Ottawa administered by the Ottawa-Carleton Institute for Civil Engineering

The undersigned recommend to the Faculty of Graduate Studies and Research, acceptance of the Thesis Entitled ***Development of a Vertical TDR Probe to Measure the Water Content Profile with Depth in Peat Columns*** submitted by Xiaoyang Zhang in partial fulfillment of the requirements for the Degree of Master of Applied Science.

Professor P. J. Van Geel, Thesis supervisor

Professor A. O. Abd El Halim
Department of Civil and Environmental Engineering

Carleton University

ABSTRACT

Time Domain Reflectometry (TDR) is used to monitor the moisture content in soils including peat. The objective of this research was to develop a TDR probe to measure the vertical moisture profile in a peat biofilter operating in the field where access to the filter is limited to the top surface.

The application of TDR to measure the water content in soils has been demonstrated by many researchers. In this research, it was demonstrated that a vertical TDR probe advanced to various depths estimated similar water content profiles with depth in peat columns compared to horizontal TDR measurements. The experiment was carried out in six columns exposed to a sequential water drainage process and two columns exposed to an organic loading to simulate a clogging process. Water content in peat columns was measured using both the vertical and horizontal TDR probes, and the gravimetric method. Water contents determined by the vertical and horizontal probes agreed well. The data was slightly more scattered in the clogging columns due to TDR signal attenuation. Total signal attenuation was observed with longer probes in clogged peat soils.

There is a consistent discrepancy between the TDR measured water contents and those determined gravimetrically, which is believed to be caused by a systematic error related to the TDR calibration curve.

ACKNOWLEDGEMENTS

I would like to thank my supervisor, Dr. P. Van Geel, for his guidance throughout this research and for his help whenever was needed.

I am grateful to Dan Patterson for providing the balance transformer and David Redman for his generous help on time domain reflectometry waveform analysis. I also wish to thank Pierre Trudel, Marie Tudoret Chow for their helpful assistance on my laboratory work.

Thanks to my family and friends for their energetic support. Especially for my parents in-law who were taking care of my daughter when I was away, for my daughter for her understanding, and for my husband and parents who are a source of unwavering encouragement.

TABLE OF CONTENTS

LIST OF FIGURES

LIST OF TABLES

SYMBOLS AND NOMENCLATURE

Δh	head change across the column (L)
Δl	length of the column across which the head change occurs (L)
Δt	time of travel (T)
A	cross sectional area of the soil column (L^2)
C	velocity of light in vacuum (LT^{-1})
F	organic content
h	head of the capillary rise (L)
i	$\sqrt{-1}$, the imaginary number
K^*	complex dielectric constant
K'	real part of the dielectric constant
K''	imaginary part of the dielectric constant or dielectric losses
K_a	apparent dielectric constant
K_s	saturated hydraulic conductivity (LT^{-1})
L	length of the probe (L)
M_{ash}	mass of ash remaining after combustion (M)
M_s	mass of oven-dried peat (M)
n	porosity
P_{air}	pressure of air ($ML^{-1}T^{-2}$)
P_c	capillary pressure ($ML^{-1}T^{-2}$)
P_{water}	pressure of water ($ML^{-1}T^{-2}$)
Q	volumetric flow rate through the soil (L^3T^{-1})
r	radius of the tube (L)
V	velocity of an electromagnetic wave (LT^{-1})
α	contact angle
γ_w	specific weight of water ($ML^{-2}T^{-2}$)
ε'	real dielectric constant of a material ($T^4Q^2L^{-3}M^{-1}$)
ε_o	real dielectric constant of vacuum ($T^4Q^2L^{-3}M^{-1}$)

ρ_b	dry bulk density (ML^{-3})
ρ_s	density of solid particles (ML^{-3})
σ	zero frequency conductivity ($T^3Q^2L^{-3}M^{-1}$)
σ'	surface tension (MT^{-2})
ω	angular frequency (T^{-1})

CHAPTER 1: INTRODUCTION

1.1 BACKGROUND

Peat is a heterogeneous mixture of plant residues under various stages of decomposition that has accumulated in a water-saturated environment with the absence of oxygen. Because of its low cost, combined with its highly porous structure, and its capacity to provide a favorable environment for microbial growth, peat offers a great potential for the biological filtration of wastewater by adsorption and microbial activity (Tinh et al., 1971; Buelna and Belanger, 1989).

Peat biofilters have been used for septic tank effluent (STE) since early the eighties with the advantage of high quality effluent, low operation cost and very little maintenance requirements of the simple system (Brooks et al., 1980). Due to the high organic content of peat soil and high organic loading of STE, microbial populations exist and grow in peat filters. Growth of biomass creates clogging problems and therefore decreases the removal efficiency of STE treatment. How long the peat can remain efficient and when it should be replaced still remains unanswered in peat filter applications.

Water content is a good indicator of microbial growth in peat filters due to two reasons: water content is the most important factor that affects microbial growth; the

overall water content (free and bound water in pores and water contained in the biomass) in peat soil increases with the growth of the microbial population. Hence, water content is cited as a critical parameter for successful biofilter operation (Helioties, 1989; Couillard, 1992). The optimum operating moisture content range (vol. basis) for biofilters is from 40-60% (Couillard, 1994). Closely monitoring water content of a boifilter sheds light on the growth of biomass in peat, and therefore the status of the filter in terms of clogging and removal efficiency.

Two methods for water content measurements in soils have been commonly used in the past for practical field application: gravimetric method and neutron meters. Gravimetric method is accurate, but destructive to the measured soil. The neutron meters involve the use of radioactive sources that require special care and precautions. Time Domain Reflectometry, generally referred as TDR, is a non-destructive, in-situ method used widely today to continually monitor moisture content in soils. TDR measures the dielectric constant (K_a) of the soil. Volumetric water content (θ_v) of the soil is calibrated by a K_a- θ_v calibration curve that is usually generated empirically.

Researchers currently use TDR to monitor the water content profiles in peat columns in the laboratory. Experiments are usually performed by inserting the TDR probes horizontally into the peat through the wall of the peat columns. The accuracy of water content measurement measured by horizontal probe insertion has been demonstrated by many researchers. The aim of this project is to develop a method to measure the water content profiles in peat columns by vertically inserting the TDR probes from the top of the columns. The vertical measuring method increases the possibility to apply TDR techniques to peat filters operating in the field.

1.2 RESEARCH SIGNIFICANCE AND PROBLEM DEFINITION

Although extensive research has been conducted for water content measurements in peat columns in the laboratory, limited research has been carried out in applying the TDR techniques to full scale biofilters (Pepin et al., 1992; Paquet et al., 1993). The objective of this research is to develop a vertical TDR probe to measure the water content profile with depth in peat columns and consequently extend the application of TDR techniques to peat filters in the field. Four potential problems were identified for the vertical probe application.

1. **Ensuring that the rods remain parallel when inserted into the soil and the impact on the TDR measurements if they do not remain parallel.**

   Parallel rods are used for TDR probes in this research. Davis et al. (1975) mentioned that to ensure accuracy, the rods did not have to be absolutely parallel, but large discrepancy should be avoided.

2. **Impact of the air space between the top of the soil and the probe connector as the rods are advanced to obtain a vertical profile.**

   In the developed method, the probe was incrementally advanced into the peat column to determine the moisture profile with depth. The electromagnetic signal will initially travel through the air (between the top of the soil and the probe head) before entering the wet peat. The impact of the portion of probe exposed in air on TDR waveforms was another concern in the vertical probe application.

3. **Impact of vertical TDR probe on the vertical hydraulic conductivity of the peat.** Hydraulic retention time is an important factor that affects the treatment efficiency in biofilters. Little impact of probe insertion on flow rate would be preferred. Small diameter rods were used in the study to minimize soil disturbance.

4. Impact of the microbial growth on the TDR calibration.

The last stage of the research was to investigate the impact of microbial growth on TDR measurements. The water content measured by TDR in clogged peat soils consists of two types of water: water in biomass and actual water. Actual water exists in the soil in two phases as free water and bound water, where free water has a K_a value of approximately 80 and bound water has a K_a value of 3 at 20°C. 80 % of the biomass is water (Van Veen and Paul, 1979). How the water in biomass impacts the TDR measurements is a question of concern. Will the water act more like free water, bound water or somewhere in between, is still an unknown. This experiment was trying to investigate the impacts of biomass on TDR measurements.

1.3 SCOPE OF THE WORK

The research consists of five stages:

1. Generate an empirical K_a-θ_v calibration curve for the type of peat under study.
2. Design guide blocks to keep the TDR rods parallel when inserted into the soil, evaluate the performance of the guide blocks and impact of rod separation on TDR readings.
3. Compare water contents in peat columns determined by vertical probes with those determined by horizontal probes and by gravimetric method.
4. Evaluate the impact of the vertical probe on the flow rate in peat columns.
5. Monitor water contents in peat columns during a clogging process and investigate the impact of biomass on TDR readings.

1.4 FORMAT OF THESIS

The research objectives and scope of the study are presented in this initial chapter. Chapter 2 provides an overview of the literature related to this study. Materials and methods used to conduct this research are presented in chapter 3, while results and discussions are presented in chapter 4, and conclusions are provided in chapter 5.

CHAPTER 2: LITERATURE REVIEW

2.1 PEAT

Peat can be described as the unconsolidated residues of aquatic plant life that accumulate in water-saturated environments over thousands of years. Due to the shortage of oxygen, the rate of decomposition of the plant matter by bacteria is less than the rate of accumulation, thus resulting in a buildup of decomposing plant material (Hamblin, 1985). The properties of peat are determined largely by the original plant species and the degree of decomposition.

Peat is a high organic material with a highly porous structure (Couillard, 1992). It contains lignin and cellulose as major constituents. These constituents, especially lignin, bear polar functional groups, such as alcohols, aldehydes, ketones, acids, phenolic hydroxides, and ethers that can be involved in chemical bonding (Coupal and Lalancetter, 1976; Ayyaswami and Viraraghavan, 1985). Partially decomposed peat has a porosity of approximately 95% and a specific area greater than 200 m^2/g (Couillard, 1994; Warith, 1996). Because of the very polar character and high specific area of this material, the specific adsorption for suspended and dissolved solids, such as transition metals and polar organic molecules, is considered to be quite high.

Because of its low cost, combined with the physical and chemical characteristics, and its capacity to provide a favorable environment for microorganisms, peat offers a great potential for the biological filtration of wastewater by adsorption and microbial activity (Tinh et al., 1971; Buelna and Belanger., 1989).

2.1.1 Types of peat

There are three typical types of peat based on the original plant species.

Sphagnum peat originated from sphagnum or hypnum mosses and is light brown to medium dark brown in color. Sphagnum peat is the most important moss today both ecologically and economically.

Sedge peat derived largely from sedges, reeds, cattails, pondweeds and other herbaceous aquatic plants of swamp areas, is generally medium dark brown to black.

Woody peat includes the remains of trees, shrubs, and other woody plants.

In literature sphagnum peat is usually referred to as "highmoor peat" while sedge and woody peat as "lowmoor peat".

Based on the degree of decomposition, peat can be classified into three types as well (Boelter, 1969; Singh et al., 1997):

Fibric peats are relatively young mosses that are only partially decomposed. It has more than two thirds of the total organic material in fibers. It usually has high water retention, low pH, low bulk density, and little ash.

Hemic peats are in their intermediate stage of decomposition. They are older and more decomposed than fibric peats. It generally has a fiber content between one-third and two-thirds.

Sapric peats are the oldest and most decomposed type of peat ranging in color from dark brown to black. It has less than one-third of the total mass of organic material made up of fibers.

Generally, fibric peat ranges between H-1 and H-3 (based on the Von Post scale, which is described in the following section); hemic peat is H-4 to H-6; and sapric peat, H-7 to H-10. The partially decomposed peat (H1-H5) is usually referred as peat moss, widely used for agriculture and wastewater treatment purposes; strongly decomposed sapric peat (H6-H10) is an excellent source of energy and used as fuel in many areas of the world (Tibbetts, 1986).

2.1.2 Decomposition of peat

Also called humification, decomposition results in plants losing their original character and turning dark brown to become peat of variable composition, ranging from material slightly decomposed that the plants can be readily identified from leaves, stems, and roots to material highly decomposed that it is like a thick structureless mud (Kaila, 1956) . As decomposition advances, the content of plant carbohydrates decreases while proteins, polyuronides, and lignin like substances and humic acids tend to accumulate (Kaila, 1956).

The properties of peat change as decomposition proceeds. It is essential to know the degree of decomposition of peat in order to gain a preliminary assessment of its use. The degree of decomposition can be expressed in different ways. The Von Post scale is the most widely used system for determining the degree of decomposition of peat in the field (Paivane, 1973). The Von Post scale is based on the direct examination of fresh samples: the color and turbidity of the water pressed by hand from the sample, and the structure and consistence of the peat residue are the main factors observed. A grading from H1 to H10 is used for the degree of decomposition, where H-1 represents totally

non-decomposed plant material while H-10 represents completely decomposed peat (Kaila, 1956).

Laboratory determination of either the physical or chemical state of decomposition of peat requires more time and equipment, but can give a more quantitative assessment of the degree of decomposition and a more accurate classification of peat materials. Two commonly used analyses are bulk density and fiber content (Farnham and Fineey, 1965; Boelter, 1969; Chason and Siegel, 1986; Shibchurn, 2001).

2.1.3 Properties of milled peat

Properties of milled peat depend on several factors, including the ambient conditions existing during its formation, the extent of its decomposition and the method of harvesting (Couillard, 1994). Properties change when peat is moved from its natural state in the bog and is drained, air or mechanically dried.

2.1.3.1 Physical and chemical properties of peat

Fiber content

Fibers are fragments or pieces of plant tissue greater than 0.10 mm in size (Bolter, 1969). Fiber content is an important indicator of peat decomposition and is used often to estimate the degree of decomposition. In general, as the degree of decomposition increases, peat becomes less and less fibrous until it gets transformed into an amorphous mushy substance without any discernible structure (Landva et al., 1980; Warith, 1996). The least decomposed peat (fibric) has more than two-thirds of the total organic material

in fibers, while the most decomposed peat (sapric) has less than one-third of the total organic material made up of fibers (Boelter, 1969).

Bulk density

The bulk density of a soil is the weight per unit volume of soil, including solid particles and pore spaces. It is normally expressed on a dry weight basis. The bulk density of peat is defined (Boelter and Blake, 1964) as the oven-dried mass of peat per unit bulk volume.

Natural peat is characterized by a low bulk density. The bulk density of highmoor peat is slightly more than half as great as that of lowmoor peat soil (Eyzerman, 1993; Paivanen, 1982). More decomposed peat has higher bulk density than younger peat for the plant remnants break down with decomposition and fill the large pores to decrease the total void space. Therefore, bulk density provides an estimate of total porosity given an approximate solid density.

Boelter (1964) reported a bulk density range of natural peat in situ from 0.020 g/cm^3(live undecomposed moss peat) to 0.237g/cm^3 (decomposed peat). Chason and Siegel (1986) reported a bulk density range from 0.06 to 0.14g/cm^3 for undisturbed peat made up mainly by sphagnum species.

Porosity and water content

Porosity is the total void space in the medium. It is the percentage of the total soil volume occupied by pores. It can be calculated by the following equation:

$$n=(1-\frac{\rho_b}{\rho_s}) \qquad (2.1)$$

Where: n: the porosity

ρ_b: the dry bulk density

ρ_s: the density of solid particles

There are two ways of expressing water content in soils: weight based and volume based. Because of the low bulk densities and its large variability, water content on a weight basis of peat is generally extremely high (500-3000%) (Landva and Pheeney, 1980) and therefore somewhat meaningless, and fails to show the actual content of water in the soil (Boelter, 1969). Boelter (1969) suggested that the water content of peat should be expressed as the portion of the total volume that is occupied by water. This volume based water content is called the volumetric water content and it is defined as a fraction equal to the volume of water over the total volume of peat.

Peat is a highly porous medium. It generally contains a large amount of water due to its porous structure. The water content of peat at saturation is considered to be equal to the total porosity (Boelter, 1969). Boelter (1964) reported that non-decomposed peat moss in nature has volumetric water contents from 95 to nearly 100% at saturation while the partially decomposed moss peat with wood inclusions, decomposed peat, and herbaceous peat, which have higher bulk densities than undecomposed moss peat, contains water between 80 to 90 %.

Particle density

Also called solid density, the particle density (ρ_s) of peat is often used to calculate the theoretical porosity (Equation 2.1). In the literature, particle density of peat is reported as 1.25-1.414 g/cm^3 (Pepin et al., 1992), 1.4 g/cm^3 (Eggelsmann et al., 1993;

Kellner et al., 2001), 1.64 g/cm^3 (Eyzerman, 1993). If organic content is known, particle density can be calculated using the following equation (Kreij and Bes, 1989):

$$\rho_s = 1/ \{F/1.5 + [(1-F)/2.7]\} \quad (2.2)$$

Where: ρ_s: the particle density

F: the organic content (mass of organic matter / mass of solids)

pH

Peat normally has a pH of around 4.0, due to the presence of humic acids (Valentin, 1986). The pH influences the structure and properties of peat. The structure of peat degrades at pH>9.0; below pH 3.0, its chelating capacity decreases (Couillard, 1994). Therefore, at pH<3, the removal of most metals will not be efficient (Couillard, 1992).

Ash content, organic content

Organic content represents the organic fraction of peat while ash content represents the inorganic fraction. Ash content is determined as the percent mineral solids that remain after the organic elements (carbon, oxygen, and hydrogen) have been burned off:

$$\text{Ash Content [\%]} = (M_{ash}/M_s)*100\% \text{ [g/g]} \quad (2.3)$$

Where: M_{ash} : the mass of ash remaining after combustion

M_s: the mass of oven-dried peat

And

$$\text{Organic Content (F)} = 100 - \text{Ash Content (\%)} \quad (2.4)$$

Peat is characteristic of low ash and high organic matter content. Ash content ranges from less than 2% (organic content >98%) for fibric peat to greater than 25%

(organic content <75%) for sapric peat (Cooper, 2003). For partially decomposed sphagnum peat, ash content is usually lower than 10% (Singh et al., 1997).

Chemical composition of peat

The chemical composition of peat is very complicated and has a large variability with different degrees of decomposition. Total ion concentrations, fixed within the peat matrix and the extractable fraction, are generally used to represent the elemental composition. Fixed ions will not leach into solution under system conditions, while extractable ions are mobile in the peat. Champagne (2001) characterized the composition of New Brunswick sphagnum peat that was used for her research by the total and extractable ion concentrations (Table 2.1).

Table 2.1: Total and extractable ion concentrations in the peat (Champagne,2001)

Element	Total Ion Concentration (µg/g)	Extractable Ion Concentration (µg/g)
Ca	7420	2120
P	440	243
K	4180	219
Mg	4070	1180
Na	n.r	390
Fe	3790 (fixed)	n.r.
Mn	16.6 (fixed)	n.r.
Mo	88.0 (fixed)	n.r.
As	93.6	34.4
Cd	0.8	b.d.
Co	24.1	6.3
Cr	15.8	b.d
Cu	301	119
Ni	7.9	1.7
Pb	13.3	2.4
Se	5.7	b.d.
Zn	53.2	23.7

b.d.= below detection limit **n.r.** = value not reported

2.1.3.2 Hydraulic properties of peat

The hydraulic properties of peat are the most important factors that affect the efficiency of wastewater treatment. They depend to a large degree on the porosity and pore-size distribution of peat soils. These are in turn related to the particle-size distribution and structure of the soil. In peat materials, the particle size, structure, and resulting porosity are determined largely by the state of decomposition (Boelter, 1969). Boelter (1969) also indicated that the dependency on pore size distribution is more significant than the difference in total porosity.

Hydraulic properties can be divided into two areas: water retention characteristics and hydraulic conductivity (Fonteno, 1993). In order to understand the hydraulic properties better, it is necessary to understand peat's pore structure.

Pore structure

Peat is a highly porous material. Particles of varying sizes make up the porous skeleton of peat. Between these particles are pore spaces varying in size and shape. Pore spaces define the ability of the media to store and drain water, and permit air movement (Hon and Gostomski, 2000).

Larger pores (diameters $>10^{-5}$cm) are called macro-pores, while micro-pores are defined as pores with sizes ranging from 10^{-9} cm to several thousand times this value in diameter (Couillard, 1994). Macro-pores contribute little to the overall surface area, but provide easier access of fluids to the interior of the soil. Most of the surface area of peat for adsorption is provided by microspores (Couillard, 1994). From geometry we know that the smaller the particle size, the larger the total external surface for a given total volume of adsorbent.

Peat exhibits a complex network of irregularly shaped and partially connected pore spaces. The pore spaces in peat could be interconnected, dead-ended or completely isolated, which makes the peat matrix different from that of granular geological porous media (Loxham, 1980; Hon and Gostomski, 2000). Large interconnected pores contribute to both the water content and the rate of water movement at saturation and movement of air when unsaturated; whereas the smaller pores and dead-end pores contribute to water storage but negligible flow. Completely isolated pores, which cannot be accessed by water at all, do not contribute to either.

Hydraulic conductivity

Hydraulic conductivity is the soil's ability to transmit water. It is defined by Darcy's law and is a function of soil water content (Fonteno, 1993).

$$K_S = \frac{Q * \Delta l}{A * \Delta h} \qquad (2.5)$$

Where: K_s: saturated hydraulic conductivity

Q: the flow rate through the soil

A: cross sectional area of the soil column

Δh: head change across the column

Δl: length of the column across which the head change occurs

Hydraulic conductivity is one of the most important physical properties that affect the retention time of water in peat and therefore the efficiency of wastewater treatment.

The hydraulic conductivity of a saturated soil may be estimated whether in the laboratory or in the field. The method used also affects the measurements. Large

differences exist among field-determined values for undisturbed peat samples, lab-determined undisturbed samples and lab-determined disturbed samples. In some cases undisturbed lab determined values were found to be 3.5-fold those found by field methods for moderately decomposed peat (Boelter, 1969; Paivanen, 1973). Boelter (1969) reported that the discrepancy might be caused by leakage along the interface between the cores and the inside wall of the sampling cylinder, the structural change due to the disturbance during sampling and transportation, and further handling of the samples.

The hydraulic conductivity of peat varies considerably because of the large differences in bulk density, structure, and porosity at various degrees of decomposition (Boelter, 1965). As the degree of decomposition increases, fibers break down, solid particles become smaller, and some pores have been totally or partially filled by finer particles. Bulk density increases while porosity decreases. Because large pores contribute more to the flow than smaller ones do, hydraulic conductivity decreases (Couillard, 1994). In their laboratory studies of undisturbed sphagnum peat, Narashiah and Hains (1988) reported that depending on the degree of decomposition, permeability of peat can vary by a factor of more than 5000. The hydraulic conductivity of slightly decomposed fibric peat can be as high as 140 cm/h (0.039 cm/s); that of highly decomposed sapric peat can be as low as 0.025 cm/h ($6.9*10^{-6}$ cm/s). Boelter (1969) reported $180*10^{-5}$ cm/s for fribric, $(2.1\text{-}180)*10^{-5}$ cm/s for hemic and $<2.1*10^{-5}$ cm/s for sapric peats for field measured values. Boelter (1969) also reported a hydraulic conductivity range $(3810\text{-}13.9)*10^{-5}$ cm/s for undecomposed sphagnum peat to moderately decomposed sphagnum peat with wood inclusions. Kennedy and Van Geel (2001) found saturated hydraulic conductivity (K_s)

ranging from $0.4x10^{-4}$ m/sec to $7.9x10^{-4}$ m/sec at various densities for disturbed, slightly decomposed sphagnum peat in the lab.

It should be mentioned that for certain peat materials, particularly the herbaceous peats formed from remains of reed and sedge-type plants, have a very pronounced horizontal laminar structure, which makes horizontal hydraulic conductivity different from the vertical one (Boelter, 1969). Malmstrom (1925) and Colley (1950) reported that horizontal hydraulic conductivity was greater than vertical hydraulic conductivity for peat. But Boelter (1969) found no significant difference between horizontal and vertical values in any of the peat types he tested. For the application studied here, the peat is milled and repacked and hence, anisotropy is not a concern.

Peat filters are designed to operate under unsaturated condition. The unsaturated hydraulic conductivity is very difficult to measure and therefore usually determined by model prediction from experimentally determined saturated hydraulic conductivity. Most models make intensive use of moisture retention curves, which describe the moisture conditions at different pressure heads (Weiss et al., 1998).

Water retention characteristics of peat

Soil water retention is a basic property of the soil that regulates the movement and storage of water within the soil profile. The total potential of soil water can be divided into the gravitational potential, the pressure potential and the osmotic potential (Paivanen, 1973).

When peat is saturated, both large and small pores are filled with water. The pore water is assumed to be continuous, with the pore water at zero gage pressure. Water flow follows Darcy's law. When peat is completely dry, all the pores are filled with air. And

when peat is unsaturated, some pores are filled with air, some are filled with water. Both water phase and air phase exist in soil pores. Water held in pores in unsaturated peat is held by tension. The tension with which water is held is called matric potential. Matric potential results from the capillary and adsorptive forces produced by the soil matrix and osmotic forces. Capillary force is caused by surface tension of water and its contact angle with the solid particles while osmotic force is due to the presence of solutes in soil water (Paivanen, 1973). In unsaturated soil, matric gradients are generally orders of magnitude more than those of osmotic suction. In addition, the salt content of peat is usually very low. Therefore the influence of the osmotic forces of the soil water relationship might be neglected.

Soil holds water in two ways, as a thin film on soil particles by adsorption, and as water stored in the pores between soil particles by capillary forces (Figure 2.1). According to how easy water can be extracted from the soil, soil water can be classified into three categories (Buckman et al., 1965):

Gravitational water or excess water contained in large pores, drains from the soil under gravity.

Capillary water contained in small pores or as films around particles.

Hygroscopic water in air dry soils, as layers on soil particles, several molecules thick, can only be moved by drying the soil under a certain temperature for a certain amount of time in the oven.

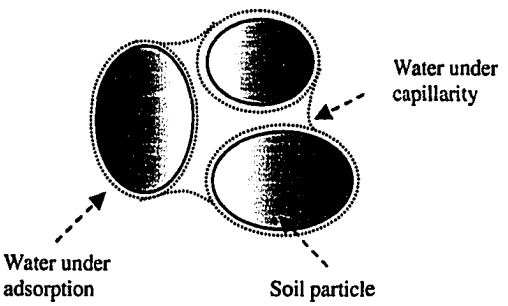

Figure 2.1: The ways that soil holds water

Pores in peat soils could be considered as a collection of capillary tubes with different diameters bundled together. Soil water is drawn up into the capillaries by the surface tension at the air-water interface (contractile skin). Capillary forces in capillaries can be illustrated by capillary tubes inserted into water (Figure 2.2).

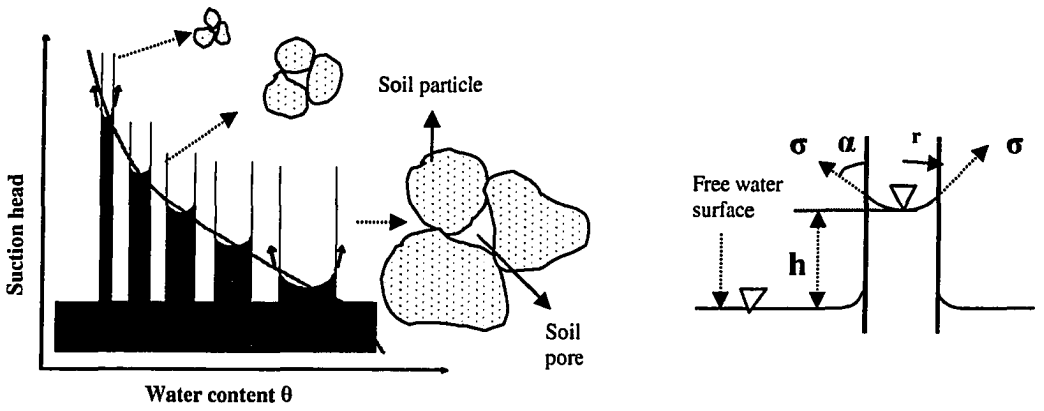

a b

Figure 2.2: Illustration of capillary pressure in a capillary tube (b) and relationship between pore size distribution and soil moisture curve (a)

The capillary pressure at the contractile skin is the pressure difference of air and water.

$$P_c=P_{air}-P_{water} \qquad (2.6)$$

Where: P_c: capillary pressure

P_{air}: pressure of air

P_{water}: pressure of water

Capillary pressure can be expressed in a head form (Figure2.2 b):

$$h = \frac{2\sigma' \cos\alpha}{\gamma_w r} \qquad (2.7)$$

Where: σ': the surface tension

r: the radius of the tube

α: contact angle

γ_w: specific weight of water

h: head of the capillary rise

Capillary pressure reflects a negative pressure with respect to the air pressure (Fredlund et al., 1993). Capillary pressure is inversely proportional to the radius of the tube. The smaller the tube diameter, the smaller the radius of curvature of the air-water interface (the more curved the meniscus), the greater the suction, or the more negative of the water pressure by which water is held. Therefore it is easier for smaller pores to draw water in but more difficult to move water out of them. As peat dries, the largest pores drain first, then the small pores and then the even smaller ones. The suctions inside of the soil capillaries become larger and larger. The relationship between water content and suction in soil is represented by soil moisture retention curve, which is also known as soil water characteristic curve.

The soil moisture curve describes how a soil behaves as it saturates or desaturates. It is an important soil function relating the water content in a soil to soil suction. The suction is usually expressed as capillary pressure or as the equivalent water-column of the negative water pressure or matric head (negative cm H_2O). Water content is expressed

either as volumetric water content (θ_v), or degree of saturation (S_w). S_w is the fraction of pores that are filled with water. It can be calculated from volumetric water content and porosity: $S=\theta_v/n$. S varies from 0 to 1.

When a soil is drained and then rewetted, the drying and wetting soil water characteristic curves are not identical. The wetting curve has a lower water content than the drainage curve over a wide range of soil water potentials (Figure 2.3). This is called soil moisture curve hysteresis. Notice that the primary drainage and primary wetting curves are the two normally occurring extremes and all points in between are possible. Therefore, the water retained in a soil does not only depend on the suction by which the water is held, but also on the wetting or the drainage history or path. According to Hillel (1971), the hysteresis effects are caused by the ink bottle effect, contact angle hysteresis, entrapped air and aging of the soil.

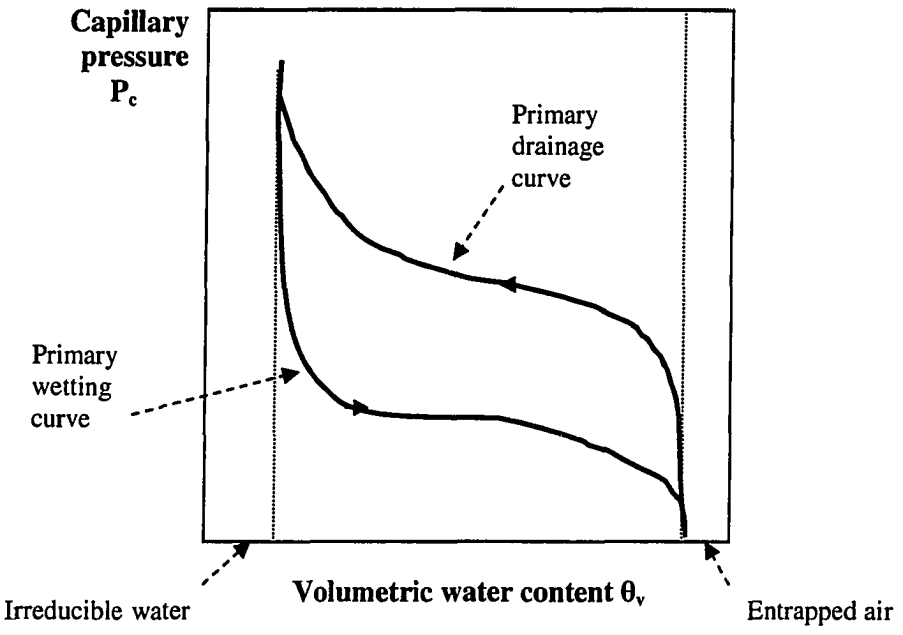

Figure 2.3: Hysteresis of soil moisture curve

Soil moisture retention curve is different for each soil type. Its actual shape is affected by the physical properties of soil such as the particle size distribution, pore size distribution, soil structure, and soil texture, uniformity of the particles, etc. Among these properties, pore size distribution is the most important factor.

Figure 2.4 shows the typical soil moisture curves for clay, loam and sand. As we can see from the figure, for all the soil types, highest water contents (saturation) are associated with zero suction, as suction increases, water content decreases. Free water or gravitational water will drain from a soil until the suction reaches field capacity (FC), approximately one-third atmospheric pressure or approximately 0.3 bars. As the soil continues to drain, wilting point is reached where plants can no longer extract water from soil. Wilting point occurs at 15 bars water potential for most plants. Between FC and WP is the water available for plants, usually referred to as available water.

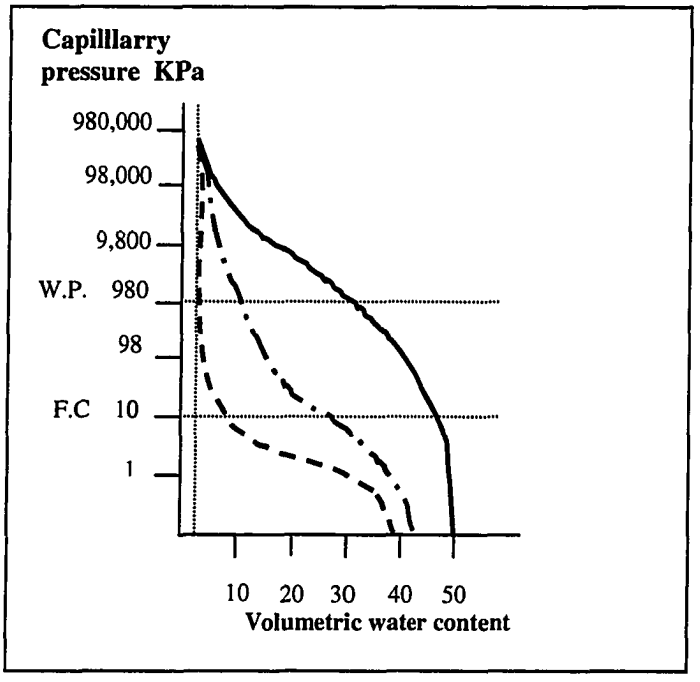

Figure 2.4: Soil moisture curves for clay, loam and sand

It can be seen from Figure 2.4 that at the same suction, clay, a fine soil that has the highest porosity and smaller-size pores (particles), retains more water than coarse soils like sand and loam. Da Silva et al. (1993) stated that when suction was increased to 2.5 Kpa (25.5 cm of H_2O), 50% of water drained out of peat. With further increase of suction to 12 Kpa (122.5 cm of H_2O), the peat still contained more than 20% of water by volume. Kennedy (1998) obtained very similar results on peat with bulk density 118.8 Kg/m^3 (46% at 25.5 cm and 19% at 122.5 cm). Figure 2.5 shows Kennedy's drainage curves of peat of two bulk densities.

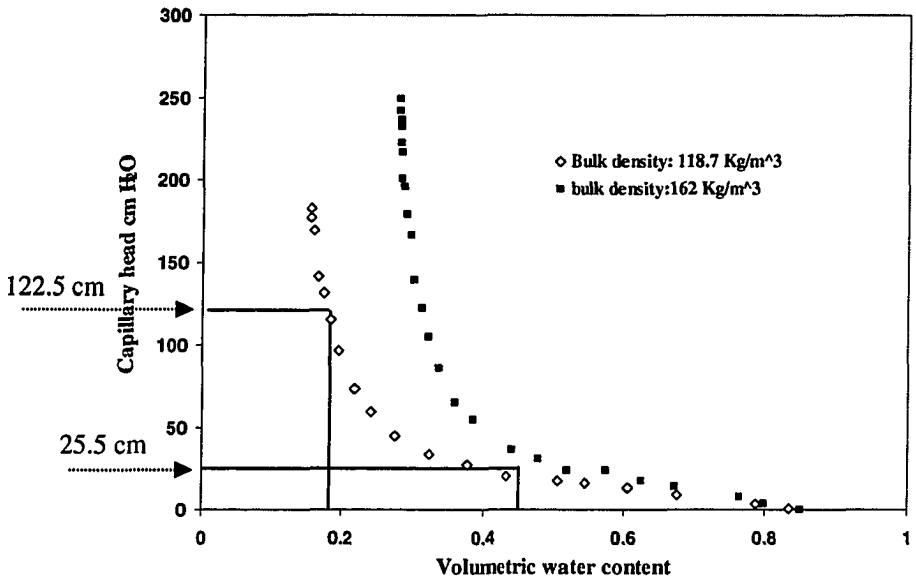

Figure 2.5: Drainage curve of peat (Kennedy, 1998)

Bulk density and degree of decomposition are two important properties that affect the pore size distribution in peat (Paivanen, 1973). In general, when bulk density is small, the pores are larger, and water would drain out of the pores easily at a low suction. Shibchurn (2001) studied the effect of bulk density on water retention properties of the sphagnum peat from the same source as in this research. Her results are presented in

Figure 2.6. It can be seen that at the same suction, peat with lower bulk densities lost water more easily, while peat with higher bulk densities had better water retention capacities.

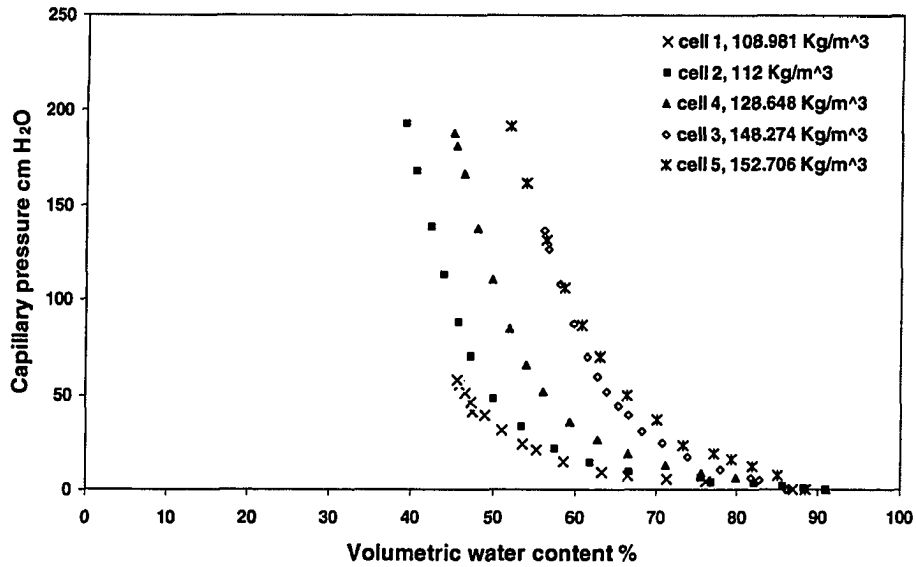

Figure 2.6: Effect of bulk density on soil moisture curves (Shibchurn, 2001)

There is no theoretical system to develop soil moisture curves. They are usually obtained from experimental data. There are several equations in use to fit the experimental data for wetting and drainage curves, of which the most common are the Brook and Corey (1964), and the van Genuchten (1980). These functions have been used to predict the hydraulic conductivity in unsaturated soils.

2.1.4 Peat filters for septic effluent treatment

On-site septic tank subsurface soil adsorption systems have long been the conventional method of treating domestic wastewater in areas where community sewage is not available. A conventional septic system consists of two main parts: the septic tank

and the soil drainfield. As a primary treatment system, where solids settle out and floatables are collected, septic tanks do not significantly reduce the polluting potential of the wastewater. The septic tank effluent (STE) is subsequently discharged into the drainage field through a soil medium for further purification (Jowett et al., 1995). However, many problems exist in the drainage field because of inadequate reduction in the pollution potential of the waste. Better treatment of STE before disposal is desirable.

It has been demonstrated (Barton et al., 1984; Couillard, 1992) that peat filtration is an efficient method of domestic wastewater treatment in the case of low volumes requiring a high degree of purification. Peat can successfully remove impurities such as suspended solids, heavy metals, odors, organic matter, oils, and nutrients from wastewater ranging in scale from the laboratory to practical application (Couillard, 1992). Solids, which are larger than the interstitial channels in peat, are filtered out. Dissolved and suspended organic matter is biodegraded as the porous structure of peat provides an effective medium for microbial growth. Peat biofilters have been used for STE since the early eighties (Brooks et al., 1980) with the advantage of high quality effluent, low operation cost and very little maintenance requirement of the simple system. The best peats for biofiltration are fibrous and intermediate decomposed peats. Peats with high degree of decomposition cause internal clogging problems because of the presence of fine particles (Buelna and Belanger, 1989).

Because of the high organic loading and the corresponding microbial growth, clogging is a problem in peat filter applications. The filter media must be periodically replaced to improve removal efficiency. How long can the peat remain efficient and when it should be replaced still remains unanswered in the application of peat biofilters.

Peat filters consist of peat materials colonized by a growth of microorganisms. These microorganisms are primarily aerobic (Pipeline, 2004). They create a biofilm surrounding peat particles. Wastewater percolating through the peat filter under gravity and by capillary forces flows over the biofilm attached to peat, is retained for a certain period of time (hydraulic residence time), and impurities are filtered out.

The growth of microorganisms acts as a key factor in the efficiency of wastewater treatment in a peat filter due to two reasons: clogging will be a problem if microorganisms block pores; the biofilm created by microorganisms surrounding peat particles is the basis of adsorption and microbial assimilation- important removal mechanisms of a peat filter. Water content, temperature and oxygen supply are important factors affecting microorganism growth, among which water content is the most important. Most review papers on biofiltration identify moisture content as the crucial operating parameter for successful biofilter operation (Helioties, 1989; Couillard, 1992) At moisture levels greater than 85%, the activity decreases slightly; while below 30%, it ceases entirely (Valentin, 1986). The optimum operating moisture content range for biofilters is from 40-60% (Couillard, 1994). Close monitoring of water content in biofilters sheds light on the growth of microorganisms in peat and therefore avoids clogging and improves the removal efficiency of a peat filter.

The most common method of measuring moisture content in biofilters is the gravimetric method. It is very destructive to the filter because a large number of soil samples have to be removed to account for the heterogeneity of peat. Time Domain Reflectometry, usually referred as TDR, is a non-destructive, in situ technique that is widely used to measure water content in soils. It is considered as the most promising

method for measuring moisture content within a filter (Reyes et al., 2000). Researchers are measuring water content using TDR in peat columns in the laboratory that simulate peat filters.

2.2 TIME DOMAIN REFLECTOMETRY (TDR) TECHNIQUES

Soil water content is the key variable to land activities, especially those involving agriculture, forestry, hydrology, and engineering. Lennox and Parsons (1975) identified the lack of adequate instrumentation and measurement techniques of soil water content. The gravimetric method has been used for many years. It is direct, simple in concept and precise. However, it is time consuming, disruptive of the measured location and additional measurements of soil bulk density are required to get water contents on a volume basis. The neutron meters involve the use of radioactive sources that require special care and precautions. To find a better technique, in 1975, the Electrical Methods Section of Geological Survey of Canada in co-operation with the Communication Research Center, Department of Communications, and the Soils Research Institute, Agriculture Canada initiated the research on measuring the dielectric constant of soils at high radio frequencies and thus moisture content in situ (Davis, 1975). The Time Domain Reflectometry (TDR) technique was first introduced by Fellner-Feldegg (1969) to measure the soil dielectric constant, which is strongly related to its water content (Davis, 1975; Annan, 1977; Topp et al., 1980, 1982). Considerable progress has been made in the application of TDR to measurement of soil water content since.

The TDR technique is based on measuring the apparent dielectric constant of a substance, which in turn is determined from the propagation velocity of an electromagnetic pulse traveling in the substance. The electric constant of a substance describes its ability, relative to that of vacuum, to store electrical potential energy while under the influence of an electrical field. A Time Domain Reflectometer, which is essentially a coaxial cable tester, was originally designed to detect faults in coaxial cables

and transmission lines. An electromagnetic pulse generated by a step pulse generator is sent down along an electromagnetic transmission line and a portion of the pulse is reflected back to the cable tester whenever there is a discontinuity (impedance mismatch) in the line. The rest of the pulse continues down the line to its end, where the entire signal is reflected from either an open or short circuit. The velocity of the guided wave traveling forward and back along the line is determined by measuring the travel time for a known length of line and can be used to infer the dielectric constant of the soil (Annan, 1977). A calibration is then needed to back calculate the volumetric water content from the dielectric constant measured by TDR. Two approaches have been developed for calibration functions: empirical polynomials (Topp et al., 1980) and theoretical dielectric mixing models (Roth et al., 1990). In this project, a calibration curve was generated using the pressure cell method.

2.2.1 Components of TDR

The TDR unit used in this project consisted of a Tektronix 1502C Metallic Time Domain Reflectometer, which is available commercially as a short-range cable tester normally used to find faults in metal cable. The metallic cable tester consists of four main components: a step pause generator, a coaxial cable, a sampler and an oscilloscope. There are some components externally connected to the TDR unit to collect and transfer data from the cable tester: balancing transformer (balun, for parallel pair probes), transmission lines, commonly called wave-guides or TDR probes. The essential components of TDR and external components are shown in Figure 2.5.

As illustrated in Figure 2.7, the cable tester applies a fast rise time step increase in voltage through its interface to the 50-ohm coaxial cable and triggers the oscilloscope scan to capture the time dependence of the interface voltage. The resulting step function wave travels down the coaxial cable, through an impedance-matching balun (for parallel-pair rods), and travels down again until it reaches the soil.

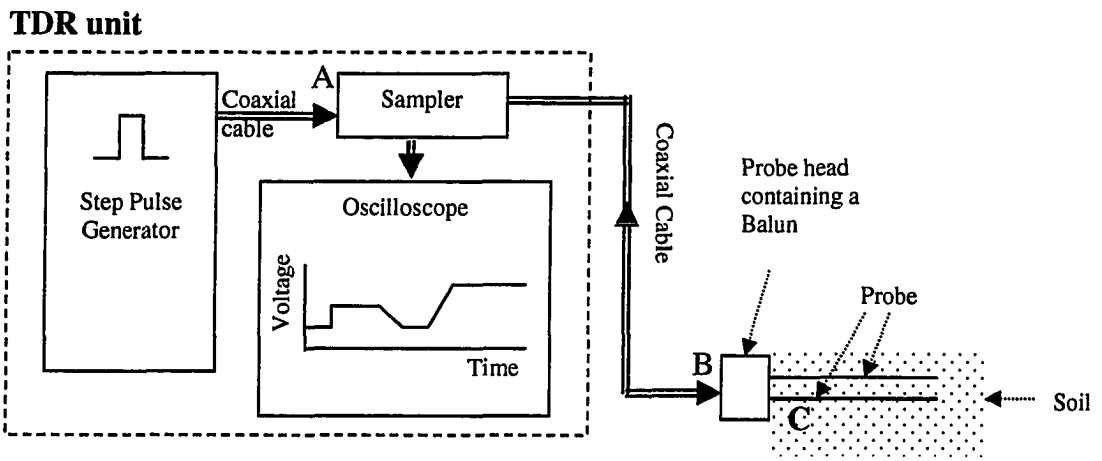

Figure 2.7: Essential components of TDR

2.2.1.1 Step pulse generator

The step pulse generator produces the electromagnetic part of the waves. An electromagnetic wave consists of both an electric and a magnetic part. Most soils are nonmagnetic and the magnetic part of the waves is therefore usually ignored. However the electric part is influenced by the soil properties and the influence is a function of the soil water content (Nissen et al., 1994).

The electric part of the electromagnetic waves consists of sine shaped waves covering a large frequency range. The Tektronix 1502C used in this project produces waves in a frequency range from 1 MHz to 1 GHz (Tektronix, 1997).

2.2.1.2 Coaxial cable

Coaxial cables connect the step pulse generator to the sampler, and the sampler to the probe (Figure 2.7). Figure 2.8 shows an illustration of a coaxial cable. In a coaxial cable, the center conductor carries the electromagnetic (EM) signal, whereas the outer conductor (the shield) is grounded and therefore has the electric potential 0.0V (Nissen et al., 2003).

When the electromagnetic waves are launched into a cable that is connected to the metallic cable tester and the probe, any change in the electric properties of the cable will cause a partial or total reflection of the waves. Changes in the electrical properties of the cable cause changes in the impedance. Impedance is the total resistance of a conductor to AC current and is measured in ohms. Most common coaxial cables, as well as the ones used in this project, have an impedance of 50 ohms (Nissen et al., 1994; Tektronix Inc., 1997).

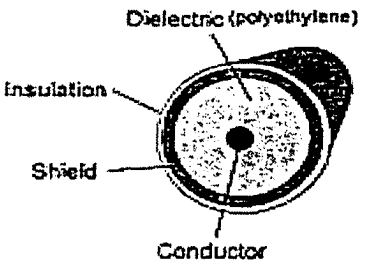

Figure 2.8: Illustration of coaxial cables (Nissen et al., 1994)

2.2.1.3 Sampler

A sampler uses an electronic sampling technique to put out a lower-frequency facsimile of the high-frequency input. The sampling principle is analogous to the principle of optical stroboscopes, which are used to make rapidly moving things appear to

be at rest or moving very slowly (Topp et al., 1980). At the same time, the sampler measures the voltage between the shield and the conductor at a certain time interval, thereby obtaining a set of data consisting of voltage as a function of time (Nissen et al., 1994). The TDR output containing this set of data is then sent to and displayed on an oscilloscope.

2.2.1.4 Oscilloscope

The oscilloscope shows the simultaneous measurements of time and voltage obtained with the sampler on a Liquid Crystal Display. This produces a curve called a waveform (Nissen et al., 1994). Figure 2.9 shows a display of an oscilloscope. The screen shown only displays a portion of the whole waveform. A cursor could be used to move the waveform back and forth by moving the screen to the left and right so that the full waveform could be seen.

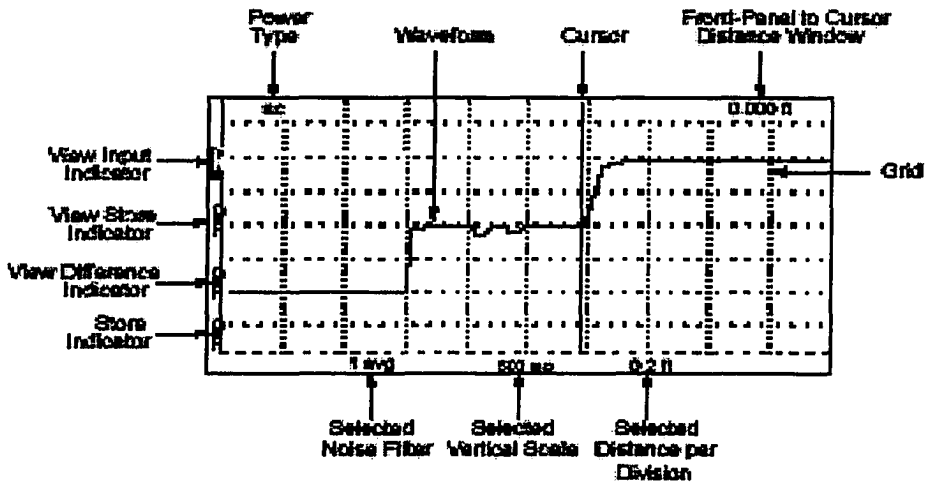

Figure 2.9: Display and indicators of oscilloscope (Tektronix Inc., 1997)

2.2.1.5 Probes

Two parallel transmission lines, generally referred to in the TDR literature as two rod probes, are one of the most popular probes currently used in lab and field studies. It consists of two stainless steel rods parallel to each other. Because there is an impedance mismatch between the coaxial cable and the parallel rods, a balancing transformer is required to avoid the unwanted noise and information loss. Two rod probes are used in this research.

Zegelin et al. (1989) introduced multirod probes to eliminate the need for a balancing transformer, the purpose of which is to reduce the complication and expense of the probe construction. He found that three-rod probes without a balun perform the same as parallel pair probes with a balun. Many researchers have successfully used three rod probes for water content measurements in soils (Zegelin et al., 1989; Topp et al., 2000; Heimovaara, 1990, 1993).

2.2.1.6 Balancing transformer

As mentioned earlier, in a coaxial cable, the center conductor carries the electromagnetic (EM) signal, whereas the shield is grounded. The signal is then referred to as unbalanced with respect to ground. In a parallel two rod probe, both conductors carry a signal, equal in magnitude but with opposite signs, and the ground plane is grounded between the center conductor and the shield (Spanns and baker, 1993, 1994; Nissen et al., 2003). This kind of signal is referred to as balanced with respect to ground. The transition from unbalanced to balanced is subject to errors and is generally unwanted (Spanns and baker, 1993; Nissen et al., 2003). The EM signal mismatch problem is traditionally solved by inserting an impedance-matching transformer, also referred as a

balun, at the transition between the coaxial and parallel rods (See figure 2.7), transforming the signal from unbalanced to balanced.

2.2.2 Dielectric constant

The dielectric properties of a substance can be described by its relative dielectric constant, also called dielectric number or relative permittivity. It is described as the ratio of the real dielectric constant (permittivity) of the material (ε') and of vacuum (ε_0), and usually defined as a complex entity:

$$K^* = \frac{\varepsilon'}{\varepsilon_\circ} = K' - i\,(K'' + \frac{\sigma}{\varepsilon_\circ \omega}) \qquad (2.8)$$

Where

ε': the real dielectric constant of a material

ε_0: the real dielectric constant of vacuum ($8.85*10^{-2}$ F/m)

K^*: complex dielectric constant

K': the real part of the dielectric constant, a function of ω

K'': the imaginary part of the dielectric constant or dielectric losses

σ: the zero frequency conductivity (Siemens/m)

ω: the angular frequency (in radians/sec)

i: $\sqrt{-1}$, the imaginary number

Davis and Annan (1977) indicated that in a frequency range from 1MHz to 1 GHz, the loss K'' is considerably smaller compared with the real part K' (K''<<K') and the real part is no longer strongly dependent on frequency. Therefore, K^* is nearly real and

constant, and can be represented as K', which can be measured by TDR (von Hippel, 1954; Davis and Annan, 1977; Ledieu et al., 1986).

In practice, however, the effects of electric loss and different frequencies do influence measurements of K' to a small extent. Therefore a measured K' value, representing the real part of the complex dielectric constant, is called apparent dielectric constant and is denoted K_a.

2.2.3 Moist soil as a dielectric material

The dielectric constant of a mixture depends on the dielectric properties and the volumetric fractions of the constituents (Roth, 1990; Kellner et al., 2001). Soil can be considered as a three-phase mixture: water, air and solid matter. In the case of wet peat, it is a mixture of air, organic matter and water. At 20°C, the K_a value of air is 1.005 (1 atm), and it is usually lossless. The K_a value of organic matter is approximately 3 and it has low losses. The K_a value of free water is 80.1 (below frequency 20 GHz) at 20°C (Condon et al., 1987; Toikka and Halikainer, 1989). The fraction of air and dry matter in wet peat is small; they have small effects on the bulk dielectric constant, and the K_a value of free water clearly differs from the other soil constituents. Therefore, a small change in the volumetric water content of the soil causes a large change in the composite dielectric constant of the bulk soil, which makes calibration of volumetric water content from dielectric constant in soil applicable.

2.2.4 TDR measurement techniques and waveform analysis

In the TDR measurement, probes of known length (L) are embedded in the soil. TDR measures the travel time (Δt) of a high frequency (1 MHz - 1 GHz) voltage pulse, as it travels to the end of the probe and reflects back. The apparent dielectric constant of the soil (K_a) can then be determined.

As mentioned before, the oscilloscope shows the waveform of time and voltage obtained with the sampler. Any change in the electrical properties of the cable will cause a partial or total reflection of the waves. Changes in the electrical properties of the cable cause changes in the impedance. The voltage amplitude of the reflected waves is a function of the change in impedance that causes the reflection. An increase in impedance causes an increase in voltage, while a decrease in impedance results in a decrease in voltage. There are two extreme cases of reflection: (I) open ended probes (the impedance tends towards infinity), (II) when probes are short circuited (the impedance tends towards 0). The waveforms of these two cases are shown in Figure 2.10.

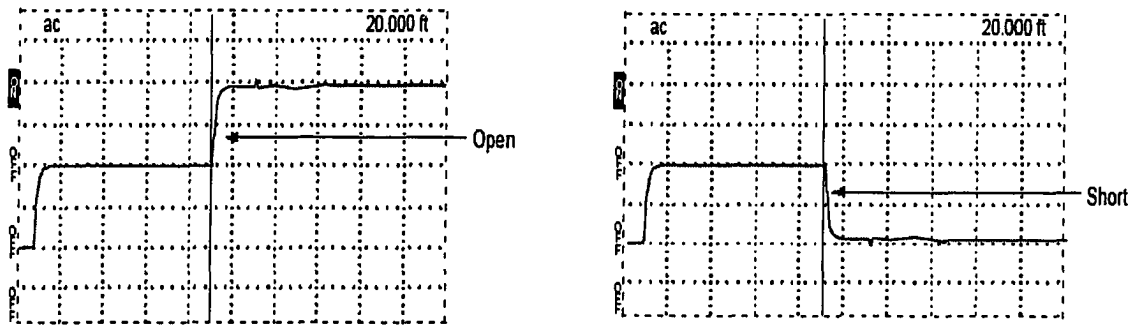

Figure 2.10: Waveforms of open-ended and short-circuited probes (1502C Metallic Time-Domain Reflectometer Service Manual, 1999)

In the application to moisture measurement in soils, the waveforms depicted in Figure 2.10 are shown in simplified form in Figure 2.11.

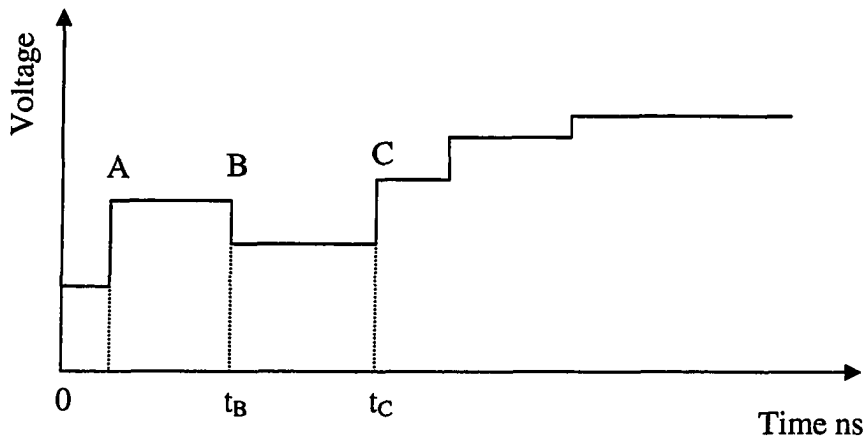

Figure 2.11: Idealized TDR waveform of a soil sample

At the time t=0, the step pulse generator starts to launch electromagnetic waves, at the same time the sampler starts to measure time (t) and voltage (V) thereby obtaining a set of data (t, V). At time t=0, the front of the voltage step has not yet reached the sampler and the sampler measures a voltage of 0. The pulse from the step generator travels along the coaxial line until it reaches the point A, where the front of the wave reaches the sampler. The sampler measures a change in voltage, results in an instantaneous rise in voltage. The wave keeps traveling down along the coaxial cable and it reaches point B, where the 50-ohm coaxial cable interfaces with a different impedance parallel transmission line embedded in soil. A part of the step pulse is reflected (first reflection) and the remainder of the wave travels to C. At C, which is an open end, the entire wave is reflected back (second reflection, assuming no losses due to radiation). At time t_B the first reflection reaches the sampler and results in a drop in voltage; at time t_C the second refection reaches the sampler and results in a rise in voltage because the impedance tends

toward infinite at an open end. The time difference between t_B and t_C is the transit time of the wave traveling from B to C along the probes and back to B again.

As described by Davis and Annan (1977), the propagation velocity of a fast rise time step is determined by the time required to travel a known length of transmission line. In the case of probes in soil, in a Δt period of time, the electromagnetic pulse has traveled double of the probe length, 2L. Therefore the propagation velocity V is:

$$V=\frac{2L}{\Delta t} \qquad (2.9)$$

Where L: length of the probe

Δt: time of travel

In a non-magnetic material, the velocity of an electromagnetic wave in a material is

$$V=\frac{C}{(K_a)^{1/2}} \qquad (2.10)$$

Where C: the velocity of light in vacuum, $3X10^8$ m/s

K_a: the apparent dielectric constant

Combining equation (2.9) and (2.10) results in:

$$\frac{2L}{\Delta t}=\frac{C}{(K_a)^{1/2}} \qquad (2.11)$$

Solving for K_a gives

$$K_a=\frac{C^2 * t^2}{(2L)^2} \qquad (2.12)$$

With a known probe length L and travel time Δt, K_a can be determined.

2.2.5 Calibration of start point and probe length

The apparent dielectric permittivity, K_a, was calculated from the travel time of the TDR signal along the probe. Before calculating travel time, the probe length and reference start point should always be calibrated (Heimovaara, 1994).

The reference point in this project was calibrated from measurements in air (K_a=1) and water of a known temperature. This calibration determines the time point where the pulse enters the soil and makes certain that both the analyses in air and water give the correct apparent dielectric permittivity.

The effective length was determined by measuring the travel time (t) of the pulse in water at known temperature and substituting the correct value for K_a in equation (2.12).

2.2.6 TDR factors affecting the soil moisture measurement

2.2.6.4 Probe configurations and sample volume

The literature provides very little information concerning the dimensions of TDR probes. Probes are usually made of stainless steel rods, with diameters ranging from 0.5 mm (microprobes, Roth, 1992) in lab application to 12.7 mm (Topp et al., 1984) in field applications, and probe lengths ranging from 5.4 cm (Roth, 1992) up to 110 cm (Topp et al., 1984). Constantz et al. (1990) and Patterson et al. (1981) have successfully used parallel lines as short as 13 and 10 cm, respectively. 50 mm is typically used for spacing, 30 mm and 25mm were also seen in the literature.

The spatial sensitivity of transmission line probes is a function of the ratio of the rod spacing to rod diameter. The scaled spatial sensitivity of the closely spaced rods may be identical to that of thick rods spaced further apart. Ease of insertion and minimizing

soil disturbance dictate that probe rods should have as small a diameter as possible. However, the effects of air gaps, measurement volume and mechanical strength of the soil may require larger diameter rods.

There are practical limits to rod spacing. It must be large enough to ensure the sampling of a representative soil volume (Patterson and Smith, 1981), but small samples are better suited for laboratory studies. Patterson and Smith (1981) found that small spacing of the rods results in steeper reflections from the end of the probe, which makes the analysis of the waveform much easier and more accurate. The soil located beyond a distance equal to twice the rod spacing has a negligible effect on the apparent dielectric constant (Davis and Chudobiak, 1975). Topp and Davis (1985) suggested that the soil measured by TDR is a cylinder whose axis lies midway between the rods and whose diameter is 1.4 times the spacing between the rods. The volume sampled corresponds to approximately the rod spacing squared multiplied by the length of the probes (Topp et al., 1982).

The sampled volume is not weighted linearly between the two rods of the transmission line. It is more heavily weighted in the region close to the transmission line elements (Baker and Lascano, 1989; Knight 1992). The transmission lines with narrow, closely spaced rods should be avoided in order to minimize the error associated with annular air gaps around transmission line rods (Whalley, 1993). Knight (1992) proposed that the ratio of rod spacing to rod diameter (B/D) should not exceed 10 for parallel-pair probes, so that too much energy will not be concentrated closely around the rods and therefore avoid the air gap problem.

A balanced two-rod system is almost twice as sensitive as multi-wire system, therefore two-rod system has greater sampling volumes (Topp et al., 1980). Three-rod design has become widely used because of the elimination of a balun. The drawback is the increased disturbance of the soil when more than two rods are used.

Lin (2003) in the simulation of TDR waveforms by varying the probe length (from 2.5 to 30 cm) revealed that the probe length did affect K_a. K_a was basically constant when the probe length is between 10 to 25 cm. However, when the length of the probe is under 5 cm, K_a is markedly higher than that determined by a probe of length between 10 and 25 cm. He concluded that the length of the probe should be at least 10 cm to ensure estimates of water content. Young et al. (1997) found that longer TDR probes gave more accurate estimates of soil water storage than did shorter probes.

2.2.6.5 Probe orientation

The probes can be installed either horizontally or vertically. Vertically installed probes have advantages such as ease of installation and removal, and measurement of total water within the depth spanned by the probe. Horizontally placed probes better integrate or average the spatial variability in the horizontal direction. The hypothesis that vertically and horizontally installed probes give the same results was tested both theoretically and experimentally in the literature (Topp et al., 1980; Topp et al., 1982; Ferre et al., 1998; Young et al., 1997 a; Baker and spaans, 1994; Nadler et al., 2002).

2.2.6.6 Cable length

Long cables are usually needed in field applications for convenience. The major effect of increasing cable lengths is that the rise time of the TDR voltage pulse increases,

spreading each reflection across a larger time interval. Smaller reflections as well as the first reflection point may no longer be visible, which influences the accuracy of the waveform analysis and causes a possible underestimation of the apparent dielectric permittivity in dry soils (Heimovaara, 1993). As a result, it is not possible to use short probes with long cable lengths. Consequently errors are smaller in media with higher dielectric constants (i.e., wet soils). Heimovaara (1993) showed that short probes (0.05 m) could not be used with cables longer than 3.2 m. The 0.10 m long probes can be used with cable lengths up to 15 m, while probes longer than 0.20 m gave reproducible results up to cable lengths of 24.1 m. Herkelrath (1991) found that cable length up to 27 m had no significant effect on the calibration curve.

2.2.7 Soil Factors affecting TDR measurement

2.2.7.1 Nonuniformity in water distribution

Strong nonuniformity in water distribution along TDR waveguides is reflected in the wavetrace. Topp et al. (1982) reported both empirically and theoretically that when water content varied with depth, the TDR gave a measure of the average water content.

2.2.7.2 Magnetic permeability of soil material

One of the soil factors that can lead to differences in calibration between soil types is magnetic permeability. The only minerals with large values of magnetic permeability are iron rich soils (Whalley, 1993). For magnetic materials, $V=\frac{C}{(K')^{1/2}}$ is no longer valid. Roth et al. (1992) have shown that at the frequencies normally used in TDR for measuring soil water content, the magnetic properties of soil do not appear to

have any significant effect on the calibration.

2.2.7.3 Soil texture and bound water

In theory, "bound water" is presumably due to an interaction between the solid and liquid phases. Water is thought to form a thin film with a paracrystalline structure around the solid phase (Dobson et al., 1985). Because of restricted rotational freedom of the water molecules in this film, its dielectric constant is lower than that of bulk water (Roth et al., 1990; Jacobsen and Schjonning, 1993; Dirkson and Dasberg, 1993). Bound water in the closest proximity of the surface is most inhibited in its movement and therefore it behaves like ice, whereas bound water further away from the surface may move more freely and therefore it resembles more like free water. The dielectric constant of bound water should be somewhere between the values of ice (≈3) and free water (Topp et al., 1980; Heimovaara et al., 1994). The magnitude of "bound water" effect depends on the surface area and surface charge and thus on the texture of the soil. At the same water content, this effect generally leads to a lower dielectric constant for fine-textured soils, compared with coarse-textured soils. Topp et al. (1980) examined the effects of soil texture for a wide range of water contents but similar bulk dry densities. Clayey soil exhibited a lower K_a at low water content but a higher K_a at high water content, than was observed for the sandy loam soil. He also noticed that for the vermiculite and organic soil, little measurable change was found in K_a until θ_v was greater than 0.1 m^3m^{-3}. He concluded that the active surface area of the soil controls the dielectric properties of the first few molecular layers of water added to the soil. The first layers acted as bound water that had very low dielectric constants.

Organic soils such as peat have different dielectric properties from mineral soils because of their lower bulk density, higher porosity and high specific surface area (Topp et al., 1980; Roth et al., 1992; Kellner et al., 2001). The high porosity causes a much larger water-content range (typically 5-95% by volume) as compared to mineral soils and the large surface area causes a larger portion of "bound" water. Different calibration functions need to be developed for organic and peat soils (Topp, 1980; Toikka et al., 1989; Roth et al., 1992; Kellner et al., 2001).

2.2.7.4 Electrical conductivity

When electromagnetic fields travel through wet porous materials, their energy can be dissipated by two major factors: polarization or electrical conductivity of the media. Polarization process is a function of the angular frequency and in a frequency range from 1 MHz to 1 GHz that is produced by TDR, polarization losses are negligible (Davis and Annan, 1977). Electrical conductivity losses can sometimes cause total attenuation of the reflected signal (White et al., 1994). Attenuation in conductive porous materials becomes a problem as the electrical conductivity increases, especially for long TDR probes.

The bulk soil electrical conductivity increases with water content but it is low even when close to saturation (Robinson et al., 1999). Topp et al. (1980, 1982) observed increased attenuation effect as soil water content increased. They found that at high water contents, the end point reflection for TDR probe (with dielectric discontinuities) longer than 60 cm were too small for confident interpretation.

Many researchers (Topp et al., 1980; Dasberg and Alton, 1985; Dalton et al., 1984; Nadler et al., 1991) have found that the presence of salt in the liquid phase of the soil-water system caused no measurable effect on the apparent dielectric constant. However, it

did increase the attenuation of the voltage step as it traveled in the soil, which increased the measurement error. More scatter was found in the relationship between K_a and θ_v where salt solution was replaced with water (Topp et al., 1980).

Some researchers (Dalton et al., 1984;, Dasberg and Dalton, 1985; Dalton and van Genuchten, 1986; Topp et al., 1988; Zegelin et al., 1989) proposed recently that the attenuation of the reflected TDR signal can be used to infer soil water electrical conductivity. In this approach, K_a and voltage levels reflected at various positions along the TDR probe are used to estimate the electrical conductivity of the soil.

2.2.7.5 Temperature

In pure water, the dielectric constant changes from 84 to 76 between 0 and 30 °C. The dielectric constants of air and solid phase are much less sensitive to temperature than that of water. The influence of temperature on the dielectric constant of wet soil increases with water content. For this project, temperature is not a significant issue because the room temperature of the laboratory has been kept at approximately 21°C. When performing seasonal measurements in soil with high water contents, field temperature corrections have to be considered.

2.2.7.6 Bulk density

Bulk density does not affect the calibration function significantly as the dielectric constant of the solid is low and bulk density does not vary significantly. But addition of bulk density to the function does improve the calibration accuracy to a relatively small extent (Jacobsen and Schjonning, 1993).

2.2.8 K_a- θ_v relationships from the literature

As mentioned in the introduction, there are two approaches to calibrate the volumetric water content with dielectric constant: empirical polynomials and dielectric mixing models. Empirical polynomials dominate in the published TDR research papers. It is well recognized that organic soils need different calibration curves from mineral soils.

Topp et al. (1980) established a universal relationship, a third order polynomial, which has been successfully and widely used by researchers in water content measurement in mineral soils. For organic soils, Topp et al. (1980) investigated a disturbed organic soil (bulk density 0.422 g/cm^2) reaching just above 50% by volume in water content. Later Roth et al. (1992) presented a calibration function for seven soil samples with organic matter contents ranging from 10.5 to 54.8% (some samples were weakly or well decomposed peat, the others were undecomposed oak leaves), extending the calibration to water contents close to 80% by volume. Herkelrath et al. (1991) provided a linear relationship between K_a and volumetric water content for organic soils. However, in poorly decomposed Sphagnum peat, soil water content regularly extends above 90% by volume. Pepin et al. (1992) evaluated 163 samples of undisturbed peat taken from 5 to 50 cm depth with porosities ranging from 83 to 95. They found that a second-order equation performed well, claiming a standard deviation of 3.4 in the range 21 to 95 % by volume. Paquet et al. (1993) also provided a third order polynomial for moderately decomposed sphagnum peat (H3 to H4 on the Von Post scale) annexed with variable amounts of sand and composed bark in a water content range from 23 to 85 %. Myllys and Simojoki (1996) suggested a third-order equation for 24 samples of cultivated

Sphagnum peat (undisturbed samples), taken from 5 to 25 cm depth. Kellner et al. (2001) came up with a third order polynomial from the undisturbed peat samples (dominantly Sphagnum spieces, von Post H2—H4) in a water content range of 10 to 95% with a porosity range of 95-97%.

The calibration functions of organic soils and peat are presented in Table 2.2 and plotted in Figure 2.12 along with Topp's universal equation for comparison.

Table2.2 Empirical K_a-θ_v calibration equations from the literature

Source	Formula	Characteristics of samples	Water Range %	Porosity	Bulk Density Kg/m^3	Rmse
Topp et al., 1980 mineral	$K_a=3.03+9.3\,\theta_v+146\theta_v^2-76.7\theta_v^3$ $\theta_v=-5.3*10^{-2}+2.92*10^{-2}*K_a-5.5*10^{-4}*K_a^2+4.3*10^{-6}*K_a^3$	Mineral soil				0.0221
Topp et al., 1980 organic	$K_a=1.74-0.34*\theta_v+135*\theta_v^2-55.3*\theta_v^3$ $\theta_v=-2.52*10^{-2}+4.15*10^{-2}*K_a-1.44*10^{-3}*K_a^2+2.2*10^{-5}*K_a^3$ (Transformed by Stein and Kane 1983)	Organic soil	3.3-55.1		442	
Roth et al., 1992 (corrected in 1993) organic	$K_a=0.994+10.51\theta_v+88.54\theta_v^2-28.92\theta_v^3$ $\theta_v=2.33*10^{-2}+2.85*10^{-2}*K_a-4.31*10^{-4}K_a^2+3.04*10^{-6}*K_a^3$	Organic soil (7 samples), weakly or well decomposed , cultivated peat 1sample of undecomposed oak leaves organic content: 10.5-54.8%	0-80	0.527 -0.786	200-770	0.1593
Herkelrath et al., 1991 organic	$\theta_v=0.1273*K_a^{0.5}-0.051$	Organic soil	10-80			0.1778
Pepin et al., 1992 peat	$\theta_v=0.085+0.0192*K_a-0.95*10^{-4}*K_a^2$	Undisturbed natural peat with mixed species including Sphagnum peat (163), organic content: 74.7-98.6% von Post: H1-H6	20.9-94.8	0. 826 –0.95	64-248	

Table2.2 Empirical K_a-θ_v calibration equations from the literature (continued)

Paquet et al., 1993 peat	$\theta_v=(-55+425*K_a-9.75*K_a^2+0.0907*K_a^3)*10^{-4}$	Moderately decomposed Sphagnum peat annexed with variable amounts of sand and composed bark Von Post: H3 to H4	23-85		293-397	
Myllys and Simojoki, 1996 peat	$\theta_v=-8.3*10^{-2}+4.32*10^{-2}K_a-8.53*10^{-4}*K_a^2+5.99*10^{-6}*K_a^3$	Cultivated Sphagnum peat (undisturbed, 24 samples) organic content: 52%	30-80	0.77	400	
Kellner et al., 2001 peat	$\theta_v=3.9*10^{-2}+3.17*10^{-2}*K_a-4.5*10^{-4}*K_a^2+2.6*10^{-6}*K_a^3$	Undisturbed natural peat (dominantly Sphagnum sp ices, von Post H2 - H4)	10-95	0.95 -0.97	29.1-66.2	
Shibchurn, 2001 sphagnum peat	$\theta_v=0.2667*Ln(K_a)-0.1405$	Milled sphagnum peat Organic content: 98.9 % Von Post H1- H3	40-90	0.88 - 0.92	109-153	

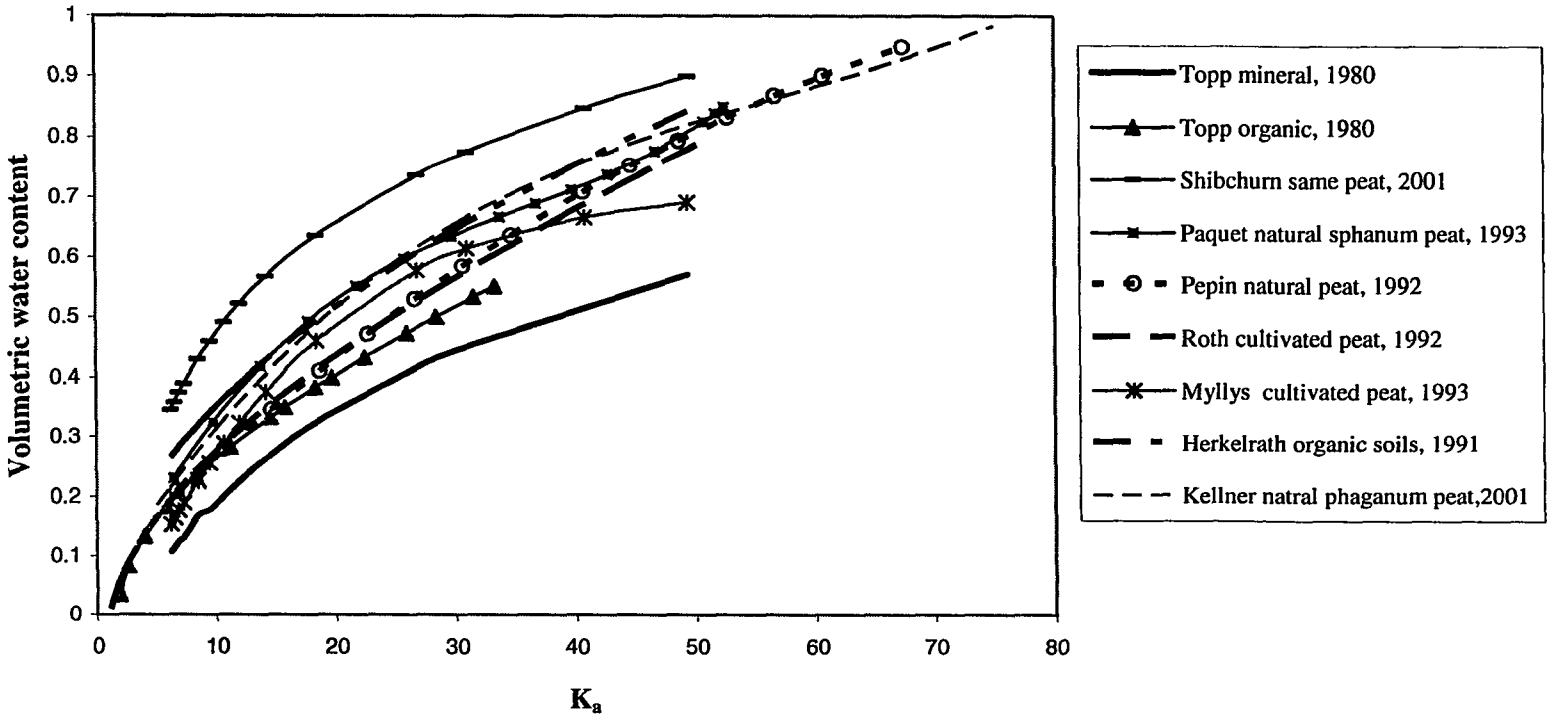

Figure 2.12: K_a-θ_v calibration curves for organic and peat Soils from the literature

CHAPTER 3: MATERIALS AND METHODS

3.1 OVERVIEW

Measurements of water content in peat columns using TDR are usually conducted by inserting probes horizontally into the soil through the wall of the columns. The accuracy of water content measurements by horizontal probe insertion has been demonstrated by many researchers. The objective of this research was to develop a method to measure the water content profile with depth in peat columns by vertically inserting TDR probes from the top of the columns, which leads to the possibility of applying TDR techniques to peat filters in the field.

As discussed in section 1.3 Scope of Work, the research consisted of five stages. The materials and methods needed to complete the research are outlined in the following sections.

3.2 WAVEFORM ANALYSIS USING WATTDR

Waveform analysis is the heart of TDR techniques. WATTDR, a software package developed by David Redman (2000), was used to permit acquisition of TDR waveforms and waveform analysis. TDR waveform analysis determines the dielectric constant (K_a) of the soil. In WATTDR, waveforms were analyzed manually by fitting tangent lines to the start and end points to determine the one-way travel time (t) along the probes embedded in the soil and then the dielectric constant could be calculated by the software. WATTDR allows the user to zoom in on different parts of the waveform in order to improve the accuracy when determining the start and end points. Redman (2004, via

email communication) explained that the WATTDR software scaled the time axis such that the time measured on this axis is the one-way travel time and hence the "2L" term in equation (2.14) is replaced by "L" and the equation becomes:

$$K_a = \frac{C^2 * t^2}{L^2} \qquad (3.1)$$

A sample output screen from WATTDR is provided in Figure 3.1. The K_a value given on the bottom of the screen is calculated based on a user-specified probe length. T1 and T2 refer to the start and end times, and t2-t1 reflects the one-way travel time along the probe in the soil. The volumetric water content value shown on the screen is calculated by WATTDR using Topp's universal K_a- θ_v calibration curve for mineral soils. The volumetric water content of peat in this study was determined from the measured K_a values using the calibration curve generated as a part of this research using pressure cell method described in section 3.4.

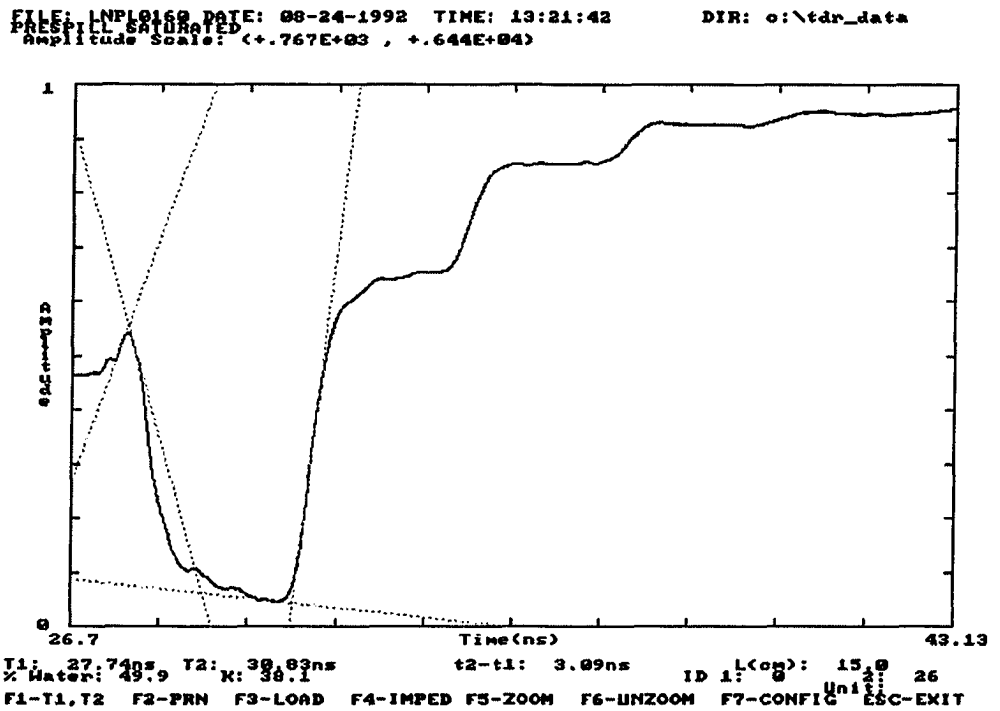

Figure 3.1: Waveform analysis in WATTDR (Redman, 2000)

3.3 PRETREATMENT AND CHARACTERIZATION OF PEAT

The sphagnum peat used in this study was provided by Premier Tech Ltd. It was received in $3.8ft^3$ plastic bags and dark brown in color. In order to avoid significant heterogeneity and channeling problems, peat had been pretreated before experiments were employed. Following the procedures that Shibchurn described in her project in 2001, twigs or sticks longer than 2.0 cm and peat clods larger than 3.0 cm in diameter were manually removed. Pretreated loose peat was soaked in a large container to achieve better saturation and to reduce the period of time to saturate the peat in comparison to the case in which the columns were packed with air dry peat and then saturated.

Shibchurn (2001) characterized the peat in her project by physical, chemical and hydraulic properties such as particle size distribution, moisture content, ash and organic content, fiber content, pH and water retention characteristics. Peat was then classified according to ASTM standards and the soil moisture curve was determined. The results were summarized and used for this research as the peat was from the same source (i.e. the same skid (15 bags) of peat delivered to Carleton University).

3.4 DETERMINATION OF K_a-θ_v CALIBRATION RELATIONSHIP

The pressure cell method is a traditional method of determining the soil moisture curve (Reginato and Bavel, 1962). In this research, the method was modified with the addition of a TDR probe inserted into the pressure cell to generate the K_a - θ_v calibration function.

3.4.1 The pressure cell

Pressure cells used in this study are made of aluminum and have two main parts: top cap and bottom cap. The top cap has an attached cylinder that can hold peat samples. Figure 3.2 shows the dimensions and assembly of a pressure cell. A ceramic plate with an air entry pressure of 1.0 bar (100 KPa) is supported on the bottom cap to prevent entry of air from the pressure cell into the drainage tube. The plate is 15.559 cm in diameter and 0.714 cm in thickness (Soil Moisture Equip Corp., 2000, Part No: 0604D06-B01M1), and was modified to a smaller diameter (14.7 cm) to fit into the bottom cap. Flat and round black rubber O-rings were installed below and on top of the plate for sealing purposes. Two holes were made at the mid height of the cylinder of the top cap in a horizontal orientation for TDR probe insertion. Rubber grommets were installed in the holes to isolate the two rods as contact with the column wall generates a short circuit.

15 cm parallel pair stainless steel rods (3 mm in diameter and 20 mm for rod spacing) were used for TDR measurement in the pressure cell. The ratio of rod spacing to rod diameter was less than 10, falling into the acceptable range indicated by Knight (1992).

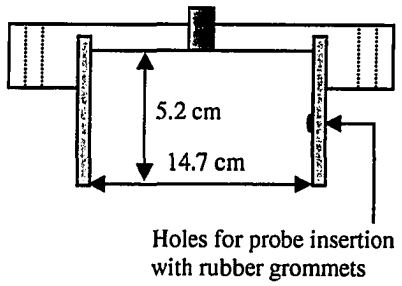

a. Top cap

b. Bottom cap

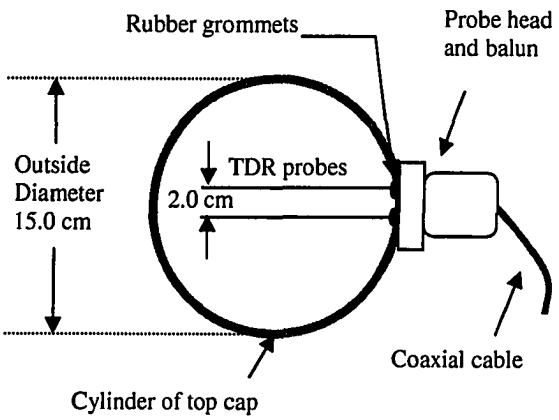

c. Plan view of a top cap connected to TDR unit

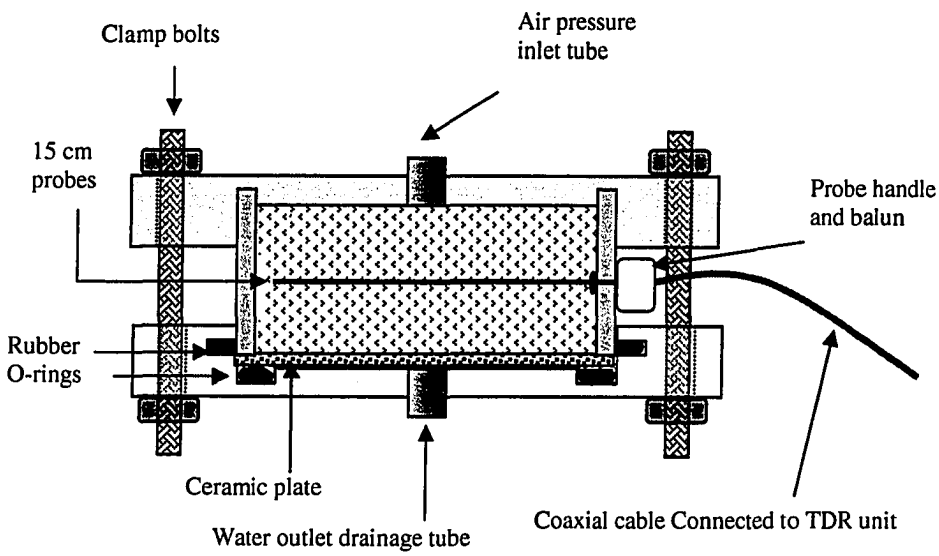

d. Assembly of a pressure cell

Figure 3.2: Dimensions and assembly of a pressure cell a. Top cap b. Bottom cap c. Plan view of a pressure cell connected to TDR unit d. Assembly of the pressure cell (Modified from Shibchurn's, 2001)

3.4.2 Calibration of the start point and probe length

Due to the influence of the probe connector and the balun, waveforms obtained in pressure cells were expected to be slightly different from the typical waveforms shown in the literature review section. At each change in impedance, a change in voltage is reflected back. This includes interference at the metal column wall and grommets that were used to isolate the metal column wall from the steel rods. Hence, identification of the start point and determination of the effective probe length became essential for further waveform analysis. Calibration of the reference start point and probe length in the pressure cell was achieved by taking measurements in air and water.

Waveforms were taken with the cell empty, or in other words, filled of air, and then when filled with water. Waveforms of air and water were plotted together. The time point where the air and water waveforms split was where the signal entered the inside of the cell and started to travel in soil. This time point was used as the reference start point for further waveform analysis.

The same waveforms of water and air were analyzed by WATTDR based on the start points determined to obtain the K_a values. Signal travel time from the start point to the end of the probes was determined by the tangent line method described by Redman (2000). With the known theoretical K_a values of water and air, effective probe length was calculated by a transformed form of equation (3.1):

$$L=\frac{C*t}{\sqrt{K_a}} \qquad (3.2)$$

Theoretical K_a of water was adjusted by the following equation at a specific temperature (Hasted, 1973):

$$K_a=87.749-0.40008T+9.398X10^{-4}T^2-1.410X10^{-6}T^3 \qquad (3.3)$$

In order to verify the reference start point and effective probe length, new waveforms were measured in a pressure cell: 8 for water and 8 for air. K_a values were analyzed based on the reference start point and effective probe length determined earlier. The measured K_a values were compared with the theoretical values of air and water using a one-sample t-test.

3.4.3 Preparation of the pressure cell

As illustrated in the assembly of the pressure cell, a ceramic plate was placed on the bottom cap to support soil drainage. To maintain good hydraulic contact between the wet soil and the water in the drainage tube, it is essential to fully saturate and deaerate the porous plate before placing the cell in operation (Reginato and Bavel, 1962). For this purpose, the dry porous plate was placed in a container with shallow water so that only half of the plate was submerged. Capillary force drew water into the plate and the plate was assumed to be saturated when water was visible over the entire top surface. This saturation process usually took several minutes.

The cavity between the ceramic plate and the drainage tube was also saturated for the same purpose. To ensure the cavity below the ceramic plate was saturated, the porous plate was placed into the bottom cap and sealed with a round rubber O-ring when the bottom cap was submerged in a water filled sink. The drainage port at the bottom cap was connected to 50 ml water-filled burette with a 3 meter long water-filled C-Flex tubing (Figure 3.3). The flat O-ring along the outer edge of the porous plate was to eliminate air movement around the plate and to maintain suction below the plate.

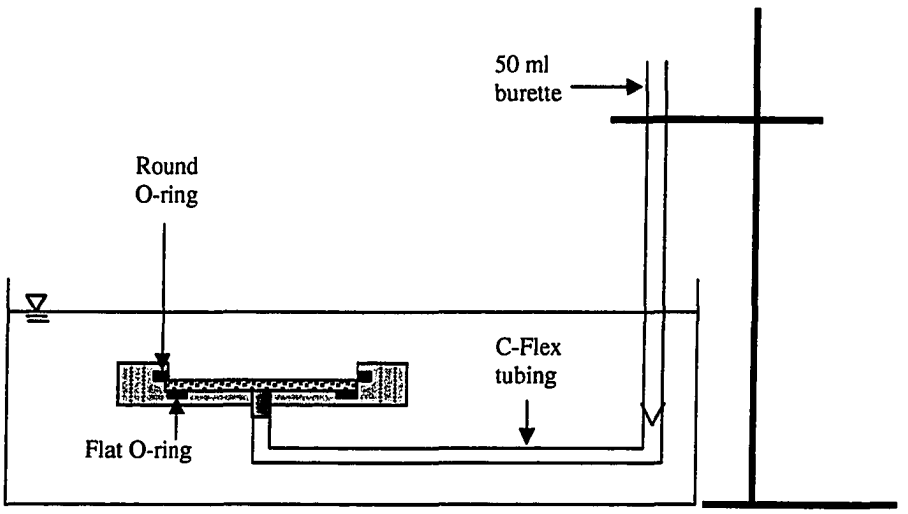

Figure 3.3: Bottom cap of a pressure cell connected to a burette

3.4.4 Final Laboratory setup

Pre-saturated peat was packed into the top cap. 15 cm pair rods were installed during the packing process to ensure they were parallel. The top cap filled with wet peat was then inverted and placed into the bottom cap that was connected to a burette in Figure 3.3. The bottom cap and top cap were fastened together by six clamp bolts. A positive hydraulic head was applied to the bottom cap by raising the burette for an hour. This allowed water to flow through the cell to maximize the chances of complete saturation. The burette was then lowered such that the water level in the burette was at the same elevation as the mid height of the cell. The TDR probe was inserted in the pressure cell and connected to the TDR unit by a coaxial cable. Figure 3.4 shows the final laboratory setup to determine the K_a-θ_v calibration relationship.

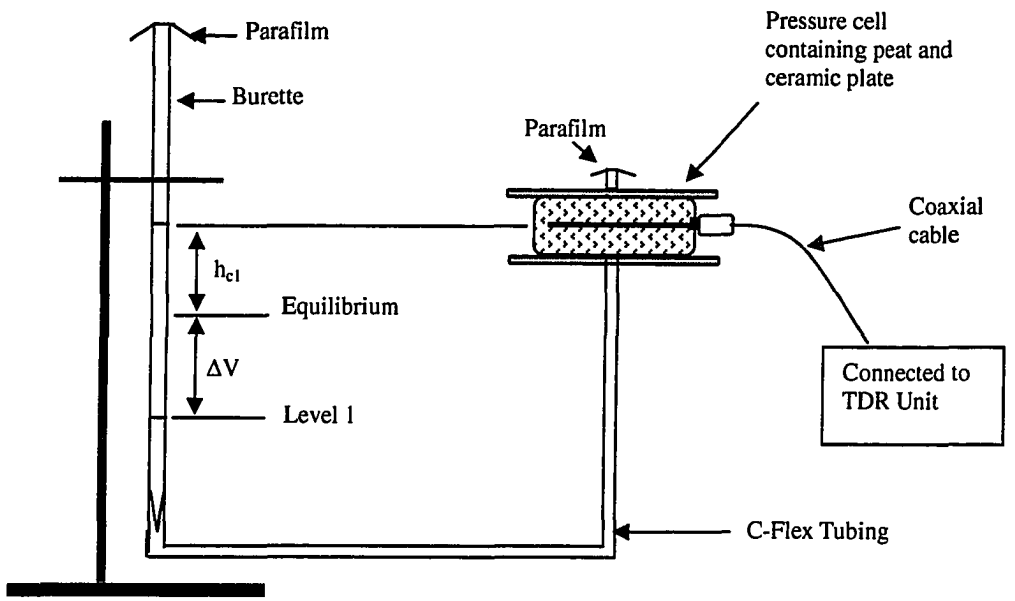

Figure 3.4: Schematic of Laboratory setup for modified pressure cell method to determine K_a-θ_v calibration function (Shibchurn, 2001)

3.4.5 Procedures to determine the K_a-θ_v calibration curve

The experiment started from saturated conditions. It was assumed that water content and suction at the mid point of the peat layer represent the whole sample as Shibchurn (2001) did in her project. The suction was therefore measured as the difference between the water level in the burette and the mid point of the pressure cell, where the TDR probes were located (Figure 3.4). With the water level in the burette at the same height as the midpoint of the cell, the K_a of saturated peat was measured by TDR. The first point on the K_a-θ_v calibration curve was determined.

To obtain another point on the curve, the water level in burette was lowered to a certain level to generate a negative pressure on the peat sample (level 1 in Figure 3.4). Under the influence of the negative pressure, water drained out from the peat soil to the burette until equilibrium was reached. At equilibrium, the amount of water drained out of

the soil (ΔV) was recorded as well as the suction (h_{cl}). The K_a of peat was measured. It should be noted that the time to reach equilibrium varied for different porous plates and for certain experiments performed with low-flow ceramic plates it took 12-60 hours to reach equilibrium. Equilibrium was assumed to be reached when the amount of water change in the burette was less than 0.5 mL in 4 hours.

The water level in burette was lowered several times to create a set of data including the amount of water collected, suction applied and K_a values. At the end, the wet peat was weighted and oven dried at 105° C to obtain the water content and the bulk density of peat in the cell at the end of the experiment. Water content at each suction level was then back calculated by sequentially adding the amount of water collected during each step. With water contents at each suction and K_a values measured by TDR, a K_a-θ_v calibration relationship could be determined. In addition, the soil moisture curve at various bulk densities was estimated.

Because of the long duration of the experiment, the air pressure inlet tube and the top of the burette were covered with parafilm to avoid evaporation. A tiny hole was poked on the parafilm to maintain the air pressure. The pressure cell was weighted at each measuring point to determine the impact of evaporation.

3.5 GUIDE BLOCK DESIGN AND TEST ON ROD SEPARATION

3.5.1 Guide blocks and the sectional ABS column

Parallel stainless steel rods were used for TDR probes to measure water contents in peat columns: 15 cm for the horizontal probes and 81 cm for the vertical probes. Both the vertical and horizontal probes had a rod diameter of 3 mm and a rod spacing of 20

mm. Davis (1975) stated that the parallel rods did not have to be exactly parallel. However, the discrepancy should not be large. Because longer probes may cause greater separation as they are inserted into the peat, special care should be taken when inserting the vertical 81 cm probe. In order to keep the rods as parallel as possible, guide blocks were designed to guide the probe during insertion. The guide blocks consisted of three components: Guide block 1 was 20 cm long with two vertical holes to guide the steel rods. This block was constructed in two half sections that can be easily removed during the measurements (Figure 3.5 c). Guide block 2 kept the top of the rods at the correct spacing and also helped advance the rods into the peat (Figure 3.5 d). Guide block 3 maintained the correct rod spacing at the top of the columns (Figure 3.5 e).

An ABS column (inside diameter: 15.2 cm, wall thickness: 0.75 cm) consisting of seven sections was designed to test the performance of the guide blocks for vertical insertion (Figure 3.5 a, b). Grooves were made on the bottom and the top of each column section to help keep good connections between sections. Assembly and dimensions of the sectional ABS column are shown in Figure 3.5 a, b. The insertion of the vertical TDR probe from the top of the sectional column using guide blocks is illustrated in Figure 3.5 b.

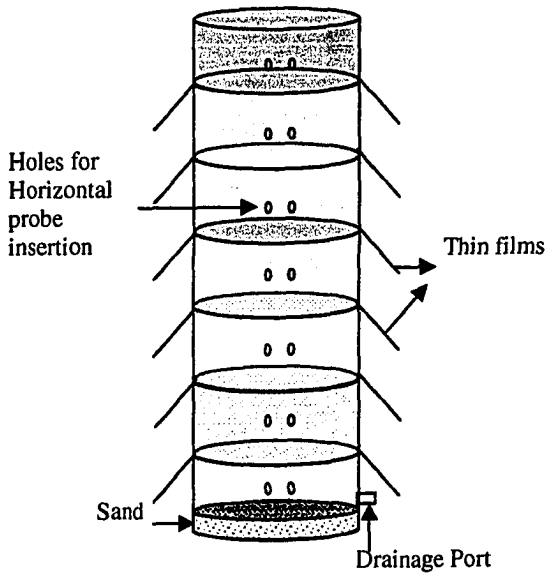

a. Black column with separate sections

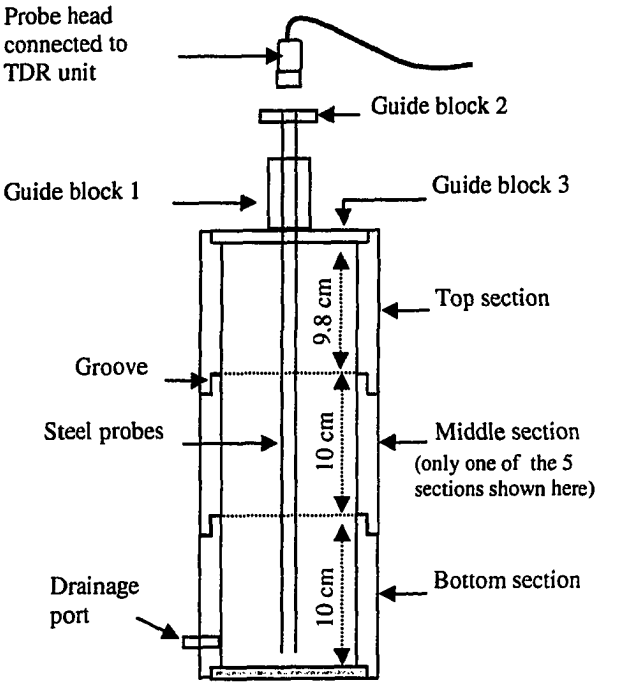

b. Illustration of black column assembly and probe insertion using guide blocks

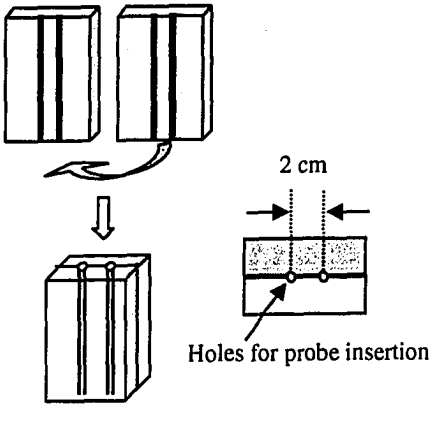

c. Guide block 1

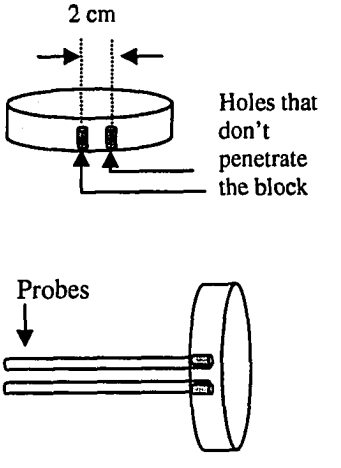

d. Guide block 2

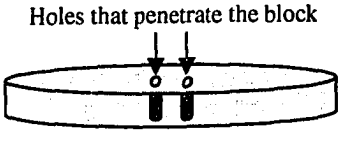

e. Guide block 3

Figure 3.5: The ABS sectional column and guide blocks

3.5.2 Performance of the guide blocks and impact of rod separation

Air dried peat was packed into the bottom section of the ABS column and a piece of thin plastic film (Saran Wrap) was placed on the top of this section. A second section was then added, packed with peat and covered with a piece of thin film. The rest of the sections were assembled and packed with peat in the same manner. Effort was made in the packing process to keep a uniform bulk density of the soil throughout the entire column. Thin films placed at the interfaces of each section were to determine the rod separation at each depth (Figure 3.5 a).

81 cm rods were inserted into peat from the top of the packed column using the guide blocks as illustrated in Figure 3.5 b. Guide blocks were removed, the TDR probe head was connected, and the K_a value of peat was measured. The column was then dismantled and distances between the two holes on the thin films caused by rod insertion were measured. The entire process was repeated six times using the same peat to determine how the rod spacing varied during probe insertion and how this spacing may have impacted the measured K_a values. Performance of guide blocks and effect of rod separation on TDR measurements were discussed.

Recognizing the potential impact of repacking on the soil structure, K_a values were also measured by inserting the 81 cm probe 6 times into the same peat column and the resulting 6 K_a values were compared.

The impact of rod separation on K_a measurements was also tested in a tall bucket containing just water. Non-conducting spacers were used to control the end separation distance of the rods. K_a values of water for different probe separations were obtained and compared with the theoretical value using a one-sample t-test.

3.6 COMPARISON OF VERTICAL TDR PROBE METHOD WITH OTHER METHODS

Water contents were measured both vertically and horizontally by TDR in peat columns during a sequential drainage experiment. Gravimetric water contents were also determined at the end of the experiment. Results were compared. In addition, the main drainage curve of the peat was evaluated.

3.6.1 Laboratory setup

Stainless steel columns (height: 61 cm; inside diameter: 16.2 cm; wall thickness: 0.3175 cm) were used for the comparison of horizontal and vertical TDR measurements (Figure 3.6).

Presaturated peat was packed into the column with a 2 cm sand layer at the bottom for drainage support. A piece of geotextile was placed on top of the sand layer to prevent leaching of fine particles from peat. C-Flex tubing was connected to the drainage port at the bottom of each column for water drainage.

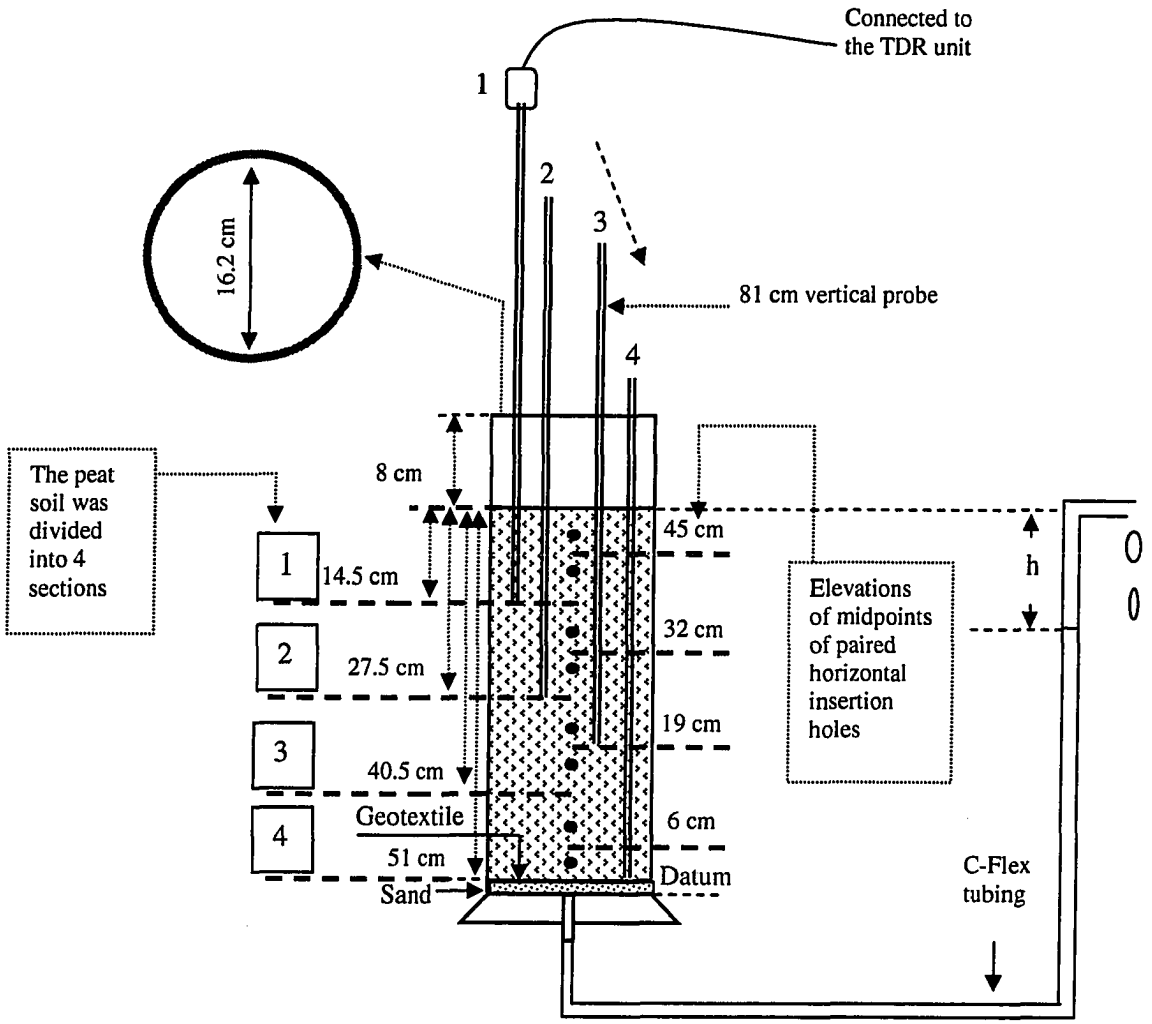

Figure 3.6: Illustration of horizontal and vertical TDR measurements in a steel column

15 cm long stainless steel rods were used for the horizontal TDR probe. Four paired holes were made in the wall of each column for horizontal probe insertion. The midpoint elevations of each paired holes were 6 cm, 19 cm, 32 cm and 45 cm respectively from the bottom to the top, based on a datum at the bottom of the sand layer.

81 cm long stainless steel rods were used for the vertical probe. The rods were

incrementally advanced 4 times (following the order 1, 2, 3, 4 in Figure 3.6) and at each probe depth, the length of probes buried in the peat soil was 14.5cm, 27.5cm, 40.5 cm and 51 cm, respectively. At probe location 1, the K_a value was determined and the average volumetric water content over the 14.5 cm depth in soil section 1 was calculated by the K_a-θ_v calibration curve. In the same manner, probe location 2 determined the average water content over the 27.5 cm depth of soil (both soil section 1 and 2). The difference in travel time for locations 1 and 2 was used to determine the average water content in section 2. The average water contents in section 3 and section 4 were determined in the same manner.

Because the horizontal probes were located at the midpoint of each of the four soil sections (small deviations existed for the top and the bottom probe locations because of the sand layer and the height of peat packed in the column), the average water contents determined by the vertical probes for each section should be similar to those determined by the horizontal probes. The main drainage curve of the peat was also evaluated in the drainage process.

3.6.2 Calibration of the start points and probe lengths

3.6.2.1 Calibration of 15 cm rods for horizontal insertion

Horizontal TDR measurements in columns had the same setup as in pressure cells but with a slightly different column diameter (16.2 cm for the column versus 14.7 cm for the pressure cell). The wall thicknesses of the pressure cell and the column are the same (0.3175 cm). The same length of probes and same size of rubber grommets were used.

Hence, the reference start point and rod length calibrated for the pressure cell could also be used for the horizontal measurements in the columns.

3.6.2.2 Calibration of 81 cm rods for vertical insertion

The start points on the vertically measured waveforms in columns should be easier to identify than on horizontal waveforms because there was no interference from the column wall. Since the probe was incrementally advanced into the peat column to determine the moisture profile with depth, the electromagnetic signal will initially travel through the air before entering the wet peat (Figure 3.6). An obvious impedance change from air to wet peat resulted in an obvious change in voltage. The point where the voltage drops occurred was taken as the reference start point. The actual probe lengths inserted in peat were assumed to be the effective probe lengths for waveform analysis.

To verify the reference start points and the corresponding probe lengths, new waveforms were taken by inserting different lengths (14.5cm, 27.5cm, 40.5cm, and 50cm) of the 81 cm probes in water and peat. The point where the waveforms in water and peat (taken with the same probe length) split was the reference start point for the corresponding probe length. In the earlier section for the 15 cm horizontal probe, waveforms of air and water were used to calibrate the start point. Peat was used instead of air for the vertical probe because there was a portion of the vertical probe exposed in air and there would be no voltage drop if the rest of the probe was inserted in air as well.

Using the reference start point determined, K_a values of water were determined based on the actual lengths inserted in water. One sample student t-test was performed to see if the measured K_a values were statistically different from the theoretical K_a value of water.

3.6.3 Determination of water content by different methods

The experiment started from saturated conditions. With the water level in the drainage tube at the same height as the peat surface in the column, average water content in the four soil sections were determined using both the horizontal and vertical TDR probes (Figure 3.6). The column was weighted. The drainage tube was then lowered to some height below the peat surface to apply a suction on the peat column and water drained out of the column. Water drained was collected in a beaker. After allowing 2 hours to reach the equilibrium, the amount of water collected, the elevation of the water level in the drainage tube (bottom of the sand layer was set as datum) and the weight of the column were recorded. Water contents in the four soils sections were determined using both the vertical and horizontal TDR probes. The drainage tube was lowered for 5 more times in the same way so that a set of data was collected.

At the end of the experiment, the peat column was dismantled into four sections. Wet peat was weighted and oven-dried at 105°C to determine the final water contents of the peat in each section. The average water content of the entire column at each suction level was then back calculated by sequentially adding the amount of water collected during each drainage step. Water contents measured using the vertical and horizontal TDR probes and the gravimetric method were compared. The experiment was repeated for five more peat columns following the same procedure.

3.7 IMPACT OF VERTICAL TDR PROBE ON FLOW RATE

The experiment to evaluate the impact of vertical TDR probe on flow rate was performed on five peat columns from a parallel research project. Peat columns in the

parallel project had the same dimensions and the same laboratory setup as illustrated in Figure 3.5 for this research. Each column was pulsed twice a day (9 am and 3 pm) and the outflow with time from the column in response to a pulse was recorded by a scale connected to a computer via an RS232 port. The water content in the column was measured by the 81 cm vertical TDR probe at 2 pm before the afternoon pulse. Flow rates of the column before the vertical probe measurement (morning pulse) and after the vertical probe measurement (afternoon pulse) were compared. After two weeks, flow rate of the afternoon pulse for the same column was measured again without moisture measurement using the vertical TDR probe. This flow rate was compared with the flow rate measured right after the vertical probe measurement.

3.8 INVESTIGATION OF CLOGGING IN PEAT COLUMNS

The two steel columns used in this part of experiment were the same as in section 3.6 and 3.7, and were packed with presaturated peat in the same manner. Then the columns were gravity drained. The gravity drained columns were pulsed with water twice a day (9 am and 3 pm) for two days and then pulsed twice a day with a high organic loading (9 am and 3 pm). The hydraulic loading for each pulse was 9.7 cm. Feed solution was made following a recipe provided by Kennedy (1998) who worked on a similar project. Table 3.1 presents the composition of the feed solution. The BOD of the feed solution was 22,000 mg/L which resulted in an organic loading of $4.27X10^6$ $mg/m^2/day$. A high organic loading was used to accelerate the clogging process such that the experiment did not take months to complete.

Table 3.1: Composition of the organic feed

Chemical Name	Chemical Formula	Concentration g/L
Glucose	$CH_2OH(CHOH)_4CHO$	13.750
Ammonium Bicarbonate	NH_4HCO_3	4.167
Potassium phosphate (mono)	KH_2PO_4	0.250
Potassium phosphate (di)	H_2HPO_4	0.167
Yeast Extract	N/A	0.150

Water contents at saturation, after gravity drainage and at various times during the clogging process were monitored with both vertical and horizontal TDR probes. Columns were weighed with each TDR measurement to perform a mass balance. At the end of the experiment, the two columns were dismantled into 8 soil sections to determine a more detailed water content profile with depth using the gravimetric method (Figure 3.7). The average water content of the entire column each time a TDR measurement was performed was back determined by adding up the column weight loss at each step to the water content at the end of the experiment.

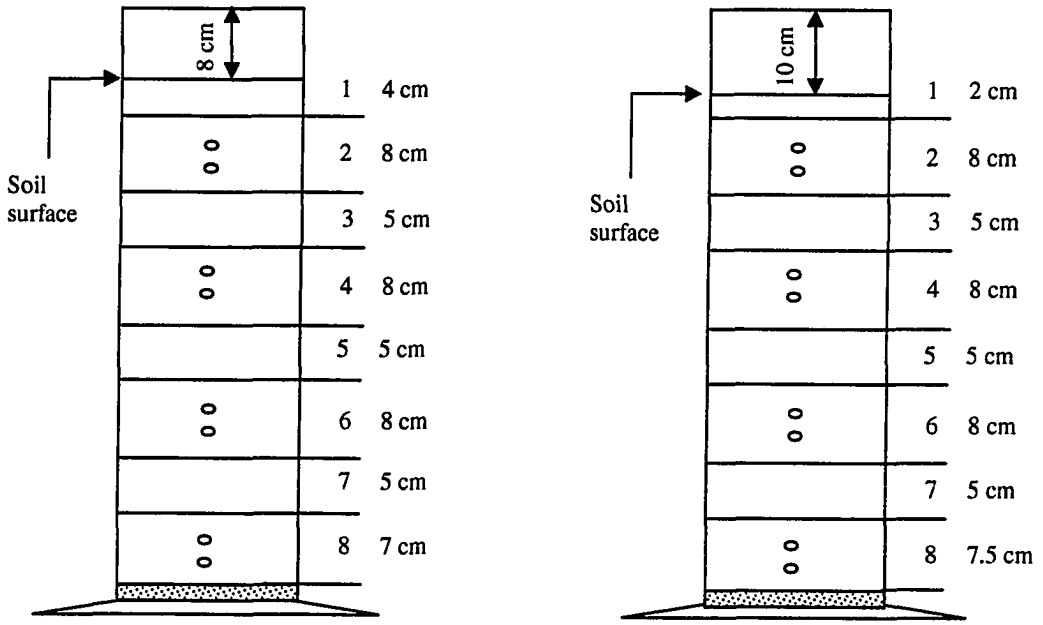

a. Dismantlement of column A *b. Dismantlement of column B*

Figure 3.7: Illustration of dismantlement of the two columns at the end of the clogging process

CHAPTER 4: RESULTS AND DISCUSSION

4.1 CHARACTERIZATION OF SPHAGNUM PEAT

4.1.1 Physical and chemical properties of peat

It is important to characterize peat before conducting experiments on it because the properties of peat are highly variable. Characterization of the peat will allow comparison of experimental results under study with those from different sources.

Shibchurn (2001) characterized the sphagnum peat used in this research. The chemical and physical properties of peat from her results are summarized in Table 4.1. The sphagnum peat examined was characterized as fibric, low ash content and highly acidic according to ASTM standards (Table 4.2).

Table 4.1: Chemical and physical properties of peat (S.D.: standard deviation)

Parameter	Ash content %	Organic content %	Fiber Content %	pH in distilled water	pH in 0.01M $CaCl_2$
Average	1.1	98.9	83.5	4.0	3.2
S.D.	0.15	0.15	2.6	0.006	0.006

Table 4.2: Classification of peat according to ASTM D4427-92 (Shibchurn, 2001)

Parameter	Ash Content	Fiber Content	pH in H_2O	pH in $CaCl_2$
Average Value	1.1%	83.5%	4.0	3.2
Classification Criteria	<5%	>67%	<4.5	<4.5
Classification [ASTM D4427-92]	Low Ash Content	Fibric, H1-H3 von Post Scale	Highly Acidic	Highly Acidic

4.1.2 The soil moisture curve of peat

The main drainage curve of the peat under study was evaluated by pressure cell method in 6 cells with bulk density ranging from 102 to 141 Kg/m^3 (Figure 4.1). Because air bubbles were found in the drainage ports of cell 3 and cell 4, the soil moisture curves observed did not follow the right trend with bulk density as what Shibchurn (2001) observed. As lower bulk density means larger pore sizes, water should drain out of the peat soil easier and peat of higher bulk density should have a larger water retention capacity. Cell 1 with the lowest bulk density (102 Kg/m^3) had the largest decreases in moisture content as the suction was increased and resulted in the lowest soil moisture curve. As the density increases, one would expect the change in moisture content to decrease in response to a change in suction since the pores are smaller. As a result, the elevation of the soil moisture curve increases as density increases. Cells 8, 11 and 5 of higher bulk densities (122-126 Kg/m^3) followed this trend. The soil moisture curves for cell 3 (bulk density 132 Kg/m^3) and 4 (bulk density 141 Kg/m^3) fell in between cell 1, 8, 11 and 5, which was not expected because the soil moisture curve for the densest sample should be the highest.

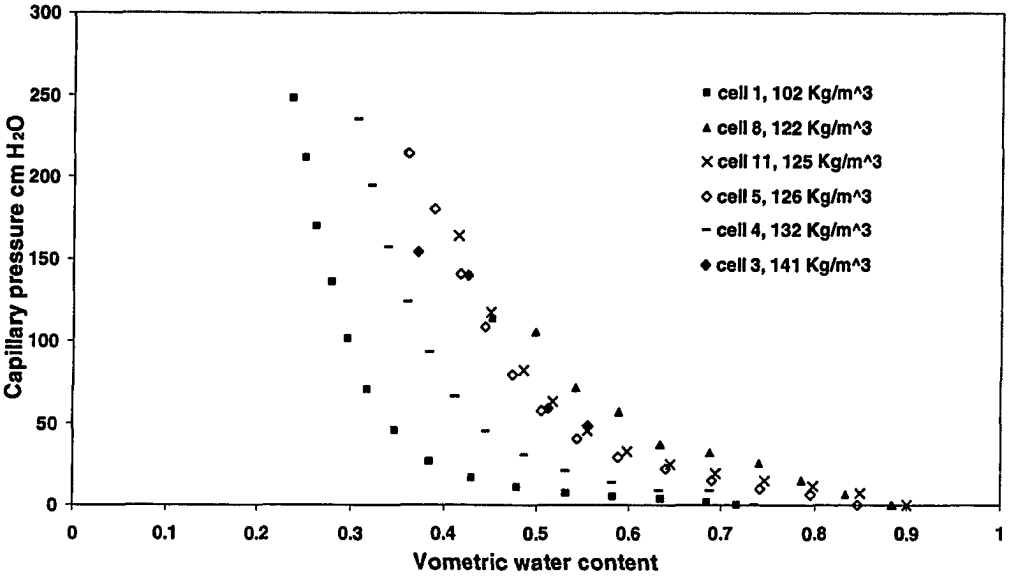

Figure 4.1: Drainage curves obtained in six cells with various bulk densities

Data obtained from cells 1, 11 and 5 are used to compare soil moisture curves of the peat under study with those from the literature (Figure 4.2). Da Silva et al. (1993) reported that at 2.5 KPa (25.5 cm of H_2O) suction, the sphagnum peat (bulk density 68 Kg/m^3, porosity 0.956) contained 50 % water and at 12 KPa (122.5 cm of H_2O) the peat still contained more than 20 % water by volume. Kennedy et al. (1998) observed similar results on the peat she was working on (bulk density 118.8 Kg/m^3, porosity 0.85). However, this was not the case in this study. At a similar bulk density of 125 Kg/m^3, cell 11 and 5 gave volumetric water contents 60 % at suction 25.5 cm H_2O and 43 % at suction 122.5 cm H_2O. These results are similar to the water retention results reported by Shibchurn (2001) on the sphagnum peat of the same source (bulk density of 112 Kg/m^3, porosity 0.90, 43 % at 122.5 cm H_2O and 60 % at 25.5 cm H_2O).

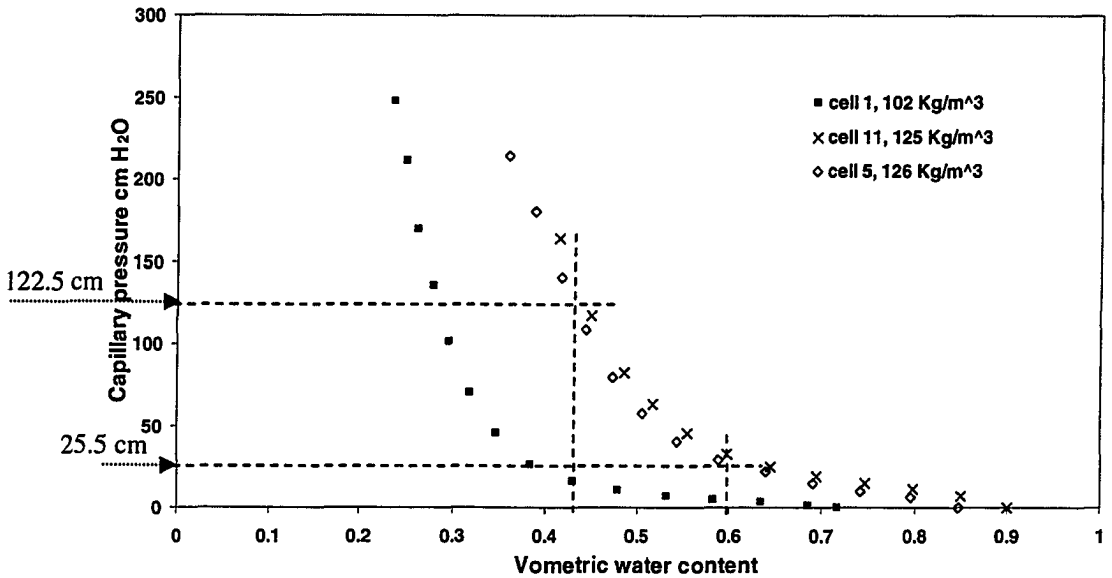

Figure 4.2: Moisture curves of cell 1, 11 and 5

4.2 RESULTS FOR K_a-Θ_v CALIBRATION RELATIONSHIP

4.2.1 Calibration of the start point and probe length

The calibration of the reference start point and effective probe length for the 15 cm horizontal probe was performed in a pressure cell. Waveforms of air and water were measured with the 15 cm probe horizontally inserted into the cell and plotted in Figure 4.3. The waveforms in air and water are coincident during the initial portion of the trace where the signal was traveling in the coaxial cable, the probe head and the rubber grommets through the cell wall. The waveforms began to separate at a later time due to different substances in the pressure cell. The point where air and water waveforms separate is where the signal started to travel inside the cell and therefore this point was taken as the reference start point. Figure 4.3 shows the calibrated start point on the

waveforms of air and water in a cell measured by the 15 cm horizontal TDR probe with a 6.5 m long coaxial cable.

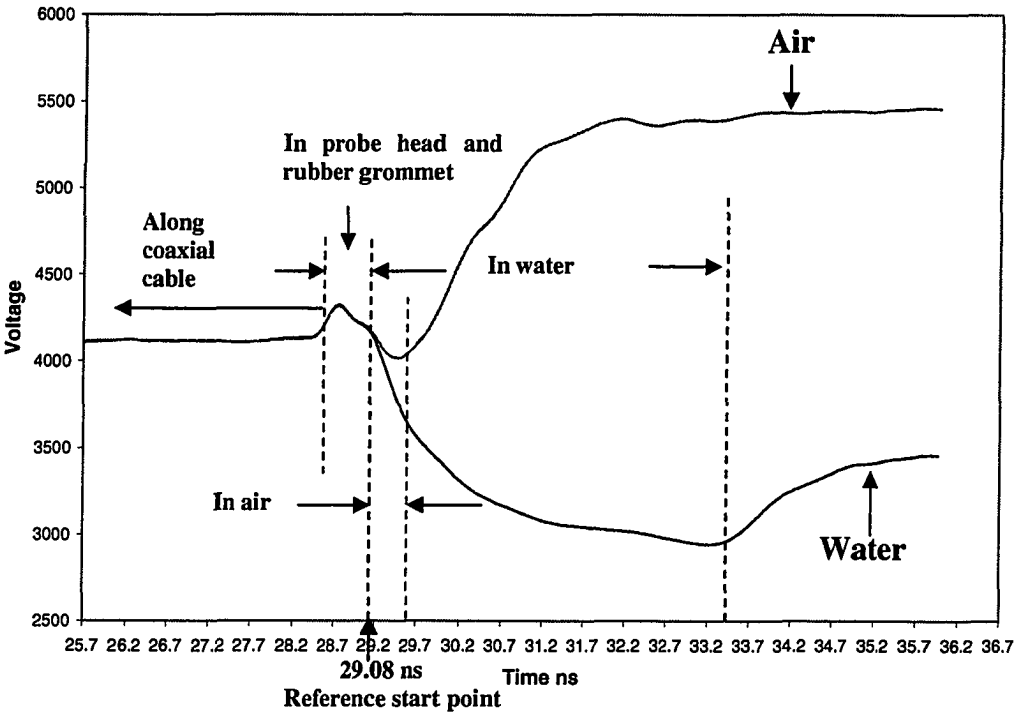

Figure 4.3: Reference start point for the 15 cm horizontal probe in a pressure cell

The waveform in water was analyzed based on the reference start point. The theoretical K_a of water at 21°C was used to determine the probe length (equation 3.2). A 14.2 cm probe length had the best performance of predicting a K_a value of 79.75 for water at 21°C (adjusted by equation 3.3 at a specific temperature). Figure 4.4 presents the waveform analysis to determine K_a of water based 14.2 cm probe lengths.

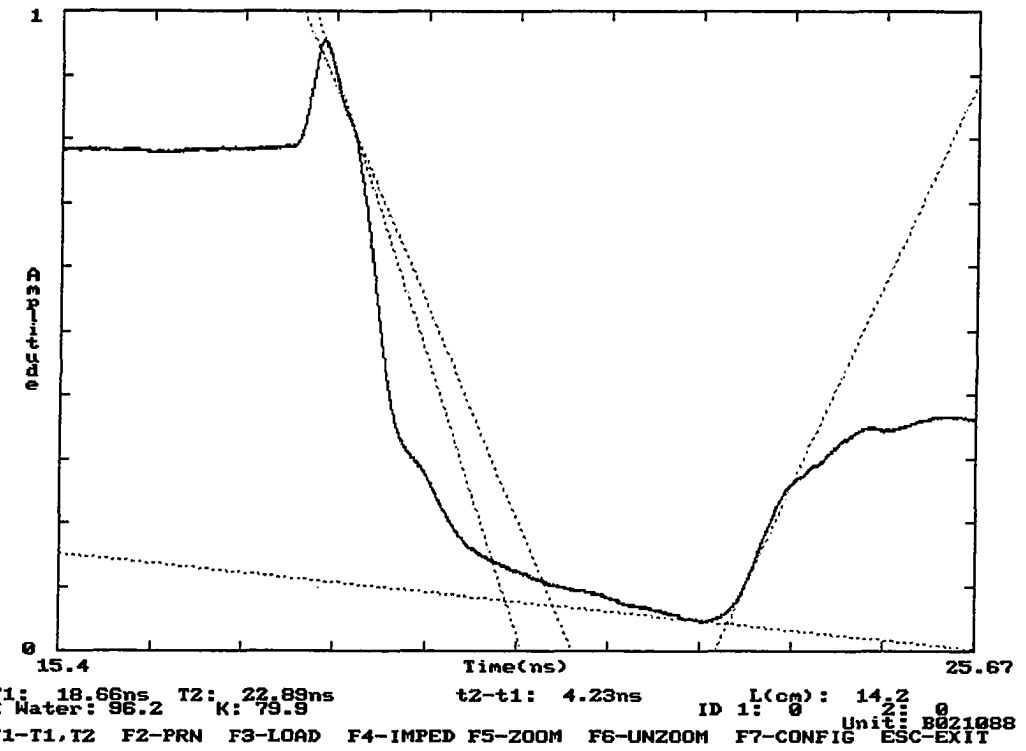

Figure 4.4: Waveform analysis of water based on 14.2 cm probe length

To verify the probe length determined, new waveforms in water and air in a pressure cell were measured with TDR and K_a values were analyzed based on the 14.2 cm probe length. The resulting K_a values were compared with the theoretical values of water and air by one-sample t-test. Results were summarized in Table 4.3 and Table 4.4.

Table 4.3: K_a values of air and water evaluated by 14.2 cm probe length

	1	2	3	4	5	6	7	8	Ave.	S.D.
Water	79.9	79.6	80.5	80.7	79.6	80.2	80	79.7	80.025	0.4132
Air	0.9	0.8	0.8	0.9	1	0.9	1.1	1	0.925	0.1035

Table 4.4: Summary of one-sample t-test on measured K_a values of water and air, significance level α=0.05

	Average K_a	Theoretical K_a (21°C)	S.D.	S.E	Statistical t^*	Critical $t_{\alpha/2}^*$	Signific -ance
Water	80.025	79.75	0.4132	0.146	1.8825	2.365	NS
Air	0.925	1	0.1035	0.037	2.04939	2.365	NS

** t ratio was calculated by the following equation: t=(Sample Mean-Population Mean)/(Sample SD/(SQRT(Sample Size))), where the theoretical K_a was taken as the population mean

** According to the significance level and the degree of freedom of the sample, critical t value was found in Table 4 in "Introduction to Probability &Statistics" (Mendenhall et. al., 1999)

** $t_{\alpha/2}$ was used for the two-tail test

Both measured K_a values of air and water showed no significant difference from the theoretical values. Therefore 14.2 cm probe length was used to analyze the waveforms obtained in the pressure cells using the 15 cm horizontal probe.

To determine the start and end points on each waveform and consequently the signal travel time, tangent lines were manually fit to the waveforms in WATTDR. The accuracy of determining the travel time is therefore dependent on the operator's experience.

4.2.2 K_a-θ_v calibration curve

The K_a- θ_v calibration relationship was generated by the modified pressure cell method with the 15 cm TDR probe horizontally inserted in the peat. Figure 4.5 presents the calibration data from 8 pressure cells with a bulk density ranging from 102 to 141 Kg/m^3.

It can be seen from Figure 4.5 that data points cover water content range from 24.4% to 91.2% and fall into two main groups. Six cells (1, 5, 7, 8, 9, and 11) are clustered to form a family group, while cell 3 and 4 are clustered as well but at a lower position. The maximum discrepancy of water contents between the two groups was over

10%. And the discrepancy became smaller at lower water contents (<40%).

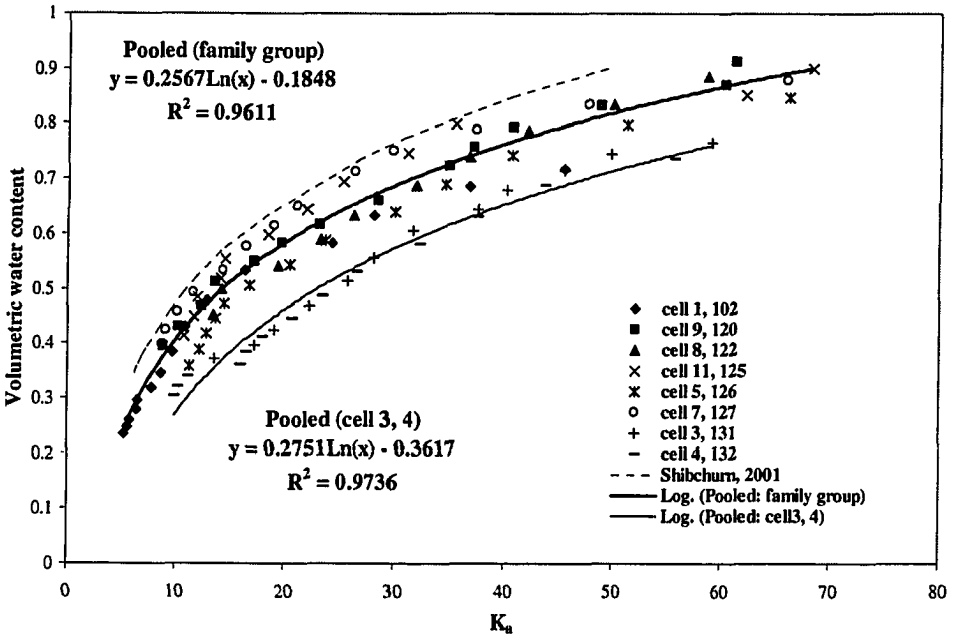

Figure 4.5: K_a-θ_v calibration results for 8 cells and best-fit curves for the pooled data

Best-fit curves were fit to each cell individually and then to the pooled data of the two groups. Polynomials and logarithmic regression types were considered. Although third-degree polynomials have been used in most calibration functions in the literature (Topp et al., 1980; Roth et al., 1992; Jacobsen and Schjonning, 1993), logarithmic was chosen in this study because of a higher coefficient of determination (R^2) and smaller residue standard deviation (S_r). A summary of the best-fit curve functions for individual cells, as well as for pooled data of the two groups and Shibchurn's calibration function of the same peat was presented in Table 4.5.

Table 4.5: Parameters for the calibration curves: θ_v=aLn(K_a)+b

Cells	a	b	R^2	S_r (Θ_v)
Cell 1	0.2305	-0.1408	0.9913	0.0161
Cell 5	0.2708	-0.2727	0.9935	0.0135
Cell 7	0.246	-0.1131	0.9876	0.0186
Cell 9	0.2583	-0.1787	0.9927	0.015
Cell 8	0.2878	-0.2973	0.9907	0.015
Cell 11	0.2513	-0.1425	0.9707	0.029
Pooled	**0.2567**	**-0.1848**	**0.9611**	**0.0353**
Cell 3	0.3018	-0.4488	0.9852	0.0169
Cell 4	0.2551	-0.3036	0.9713	0.025
Pooled (3, 4)	**0.2751**	**-0.3671**	**0.9736**	**0.0244**
Shibchurn (2001)	0.2667	-0.1405	0.9564	N/A

**The goodness of curve fit is indicated by the Coefficient of Determination (R^2) and Residue Standard Deviation (S_r) of Θ_v

** Residue Standard Deviation (S_r) was calculated by $S_{res}=\sqrt{\frac{\sum(Y_{observed}-Y_{predicted})^2}{df}}$, where $Y_{observed}$ are water content values determined gravimetrically and $Y_{predicted}$ are the calculated water contents by the calibration equation.

It can be seen from Table 4.5 that all calibration equations have very similar slopes, but different intercepts. The coefficients of determination are high (R^2>0.9611); residue standard deviations were low (S_r<0.0353), indicating a very good correlation between K_a and θ_v. However, pooling all the data for the family group of six cells slightly decreased R^2 and increased the residue standard deviation.

At the same water content, a higher bulk density may result in a slightly higher dielectric constant due to a larger contribution from the solid phase to the bulk dielectric constant of the soil. However, an increase in the specific area associated with higher density and corresponding increase in bound water may result in a slight decrease in the dielectric constant. The balance between these two effects governs the variation of the dielectric constants with bulk densities and this variation is expected to be small. Topp et al. (1980) did not observe any effect of dry bulk density on the dielectric constant of

mineral soils over a bulk density range from $1.32X10^3$ to $1.44X10^3$ Kg/m^3. Shibchurn (2001), who worked on the sphagnum peat from the same source as in this research, did not see significant variation in the calibration data with a bulk density range of 108.98 – 152.7 Kg/m^3. Jacobsen and Schjonning (1993), however, reported higher dielectric constants at higher densities in a density range of 135-155 Kg/m^3. They found that the bulk density effect would not change the shape of the calibration curve but would only change the level. They also noted that at the same dielectric constant, the variation in water contents caused by different bulk densities was of the same magnitude as the standard deviation of the estimated water content (0.01). Ledieu et al. (1986) also observed the effect of bulk density on the calibration curve, and indicated that the effect was rather small compared with the measurement error.

In the case of this study, all of the calibration equations have similar slopes but different intercepts, which is in agreement with Jacobsen and Schjonning's observation of density effect. Cell 3 (bulk density 131Kg/m^3) and 4 (bulk density 132 Kg/m^3), which are located at a lower position in Figure 4.5, had the highest densities. At the same water content, K_a values measured from these two cells were higher than those from the others. However, no similar trend was found in other cells with bulk density ranging from 102 to 127 Kg/m^3. Hence, the density effect is rather small and should not, or should not solely, account for the deviations of the intercepts among different cells, especially not for a discrepancy as large as 10% between the two main groups.

The impact of packing on peat soil structure was also considered to explain the intercept deviations. The impact of soil structure on K_a values was tested by repacking

the same volume of peat of the same water content in a beaker 6 times. The resulting K_a values were summarized in Table 4.6.

Table 4.6: K_a values of peat measured in a beaker by repacking the same peat

Test	1	2	3	4	5	6	Average	S.D.
K_a	39.9	42.4	41.1	40.6	42.3	40	41.05	1.1

The K_a values measured for the 6 repacked peat samples are similar to each other with a standard deviation of 1.1. The repacking of peat should not account for the standard deviation solely because there was also error associated with measurement and waveform analysis. However, the soil structure does not appear to explain the differences between the two groups of data.

Evaporation was considered as another factor that might affect the calibration curve. Impact of evaporation was evaluated by weighing the pressure cell every time a TDR reading was taken. The weight loss of the cell was compared with the corresponding amount of water collected in the burette. The comparison result showed that evaporation did not have a significant impact on the calibration curve determined by the modified pressure cell method. The amount of water lost by evaporation during an entire experiment was approximately 1% on a volume basis.

What has caused the large discrepancy is still unknown. The calibration equation from the pooled data of the family group was used to calibrate the volumetric water contents in the analysis presented in the later sections.

$$\theta_v = 0.2567 * \mathrm{Ln}(K_a) - 0.1848 \qquad (4.1)$$

Where θ_v: the volumetric water content of the soil

K_a: the dielectric constant of the soil

Equation (4.1) estimates water contents ranging from 24.4 to 91.2 % for peat with a standard deviation of 0.0353. This water content range covers the optimum moisture content range (40-60 %) for biofilters.

The calibration curve obtained from equation 4.1 was extrapolated up to the θ_v value 1.0 and down to the θ_v value 0 (Figure 4.6). At 0 water content, a K_a value of 2 was observed. The K_a value is consistent with the K_a of dry organic matter or dry peat reported by other researchers (Pepin et al., 1992: 2.0 for dry peat; Topp et al., 1980: 2.5 for dry organic soil; Myllys et al., 1996: 2.8 for dry peat; Roth et al., 1990: 5.0 for dry peat). However, the extrapolation gave a K_a value over 90 for θ_v value 1.0, much higher than the dielectric constant of free water at 21 °C (79. 75). Although the water content range from 95 to 100 % does not represent true situation as the water content can not be higher than the total porosity, the very high K_a value obtained at the assumed 100 % saturation is still a suspicion of error of the calibration curve.

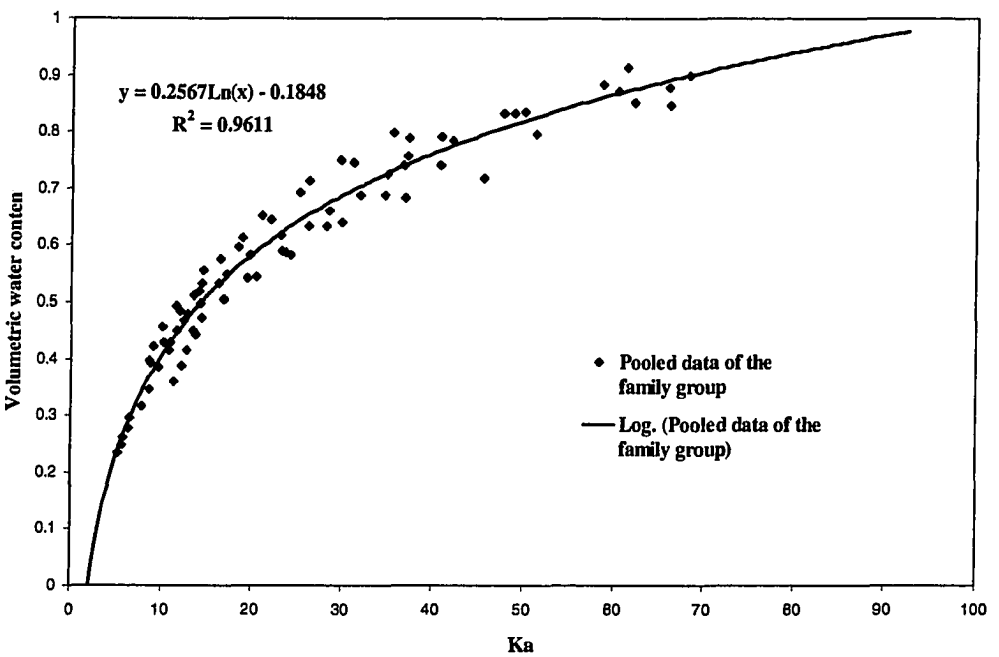

Figure 4.6: Extrapolation of the calibration curve

4.2.3 Comparison of the calibration curve to the literature

The K_a-θ_v calibration curve from the pooled data of the family group was plotted with those of organic soils and peat from the literature for comparison (Figure 4.7). The calibration curve generated in this study lies at the upper edge of the calibration curves from the literature. The curve in this study calibrates lower water contents in wet soils (> 83 %) and higher water content in drier soils (<83 %).

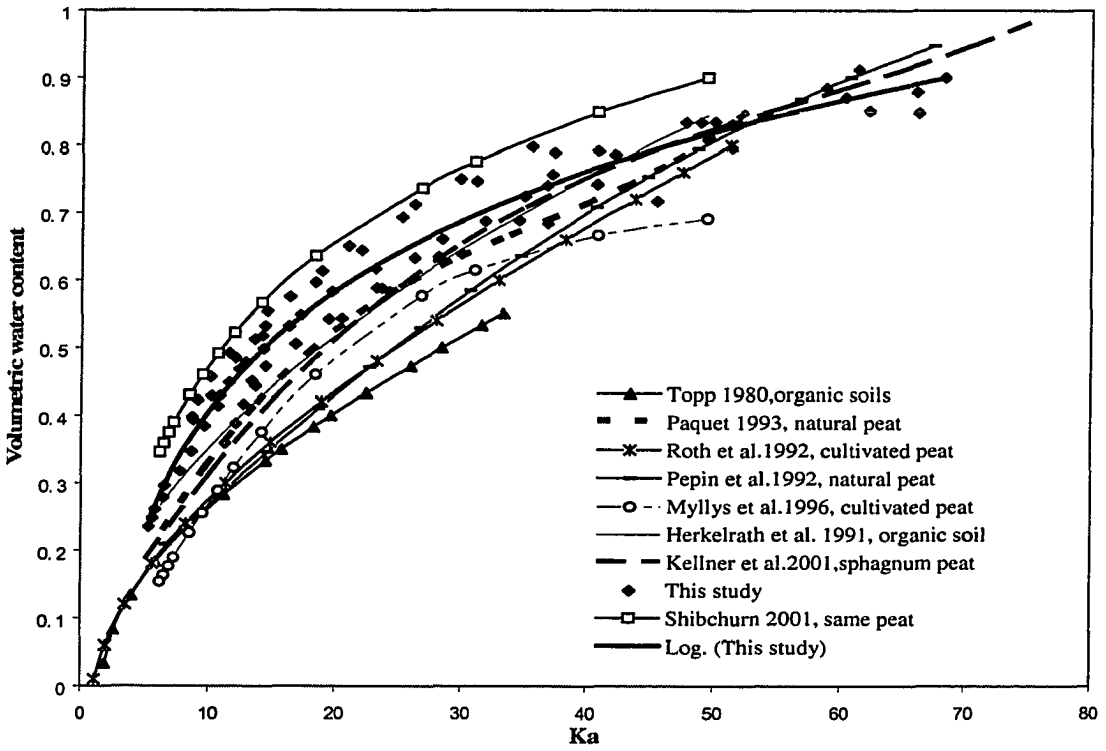

Figure 4.7: Comparison of the K_a-θ_v calibration curve in this study to the literature

The shape of the curve is similar to those of Shibchurn (2001) of milled sphagnum peat and Myllys (1996) of cultivated sphagnum peat. The curve under study has shifted approximately 7 % down from Shibchurn's relationship and 7 % up from Myllys' relationship. At water contents over 60 %, Myllys' curve levels off faster. The

sphagnum peat Myllys worked on had a low organic content organic content of 52 % and a very high bulk density of 400 Kg/m^3, both of which indicate a higher dielectric constant at the same water content. Shibchurn (2001) worked on sphagnum peat from the same source and used the same pressure cells to generate her calibration curve. There should not be much difference between her calibration curve and the calibration curve in this study. What has caused the discrepancy from Shibchurn's calibration is still not known.

There is a large deviation between the curve under study and that of Roth et al. (1992). However, Roth's curve was derived from a mix of cultivated peat at various degrees of decomposition and undecomposed oak leaves, which had a low organic content range of 10.5-54.8 % and a very high bulk density range of 220 -700 Kg/m^3. The high organic content (98.9 %) and lower bulk density (102- 141 Kg/m^3) of the peat in this study infers a lower dielectric constant at the same water content, which is a good explanation of the higher position of the calibration curve.

Both Pepin et al. (1992) and Kellner et al. (2001) worked on peat soils that had similar properties with the peat under study (Table 4.7). The calibration curve determined in this research is close to Kellner's curve with a slightly different slope. Pepin et al.'s curve (with the lowest bulk density) is surprisingly located at the lowest position, in disagreement with the explanation of density effect on dielectric constants. The bulk density effect being small is proven again here.

Table 4.7: Comparison of the peat under study to those of Pepin et al. and Kellner et al.

	Soil type	Organic content %	Degree of Decomposition von Post	Porosity	Bulk density Kg/m^3
Pepin et al. 1992	Undisturbed natural peat including sphagnum peat	74.7-98.6	H1- H6	0.826-0.95	64-248
Kellner et al. 2001	Undisturbed natural peat, dominantly sphagnum species	N/A	H2 - H4	0.95-0.97	29.1-66.2
This study	Disturbed sphagnum peat	98.9	H1-H3	0.91-0.93	102-141

Considering the possible factors that could affect the calibration curve, the first concern was the oven-drying temperature of peat at the end of the experiments. It is the gravimetric water content at the end of the experiment that fixes the position of the calibration curve since the water drained during each drainage step is added to this value to determine the moisture content. Hence, any error in determining this point will cause the entire curve to shift vertically in the plot of water content versus K_a. To determine the gravimetric water content at the end of the experiment, the peat was dried at 105°C. Some researchers working on peat preferred lower temperatures (65°C, Myllys et al., 1996; 65°C, Pepin et al., 1992; 70°C, Kellner et al., 2001) to prevent burning of any organic matter. If some organic matter was burned and attributed to water loss, then the actual water content would be lower than the water contents that were used to generate the calibration curve, which would shift the curve down without changing its shape. Peat samples were prepared and dried in the oven at 65 ° C, and then at 105°C. Little change of sample weight has been observed with different temperatures.

The second factor tested was the height of the pressure cell. Whalley (1993) reported that the soil located at a distance equal to twice or more the rod spacing has negligible effect on K_a. The spacing of the parallel rods used in this study was 2 cm and the cell height was 5.2 cm, which gives a reasonable sensitivity range for the TDR probe in theory. To test if the top and bottom aluminum caps located 2.6 cm from the probe affect the TDR readings, a pressure cell 10 cm in height and made of the same material was designed to generate two more sets of calibration data, the result was plotted with the calibration data of the 5.2 cm cell in Figure 4.8. The two sets of data from the 10 cm high cell fell into the range of the data from the 5.2 cm cells, which indicates that the top and bottom aluminum cap of the 5.2 cm cell did not affect the TDR readings.

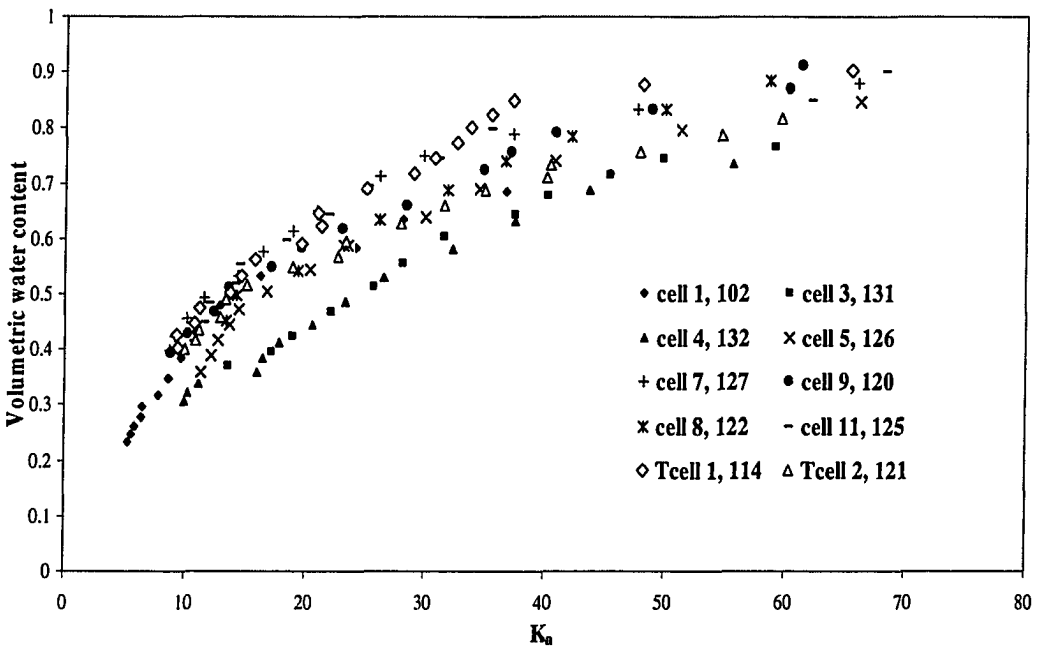

Figure 4.8: Comparison of the calibration data from 5.2 cm cells with 10 cm cells (Tcell 1, 2)

As indicated by Jacobsen and Schjonning (1994), the comparison between different laboratory calibrations doesn't necessarily tell how well the TDR performs. Some other more technical factors such as differences in measuring systems, probe configuration, length of coaxial cable and probe installation problems might influence the variation between the calibration curves. Temperature effect was also cited as one of the factors that could account for the difference between calibration curves obtained by different researchers.

4.3 PERFORMANCE OF THE GUIDE BLOCKS

Attention should be paid to vertical measurements using 81 cm parallel rods because longer probes result in variable separation distances due to their length. As outlined in section 3.5.2, thin plastic films were placed between each section of a sectional column to evaluate the variability in the separation distance (Figure 4.9).

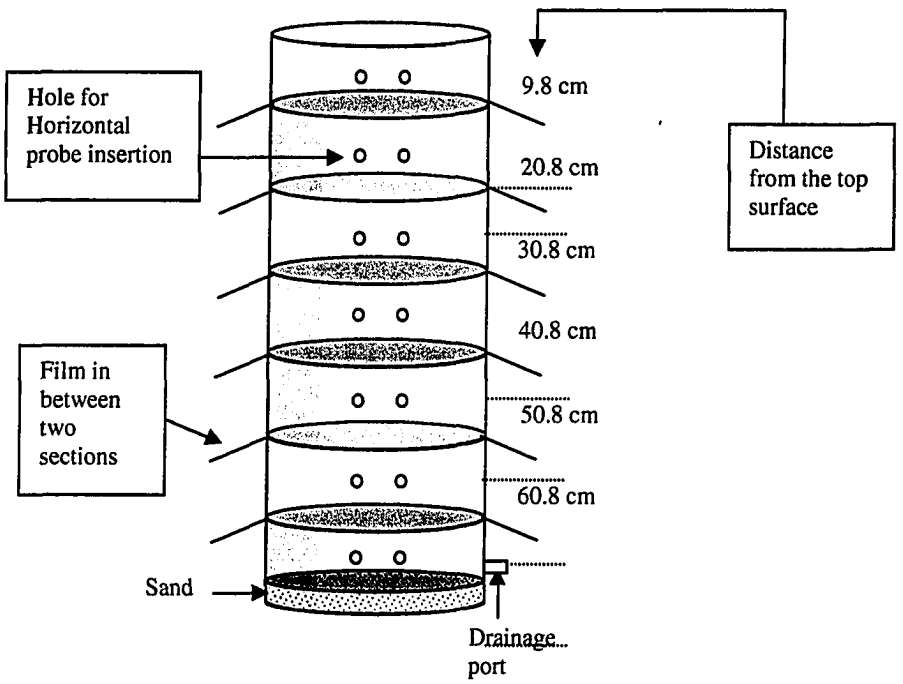

Figure 4.9: Locations of the thin films in the sectional Column

The column was packed with the same peat 8 times. K_a value of peat was measured by the vertical TDR probe each time and the distances between two holes on the thin films were recorded. The results were summarized in Table 4.8.

From Table 4.8, it can be seen that for the probe insertion starting with a rod separation of 2 cm at the top of the column, the guide blocks performed well except for test 8. Test 3 and 6, which started from a narrower separation, the performance of the guide blocks became worse. Therefore making sure that rods enter the soil with the right separation before the insertion is very important. All 8 tests gave very close K_a values, except test 6, which had a narrow (0.5 cm) rod separation at the end. No dependence of K_a values was observed on rod separation.

Table 4.8: Distances of the two holes on the films and K_a values measured in peat

Distance from the top cm	**Test number and probe separation on films cm**							
	1	**2**	**3**	**4**	**5**	**6**	**7**	**8**
9.8	2	2	1.5	2	2	1.5	2	2
20.8	2	2	1.5	2	2	1.5	1.5	2
30.8	2	2	1.5	2	1.5	1	1.5	3
40.8	2	2	1.5	2	1.5	1	1.2	4
50.8	2	2	2	1.8	1.5	1	1	5
60.8	2	1.5	3	1.7	1.5	0.5	0.5	6
K_a Measured	3.1	3.1	2.9	3	2.9	2.6	3	2.9
Average (K_a)	2.9375		**S.D. (K_a)**		0.1598	**S.E. (K_a)**		0.056

To evaluate the impact of potential changes in K_a due to inserting the probe multiple times, vertical measurements were taken in a peat column by inserting the probe for 6 times without repacking the soil. Results are presented in Table 4.9.

Table 4.9: Measured K_a values of peat in the same column

Measurement	1	2	3	4	5	6
K_a	56.2	56.6	57.1	57.3	56.6	57.3
Average	56.68	S.D.	0.685	S.E.	0.28	

It can be seen again in table 4.9, very close K_a values were obtained by inserting the vertical probe in the same column (without repacking the peat) for 6 times, which is in agreement with the results from the sectional column that the rod separation did not significantly affect TDR measurements.

The impact of different rod separations on TDR measurements was tested again in water. K_a values of water at 20°C were measured using the 81 cm probe with different rod separations at the end. Measured K_a values were compared with the theoretical value using a one sample t-test (Table 4.10).

Table 4.10: Measured K_a values of water with different rod separations and the result of one-sample t-test, significance level α=0.05

Separation at the end of the 81 cm probes cm	K_a
0.5	80.7
1	80.7
1.5	80.4
2	79.4
2.5	80.1
3	80.6
3.5	80
4	79.4
4.5	79.5
5	79.9
5.5	79.5
6	79.9
7	79.4
8	80
9	80.5
10	79.9

AveraAverage of K_a	79.99
Standard Deviation	0.4739
Standard Error	0.118
Theoretical K_a at 20°C	80.1
One sample t-test result	
Estimated t	0.8967
Critical $t_{\alpha/2}$	2.131
Significance	NS

One sample t-test results show no significance difference (at significance level α=0.05) between the measured K_a values and the theoretical K_a with rod separations ranging from 0.5cm to 10 cm, which is in agreement with the results in peat. This does not support the conclusions drawn by Davis (1975) that the parallel pair rods do not have to be completely parallel but a large discrepancy should be avoided. Topp et al. (1980) did not observe any difference in the water content measurements between the 1.05 m vertical probes that were installed with or without pilot holes. They used parallel rods 12.7 mm in diameter, which is quite large, and up to 1 m in length for a corn field application and stated that it was unnecessary to use pilot holes for the vertical installations if rods of smaller diameter are used, which is in agreement with the results in this study.

For vertical insertion in the steel columns using the 81 cm probe, concern arose if the two rods were touching each other or the separation was so wide that the rods were in contact with the metal wall of the column. These phenomena should give short-circuited waveforms like the one shown in Figure 2.10 in the Literature Review. The special shape of the short-circuited waveform is very easy to recognize and was not encountered in the TDR measurements.

The accuracy of probe length was an important factor that affected the accuracy of TDR readings. For example, in the K_a measurement of water in a bucket, the water level a bit lower than the 27.5 cm or a bit higher did make a recognizable difference on the K_a values because a 27.5 cm length was used to analyze the waveforms. Special care was needed to accurately control the probe length inserted in soil to eliminate this

operating error. In this research, 14.5, 27.5, 40.5, 50 cm from the end of the probe were marked on the steel rods using a permanent marker before the insertion.

4.4 COMPARISON OF DIFFERENT METHODS FOR WATER CONTENT MEASUREMENT

4.4.1 Calibration of the start point and probe length

Horizontal TDR measurements in the steel columns had the same setup as in the pressure cells that were used to determine the calibration curve. Hence, the reference start point and rod length calibrated for the pressure cell were also used for the horizontally measured waveforms in the columns.

As expected, start points on the waveforms measured by the vertical probe were easier to identify than those measured by the horizontal probe because there was an obvious impedance change at the air-soil interface. Figure 4.10 presents waveforms taken by the 81 cm vertical probe with 14.5 cm inserted in water and peat. The time when the signal enters the peat (or water) occurs when the two waveforms split just prior to the large voltage drop and this point was considered as the reference start point. Waveforms taken with 14.5, 27.5, 40.5, 50 cm of the 81 cm probe inserted in water were plotted in Figure 4.11 and the reference start points for the corresponding lengths were indicated.

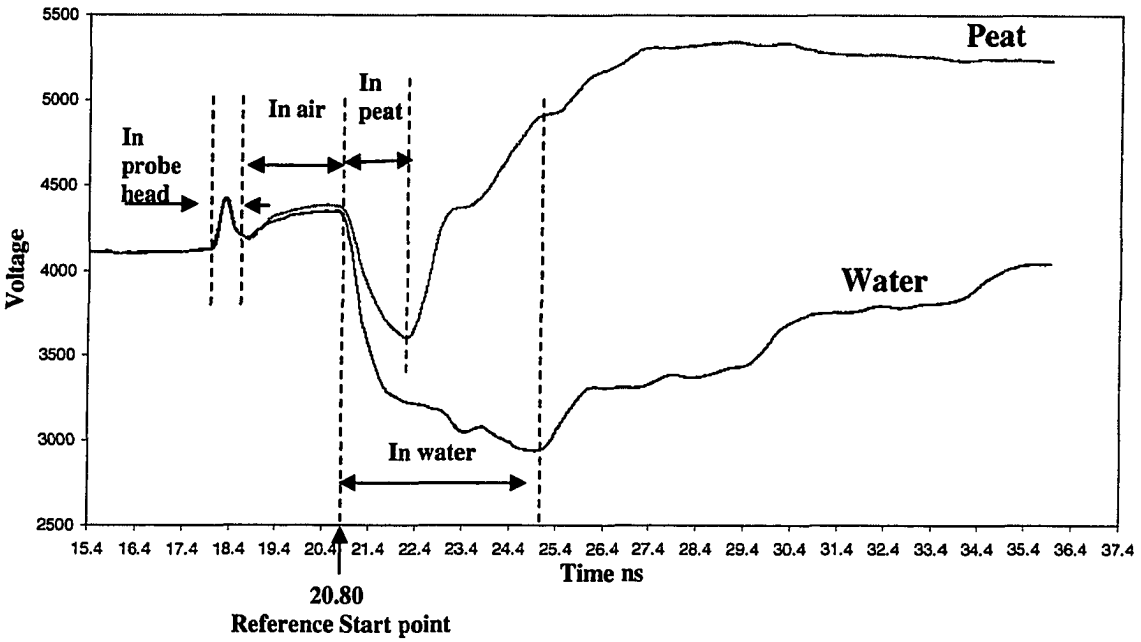

Figure 4.10: Reference start point on the waveform taken by the 81 cm vertical probe with 14.5 cm inserted in water and peat

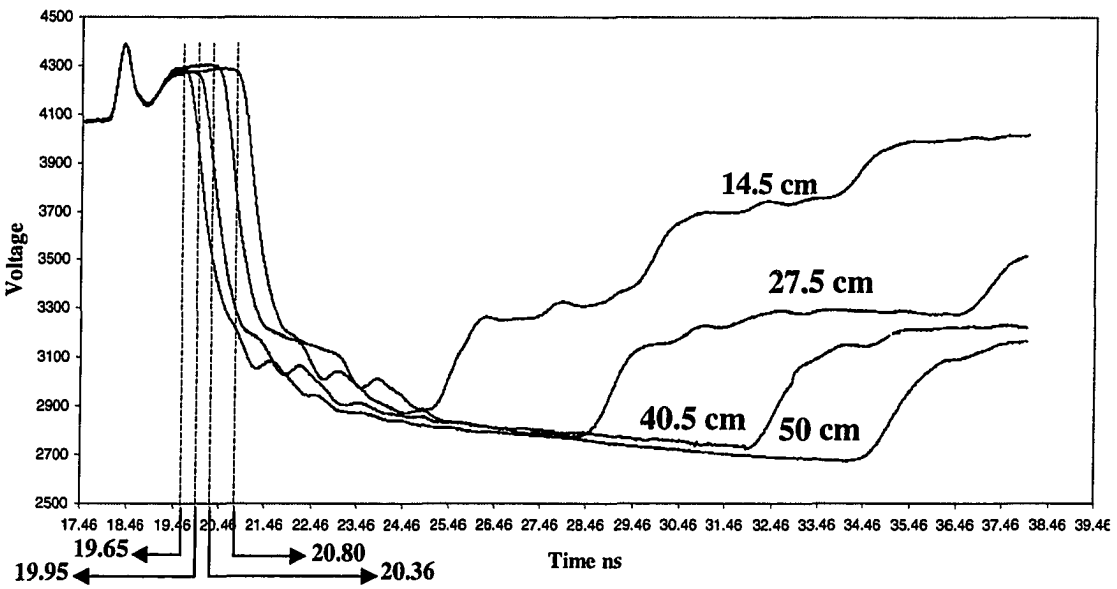

Figure 4.11: Reference start points on waveforms taken by the 81 cm vertical probe with 14.5, 27.5, 40.5 and 50 cm inserted in water

To verify the start points determined, new waveforms were taken using the 81 cm probe with the 4 different lengths inserted in water at 20°C (theoretical K_a=80.1). The actual probe lengths inserted in water were used to analyze the K_a values. Measured K_a values were compared with the theoretical K_a value of water using a one sample t-test. The results were presented in Table 4.11.

Table 4.11: One-sample t-test for comparison of K_a values of water measured by the vertical probe with the theoretical value, significance level α=0.05

Length of Probes cm	K_a measured		Length of Probes inserted in water cm		K_a measured	
14.5	80.8		40.5		80	
14.5	79.1		40.5		80.5	
14.5	79.6		40.5		80.6	
27.5	81		50		80.9	
27.5	80.5		50		80.6	
27.5	80.2		50		80.7	
One sample t-test results	Ave.	S.D.	S.E.	Statistical t	Critical $t_{\alpha/2}$	Significance
	80.375	0.563	0.1624	1.693	2.201	NS

The one-sample t-test result indicates that there was no significant difference (at significance level 0.05) between the theoretical value and the K_a values analyzed based on the reference start point and actual probe length inserted in water. Therefore the determined start points and actual probe lengths were used to analyze the vertically measured waveforms in the columns.

4.4.2 Comparison of water contents determined by different methods

The experiment to compare the horizontal TDR, vertical TDR and gravimetric water contents took place in 6 peat columns during a sequential drainage process. Peat soil in the column was divided into 4 sections as illustrated in Figure 3.6 in section 3.6.1.

Average water contents for the four sections (with midpoint elevations: 6, 19, 32, 45 cm from the bottom of the column) were determined both vertically and horizontally by TDR at each measuring point during drainage. Gravimetric water contents were measured at the end of the experiments by oven-drying the wet peat. In addition, the soil moisture curve (the main drainage curve) was evaluated to characterize the sphagnum peat under study.

Water contents in the 6 columns determined by the vertical and horizontal TDR probes were plotted in Figure 4.12 for comparison. Figure 4.12 showed a reasonable 1:1 correspondence between the water contents measured by the vertical and horizontal probes. The best fit line has a slope of 0.973 and a small intercept 0.0121, with a correlation coefficient 0.9349. The standard deviation from the 1:1 line is 0.047. The water contents measured by the vertical probe were both above and below those determined by the horizontal probe. Other researchers have also observed this scatter phenomena with their experimental data measured with vertical and horizontal TDR probes for different kind of soils (Jones and Friedman, 2000; Wang and Schmugge, 1980). Nadler et al. (2002) suggested that the alternating deviations were caused by the averaging process, which may be the source of scatter in this research as well.

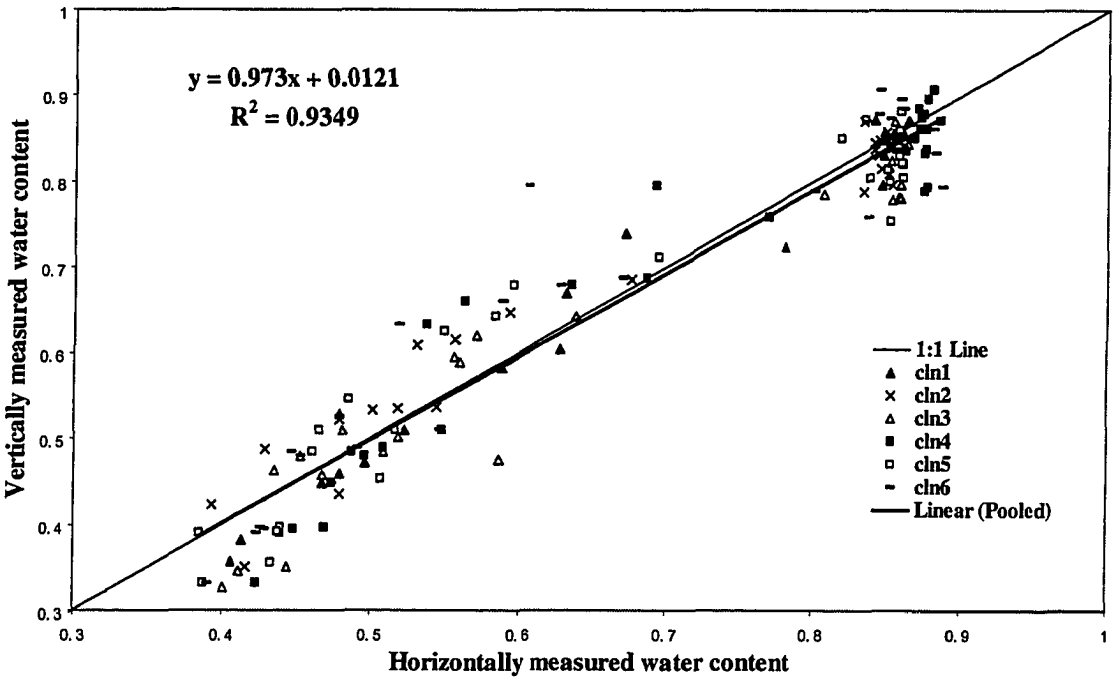

Figure 4.12: Comparison of water contents measured by the vertical TDR probe with those determined by the horizontal probe in six columns

A two-tail paired t-test was performed and the result showed that there was no significant difference between the vertical and horizontal methods at significance level of 0.05 (Table 4.12).

Table 4.12: Paired t-test (two-tail) results of water contents measured by the vertical probe with those determined by the horizontal probe in six columns

n	Mean (Θ_v- Θ_h)	S. D.	S. E.	Statistical t	Critical $t_{\alpha/2}$	P	Signifi -cance
60	0.0064	0.047	0.0037	1.73	1.975	0.0848	NS

** n: number of paired observations, S.D.: standard deviation of differences, S.E.: standard error of differences
**Θ_h, water content determined by the horizontal probe
**Θ_v, water content determined by the vertical probe

Gravimetric sampling for each section of the column was only possible at the end of the experiments. Gravimetric water contents at saturation and after each drainage step could be only obtained as the average of the entire column since the column was weighed

initially and after each drainage step. TDR determined average water contents in the column were calculated by averaging the water contents in the four sections. Average water contents in the columns determined by the vertical and horizontal TDR probes were plotted in Figure 4.13.

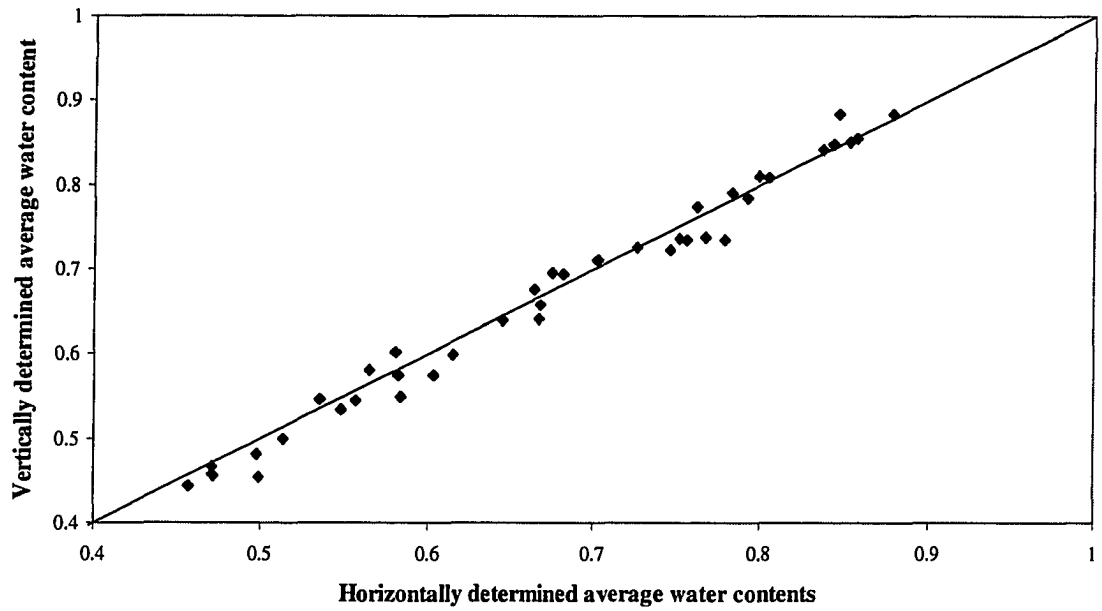

Figure 4.13: Comparison of TDR measured water content with the gravimetric water content in six columns

It can be seen from Figure 4.13 that the data points are highly clustered along the 1:1 line. The vertical and horizontal average water contents showed a much better agreement over a water content range of 40-85% than the water contents determined by the TDR probes in the four individual sections (a residue standard deviation 0.019 from the 1:1 line for the average compared with 0.0476 for the individual). The larger variation in the four individual soil sections might be due to the redistribution of water in the columns and error associated with the averaging.

The accuracy of water content measurement using horizontal TDR probes has been demonstrated by many researchers. The hypothesis that horizontal and vertical TDR probes give similar results was verified both theoretically and experimentally (Topp et al., 1980; Ferret et al., 1996; Baker and spaans, 1994; Young et al., 1997 a, b). Topp et al. (1980) used vertical TDR probes as long as 1 meter and stated that the difference between the water contents measured by vertical and horizontal TDR probes was always $< 0.03\ cm^3cm^{-3}$. The comparison results in this study are in agreement with the literature.

However, there is a discrepancy between the TDR measured water contents and those determined gravimetrically. TDR measured average water contents in the columns were plotted with those determined gravimetrically in Figure 4.14.

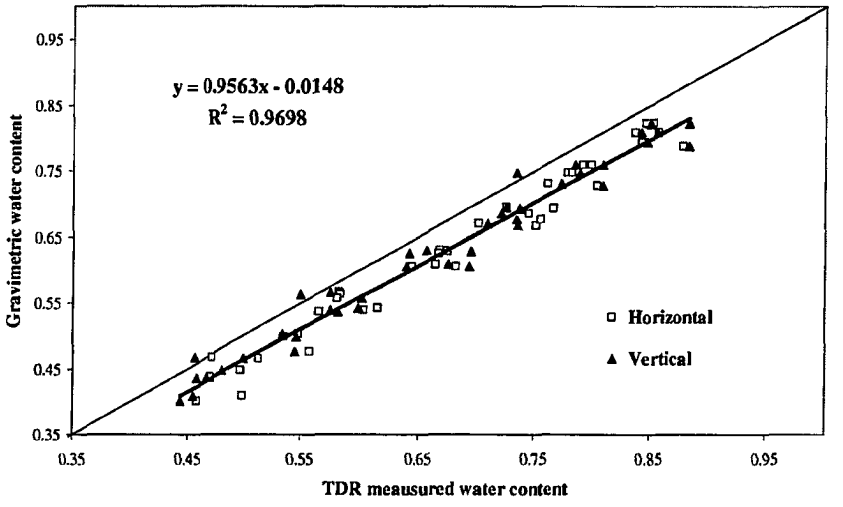

Figure 4.14: Comparison of the TDR measured average water content with the gravimetric in six columns

TDR gave higher water content values than the gravimetric method. In Figure 4.14, most of the data points were located below the 1:1 line. And the best fit line is

almost parallel to the 1:1 line (slope=0.9563), which indicates that the discrepancies for all the points in a water content range of 40-90% are very consistent. The mean of the difference between the TDR measured and gravimetric water contents is 0.044 with a standard deviation of 0.023. This indicated that the discrepancy might be caused by systematic errors. Recall that the calibration curve generated in this study was above the others noted in the literature (Figure 4.7). For the same K_a value, the calibration function determined in this study resulted in a higher water content. The calibration curve generated by Shibchurn (2001) on the same peat using the same method was located at a even higher position (approximately 0.07 above the curve under study). The uncertainty of the calibration curve might have caused the overestimation of water contents by TDR.

The statistical analysis of the comparison of TDR measured water contents to the gravimetric water contents is presented in Table 4.13. The similar means and standard deviations of the measurement differences between the TDR and gravimetric water contents indicated the horizontal and vertical TDR measurements were consistently higher than the gravimetric values.

Table 4.13: Paired t-test (two-tail) results for comparison of TDR water content with the gravimetric water content in six columns

	n	Mean	S. D	S. E	Stat. t	Critical t	Significance
$\Theta_h - \Theta_g$	40	0.047	0.022	0.0034	13.7	2.02	S
$\Theta_v - \Theta_g$	40	0.041	0.024	0.0038	10.8	2.02	S
$\Theta_{TDR} - \Theta_g$	80	0.044	0.023	0.0026	17.13	1.99	S

**Θ_h, water content determined by the horizontal probe
**Θ_v, water content determined by the vertical probe
**Θ_g, water content determined by the gravimetric method
**Θ_{TDR}, pooled data of Θ_v and Θ_h

4.4.3 Moisture profiles with depth

Figures 4.15, 4.16, 4.17 show the moisture profiles with depth determined both vertically and horizontally by TDR in 3 columns: at saturation and after each of the 5 drainage steps. The other 3 columns had similar results and are presented in Appendix B. All of the columns had similar bulk densities ranging from 101 Kg/m^3 to 109 Kg/m^3, which was reflected by the similar moisture profiles (85-90%) at saturation.

The vertical and horizontal probes gave comparable values. No dependence on measuring method was observed. At saturation, water contents were quite uniform along the column while after gravity drainage, water contents increased with depth.

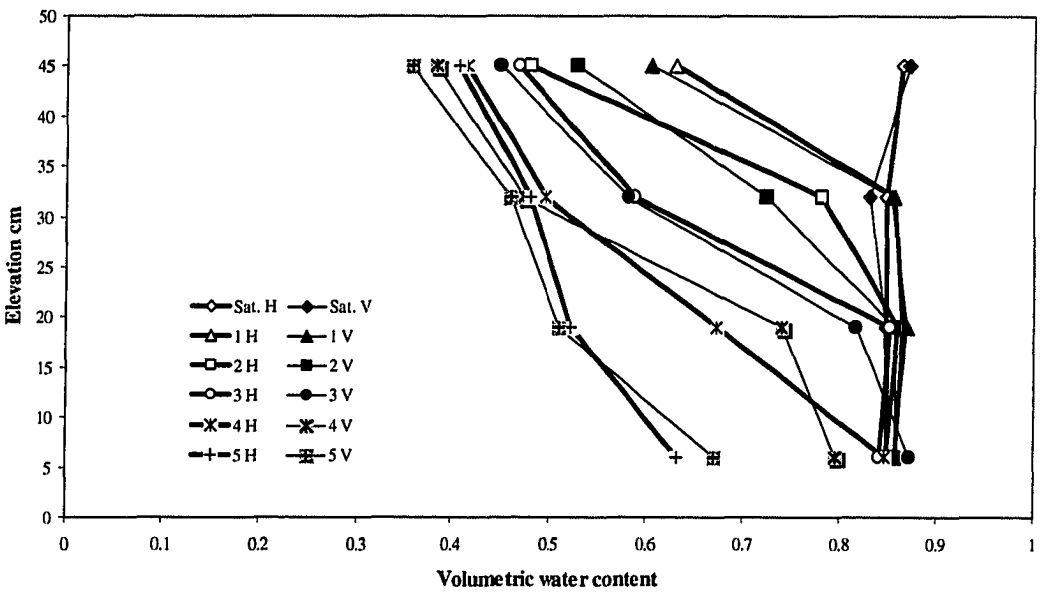

Figure 4.15: Water content profiles with depth during a drainage process in column 1 (bulk density: 107 Kg/m^3)

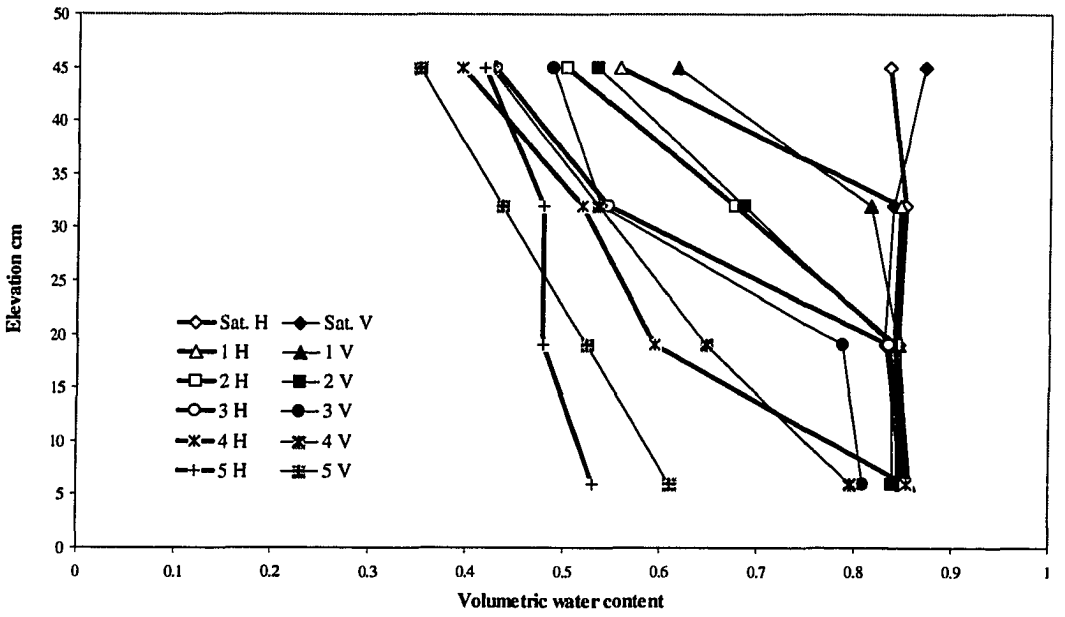

Figure 4.16: Water content profiles with depth during a drainage process in column 2 (bulk density: 107.5 Kg/m^3)

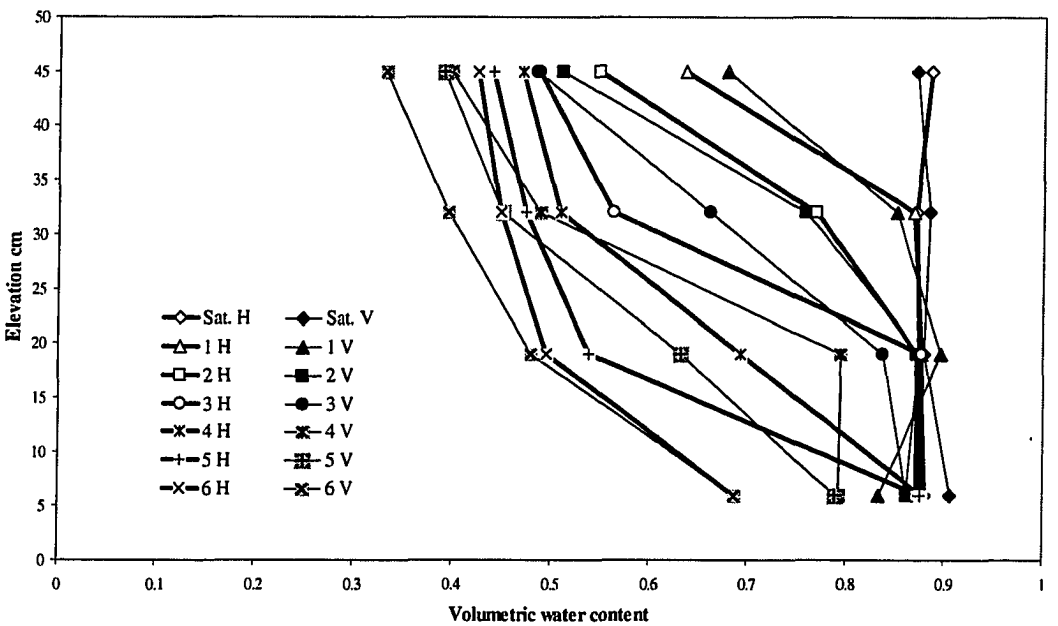

Figure 4.17: Water content profiles with depth during a drainage process in column 4 (bulk density: 102 Kg/m^3)

At the end of the experiment, water contents in the four sections were determined by the gravimetric method. Moisture profiles at the end of the experiments determined by both TDR and the gravimetric method were plotted in Figure 4.18.

It can be seen in Figure 4.18 that the vertical and horizontal TDR probes gave comparable measurements. TDR estimated higher water contents than the gravimetric method. However, the deviation of the TDR determined water contents from those determined by the gravimetric method is not consistent as observed earlier in Figure 4.14 for the average water contents of the entire column. Water contents in the four soil sections were averaged to obtain the average water content in each column at the end of the experiment. And the average water contents determined by TDR and the gravimetric method were plotted in Figure 4.19.

The average water contents at the end of the experiments followed the same trend as in Figure 4.14. The average water contents determined by TDR were higher than those determined by the gravimetric method and the deviation is quite consistent. The mean of the difference between the TDR measured and gravimetric water contents is 0.036 with a standard deviation of 0.025, similar to the magnitude determined in Figure 4.14 for all the data points. The deviation between the TDR water contents and the gravimetric in the individual sections may have been caused by the redistribution of the water in the column and the measurement error associated with dismantling the columns.

The first factor that might have affected the distribution of water in the column was the disturbance of soil structure when collecting the sample. When the columns were dismantled, the peat still had a relatively high water content (approximately from 33 % at the top soil section up to 86 % at the bottom), disturbance of the soil structure when

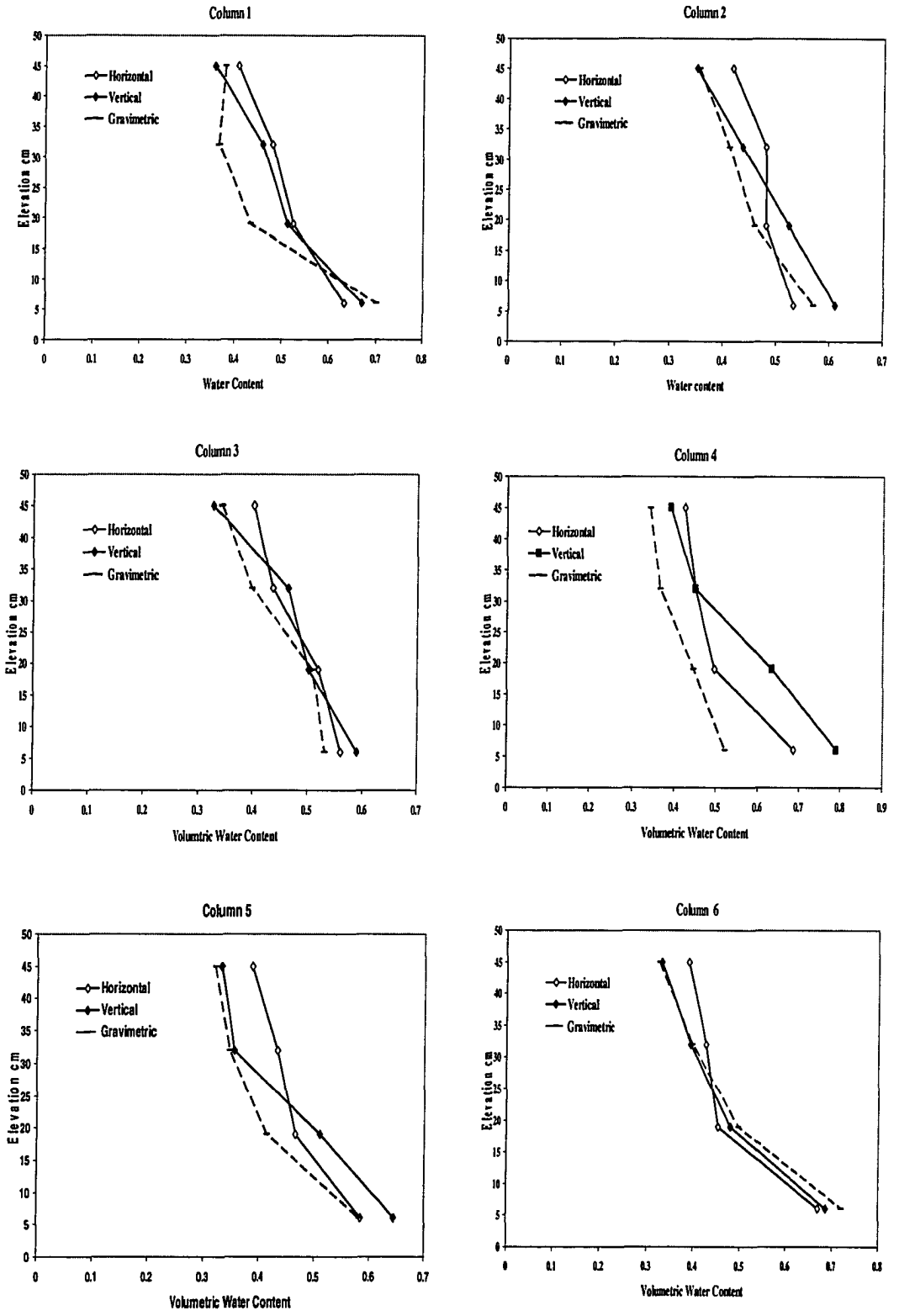

Figure 4.18: Comparison of water content profiles with depth determined by TDR and the gravimetric method at the end of the experiment in six columns

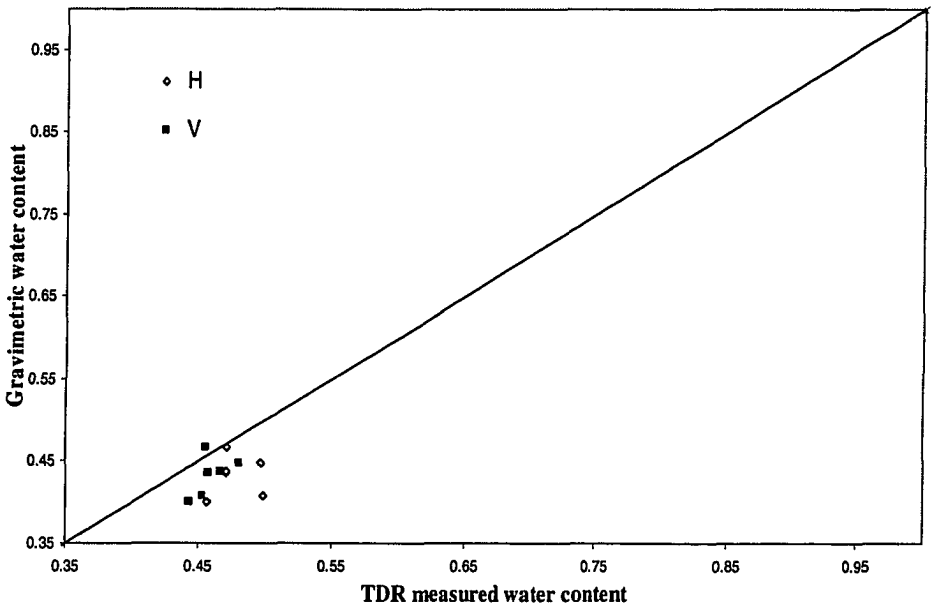

Figure 4.19: Average water contents at the end of the experiment determined by TDR and the gravimetric method

taking the peat out section by section may have caused a portion of the water to drain to the lower sections, which explains the relatively higher water content at the bottom.

Difficulties of identifying when equilibrium was reached after drainage increased the measurement error associated with water distribution as well. After drainage, TDR readings were taken after two hours to let the water redistribute in the column. It was hard to determine when equilibrium was reached. The deviations might be created when the equilibrium was not actually reached, and therefore water contents in the column were actually changing during the measurement process.

4.5 EFFECT OF VERTICAL TDR PROBE ON FLOW RATE

The flow rate test was performed in five columns used by a parallel project. The five columns were pulsed twice a day (9 am and 3 pm) with similar loadings as in this research and the outflow with time from the columns in response to a pulse was recorded

by a scale connected to a computer via an RS232 port. Water content in each column was measured by the 81 cm vertical TDR probe at 2 pm prior to the afternoon pulse. The outflow rate for the afternoon pulse right after the water content measurement using the vertical TDR probe and the outflow rate of an afternoon pulse two weeks later, during which time the TDR probe was not inserted, were compared. Flow rates before the vertical probe measurement (morning pulse), after the vertical probe measurement (afternoon pulse at the same day) and after two weeks are presented in Figures 4.20-4.24 for comparison. Bulk densities of the columns varied and are noted for each column.

Column 2: 115 Kg/m^3

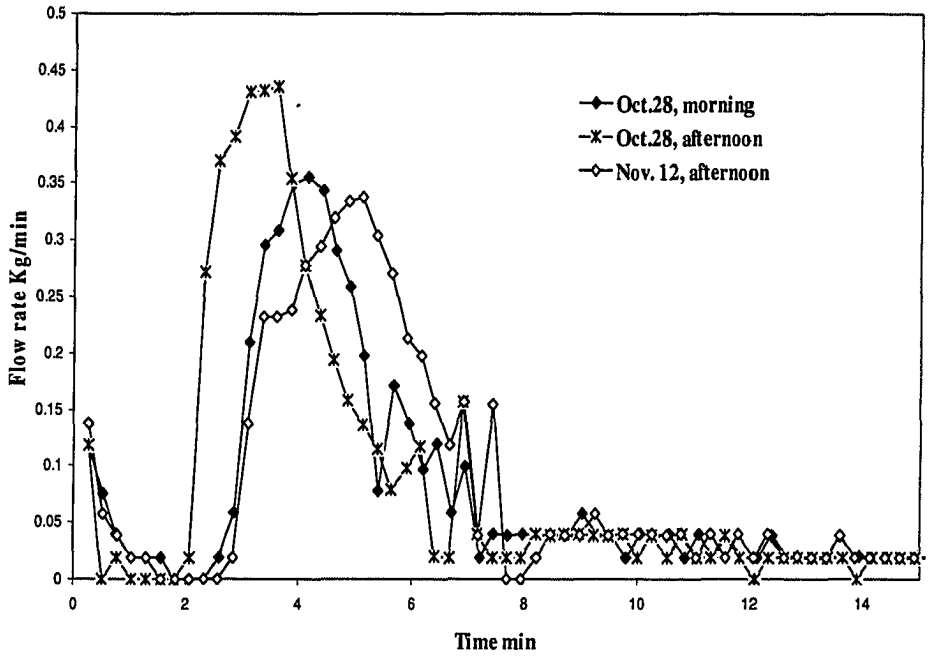

Figure 4.20: Impact of vertical probe on flow rate: column 2

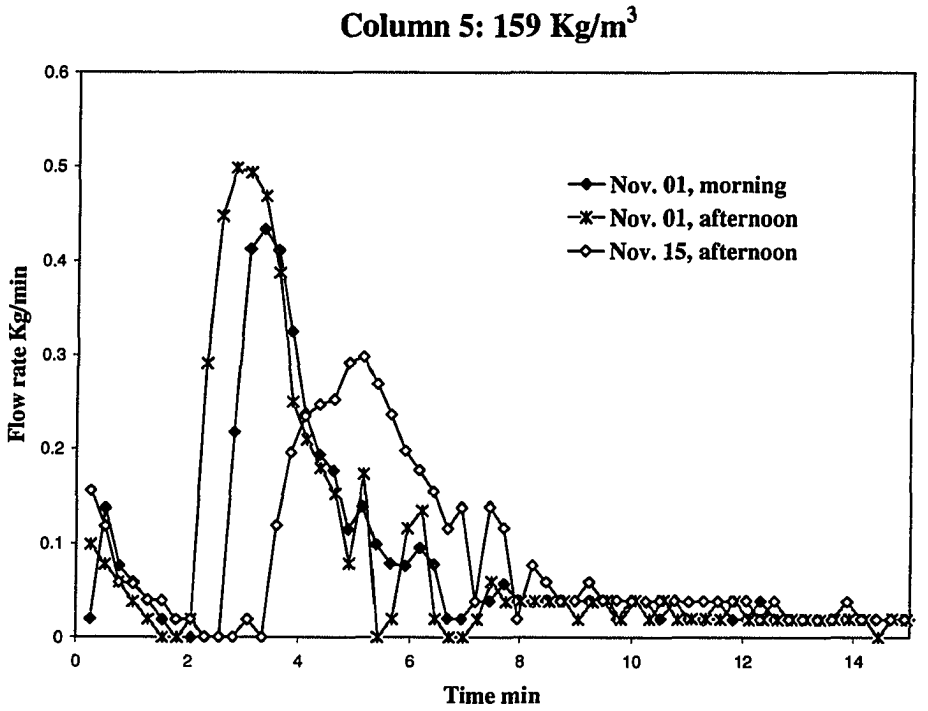

Figure 4.21: Impact of vertical probe flow rate: column 5

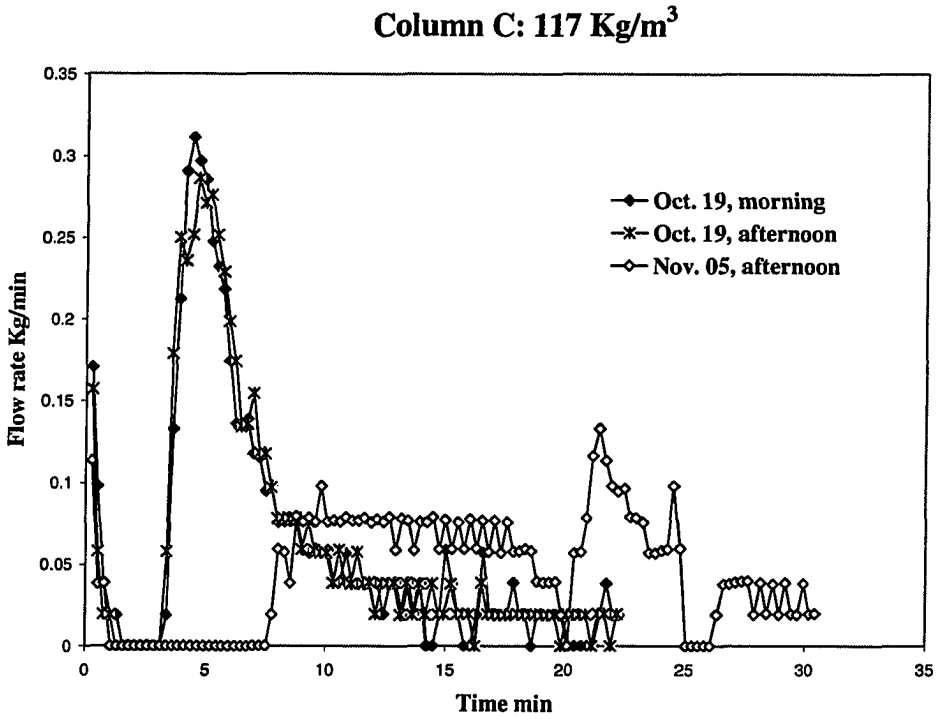

Figure 4.22: Impact of vertical probe on flow rate: column C

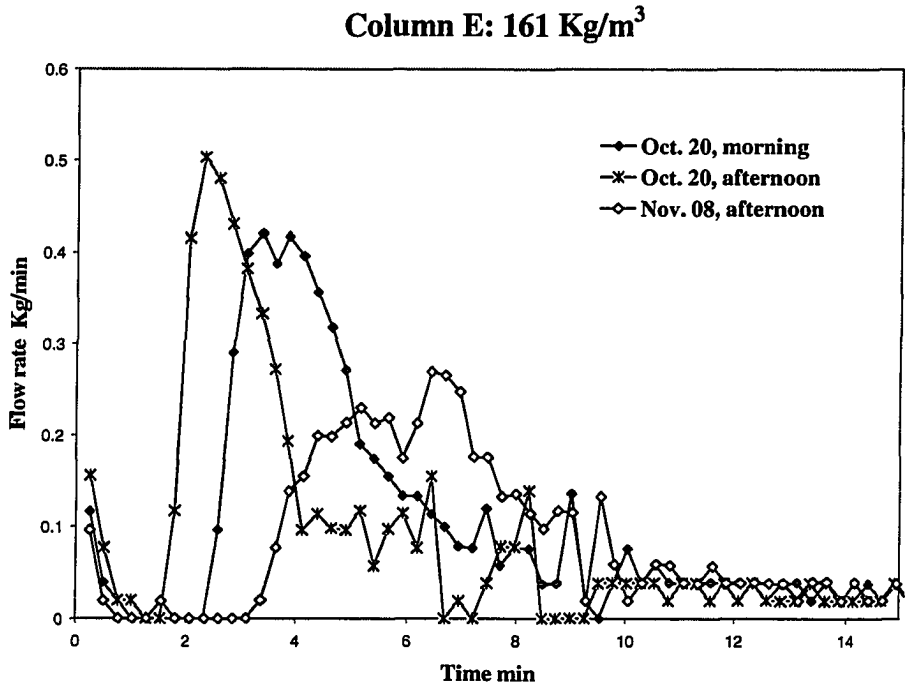

Figure 4.23: Impact of vertical probe flow rate: column E

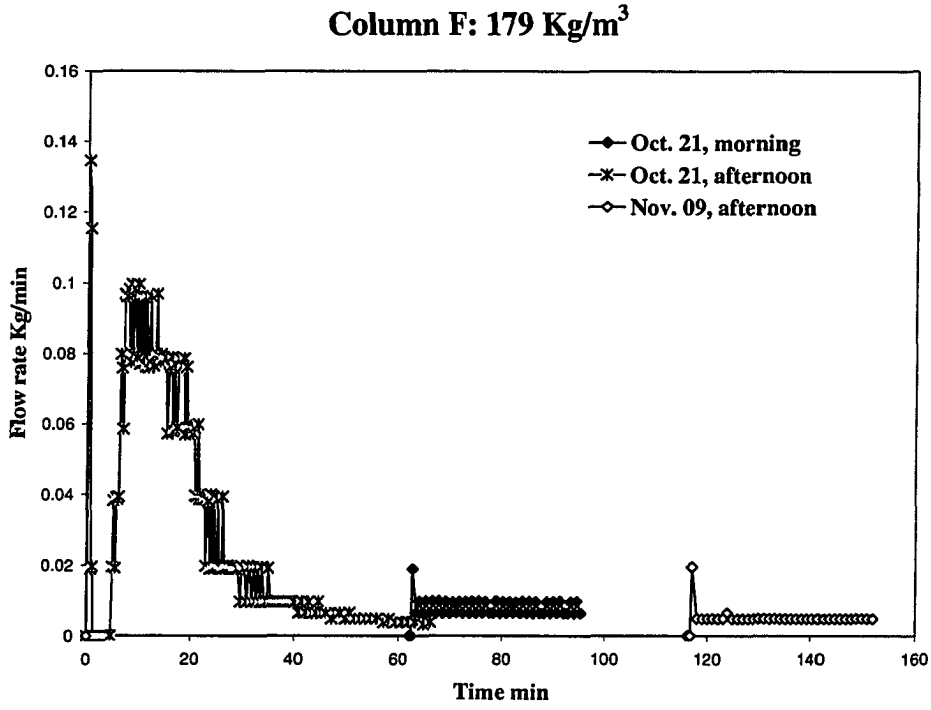

Figure 4.24: Impact of vertical probe on flow rate: column F

It can be seen from Figure 4.20-24, the vertical probe insertion did affect the flow rate of the peat columns right after the vertical probe removal. The peak values of the flow rate increased and arrived earlier for all the columns except column C, which had a lower bulk density (117 Kg/m^3). However, there was an impact on column 2, which had a similar bulk density (115 Kg/m^3) as column C. For column F, which had the highest bulk density (179 Kg/m^3), the impact was larger. The peak of the flow rate moved from 60 minutes (0.02 Kg/min) to 15 minutes (0.1 Kg/min). The flow rate changes on the other four columns (bulk density range 115-161 Kg/m^3) were small. However, it should be noticed that the flow rates for the morning and afternoon pulses may be slightly different since the morning pulse had a longer time to drain, 18 hours in comparison to 6 hours for the afternoon pulse.

After two weeks, the flow rates for all columns did not indicate any residual impact due to the vertical TDR probe and in fact, a lower flow rate and later time to reach the peak was observed as these columns were pulsed with a suspended and/or dissolved organic loading to cause clogging. The moisture content measurement in peat filters operating in the field will not be performed frequently, and hence, the disturbance from the vertical TDR probe should not be a concern.

4.6 IMPACT OF MICROORGANISMS ON TDR MEASUREMENTS

Two steel columns were packed with presaturated peat, gravity drained and pulsed with high organic loading twice a day. Peat soil in the columns clogged gradually due to microbial growth. Water contents were monitored by both the horizontal and vertical TDR probes during the process, and by the gravimetric method at the end of the

experiment. The water contents determined by the different methods were compared, the moisture profiles with depth were generated and the impact of biomass on TDR readings was evaluated.

4.6.1 TDR signal attenuation and difficulties of identifying the end points

For water content measurements using the vertical TDR probe in the clogging columns, difficulties were encountered to identify the end points on the waveforms, and this phenomenon was more obvious with longer probes. Figure 4.25 presents the waveforms taken with the 15 cm horizontal probe and Figure 4.26 through 4.28 present the waveforms taken with the 81 cm vertical probe in column A at different stages of the clogging process. Column A was packed with saturated peat and gravity drained. The waveform recorded on Aug. 11 was taken after the gravity drainage prior to pulsing with an organic load and the others at various times during the clogging process.

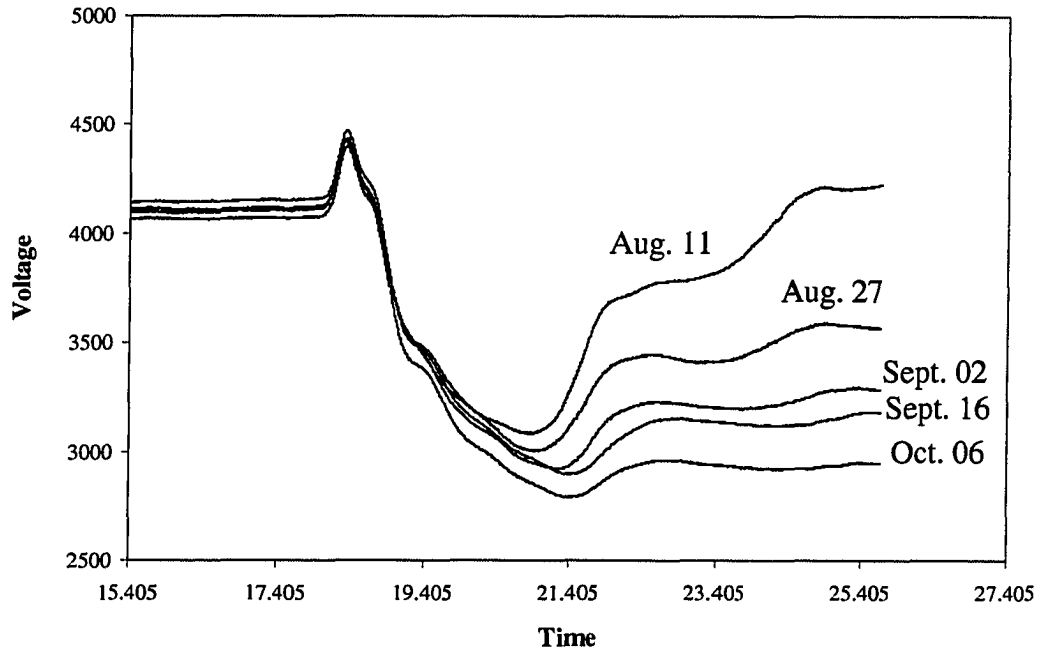

Figure 4.25: Waveforms during clogging in column A taken by the 15 cm horizontal TDR probe (bottom port)

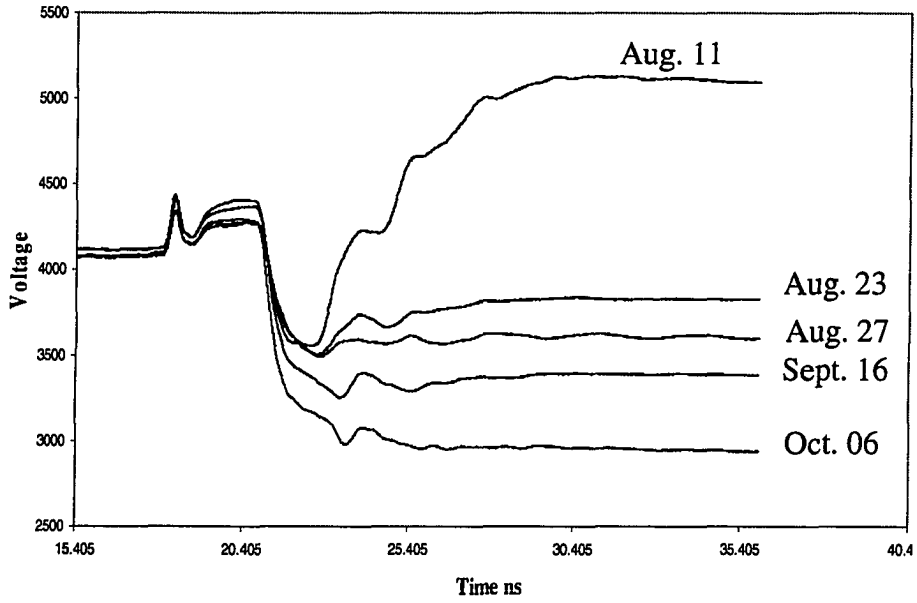

Figure 2.26: Waveforms during clogging in column A taken by the 81 cm vertical probe with 14.5 cm inserted in peat

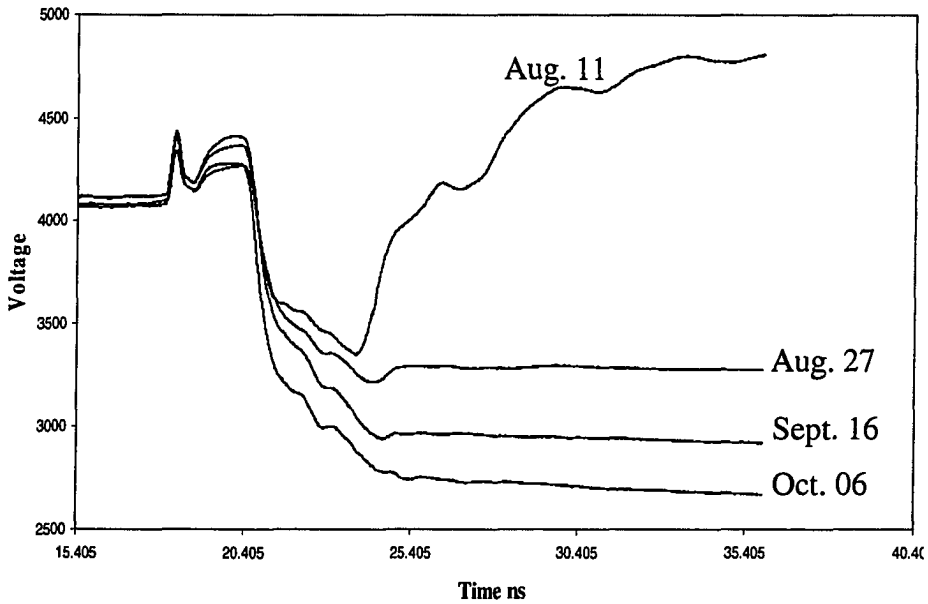

Figure 2.27: Waveforms during clogging in column A taken by the 81 cm vertical probe with 27.5 cm inserted in peat

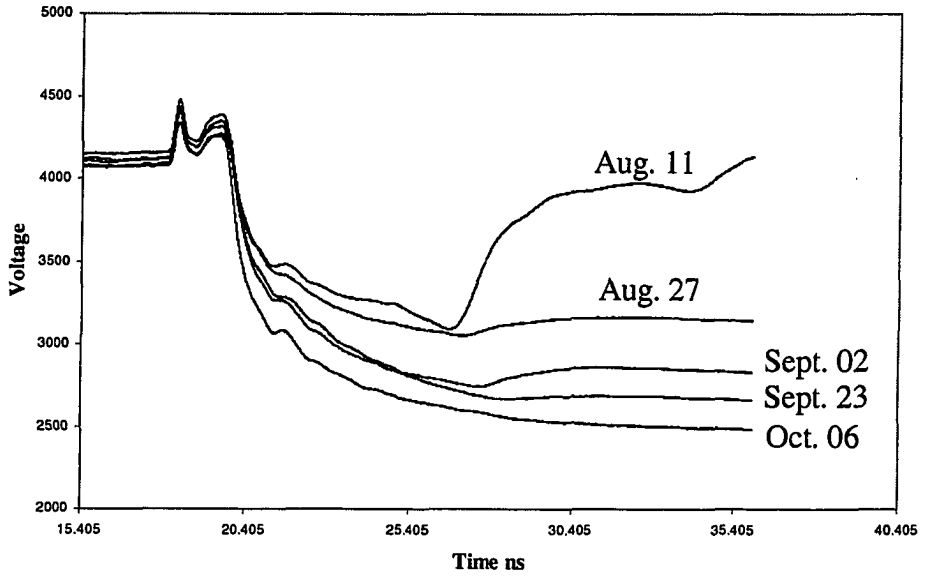

Figure 2.28: Waveforms during clogging in column A taken by the 81 cm vertical probe with 50 cm inserted in peat

It can be clearly seen from all the waveforms that water content increased as the microbial growth increased in the column. As the clogging process continued, the signal was attenuated and the end reflection points flattened out. There was an increased attenuation effect on the waveforms obtained by longer probes. On Oct. 06, the end points on the waveforms from the 15 cm horizontal and 14.5 cm vertical probes could still be identified while the end points on the waveforms from the 27.5 cm and longer probes could not be identified. According to the horizontal measurements, the average water content along the 27.5 cm vertical probe on Oct. 06 was approximately 64 % in column A. And in column B, the average water content was found to be 66 % for the 27.5 cm probe to lose the end point refection.

Several reasons were considered to explain the attenuation. The first factor considered was the increased water contents in the columns with the advance of clogging. Waveforms measured with 14.5, 27.5, 40.5, 50 cm of the 81 cm vertical probe inserted in

pure water, in saturated and gravity drained peat columns (water saturated, no biomass involved) were presented in Figure 4.29 and 4.30 for comparison.

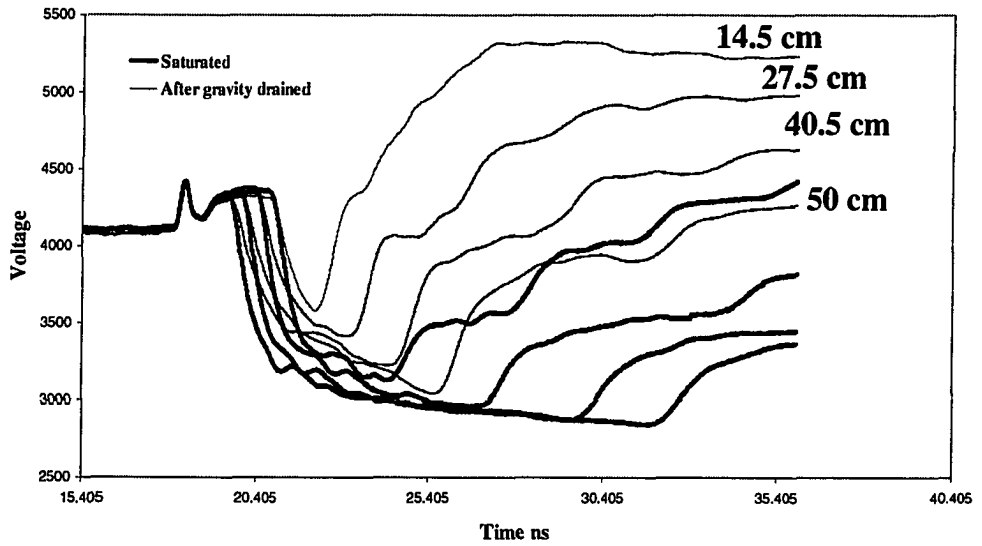

Figure 4.29: Waveforms measured by the 81 cm vertical probe in saturated and gravity drained peat columns

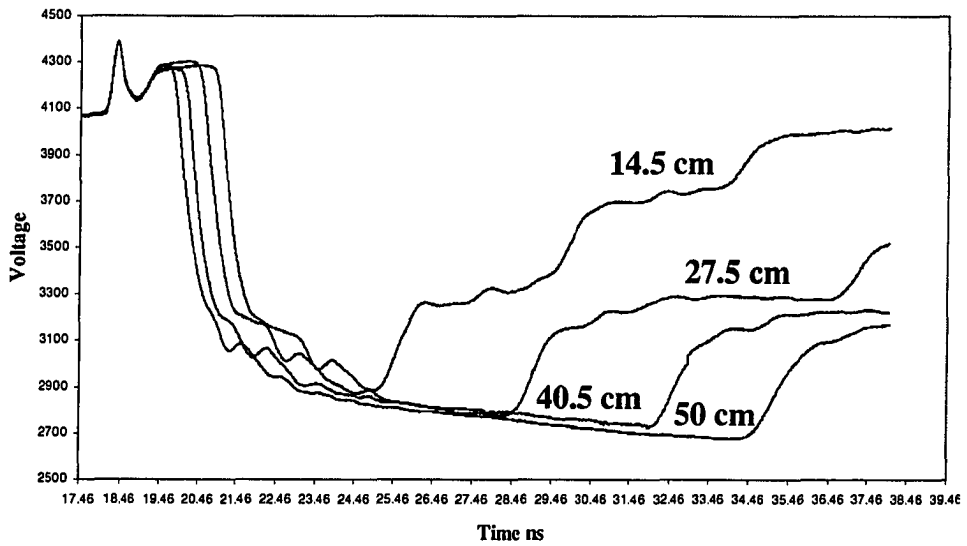

Figure 4.30: Waveforms measured by the 81 cm probe in pure water

Comparing the waveforms taken in the gravity drained and saturated column (Figure 4.29), one can see that the end reflections was attenuated to a small extent with the increased water content, but the reflections were still very strong for confident end point identification, even for the 50 cm probe in the extreme case of pure water (Figure 4.30). This result is in agreement with the observation of Topp et al. (1980) and Robinson et al. (1999) that increased water content increases the signal attenuation but the effect is rather small. However, high water content should not solely account for the total attenuation of the signal in the clogging columns in this research.

Some researchers (Topp et al., 1980; Nadler et al., 1984; Dabson et al., 1985; White et al., 1994) have reported the attenuation of the TDR wave caused by abrupt dielectric property changes along the TDR probe such as a sharp water front or in layered soils, especially for longer probes. Multiple reflections along the TDR probe might cause total signal attenuation at the end of the probe. Topp et al. (1980) observed that for the probes longer than 60 cm placed in soils with discontinuities (abrupt dielectric property change), the reflections were too small for confident interpolation at high water contents. In the case of this study, the water content in the horizontal orientation was quite uniform. Water content changed gradually with depth in the columns. The nonuniformity of water content with depth along the vertical probe was reflected as more fluctuations on the waveforms measured after gravity drainage compared with those at saturation (Figure 4.29). However, there was no abrupt water content change in the column. Waveforms taken with the vertical probe in the peat columns (Figure 4.29) have proven that the non-uniformity of water content with depth did not affect the attenuation of the signal significantly.

After the consideration of the factors that might have affected the attenuation of the TDR signal, it was concluded that the increased electrical conductivity of the soil solution with clogging caused the total attenuation of the end refection. Electrical conductivity is stated as one of the two major sources that could cause total attenuation of the TDR signal (White et al., 1994). In the case of this study, one possible source for the conductivity increase is the leaching ions from the peat particles. Further study is needed to determine if it is the leaching ions that have caused the increased conductivity of the soil solution and if this is the case, what has caused the leaching of ions from peat particles.

4.6.2 Comparison of water contents determined by different methods and investigation of the impact of microbial on TDR measurements

Water contents in each soil section and the average water contents of the clogging columns determined by both the vertical and horizontal probes were plotted in Figures 4.31 and 4.32. The result is similar to that obtained in the drainage columns without clogging. The vertical and horizontal probe agreed reasonably well. The water contents determined by the vertical probe were both above and below the 1:1 line with a standard deviation of 0.050. For the average water content in the entire column, the data was less scattered, with a standard deviation of 0.026 from the 1:1 line.

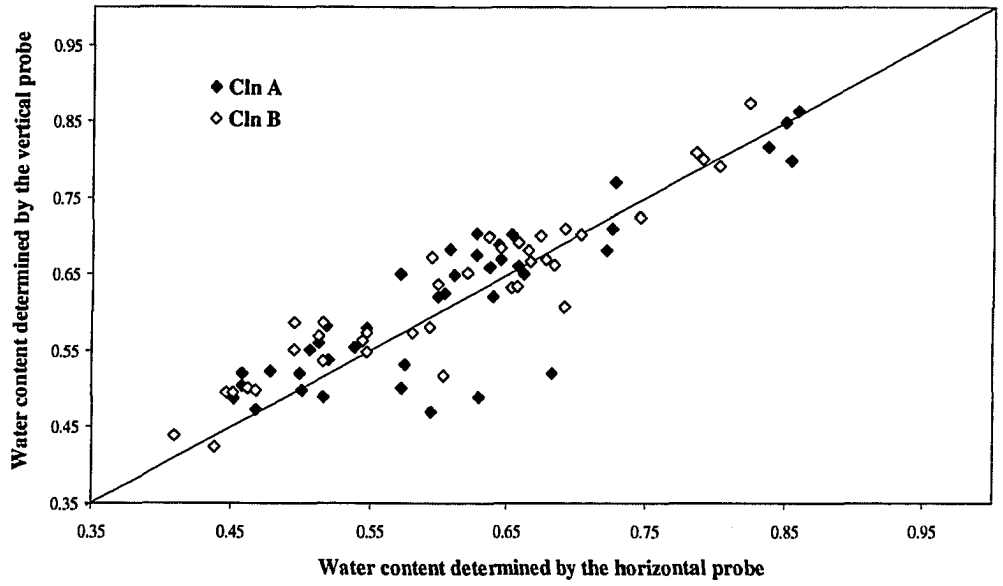

Figure 4.31: Comparison of water contents determined by the vertical and horizontal probes in the columns during clogging

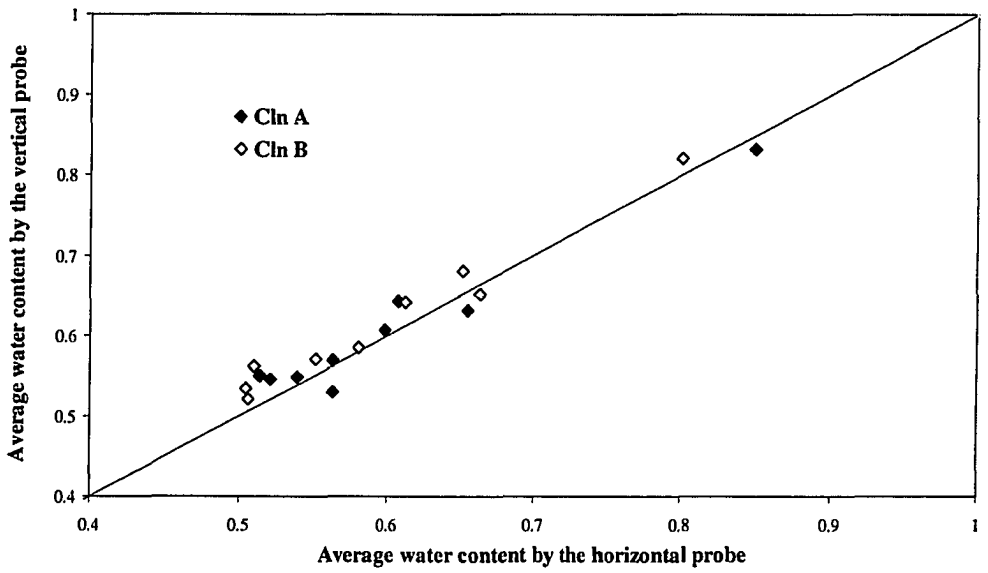

Figure 4.32: Comparison of the average water contents determined by the vertical and horizontal probes in the columns during clogging

The paired t-test results for the water contents measured in each soil section by the vertical and horizontal TDR probes were shown in Table 4.14. There was no

significant difference between the two methods at significance level of 0.01. At significance level 0.05, the statistical t is slightly higher than the corresponding critical t value. This may be caused by the larger scatter of the data due to the increased signal attenuation. Compare the deviations from the clogging columns (Table 4.14) with those from the drainage columns (Table 4.12), we can see that the data in the clogging columns was more scattered. The scatter effect might have been caused by the increased attenuation in the soil solution with the advance of clogging.

Table 4.14: Paired t-test (two-tail) results for the vertical and horizontal water contents in the clogging columns

n	Mean (Θ_v- Θ_h)	S. D.	S. E.	Statis. t	Critical t (α=0.05)	Critical t (α=0.01)	Significance
8	0.012	0.048	0.005	2.217	1.99	2.64	NS at α=0.01

**Θ_h, water content determined by the horizontal probe
**Θ_v, water content determined by the vertical probe

One of the objectives of this research was to investigate the impact of biomass on TDR readings. Water content increases with microbial growth in the peat column. Therefore, the water content measured by TDR in clogged peat soils consists of two types of water: water in biomass and actual water (free water and bound water). If the water in the biomass behaves more like bound water, the TDR technique would underestimate the actual water contents because the dielectric constant of bound water is much lower than free water. Or, if the water in the biomass behaves more like free water, it will not affect the TDR measurement. Comparison of TDR measured water contents and those obtained by the gravimetric method (taken as the actual water content) in the clogged soil infers the dielectric behavior of the water in biomass. If the comparison of the TDR and gravimetric methods in the clogged columns is similar to that for the regular columns, it

could be inferred that the dielectric constant of the water in the biomass was similar to that of free water.

As discussed earlier for the drainage columns, the gravimetric water contents for each soil section in the clogging columns could only be performed at the end of the experiment. The gravimetric water contents at various times during the clogging process were obtained as the average of the entire column. The average TDR measured water contents and those determined by the gravimetric method were plotted in Figure 4.33.

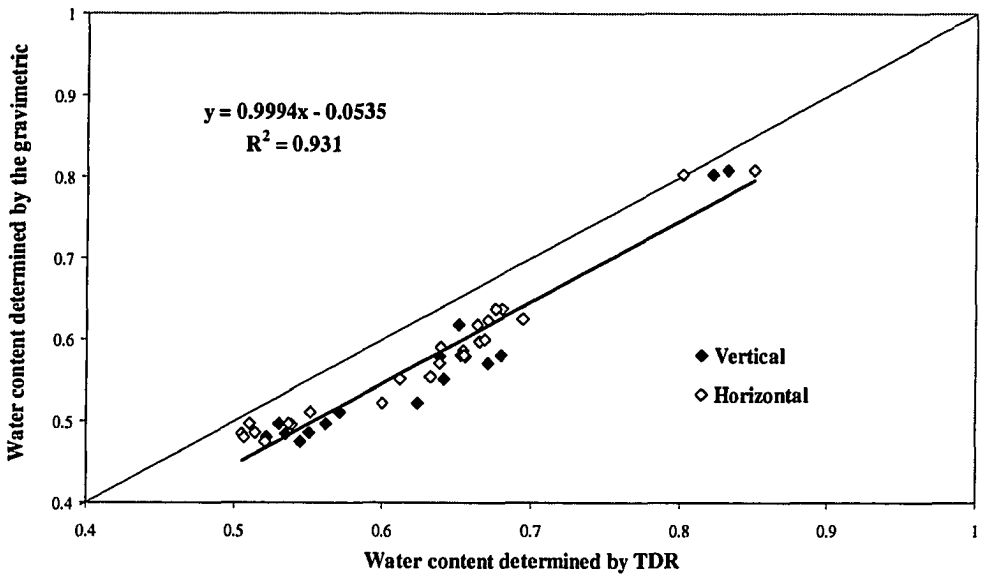

Figure 4.33: Comparison of TDR and gravimetric water contents in the clogging columns

Paired t-test results to compare the water contents determined by TDR and those by the gravimetric method are presented in Table 4.15. The same trend was found as for the drainage columns. The TDR technique gave higher water content values than the gravimetric method with a consistent discrepancy, which was attributed to the error in the calibration curve. However, the mean difference is slightly higher (0.054 with a standard

deviation of 0.024) compared with that obtained in the drainage columns without clogging (0.044 with a standard deviation of 0.023). The slightly higher mean difference likely resulted from the increased scatter in the data associated with signal attenuation caused by the increased electrical conductivity of the soil with clogging. Therefore, it was concluded that the existence of the biomass did not affect the TDR readings significantly, which infers that the water in biomass has a dielectric constant close to that of free water.

Table 4.15: Paired t-test (two-tail) results for TDR and the gravimetric method in the two columns during clogging

	n	Mean	S. D.	S. E	Statis. t	Critical t	Significance
$\Theta_h - \Theta_g$	28	0.050	0.021	0.004	12.59	2.05	S
$\Theta_v - \Theta_g$	15	0.061	0.028	0.007	8.38	2.14	S
$\Theta_{TDR} - \Theta_g$	43	0.054	0.024	0.004	14.7	2.02	S

**Θ_h, water content determined by the horizontal probe
**Θ_v, water content determined by the vertical probe
**Θ_g, water content determined by the gravimetric method
**Θ_{TDR}, pooled data of Θ_v and Θ_h

4.6.3 Moisture profiles

Moisture profiles of column B at saturation, after gravity drainage and at different stages of clogging were shown in Figure 4.34. Those measured by the vertical probe at the end of the experiment were not plotted because of the increasing attenuation of the TDR signal with the longer probes.

Over time, water contents in the peat column increased because a portion of the pore space was occupied by microbial growth and 80 % of the biomass is water by volume (Van Veen and Paul, 1979). The water content increase in the top layer of the soil was the largest. From Aug. 09 to Oct. 27, the water content increase of the top portion (elevation 45 cm at a datum of the bottom of the sand) is over 30 % (moisture profiles by

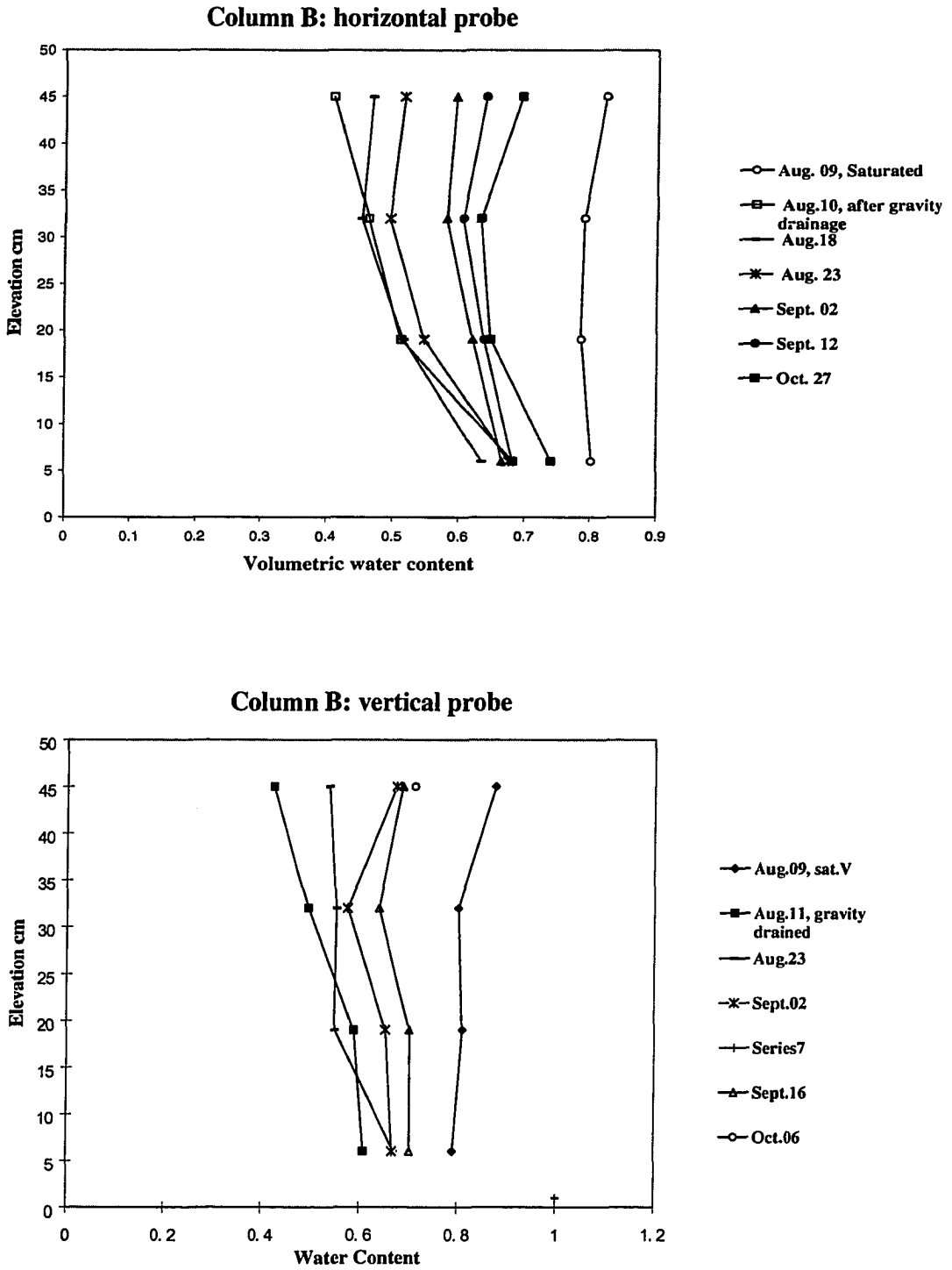

Figure 4.34: Water content profiles with depth in column B during clogging

the horizontal probe), and of the second, third and fourth locations (elevations 6, 19, 32 cm) is approximately 20, 15, 10 %, respectively.

At the end of the experiment, the columns were dismantled into 8 sections to determine the gravimetric water contents of each soil section as illustrated in Figure 3.7 in section 3.8. The results are summarized in Table 4.16.

Table 4.16: Dismantlement of the two columns at the end of the clogging process

Soil section	Column A		Column B	
	Thickness of the layer cm	Volumetric water content	Thickness of the layer cm	Volumetric water content
1	4	73.6 %	2	73.3 %
2	8	53.3 %	8	62.4 %
3	5	58.2 %	5	56.4 %
4	8	56.6 %	8	55.1 %
5	5	63.2 %	5	51.9 %
6	8	59.4 %	8	63.8 %
7	5	58.5 %	5	70.6 %
8	7	81 %	7.5	79.3 %

The peat in the top two sections appeared very dark in color and turned into hard chunks in large pieces after oven-dried, especially in the very top layers. The gravimetric water content for the top layer turned out to be extremely high, more than 73% for both columns.

Combining the results from the TDR technique and the gravimetric method, water content change with depth during clogging suggested that microbial growth occurred mainly at the top of the soil column, where oxygen was sufficient. The microbial population decreased with depth in the column. The high water contents in the bottom sections resulted from the higher base water contents after the gravity drainage.

CHAPTER 5: CONCLUSIONS

The use of a Time Domain Reflectometry (TDR) probe to measure the vertical moisture content profile in peat columns during biological clogging was evaluated. A comparison of horizontal and vertical TDR measurements in columns exposed to just water under various drainage conditions and columns exposed to an organic loading indicate that the vertical moisture profile measured using a vertical TDR probe advanced to various depths was in good agreement with horizontal measurements. The mean water content difference between the two methods was 0.0064 for the water columns and 0.012 for the columns experiencing clogging. The slight increase of the deviation for the columns experiencing clogging was due to the increased attenuation of the TDR signal in the presence of the microbial growth. The scatter of the data in both situations may have been caused by the averaging process of the water contents, measurement error, and TDR waveform analysis.

Compared with the gravimetric method, TDR overestimated the water contents. The discrepancy between the TDR measured water contents and those determined gravimetrically was very consistent, even in the clogged soils, which indicates that the discrepancy might have been caused by a systematic error, possibly the error in the TDR calibration curve that was generated by the modified pressure cell method. The cause of the error is still not known.

The discrepancy between the TDR and gravimetric water contents in the columns during clogging had no significant difference from that in the regular columns with a mean difference between the TDR and gravimetric methods of 0.054 for the clogging

columns compared with 0.044 for the regular columns. The slightly larger mean difference probably resulted from the increased scatter of the data caused by the signal attenuation in the clogging columns. The similar results for the clogged and regular columns support the conclusion that the water in the biomass has a similar dielectric constant as free water.

The water contents in two columns exposed to an organic loading increased with time as the microbial mass established. The magnitude of the water content increase decreased from the top (over 30% increase in a two month period) to the bottom (10% increase) of the column, which indicated that the growth of the microbial community occurred mainly in the top layer where oxygen was sufficient.

The impact of the vertical TDR probe on the vertical conductivity was evaluated. The vertical flow rates measured before and after use of the vertical TDR probe indicated that there was no significant impact. However, signal attenuation remains a problem. Total attenuation of the TDR signal was observed with the longer vertical probes in the clogged columns. When the probe was inserted 27.5 cm into the columns impacted by microbial growth, the end point reflection was lost at water contents over approximately 60%. The attenuation was believed to be caused by the increased conductivity of the soil solution due to the microbial growth in the soil.

The objective of the research was to develop or evaluate the use of a TDR probe to measure the vertical moisture profile in peat filters operating in the field. The vertical moisture profile could then be used to infer the status of the filter. The attenuation noted in this research does limit this application. However, the attenuation of the signal may be used to infer the microbial growth in the clogged soil since they are strongly related.

REFERENCES

Annan, A.P., 1977 "*Time-Domain Reflectometry—Air-gap Problem for Parallel Wire Transmission Lines*", Geol. Surv. Can., Paper 77-1B: 59-62

Ayyaswami, A. and Viraraghavan, T., 1985 "*Septic Tank Eluent Teatment Using Peat*", Canadian Society for civil Engineering Annual Conference, Saskatoon, Sk., May 27-31, 1985: 343-362

Baker, J.M. and Spaans, E.J.A., 1994 "*Measuring Water Exchange Between Soil Water and Atmosphere with TDR-microlysimetry*", Soil Sci. 158: 22-30

Baker, J.M. and Lascano, R.J., 1989 "*The Spatial Sensitivity of Time Domain Reflectometry*", Soil Science, Vol. 147, No. 5: 378-383

Barton P., Buggy M., Deane S., Kelly J. and Lyons H.J., 1984 "*Some Applications of Irish Moss Peat in Effluent Treatment*", Proceedings of the Seventh International Peat Congress, Dublin, Ireland, 2: 148-156, International peat society, Helsinki, Finland

Boelter, D.H., 1964 "*Water Storage Characteristics of Several Peats In-Stu*", Soil Sc. Soc. Am. Proceedings 28: 433-435

Boelter, D.H., 1965 "*Hydraulic Conductivity of Peats*", Soil Science, Vol. 100, No. 4: 227-231

Boelter, D.H., 1969 "Physical *Properties of Peats as related to Degree of Decomposition*", Soil Sci. Soc. Am. Proceedings 33: 606-609

Boelter, D.H. and Blake G.R., 1964 "*Importance of Volumetric Expression of Water Contents of Organic soils*", Soil Sci. Soc. Am. Proceedings 28: 176-178

Brook, R.H. and Corey, A.T., 1964 "*Hydraulic Properties of Porous Media*", Civil Engineering Departement Report, Colorado State University, Fort Collins, CO.

Brooks, Joan L., Rock, Chet A., Strchtemeyer, Roland A. and Woodrd, Franklin E., 1980 "*The Use of Sphagnum Peat for Treatment of Septic Tank Effluent*", University of Maine, Orono, Maine, U.S.A.: 442-461

Buckman, H.O. and Brady, N.C., 1965 "*The Nature and the Properties of Soils*", New York, p25

Buelna, G. and Belanger, G., 1989 "*Peat-based Biofilters for Municipal Wastewater Treatment: Choice of Peat*", Proceedings of Symposium's 89 Peat and Peatlands: Diversification and Innovation, 6-10 August, 1989, Quebec City, Canada, II-New Products: 122-126

Champagne-Hartley, P., 2001 "*A Combined Passive System for the Treatment of Acid Mine Drainage*", PHD Thesis, Carleton University, Ottawa, Canada

Chason, D. B. and Siegel D. I., 1986 "*Hydraulic Conductivity and Related Physical Properties of Peat, Lost River Peatland, Northern Minnesota*", Soil Science, Vol. 142, No. 2: 91-99

Colley, B.E., 1950 "*Construction of Highways over Peat and Muck Areas*", Am. Hghways, 29: 3-6

Condon, E.U. and Odishaw, H., 1987 "*Handbook of Physics*", *Chapter 7 Dielectrics*, McGraw-Hill Book Company, Inc., New York, Toronto, London

Constantz. J. and Murphy, F., 1990 "*Monitoring Moisture Storage in Trees Using Time Domain Reflectometry*", J. Hydrol. 119: 31-42

Cooper, T., 2003 "*Course 2125*", Basic Soil Science web pages, University of Minnesota, http://www.soils.umn.edu/academics/classes/soil2125/doc/s10chap2.htm, Aug. 05, 2003

Couillard, D., 1992 "*Appropriate Wastewater Management Technologies Using Peat*", J. Envir. Syst. 21: 1-19

Couillard, D., 1994 "*The Use of Peat in Wastewater Treatment*", Water Resources, Vol. 28, No. 6: 1261-1274

Coupal, Bl. and Lalancetter, J.M, 1976 "*The Treatment of Wastewaters with Peat Moss*", Water Research 10: 1071-1076

da Silva, F.F., Wallach, R. and Y. Chen, 1993 "*Hydraulic Properties of Sphagnum Peat Moss and Tuff and Their Potential Effects on Water Availability*", Plant and Soil 154: 119-126

Dalton, F.N., Herkekrath, W.N., Rawlins, D.S. and Rhoades, J.D., 1984 "*Time Domain Reflectometry: Simultaneous Measurement of Soil Water Content and Elecrical Conductivity with a Single Probe*", Science (Washington, DC) 224: 989-990

Dalton, F.N. and van Genuchten, M.T., 1986 "*The Time-Domian Reflectometry Method for Measuring Soil Water Content and Salinity*", Geoderma 38: 237-250

Dasberg, S. and Dalton, F.N., 1985 "*Time Domain Reflectometry Field Measurements of Soil Water Content and Electrical conductivity*", Soil Sci. Soc. Am. J. 49: 293-297

Davis, J.L. and Annan, A.P., 1977 "*Electromagnetic Detection of Soil Moisture: Progress Report*", Canadian J. of Remote Sensing, Vol. 3, No. 1: 76-86

Davis, J.L. and Chudobiak, W.J., 1975 "*In Situ Meter for Measuring Relative Permittivity of Soils*", Geol. Surv. Can., Paper 75-1A: 75-79

Davis, J.L. and Chudobialk, W.J., 1975 "*Relative Permittivity Measurements of a Sand and Clay Soil in SITU*", Geol. Surv. Can., Paper 75-1C: 361-365

Dirksen, C. and Dasberg, S., 1993 "*Improved Calibration of Time Domain Reflectometry Soil Water Content Measurements*", Soil Sci. Soc. Am. J. 57: 660-667

Dobson, M.C., Ulaby, F.T., Halllikainen, M.R. and El-Rayes, M.A, 1985 "*Microwave dielectric behaviour of wet soil-ParII: Dielectric Mixing Models*", Institution of Electrical and Electronic Engineers Transactions on Geoscience and Remote Sensing GE-23: 35-46

Eggelsmann, R., Heathwaite, A.L., Grosse-Brauckmann, G., Kuster, E., Naucke, W., Schuch, M. and Schweichle, V., 1993 "*Physical Processes and Properties of Mires*", In: Heathwaite, A.L. and Gottlich, K.H., Mires: Process, Exploitation and Conservation, John Wiley and Sons, Chichester, UK: 171-262

Eyzerman, N.I., 1993 "*Physical Properties and Drainage Depth Standards of Forest Peat Soils*", Eurasian Soil Science, Vol. 25, No. 2: 104-110

Farnham, R.S. and Finney, H.R., 1965 "*Classification and Properties of Organic Soils*", Advances in Agronomy 17: 115-162

Fellner-Feldegg, J., 1969 "*The measurement of Dielectrics in the Time Domain*", J. Phys. Chem. 73: 616-623

Ferre, P.A., Rudolph, D.L. and Kachanoski, R.G., 1998 "*Spatial Averaging of Aater Content by Time Domain Reflectometry: Implications for Two Rods Probes with and without Dielectric Coatings*", Water Resour. Res. 32: 271-279

Fonteno, William C., 1993 "*Problems & Considerations in Determining Physical Properties of Horticultural Substrates, Substrates in Horticulture*", Acta Horticulture, 342: 197-204

Fredlund, D.G. and Rahrdjo, H., 1993 "*Soil Mechanics for Unsaturated Soils*", Wiley, New York, USA

Hasted, J.B., 1973 "*Aqueous Dielectrics*", Chapman and Hall Ltd., London

Hamblin, W.K., 1985 "*The Earth's Dynamic Systems: a Textbook in Physical Geology*", 5th edition, MacMillan Publishing Co., New York

Heimovaara, R.J., 1993 "*Design of Triple-wire Time Domain Reflectometry Probes in Practice and Theory*", Soil Sci. Soc. Am. J. 57: 1410-1417

Heimovaara, T.J. and Bouten, W., 1990 "*A computer-Controlled 36-Channel Time Domain Reflectometry System for Monitoring Soil Water Contents*", Water Resources Research, Vol. 26, No. 10: 2311-2316

Heimovaara, T.J., Bouten, W. and Verstraten, J.M. , 1994 "*Frequency Domain Analysis of Time Domain Reflectometry Waveforms 1: Measurement of the Complex Dielectric Permittivity of Soils*", Water Resources Research, Vol. 30, No. 2:189-199

Heimovaara, T.J., Bouten, W. and Verstraten, J.M, 1994 "*Frequency Domain Analysis of Time Domain Reflectometry Waveforms 2: A Four-component Complex Dielectric Mixing Model for Soils*", Water Resources Research, Vol. 30, No. 2: 201-209

Helioties, F.D., 1989 "*Water Storage Capacity of Wetland Used for Wastewater Treatment*", Journal of Environmental Engineering, Vol. 115, No. 4: 822-834

Herkelrath, W.N., Hamburg, S.P. and Murphy, F., 1991 "*Automatic, Real-Time Monitoring of Soil Moisture in a Remote Field Area with Time Domain Reflectometry*", Water Resource Research, Vol. 27, No. 5: 857-864

Hillel, D., 1971 "*Soil and Water: Physical Principles and Processes*", Academic press, New York, London

Hon, A. S. and Gostomski, P. A. , 2000 "*Unsaturated Water Conductivity Measurements in Biofilter media*", Proceedings of the AWMA's 3rd Annual Conference and Exhibition, Salt Lake City, Utah, June 18-20

Jacobsen, O.H. and Schjonning, P., 1993 "*A Laboratory Calibration of Time Domain Reflectometry for Soil Water Measurement Including Effects of Bulk Density and Texture*", J. Hydrology 151: 147-157

Jacobsen, O.H. and Schjonning, P., 1994 "Comparison of TDR Calibration Functions for Soil Water Determination", Proceedings of the Symposium: TDR Applications in Soil Science

Jones, B.S., and Friedman, S.P., 2000 "*Partical Shape Effects on the Effective Permittivity of Anisotropic or Isotropic Media Consisting of Aaligned or Randomly Oriented Ellipsoidal Particles*", Water Resour. Re. 36: 2821-2833

Jowett, E.C., M.L. McMaster, 1995 "*On-Site Wastewater Treatment Using Unsaturated Absorbent Biofilters*", Journal of Environmental Quality 24: 86-95

Kaila A., 1956 "*Determination of the Degree of Humification in Peat Samples*", J. Scientific Agricultural Society of Findland 28: 18-25

Kellner, E. and Lundin, Lars-Christer, 2001 "*Calibration of Time Domain Reflectometry for Water Content in Peat Soi*l", Nordic Hydrology 32(4/5): 315-332

Kennedy, P., 1998 "*Investigation of Flow through Peat Filters*", M.Eng. Thesis, Carleton University, Ottawa, Canada

Kennedy, P. and P. J. van Geel, 2001 "*Impact of Density on the Hydraulics of Peat Filters*", Canadian Geotechnical Journal, Vol. 38, No. 6:1213-1219

Knight, J.H., 1992 "*Sensitivity of Time Domain Reflectometry Measurement to Lateral Variations in Soil Water Content*", Water Res. Research 28: 2345-2352

Kreij, C.de and Bes, S.S. de, 1989 "*Utilization of Tempe Cells in Determination of Physical Properties of Peat Based Substrates*", Acta Hortic. 238: 23-36

Landva. A.O. and Pheeney, P.E., 1980 "*Peat Fabric and Structure*", Can. Geotech. J. 17: 416-415

Ledieu, J.P., Ridder, D., Clerck, P.D., and Dautrebande, S., 1986 "*A method of measuring soil moisture by time-domian reflectometry*", Journal of Hydrology 88: 319-328

Lennox, D.H. and Parsons, M.L., 1975 "*Subsurface Hydrology in Canada during the International Hydrological Decade*", In Canadian Hydrology Symposium-75 Proceedings, Associate Committee on Hydrology. National Research Council of Canada, Ottawa: 306-325

Lin, Chih-Pin, 2003 "*Frequency Domain versus Travel Time Analyses of TDR Waveforms for Soil Moisture Measurements*", Soil Sci. Soc. Am. J. 67: 720-729

Loxham, M., 1980 "*Theoretical Considerations of Transport of Pollutants in Peats*", International peat society proceedings of the 6th international peat congress, Duluth, Minnesota, U.S.A., August 17-23, 1980: 600-606

Malmstrom, C., 1925 "*Some Pointers for the Drainage of Peat Soils in Norrland*", Skogliga Ron 4

Mendenhall, W., Beaver, R.J. and Beaver, B.M., 1999 "*Introduction to Probability and Statistics*", 10th Edition, Duxbury Press, Brooks/Cole Publishing Company

Myllys, M. and Simojoki, A., 1996 "*Calibration of Time Domain Reflectometry (TDR) for Soil Moisture Measurements in Cultivated Peat Soils*", Suo 47: 1-6

Nadler, A., Dasberg, S., and Lapid, I., 1991 "*Time Domain Reflectometry Measurements of Water Content and Electrical Conductivity of Layered Soil Columns*". Soil Sci. Soc. Am. J. 55: 938-943

Nadler, A., Green, S.R., Vogeler, I. and Clothier, B.E., 2002 "*Horizontal and Vertical TDR Measurements of Soil Water Content and Electrical Conductivity*", Soil Sci. Soc. Am. J. 66: 735-743

Nadler, A., Fenkel, H., and Mantell A., 1984 "*Applicability of the Four-Probe Technique under Extremely Variable Water Contents and Salinity Distribution*", Soil Sci. Soc. Am. J. 48: 1258-1261

Narashiah K.S. and Hains L, 1988 "*Tertiary Treatment of Aerated Lagoon Effluents by Sphagnum Peat Moss: Laboratory Studies*", Envir. Technol. Lett. 9: 1213-1222

Nissen, H.H., Ferre, P.A. and Moldrup, P., 2003 "*Time Domian Reflectometry Developments in Soil Science: 1. Unbalanced Two-rod Probe Spatial Sensitivity and Sampling Volume*", Soil Science, Vol. 168, No. 2: 77-83

Nissen, H. and Moldrup, P., 1994 "*Theoretical Background for the TDR Methodology*", Proceedings of the Symposium: Time Domain Reflectometry Applications in Soil Science, Denmark: 9-23

Paivanen, J., 1969 "*The Bulk Density of Peat and Its Determination*", Silva Fennica, Vol. 3, No. 01: 1-19

Paivanen, J., 1973 "*Hydraulic Conductivity and Water Retention in Peat Soils*", Report from the Faculty of Agriculture and Forestry of the University of Helsinki, Finland, Acta Forestalia Fennica 129: 1-70

Paivanen, J., 1982 "*Physical Properties of Peat Samples in Relation to Shrinkage Upon Drying*", Silva Fennica, Vol. 16, No. 3: 247-263

Paquet, J.M. and Caron, J., 1993 "*In-situ Determination of the Water Desorption Characteristics of Peat Substrates*", Canadian J. of Soil Science 73: 329-339

Patterson, D.E. and Smith, M.W., 1981 "*The Measurement of Unfrozen Water Content by Time Domain Reflectometry: Results from Laboratory Tests*", Can. Geotech. J. 18: 131-144

Pepin. S., Planmondon, A.P. and Stein, J., 1992 "*Peat Water Content Measurement Using Time Domain Reflectometry*", Can J. for Res. 2: 534-540

PIPELINE , 2004, V0l. 15, No. 1, published quarterly by the National Small Flows Clearinghouse at West Virginia University, P.O. Box 6064, Morgantown, WV 26506-6064, Winter (2004)

http://www.google.ca/search?q=cache:zZ13ud04GBsJ:www.nesc.wvu.edu/nsfc/pdf/pipline/PL_w04.pdf+biofilters,+anaerobic,+aerobic,peat&hl=en , Aug. 24, 2004

Redman, D., 2000 "*WATTDR User's Guide*", Environmental Geophysics Facility, Department of Earth Sciences, University of Waterloo

Reginato, Robert J. and van Bavel, C. H. M, 1962 "*Pressure Cell for Coil Cores*", Soil Sci. Soc. of Am. Proceedings, January-February 1962, Vol. 26, No.1: 1-3

Reyes, P.O., Ergas, S.J. and Djaferis, T.E., 2000 "*An Automatic Moisture Control System for Biofiltration*", Proceedings of the Air and Waste Management Association's 93rd annual conference and Exhibition: 1-20

Robinson, D.A., Gardner, C. M. K. and Cooper, J. D., 1999 "*Measurement of Relative Permittivity in Sand Soils Using TDR, Capacitance and Theta Probes: Comparison, Including the Effects of Bulk Soil Electrical conductivity*", Journal of Hydrology 223: 198-211

Roth, C.H., Malicki, M.a. and Plagge, R., 1992 "*Empirical Evaluation of the Relationship between Soil Dielectric Constant and Volumetric Water Content as the Basis for Calibrating Soil Moisture Measurements by TDR*", J. of Soil Science 43: 1-13

Roth, K., Schulin, R., Fluhler, H. and Attinger, W., 1990 "*Calibration of Time Domain Reflectometer for Water Content Measurement Using a Composite Dielectric Approach*", Water Resources Research, V. 26, No. 10: 2267-2273

Shibchurn, A., 2001 "*Water Content Measurement in Peat Using Time Domain Reflectometry*", M. Eng. Thesis, Carleton University, Ottawa, Canada

Singh,H., Huat, B.B.K and Bahia, H.M., 1997 "*Varying Perspective on Peat, It's Occurrence in Sarawak and Some Geotechnical Properties*", Proceedings of Conference on Recent Advances in Soft Soil Engineering, eds., Kuching, Sarawak, 5-7 March, 1997: 135 – 149

Spanns, E.J.A., Baker, J.M., 1993 "*Simple Baluns in Parallel Probes for Time Domain Reflectometry*", Soil Sci. Soc. Am. J. 57: 668-673

Tektronic Inc., 1999 "*1502 C Metallic Time-Domain Reflectometer Service Manual 070-7168-03*", Tektronix, Inc., Oregon, USA

Tibbetts, T.E., 1986 "*N.R.C Peat Program Overview: 1982-1985*", National Research Council of Canada, April 1986

Tinh, V.Q., Leblance, R., Janssens, J.M. and Ruel, M., 1971 "*Peat Moss-natural Adsorbing Agent for the Treatment of Polluted Water*", Can. Min. Metal. Bull. 64: 99-104

Toikka, M.V., Halikainer, M., 1989 "*A Practical Electric Instrument for In Situ Measurement of Peat Properties*", Agricultural engineering: proceedings of the Eleventh International Congress on Agricultural Engineering, Dublin, September 8, 1989: 101-1054

Topp, G.C. and Davis, J. L., 1985 "*Measurement of Soil Water Content Using Time Domain Reflectometer (TDR): A Field Evaluation*", Soil Sci. Soc. Am. J. 49: 19-24

Topp, G.C., Davis, J.L. and Annan, A.P., 1982 "*Electromagnetic Determination of Soil Water Content Using TDR: I. Applications to Wetting Fronts and Steep Gradients*", Soil Sci. Soc. Am. J. 46: 672-678

Topp, G.C., Davis, J.L. and Annan, A.P., 1982 "*Electromagnetic Determination of Soil Water Content Using TDR: II. Evaluation of Installation and Configuration of Parallel Transmission Lines*", Soil Sci. Soc. Am. J. 46: 678-684

Topp, G.C., Davis, J.L., Baileyk W.G. and Zebchuck, W.D., 1984 "*The Measurement of Soil Water Content Using a Portable TDR Hand Probe*", Canadian J. of Soil Science 64: 313-321

Topp, G.C., Davis, J.L. and Annan, A.P., 1980 "*Electromagnetic Detection of Soil Water Content: Measurements in Coaxial Transmission Lines*", Water Resource Research, Vol. 16, No. 3: 574-582

Topp, G. C., Yanuka, M., Zebchuck, W. D. and Zegelin, S., 1988 "*Multiple reflections and attenuation of TDR pulses: Theoretical considerations for application to soil and water*". Water Resource Research 24: 939-944

Topp G.C., Zegelin, S. and White I., 2000 "*Impacts of the Real and Imaginary Components of Relative Permittivity on Time Domain Reflectometry Measurements in Soils*", Soil Sci. Soc. Am. J. 64: 1244-1252

Valentin F.H.H., 1986 "*Peat Beds for Odour Control: Recent Developments and Practical Details*", Filtn Sepn 23: 224-226

Van Genuchten, M.T., 1980 "*A Closed-form Equation for Predicting the Hydraulic Conductivity of Unsaturated Soils*". Soil Sci. Soc. Am. J. 49: 12-19

Van Veen, J.A. and Paul, E.A., 1979 "*Conversion of Biovolume Measurements of Soil Organisms, Grown Under Various Moisture Tensions, to Biomass and Their Nutrient Content*". Applied and Environmental Microbiology, Vol. 37, No. 4: 686-692

Von Hippel, A.R., 1954 "*Dielectric Materials and Applications: MIT Press*", Massachusetts Institute of Technology, Cambridge, Massachusetts

Wang, J.R. and Schmugge, T.J., 1980. "*An Empirical Model for the Complex Dielectric Permittivity of Soils as a Function of Water Content*", Institution of Electrical and Electronic Engineers Transactions on Geoscience and Remote Sensing GE-18: 288-295

Warith, Mostafa A., 1996 "*Evaluation and Design of Peat Filter to Attenuate Landfill Leachate*", Water Quality Resources, Canada, V. 31, No. 1, 65-83

Weiss, R., Alm, J., Laiho, R. and Laine, J., 1998 "*Modeling Moisture Retention in Peat Soils*", Soil Sci. Soc. Am. J. 62: 305-313

Whalley, W.R., 1993 "*Considerations on the Use of Time Domain Reflectometry (TDR) for Measuring Soil Water Content*", J. of Soil Science 44: 1-9

White, I., Knight, J.H., Zegelin,S.J. and Topp, G.C., 1994 "*Comments on 'Considerations on the Use of Time-domian-reflectometry (TDR) for Measuring Soil Water Content' by W.R. Whalley*", European Journal of Soil Science 45: 503-508

Young, M.H., Wierenga, J.B. and Warrick, W.A., 1997a "*Rapid Laboratory Calibration of Time Domain Reflectometry Using Upward Infiltration*", Soil Sci. Soc. Am. J. 61: 707-712

Young, M.H., Wierenga, P.J. and Mancino C.F., 1997b "*Monitoring Near-Surface Soil Water Storage in Turfgrass using Time Domian Reflectometry and weighing Lysimetry*", Soil Sci. Soc. Am. J. 61: 1138-1146

Zegelin,S.J. and White, I., 1989 "*Improved Field Probes for Soil Water Content and Electrical Conductivity Measurement Using Time Domain Reflectometry*", Water Resources Research, Vol. 25, No. 11: 2367-2376

APPENDIX A
DATA FROM THE PRESSURE CELL MOTHOD

Experimental procedure

The pressure cell was packed with presaturated peat and the lab setup was illustrated in Figure 3.4 in section 3.4.4. The experiment started from saturated conditions. K_a of saturated peat was measured. The burette was lowered several times to obtain a set of data of the amount of water collected in the burette, K_a measured by TDR and suction applied to the peat. At the end of the experiment, wet peat in the cell was weighted and oven dried to determine the gravimetric water content, which was considered as the actual water content. The K_a-Θ_v calibration curve and soil drainage curve were determined. The pressure cell was weighed at each step for a check of the evaporation impact. The same procedure was performed on 10 pressure cells (8 with height of 5.2 cm and 2 with height of 10 cm).

The theoretical porosity of peat was calculated using Equation (2.1) from section 2.1.3, $n=(1-\frac{\rho_b}{\rho_s})$, where ρ_b is the dry bulk density and ρ_s is the density of solid particles of peat. ρ_s was calculated by Equation (2.2) from the same section, $\rho_s = 1/\{F/1.5 + [(1-F)/2.7]\}$. F is the organic content and the organic content of the peat under study was determined by Shibchurn (2001).

A 1: RAW DATA SETS

Table A.1: Pressure cell data set #1: cell 1

Volume of the cell cm^3:	882.0794	**ρ_s Kg/m^3**	1.507
Top cap1+rods+wet peat g:	1232.5		
Top cap1+rods+dry peat g:	1025.5	**Theoretical Porosity n**	0.932
Top cap1+rods g:	935.5		
Amount of water at the end g:	207		
Water content at the end:	0.2346728		
Dry bulk density kg/m^3:	102.03163		
Elevation of the midpoint of the cell cm: (the cell was placed on counters of different heights to achieve proper suctions when low the burette)		1--4	75.8
		5--13	145.3
		14	181.7
Initial amount of water in peat g:		632.55	

No. of time to low burette		**W.L. in burette ml**	**W.E. from Datum cm**	**Suction cm H2O**	**ΔV g**	**Accum. Water g**	**Total Water in g**	**K_s**	**Θ_v actual**
Sat.		36.4	75.8	0	0	0	632.55	45.42	0.717
1	start	36.4							
	eqm	7.7	74.5	1.3	28.7	28.7	603.85	36.76	0.685
2	start	49.2							
	eqm	4.55	72.4	3.4	44.6	73.35	559.2	28.12	0.634
3	start	49							
	eqm	4.1	70.8	5	44.9	118.25	514.3	24.23	0.583
4	start	50							
	eqm	4.5	68.5	7.3	45.5	163.75	468.8	16.28	0.531
5	start	50							
	eqm	3.5	134.5	10.8	46.5	210.25	422.3	12.90	0.479
6	start	50							
	eqm	6.5	128.8	16.5	43.5	253.75	378.8	10.86	0.429
7	start	50							
	eqm	10.3	118.8	26.5	39.7	293.45	339.1	9.64	0.384
8	start	50							
	eqm	16.7	100	45.3	33.3	326.75	305.8	8.62	0.347
9	start	50							
	eqm	24.4	75	70.3	25.6	352.35	280.2	7.78	0.318
10	start	50							
	eqm	30.4	44	101.3	19.6	371.95	260.6	6.53	0.295
11	start	50							
	eqm	34.8	9.5	135.8	15.2	387.15	245.4	6.43	0.278
12	start	50							
	eqm	34.8	-24.5	169.8	15.2	402.35	230.2	5.80	0.261
13	start	50							
	eqm	38.8	-65.8	211.1	11.2	413.55	219	5.60	0.248
14	start	50							
	eqm	38	-66.1	247.8	12	425.55	207	5.30	0.235

Table A.2: Pressure cell data set #2: cell 3

Volume of the cell cm^3:		882.0794		Cell weight at saturation g:				3570
Top cap+rods+wet peat g:		1388.5		Cell weight after ended g:				3210
Top cap1+rods+dry peat g:		1061.3		Cell weight loss g:				360
Top cap1+rods g:		936.2		Total water collected g:				348.8
Amount of water at the end g:		327.2		Water lost through evap. g:				11.2
Water content at the end:		0.371		Percentage water lost:				0.013
Dry bulk density kg/m^3:		141.824		Experiment period day:				25
Elevation of the midpoint of the cell cm:	1--2	75.8		ρ_s kg/m^3				1.507
	3--4	181.7		Theoretical Porosity n				0.906
Initial amount of water in peat g:		675.5						

No. of time to low burette		W.L in burette ml	W.E from Datum cm	Suction cm H_2O	ΔV g	Accu. water g	Total water in g	Ka	Θ_v actual
Sat.			75.8	0	0	0	675.5	59.14	0.766
1	start	50							
	stop	31.2			18.8	18.8	656.7	49.79	0.744
	start	49.9							
	stop	23.2			26.7	45.5	630	45.42	0.714
	start	49.7							
	stop	18.2			31.5	77	598.5	40.17	0.679
	start	49							
	stop	18.1			30.9	107.9	567.6	37.54	0.643
	start	50							
	stop	16.2			33.8	141.7	533.8	31.58	0.605
	start	49.4							
	eqm	5.8	27.6	48.2	43.6	185.3	490.2	28.12	0.556
2	start	49.4							
	eqm	11.5	16.7	59.1	37.9	223.2	452.3	25.71	0.513
3	start	49.6							
	stop	10			39.6	262.8	412.7	22.20	0.468
	start	49.5							
	eqm	11.1	41.8	139.9	38.4	301.2	374.3	18.94	0.424
4	start	49.3							
	stop	24			25.3	326.5	349	17.15	0.396
	start	49.6							
	eqm	27.8	27.8	153.9	21.8	348.3	327.2	13.51	0.371

Table A.3: Pressure cell data set #3: Cell 4

Volume of the cell cm^3:	882.0794	ρ_s Kg/m^3	1.507
Top cap + rods + wet peat g:	1321		
Top cap1+ rods+ dry peat g:	1052	Theoretical Porosity n:	0.912
Top cap1+rods g:	935.1		
Amount of water at the end g:	269		
Water content at the end:	0.304961		
Dry bulk density kg/m^3:	132.5278		
Elevation of the midpoint of the cell cm:		1--8	75.8
		9--12	181.7
Initial amount of water in peat g:		648.4	

No. of time to low burette		W.L in burette ml	W.E from Datum cm	Suction cm H2O	ΔV g	Accum. water g	Total water in g	K_a	Θ_v actual
Sat.			75.8	0	0	0	648.4	55.62	0.735
1	start	50							
	eqm	7.8	67	8.8	42.2	42.2	606.2	43.73	0.687
2	start	50							
	eqm	1.3	67.3	8.5	48.7	90.9	557.5	37.54	0.632
3	start	50							
	eqm	4.7	62.5	13.3	45.3	136.2	512.2	32.30	0.581
4	start	50							
	eqm	6.1	55.5	20.3	43.9	180.1	468.3	26.57	0.531
5	start	50							
	eqm	10.4	45.5	30.3	39.6	219.7	428.7	23.41	0.486
6	start	50							
	eqm	13.7	31	44.8	36.3	256	392.4	20.63	0.445
7	start	50							
	eqm	20.6	9.7	66.1	29.4	285.4	363	17.85	0.412
8	start	50							
	eqm	25	-16.8	92.6	25	310.4	338	16.45	0.383
9	start	50							
	eqm	29.5	58.1	123.6	20.5	330.9	317.5	15.94	0.360
10	start	50							
	eqm	31.3	24.8	156.9	18.7	349.6	298.8	11.142	0.339
11	start	50							
	eqm	34	-12.9	194.6	16	365.6	282.8	10.18	0.321
12	start	50							
	eqm	36.2	-52.8	234.5	13.8	379.4	269	9.91	0.305

Table A.4: Pressure cell data set #4: cell 5

Volume of the cell cm^3:	882.0794	**Weight of cell at saturation g:**	3640
Top cap1+rods+wet peat g:	1363.1	**Weight of cell at the end g:**	3205
Top cap1+rods+dry peat g:	1046.2	**Water lost during the process g:**	435
Top cap1+rods g:	935.2	**Water collected in burette:**	430.5
Amount of water at the end g:	316.9	**Water lost by evaporation g:**	4.5
Water content at the end:	0.359	**Percentage of water loss:**	0.5%
Dry bulk density kg/m^3:	125.839	**Experiment duration day:**	16
Elevation of midpoint of top cap 1 cm:	1--8 75.8 9--12 181.7	**ρ_s Kg/m^3:** **Theoretical porosity n:**	1.507 0.916
Initial water in peat g:	747.4		

No. of time to low burette		W.L in burette ml	W.E from Datum cm	Suction cm H2O	ΔV g	Accum. water g	Total water in g	Ka	Θv actual
Sat.			75.8	0	0	0	747.4	66.15875	0.847
1	start	50.1							
	eqm	4.8	69.6	6.2	45.3	45.3	702.1	51.29384	0.796
2	start	49.7							
	eqm	1.9	66	9.8	47.8	93.1	654.3	40.70799	0.741
3	start	49.9							
	eqm	3.5	61.2	14.6	46.4	139.5	607.9	34.49494	0.689
4	start	49.7							
	eqm	5.6	54	21.8	44.1	183.6	563.8	29.94093	0.639
5	start	49.9							
	eqm	4.6	46.9	28.9	45.3	228.9	518.5	23.61139	0.588
6	start	49.6							
	eqm	10.3	35.6	40.2	39.3	268.2	479.2	20.44059	0.543
7	start	49.9							
	eqm	16	18.7	57.1	33.9	302.1	445.3	16.79845	0.505
8	start	49.8							
	eqm	21.3	-3.8	79.6	28.5	330.6	416.8	14.46142	0.472
9	start	50							
	eqm	24.5	73	108.7	25.5	356.1	391.3	13.66916	0.444
10	start	50							
	eqm	25.8	41	140.7	24.2	380.3	367.1	12.74792	0.416
11	start	50							
	eqm	25.4	1.8	179.9	24.6	404.9	342.5	12.15161	0.388
12	start	49.6							
	eqm	24	-32.8	214.5	25.6	430.5	316.9	11.28392	0.359

Table A.5: Pressure cell data set #5: cell 7

Volume cm^3:	882.0794	Weight of cell at saturation g:	3675					
Top cap+rods+wet peat g:	1397.7	Weight of cell at the end g:	3238					
Top cap+rods+dry peat g:	1046.9	Weight loss g:	437					
Top cap+rods g:	935.1	Water collected from burette g:	424.2					
Amount of water at then end g:	350.8	Water loss by evaporation g:	12.8					
Water content at the end:	0.397697	Percentage of water loss g:	1.45					
Dry bulk density kg/m^3:	126.746							
Elevation of midpoint of the cell cm:	1--8	75.8	ρ_S Kg/m^3:	1.507				
	9--12	181.7	Theoretical Porosity n:	0.916				
Initial water in peat g:	775							

No. of time to low burette		W.L in burette ml	W.E from Datum cm	ΔV g	Accum. water g	Total water in g	TDR file name	K_a	Θ_v actual
Sat.			75.8	0	0	775	ce70	66	0.878606
1	start	49.9							
	stop	10.2	63.9	39.7	39.7	735.3	ce71	47.7	0.833598
2	start	49.6							
	stop	10.3		39.3	79	696	ce721	37.3	0.789045
	start	50							
	stop	15.2		34.8	113.8	661.2	ce722	29.8	0.749592
	start	49.2							
	stop	16.6		32.6	146.4	628.6	ce723	26.2	0.712634
	start	49.7							
	stop	-5.1	52	54.8	201.2	573.8	ce72	21	0.650508
3	start	49.6							
	stop	16.7		32.9	234.1	540.9	ce731	18.9	0.61321
	start	49.7							
	stop	16.5		33.2	267.3	507.7	ce732	16.4	0.575572
	start	49.4							
	stop	10.9	24.8	38.5	305.8	469.2	ce733	14.4	0.531925
4	start	49.7							
	stop	14.7		35	340.8	434.2	ce741	11.6	0.492246
	start	49.8							
	stop	18.7		31.1	371.9	403.1	ce742	10.1	0.456988
	start	49.5							
	stop	19.2		30.3	402.2	372.8	ce743	9.1	0.422638
	start	49.4							
	stop	27.4	-3.8	22	424.2	350.8	ce744	8.7	0.397697

Table A.6: Pressure cell data set #6: cell 8

Volume of the cell cm^3	882.0794		Weight of cell at saturation g:		3734
Top cap+rods+wet peat g:	1440		weight of cell at the end g:		3355
Top cap+rods+dry peat g:	1042.5		Weight loss of the cell g:		379
Top cap+rods g:	934.5		Water collected in burette g:		382.2
Water at the end g:	397.5		Water loss by evaporation g:		-3.2
water content at the end:	0.45064		Variation in volumetric water content:		-0.0036
Dry bulk density kg/m^3:	122.438		ρ_s Kg/m^3 :		1.507
Elevation of midpoint of the cell cm:	1--8	75.8	Theoretical porosity n :		0.919
	8--9	181.7			
Initial water in cell g:	779.7				

No. of time to low burette		W.L in Burette ml	W.E cm	Suction cm H2O	ΔV g	Accum. Water g	Total water g	TDR Ffile name	Ka	Θv Actual	Weight of Cell	Weight Loss g
Sat.			75.8	0	0	0	779.7	ce8s	58.7	0.883	3734	
1	start	50										
	eqm	6	69.7	6.1	44	44	735.7	ce81	50	0.834	3688.2	45.8
2	start	50										
	eqm	7.1	61.2	14.6	42.9	86.9	692.8	ce82	42.1	0.785	3645.6	42.6
3	start	49.8										
	eqm	10.2	50	25.8	39.6	126.5	653.2	ce83	36.7	0.740	3605.6	40
4	start	49.3										
	eqm	2.6	43.7	32.1	46.7	173.2	606.5	ce84	31.8	0.687	3555	50.6
5	start	49.9										
	eqm	1.9	38.8	37	48	221.2	558.5	ce 85	26.2	0.633	3505	50
6	start	49.8										
	eqm	10.8	19	56.8	39	260.2	519.5	ce86	23.2	0.589	3465	40
7	start	50										
	eqm	8.5	4.1	71.7	41.5	301.7	478	ce87	19.4	0.542	3425	40
8	start	50										
	eqm	11.4	76.3	105.4	38.6	340.3	439.4	ce88	14.3	0.498	3385	40
9	start	50										
	eqm	8.1	67.7	114	41.9	382.2	397.5	ce89	13.4	0.451	3355	30

Table A.7: Pressure cell data set #7: cell 9

Volume of the cell cm^3:		882.0794			**Weight of Saturated cell g:**			3675					
Top cap+rods+wet peat g:		1385			**Weight of cell at the end g:**			3238					
Top cap+rods+dry peat g:		1038.1			**Weight loss during the process g:**			437					
Top cap+rods g:		932.3			**Water collected in burette g:**			457.3					
End water g:		346.9			**Water loss by evaporation g:**			-20.3					
End water content:		0.393275			**Percentage of water loss g:**			-0.02301					
Dry bulk density kg/m^3:		119.9439			**ρ_s Kg/m^3 :**			1.507					
Initial water in the cell g:		804.2			**Theoretical porosity n:**			0.920					
No. of time to low burette		**W.L in burette ml**	**ΔV g**	**Accum. water g**	**Total water in g**	**TDR file name**	**Ka**	**Θv actual**	**Weight of cell g**	**Cell weight lost g**	**Accum. water lost g**	**Total water in cell g**	**Θ_v basesd on**
Sat.			0	0	804.2	**ce9s**	61.3	0.911709	3697.2				0.911709
1	start	49.8											
	eqm	13.5	36.3	36.3	767.9	**ce911**	60.3	0.870557	3650	47.2	47.2	757	0.858199
2	start	49.8											
	eqm	16.9	32.9	69.2	735	**ce912**	48.9	0.833258	3620.2	29.8	77	727.2	0.824416
3	start	50											
	eqm	13.3	36.7	105.9	698.3	**ce913**	40.8	0.791652	3583.7	36.5	113.5	690.7	0.783036
4	start	49											
	eqm	18.1	30.9	136.8	667.4	**ce914**	37.1	0.756621	3545	38.7	152.2	652	0.739162
5	start	49.3											
	eqm	20.8	28.5	165.3	638.9	**ce915**	34.9	0.724311	3519.7	25.3	177.5	626.7	0.71048
6	start	49.3											
	eqm	-6.7	56	221.3	582.9	**ce916**	28.4	0.660825	3463.2	56.5	234	570.2	0.646427
7	start	50											
	eqm	11.5	38.5	259.8	544.4	**ce917**	23.1	0.617178	3420	43.2	277.2	527	0.597452
8	start	50											
	eqm	19.8	30.2	290	514.2	**ce918**	19.7	0.582941	3390	30	307.2	497	0.563441
9	start	50											
	eqm	19.5	30.5	320.5	483.7	**ce919**	17.2	0.548363	3360	30	337.2	467	0.529431
10	start	50											

	eqm	18.3	31.7	352.2	452	ce920	13.6	0.512426	3333	27	364.2	440	0.498821
11	start	48.8											
	eqm	10	38.8	391	413.2	ce921	12.4	0.468439	3290	43	407.2	397	0.450073
12	start	49.9											
	eqm	15.1	34.8	425.8	378.4	ce922	10.2	0.428986	3255	35	442.2	362	0.410394
13	start	49.2											
	eqm	17.7	31.5	457.3	346.9	ce923	8.8	0.393275	3220	35	477.2	327	0.370715

Table A.8: Pressure cell data set #8: cell 11

Volume of the cell cm^3:	882.0794	Weight of Saturated cell g:	3799
Top cap+rods+wet peat g:	1410	Weight of cell at the end g:	3360
Top cap+rods+dry peat g:	1044.8	Weight loss during the process g:	439
Top cap+rods g:	934.6	Water collected in burette g:	428.7
Water at the end g:	365.2	Water loss by evaporation g:	10.3
Water content at the end:	0.414022	Percentage of water loss g:	0.011677
Dry bulk density kg/m^3:	124.9321	p_s Kg/m^3 :	1.507
Elevation of midpoint of the cell cm:	1--9	75.8	
	10--11	181.7	Theoretical porosity n: 0.917
Initial water in the cell g:	793.9		

No. of time to low burette		Water level in burette ml	W.E from Datum cm	Suction cm H2O	ΔV g	Accum. water g	Total water in g	Ka	Θv actual	Weight of cell	Cell weight Loss g	Accum. weight Loss g	Wate in cell g	Θv based on weight loss
Sat.			75.8	0	0	0	793.9	68.3	0.9	3799	0	0	793.9	0.900032
1	start	49.8												
	eqm	5.9	68.5	7.3	43.9	43.9	750	62.2	0.85	3740	59	59	734.9	0.833145
2	start	49.6												
	eqm	3.5	64.7	11.1	46.1	90	703.9	35.5	0.798	3695	45	104	689.9	0.782129
3	start	50												

	eqm	4.2	60.8	15	45.8	135.8	658.1	31.1	0.746	3650	45	149	644.9	0.731113
4	start	50												
	eqm	3.8	56.9	18.9	46.2	182	611.9	25.2	0.694	3605	45	194	599.9	0.680098
5	start	49.8												
	eqm	6.4	50.9	24.9	43.4	225.4	568.5	22	0.644	3569.7	35.3	229.3	564.6	0.640078
6	start	49.5												
	eqm	7.6	43	32.8	41.9	267.3	526.6	18.4	0.597	3527.3	42.4	271.7	522.2	0.59201
7	start	49.7												
	eqm	11.9	30.2	45.6	37.8	305.1	488.8	14.6	0.554	3485	42.3	314	479.9	0.544055
8	start	49.6												
	eqm	17.4	13	62.8	32.2	337.3	456.6	14.2	0.518	3450	35	349	444.9	0.504376
9	start	49.6												
	eqm	20.5	-6.5	82.3	29.1	366.4	427.5	12.1	0.485	3428.9	21.1	370.1	423.8	0.480456
10	start	50												
	eqm	18.5	65	116.7	31.5	397.9	396	11.6	0.449	3396.6	32.3	402.4	391.5	0.443838
11	start	50												
	eqm	19.2	18.2	163.5	30.8	428.7	365.2	10.7	0.414	3360	36.6	439	354.9	0.402345

Table A.9: Pressure cell data set #9: tall cell 1

Volume cm^3:	1696.3065	**Weight of Saturated cell g:**			4800
Top cap+rods+wet peat g:	2005	**Weight of cell at the end g:**			3930
Top cap+rods+dry peat g:	1320	**Weight loss during the process g:**			870
Top cap+rods g:	1126.1	**Water collected in burette g:**			847.7
Water at the end g:	685	**Water loss by evaporation g:**			22.3
Water content at the end:	0.40381853	**Percentage of water loss g:**			0.013146
Dry bulk density kg/m^3:	114.307173		**ρ_s Kg/m^3**		1.507
Elevation of midpoint of the cell cm:	1--9	75.8			
	10--11	181.7	**Theoretical porosity n:**		0.924
Initial water in peat g:	1532.7				

No. of time to low burette		**W.L in burette ml**	**ΔV g**	**Accum. Water g**	**Total Water in g**	**Suction cm H2O**	**Ka**	**Θv actual**	**Weight of Cell g**	**Cell weight loss g**	**Accum. Weight loss g**	**Water in Cell g**	**Θv based on weight loss**
Sat.			0	0	1532.7	0	65.4	0.904	4800		0	1532.7	0.904
1	start	49.3											
	eqm	4.9	44.4	44.4	1488.3	75.8	48.2	0.877	4750	50	50	1482.7	0.874
2	start	50											
	eqm	1.8	48.2	92.6	1440.1	75.8	37.3	0.849	4700	50	100	1432.7	0.845
3	start	50											
	eqm	8.6	41.4	134	1398.7	75.8	35.5	0.825	4660	40	140	1392.7	0.821
4	start	50											
	eqm	11.2	38.8	172.8	1359.9	75.8	33.8	0.802	4620	40	180	1352.7	0.797
5	start	50											
	eqm	1.5	48.5	221.3	1311.4	75.8	32.6	0.773	4570	50	230	1302.7	0.768
6	start	50											
	eqm	3.6	46.4	267.7	1265	75.8	30.7	0.746	4525	45	275	1257.7	0.741
7	start	50											

	eqm	4.2	45.8	313.5	1219.2	75.8	29	0.719	4480	45	320	1212.7	0.715
8	start	50											
	eqm	2	48	361.5	1171.2	75.8	25.1	0.690	4430	50	370	1162.7	0.685
9	start	49.6											
	eqm	-24	74	435.5	1097.2	75.8	21.1	0.647	4356.3	73.7	443.7	1089	0.642
10	start	50											
	eqm	7.4	42.6	478.1	1054.6	181.7	21.3	0.622	4313.1	43.2	486.9	1045.8	0.617
11	start	50											
	eqm	-2.4	52.4	530.5	1002.2	181.7	19.7	0.591	4261.1	52	538.9	993.8	0.586
12	start	50											
	eqm	3.5	46.5	577	955.7		15.8	0.563	4214.9	46.2	585.1	947.6	0.557
13	start	50											
	eqm	-3.6	53.6	630.6	902.1		14.7	0.532	4161.8	53.1	638.2	894.5	0.527
14	start	50											
	eqm	0.1	49.9	680.5	852.2		13.7	0.502	4111.6	50.2	688.4	844.3	0.498
15	start	50											
	eqm	1.2	48.8	729.3	803.4		11.2	0.474	4050	61.6	750	782.7	0.461
16	start	50											
	eqm	5.3	44.7	774	758.7		10.8	0.447	4010	40	790	742.7	0.438
17	start	49.7											
	eqm	12.9	36.8	810.8	721.9		9.3	0.426	3975	35	825	707.7	0.417
18	start	50											
	eqm	13.1	36.9	847.7	685		9.4	0.404	3930	45	870	662.7	0.391

Table A.10: Pressure cell data set #10: tall cell 2

Volume of the cell cm^3:	1696.307		Weight of Saturated cell g:	4656	
Top cap+rods+wet peat g:	2012.4		Weight of cell at the end g:	3910	
Top cap+rods+dry peat g:	1332.1		Weight loss during the process g:	746	
Top cap1+rods g:	1126.1		Water collected in burette g:	704	
Water at the end g:	680.3		Water loss by evaporation g:	42	
Water content at the end:	0.401048		Percentage of water loss g:	0.02476	
Dry bulk density kg/m^3:	121.4403		ρ_s Kg/m^3	1.507	
Elevation of midpoint of the cell cm:	1--9	75.8			
	10--11	181.7	Theoretical porosity n:	0.919	
Initial water in peat g:	1384.3				

No. of Ttime to Low Burette		Water Level in Burette ml	ΔV g	Accum. Water g	Total Water in g	TDR File Name	Ka	Θ_v actual	Weight of Cell g	Weight Loss g	Accum. Water g	Water in Cell	Θ_v based on Weight Loss
Sat.			0	0	1384.3	tcell2s	59.7	0.8161	4656		0	1384.3	0.9036
1	start	49.6											
	stop	0	49.6	49.6	1334.7	tcell21	54.7	0.7868	4613	43.1	43.1	1341.2	0.7907
2	start	49.6											
	stop	0.1	49.5	99.1	1285.2	tcell22	47.9	0.7576	4563	49.9	93	1291.3	0.7612
3	start	49.7											
	stop	7.5	42.2	141.3	1243	tcell23	40.4	0.7328	4522	40.6	133.6	1250.7	0.7373
4	start	49.8											
	stop	13.9	35.9	177.2	1207.1	tcell24	40.1	0.7116	4486	36	169.6	1214.7	0.7161
5	start	49.7											
	stop	10.3	39.4	216.6	1167.7	tcell25	35	0.6884	4447	39.6	209.2	1175.1	0.6927
6	start	49.8											
	stop	0.5	49.3	265.9	1118.4	tcell26	31.6	0.6593	4398	48.8	258	1126.3	0.664
7	start	50											
	stop	-6	56	321.9	1062.4	tcell27	27.9	0.6263	4340	58.2	316.2	1068.1	0.6297
8	start	49.4											
	stop	-4	53.4	375.3	1009	tcell28	23.4	0.5948	4270	69.8	386	998.3	0.5885
9	start	49.5											

	stop	2.4	47.1	422.4	961.9	tcell29	22.7	0.5671	4230	40	426	958.3	0.5649
10	start	49.9											
	stop	20	29.9	452.3	932	tcell210	18.9	0.5494	4200	30	456	928.3	0.5472
11	start	50											
	stop	-5.3	55.3	507.6	876.7	tcell211	15.1	0.5168	4145	54.9	510.9	873.4	0.5149
12	start	50											
	stop	7	43	550.6	833.7	tcell212	13.4	0.4915	4095	50.1	561	823.3	0.4853
13	start	50											
	stop	-6	56	606.6	777.7	tcell213	12.9	0.4585	4035	60	621	763.3	0.45
14	start	50											
	stop	11.3	38.7	645.3	739	tcell214	11.1	0.4357	3995	40	661	723.3	0.4264
15	start	50											
	stop	16.5	33.5	678.8	705.5	tcell215	10.9	0.4159	3960	35	696	688.3	0.4058
16	start	49.7											
	stop	24.5	25.2	704	680.3	tcell216	9.9	0.401	3910	50	746	638.3	0.3763

A2: CALIBRATION CURVES FOR INDIVIDUAL CELLS

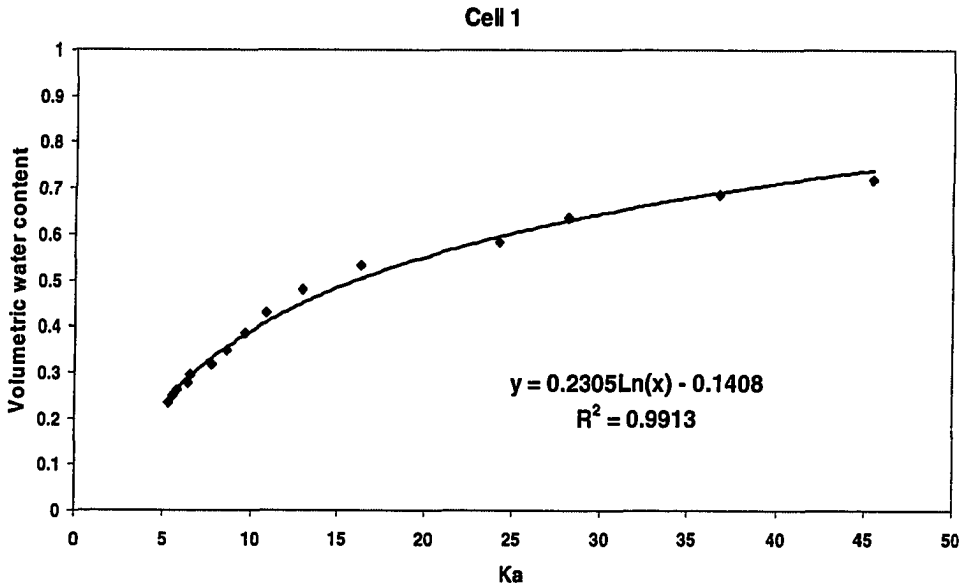

Figure A. 1: Calibration curve for cell 1, bulk density 102 Kg/m^3

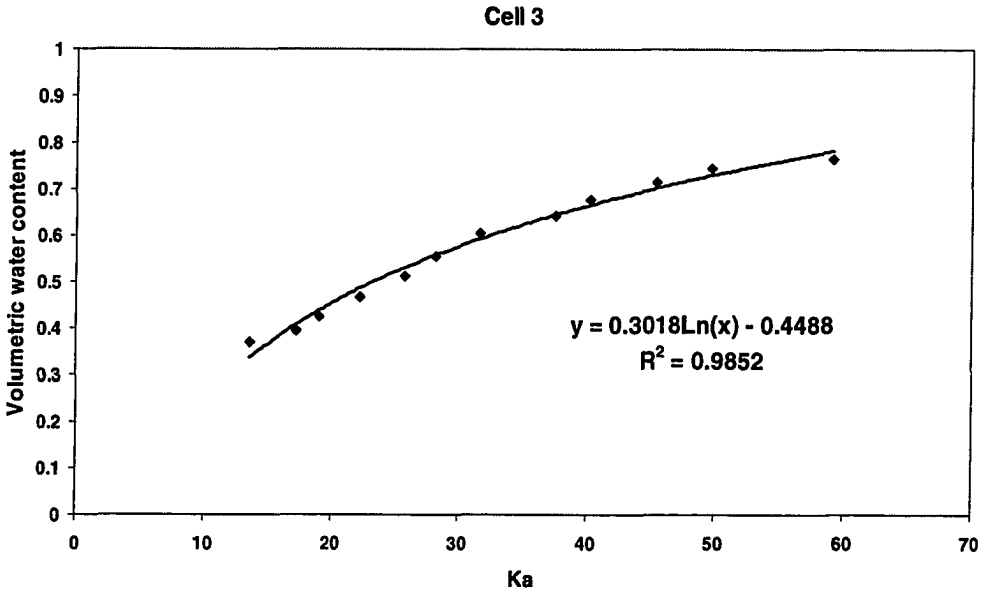

Figure A.2: Calibration curve for cell 3, bulk density 141 Kg/m^3

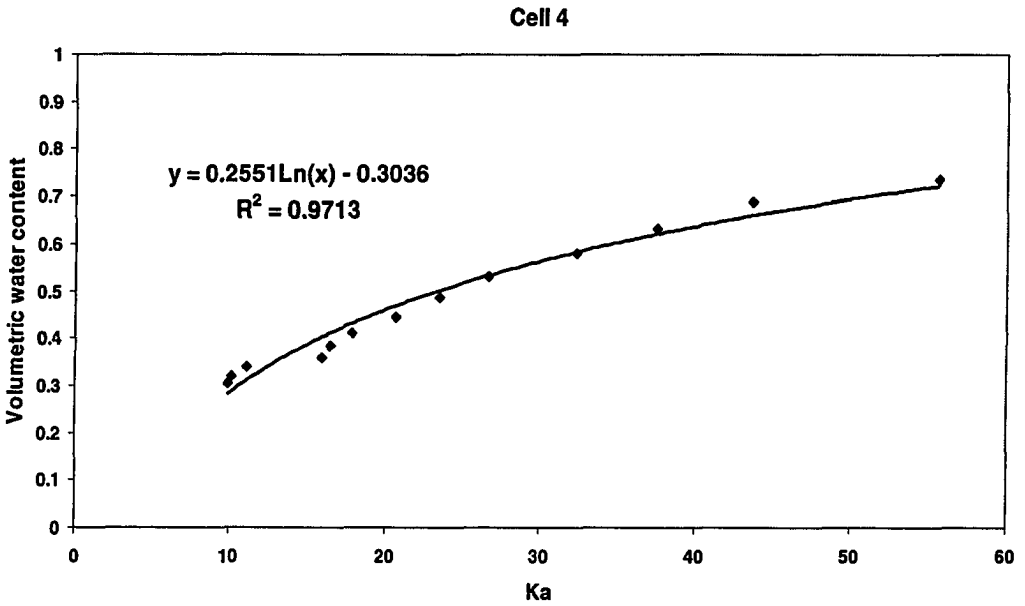

Figure A.3: Calibration curve for cell 4, bulk density 132 Kg/m^3

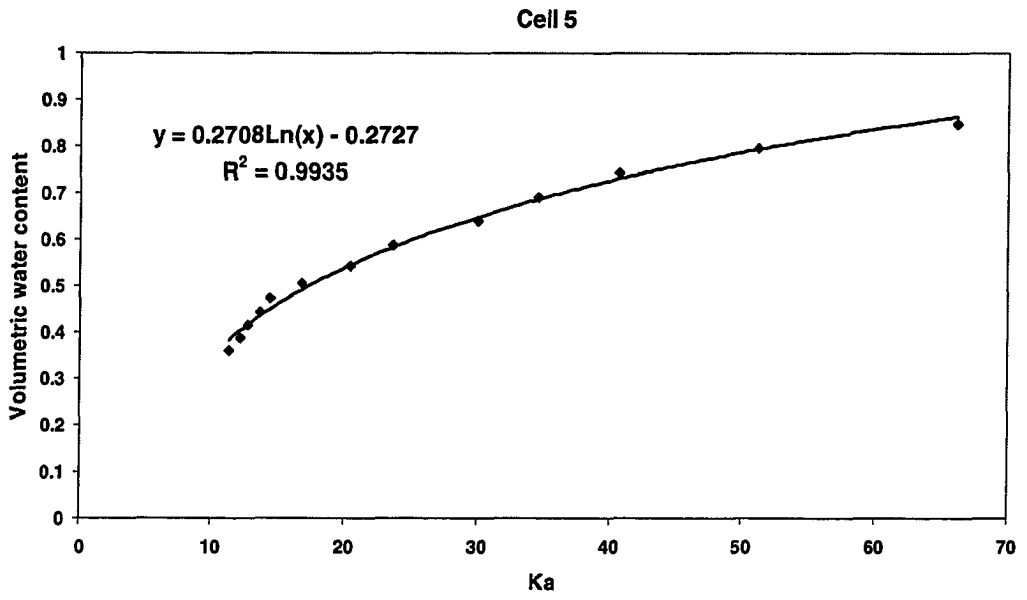

Figure A.4: Calibration curve for cell 5, bulk density 126 Kg/m^3

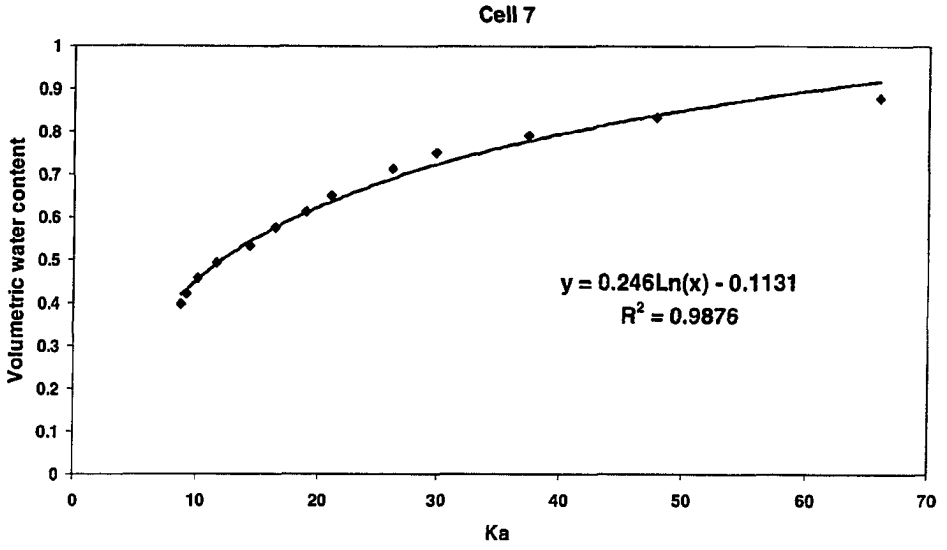

Figure A.5: Calibration curve for cell 7, bulk density 127 Kg/m^3

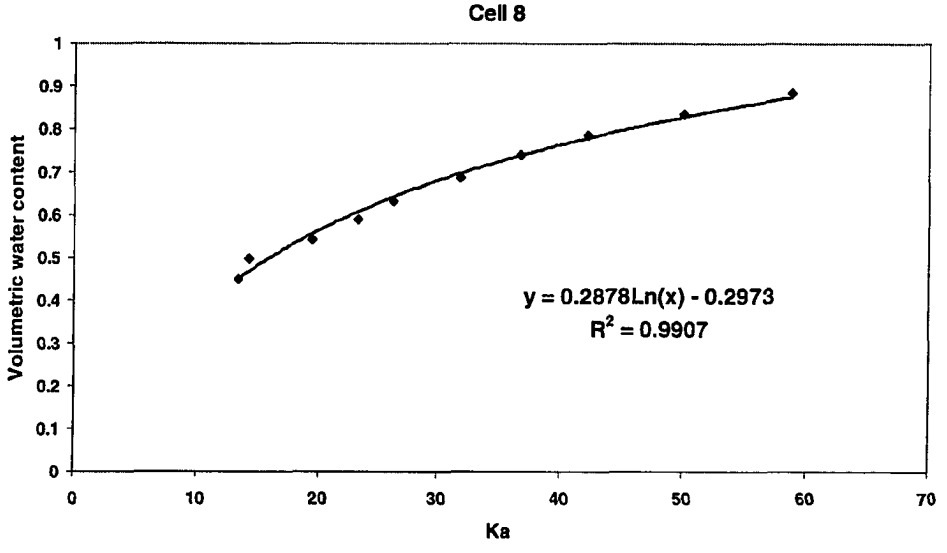

Figure A.6: Calibration curve for cell 8, bulk density 122 Kg/m^3

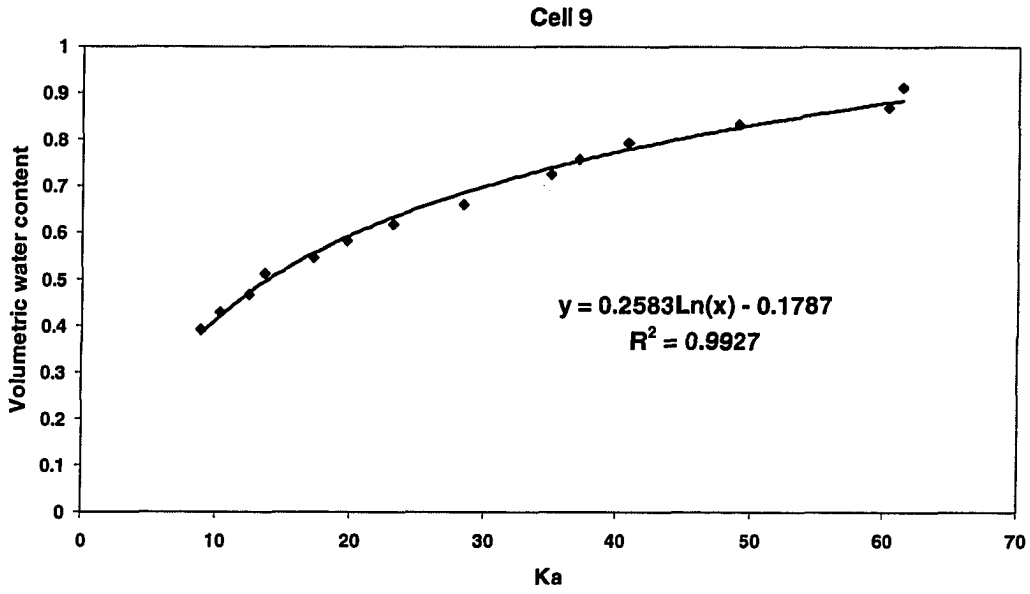

Figure A.7: Calibration curve for cell 9, bulk density 120 Kg/m^3

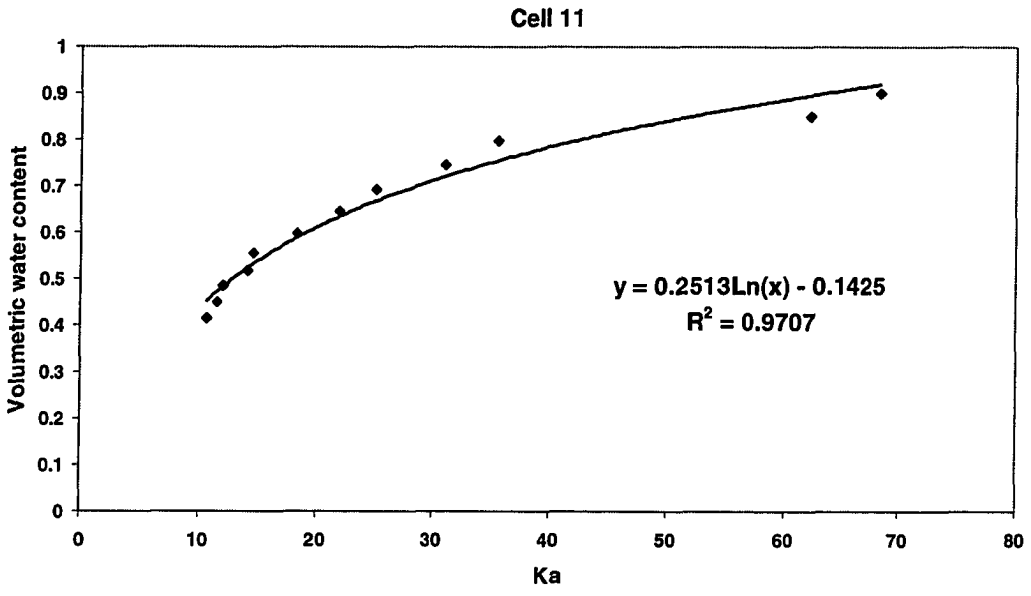

Figure A.8: Calibration curve for cell 11, bulk density 125 Kg/m^3

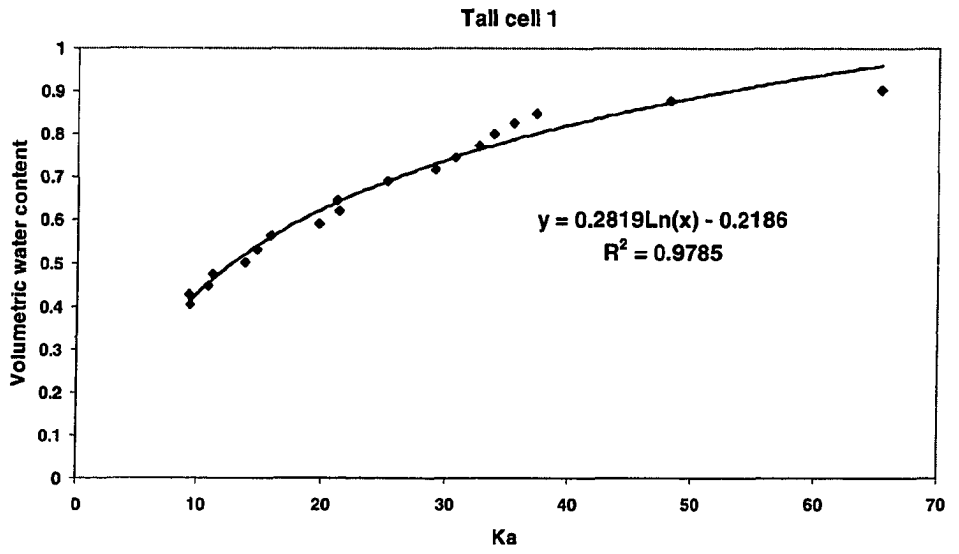

Figure A.9: Calibration curve for tall cell 1, bulk density 114 Kg/m^3

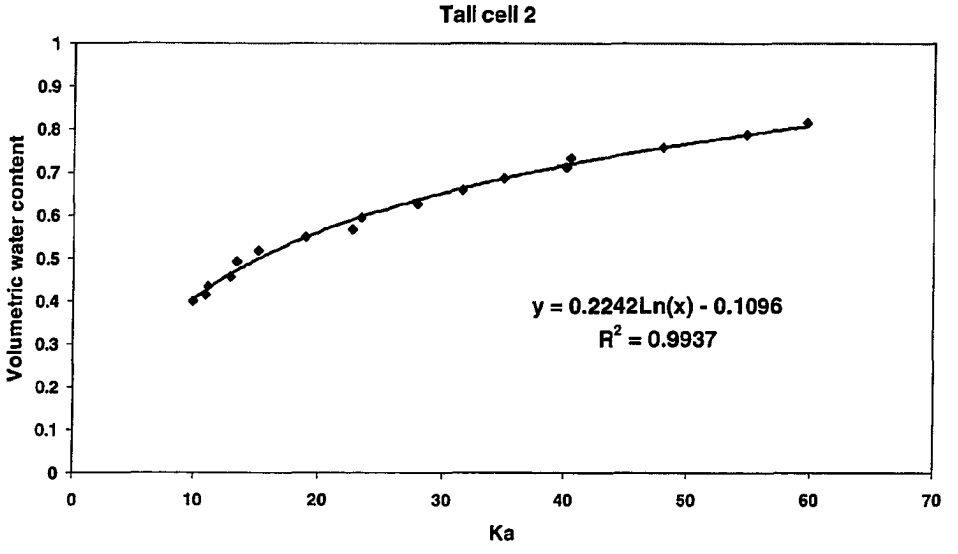

Figure A.10: Calibration curve for tall cell 2, bulk density 121 Kg/m^3

A 3: IMPACT OF EVAPORATION ON CALIBRATION CURVES

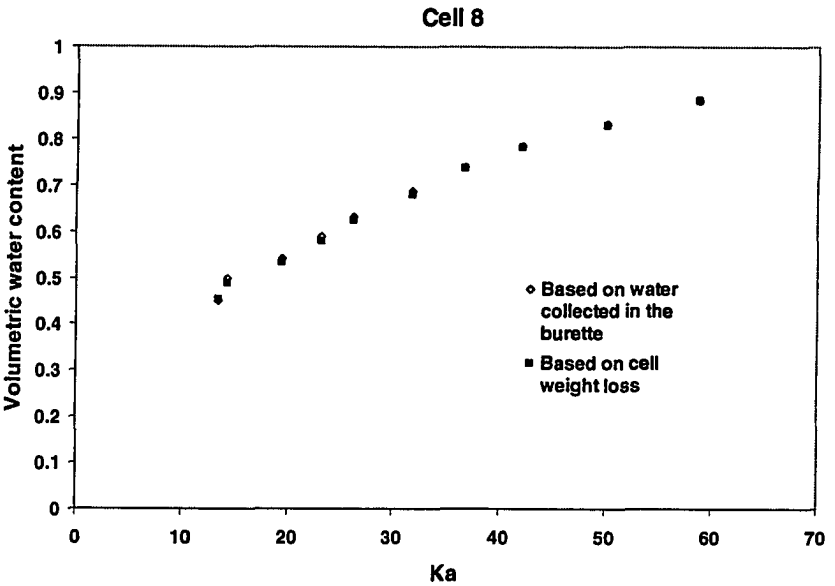

Figure A.11: Calibration curves based on water collected in burette and cell weight loss for cell 8

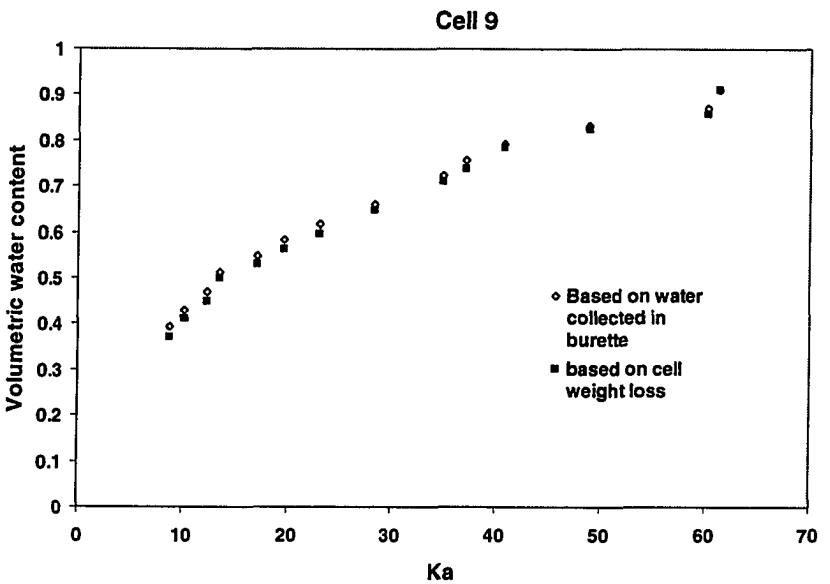

Figure A. 12: Calibration curves based on water collected burette and cell weight loss for cell 9

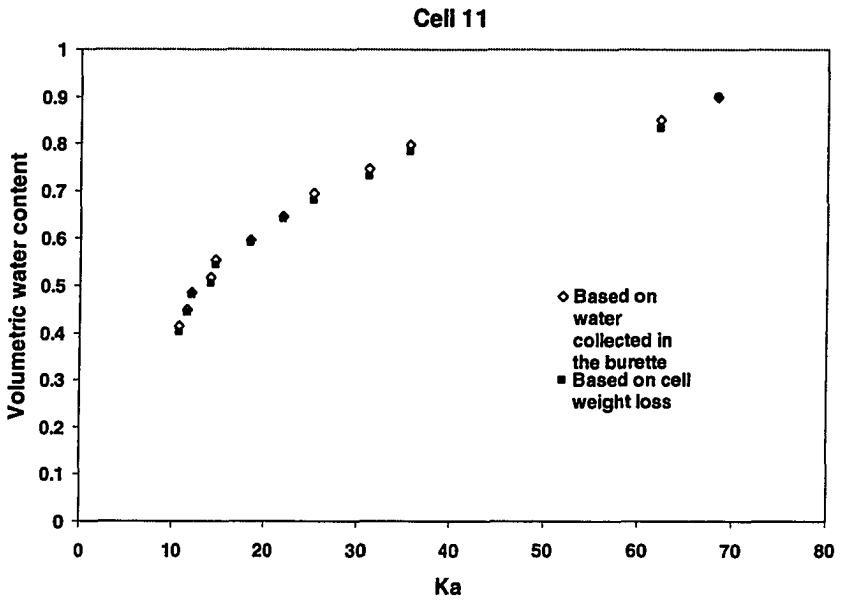

Figure A. 13: Calibration curves based on water collected in burette and cell weight loss for cell 11

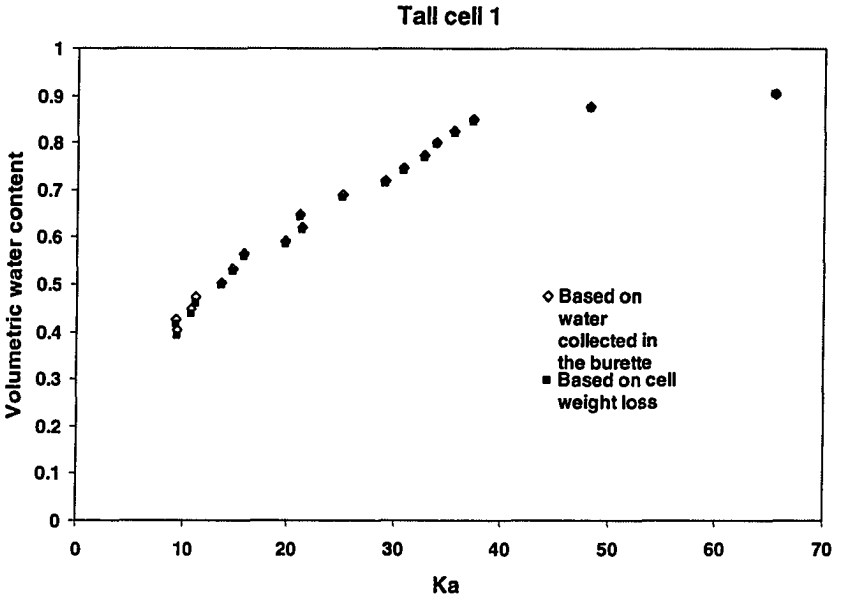

Figure A. 14: Calibration curves based on water collected in burette and cell weight loss for tall cell 1

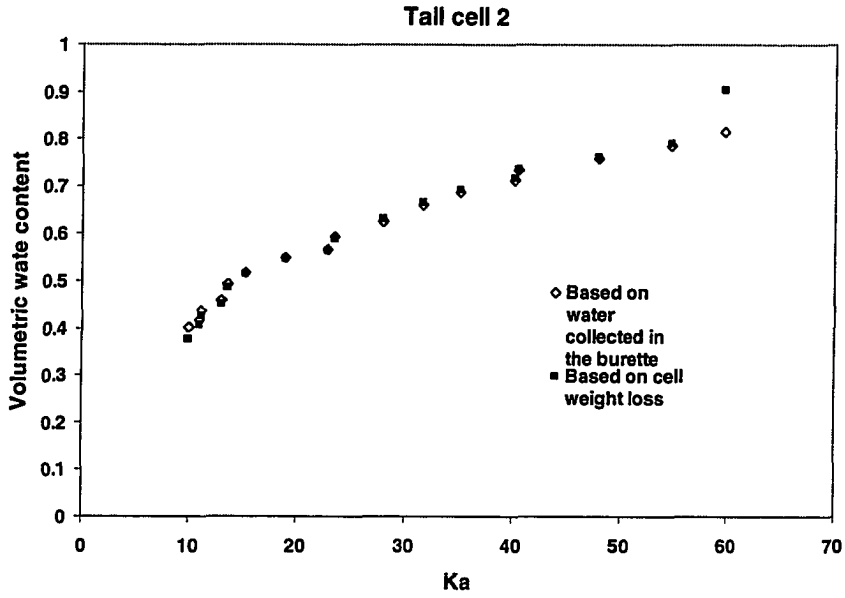

Figure A. 15: Calibration curves based on water collected in burette and cell weight loss for tall cell 1

A 4: TDR WAVEFORMS OF TEN PRESSURE CELLS OF DIFFERENT BULK DENSITIES FOR VARIOUS VOLUMETRIC WATER CONTENTS

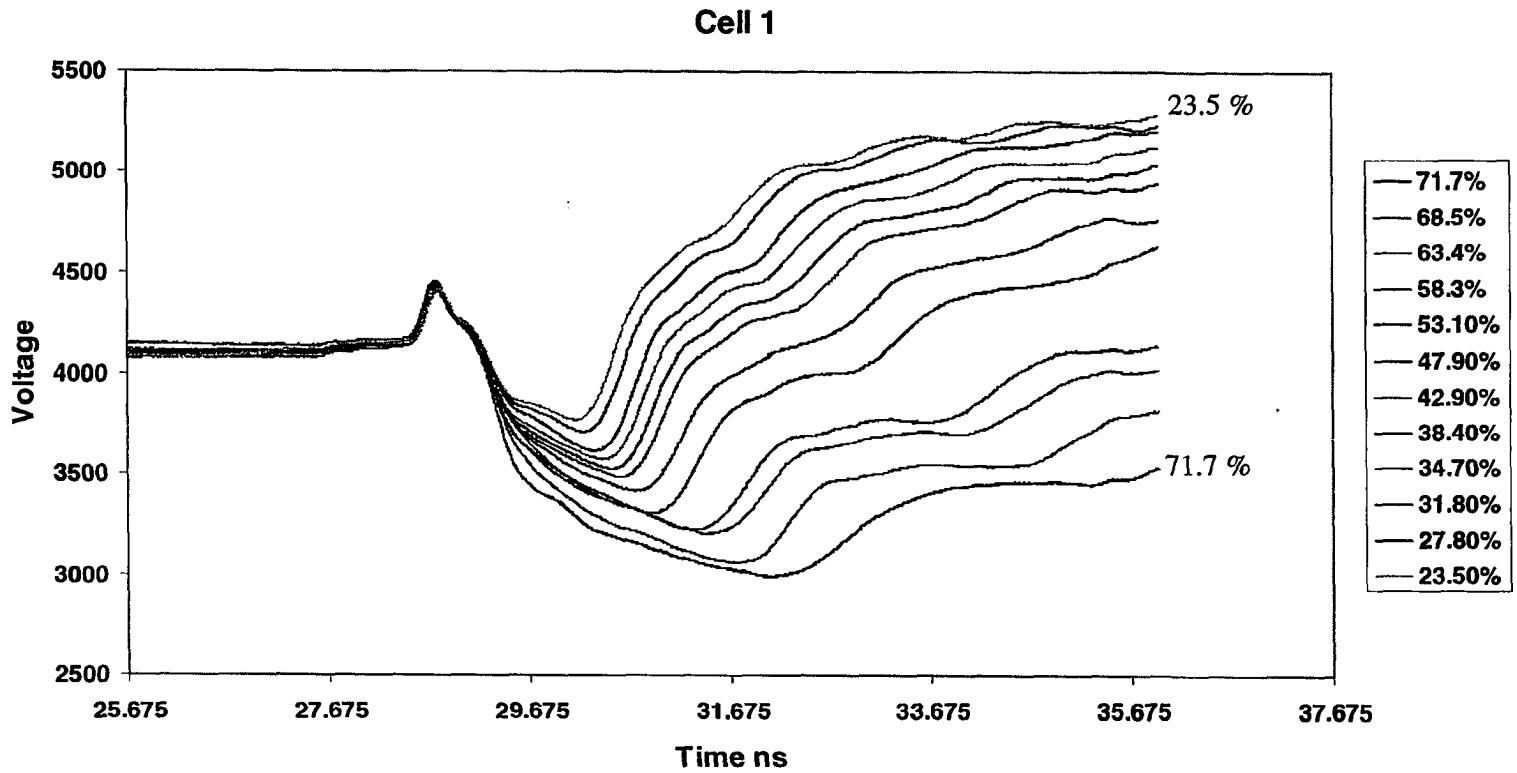

Figure A. 16: Waveforms for cell 1, bulk density 102 Kg/m^3

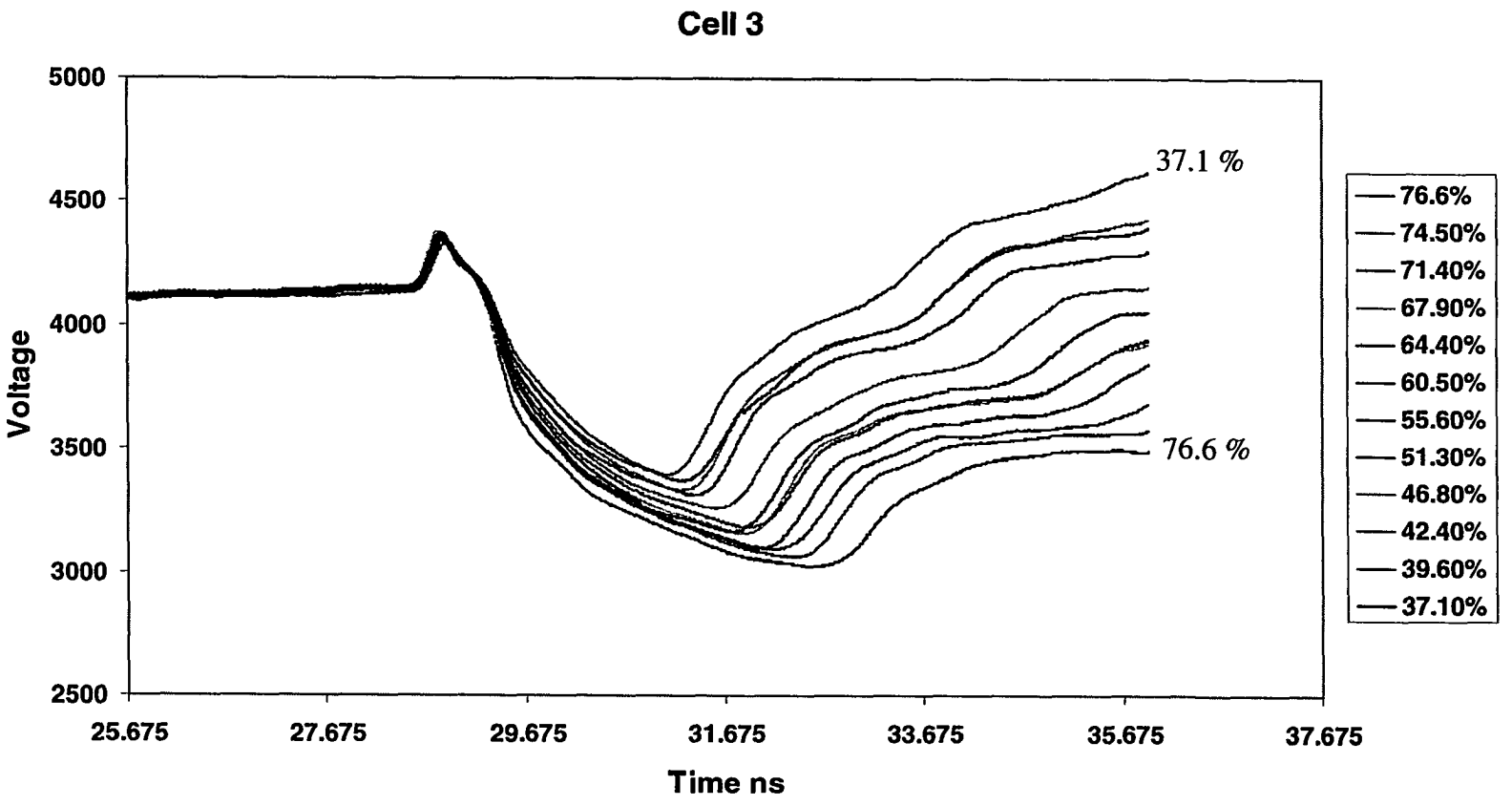

Figure A. 17: Waveforms for cell 3, bulk density 141 kg/m^3

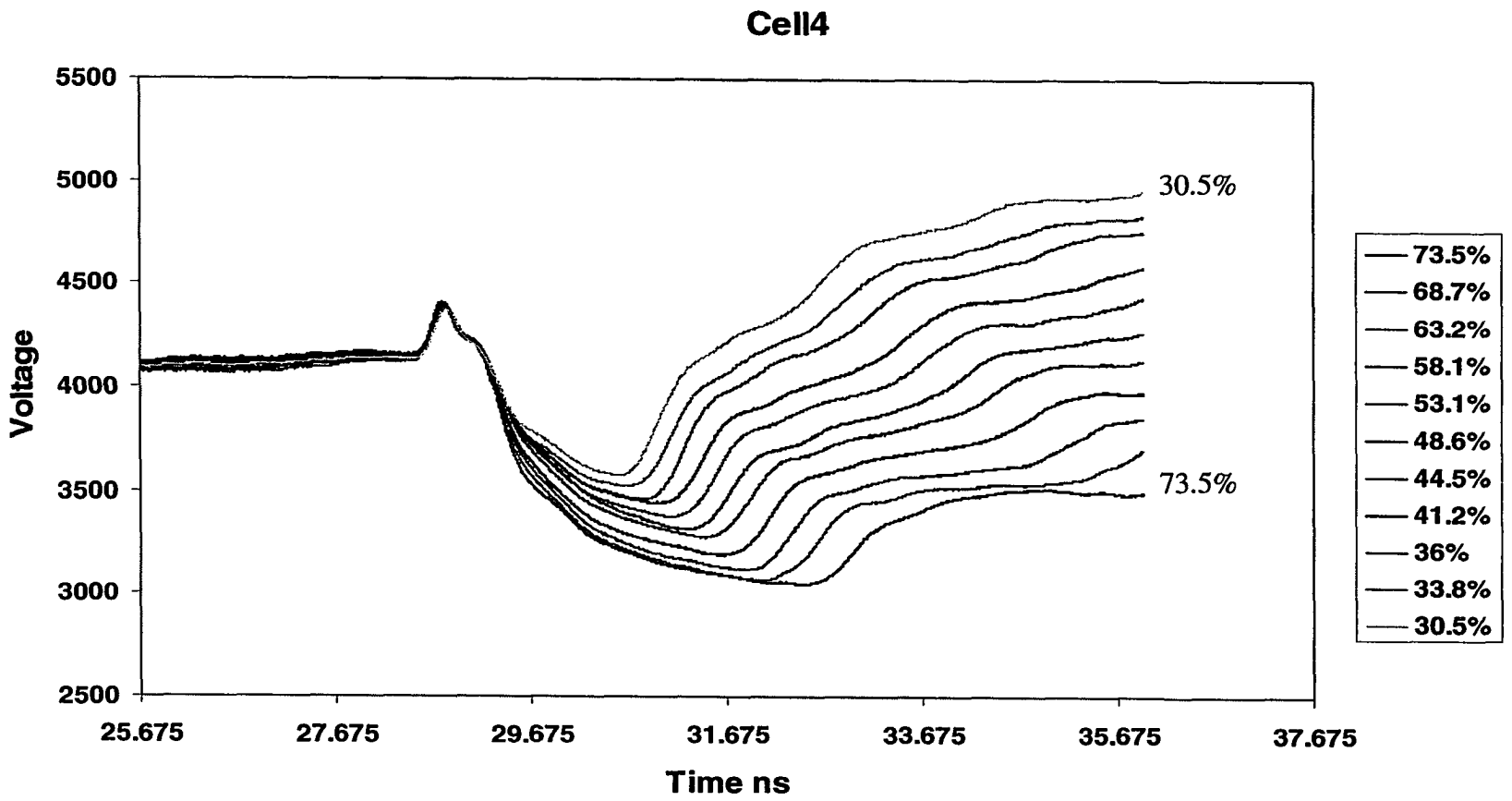

Figure A. 18: Waveforms for cell 4, bulk density 132 Kg/m^3

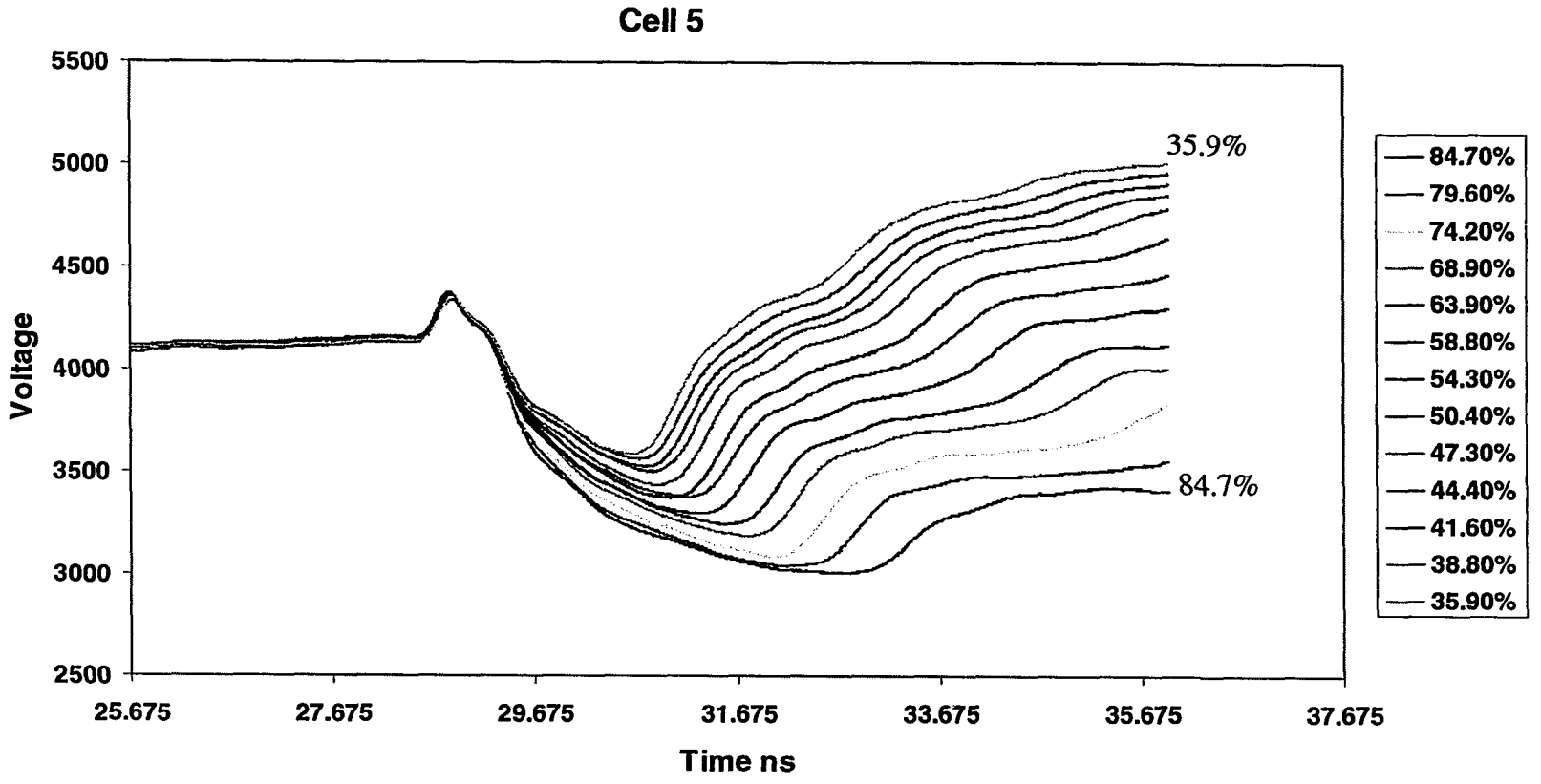

Figure A. 19: Waveforms for cell 5, bulk density 126 Kg/m^3

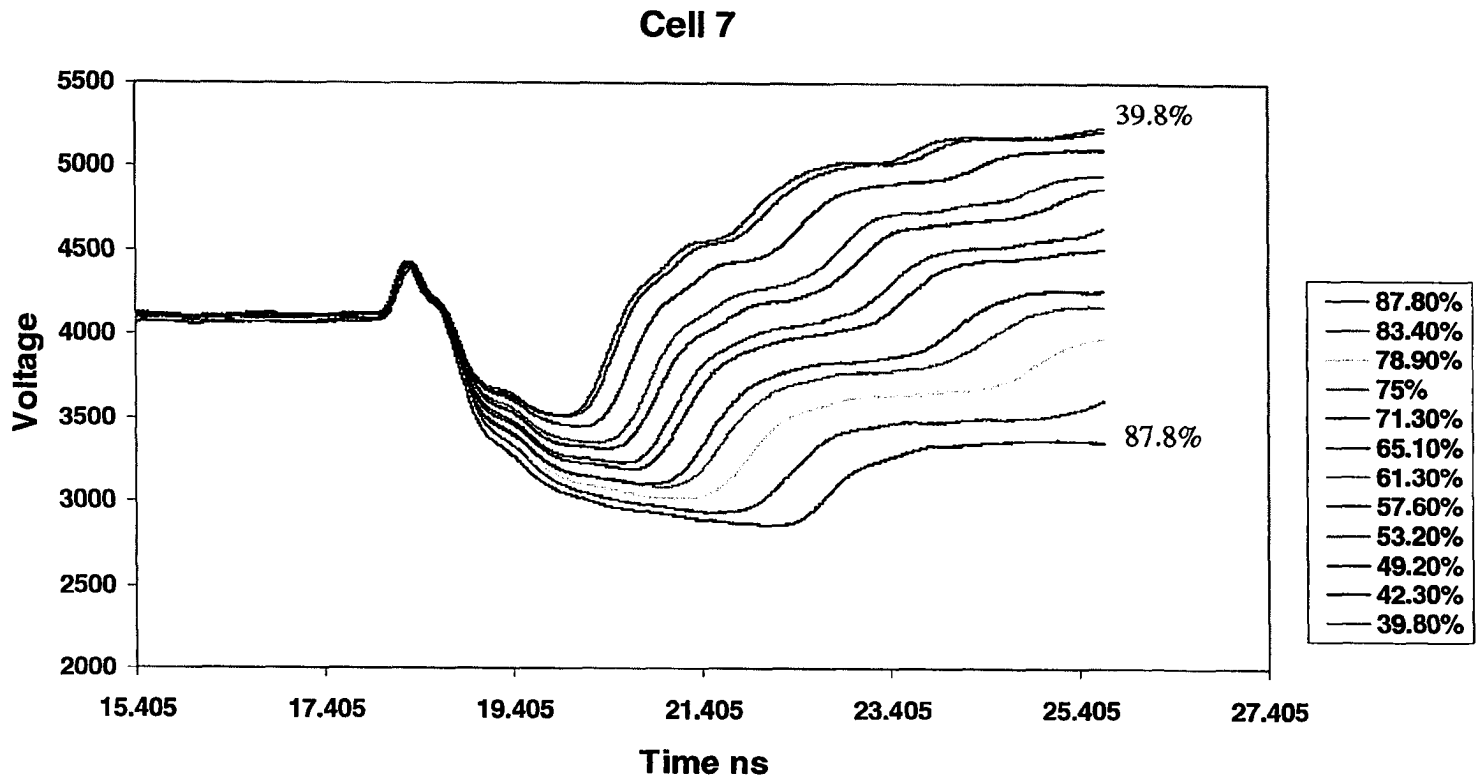

Figure A. 20: Waveforms for cell 7, bulk density 127 Kg/m^3

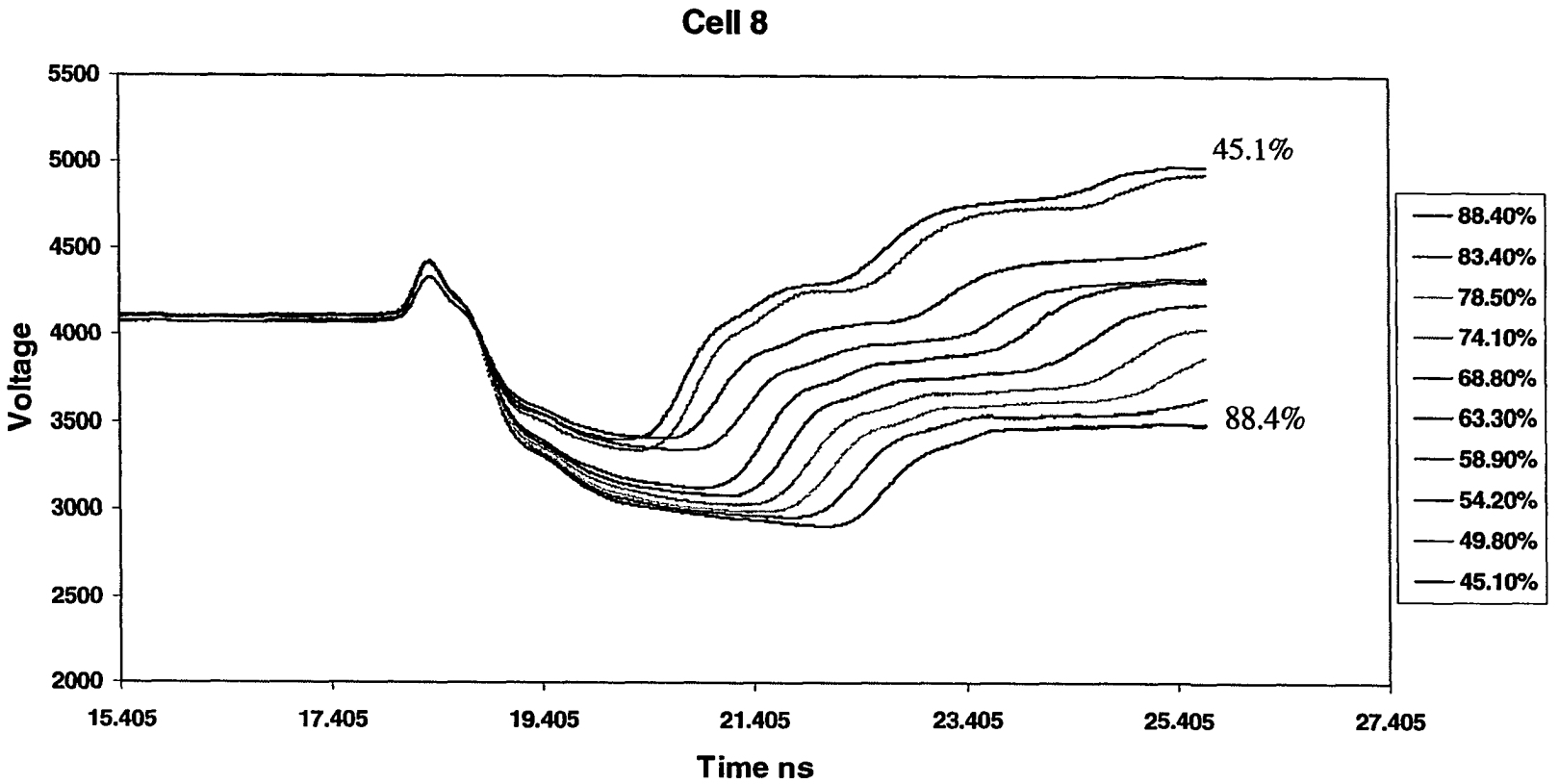

Figure A. 21: Waveforms for cell 4, bulk density 122 Kg/m^3

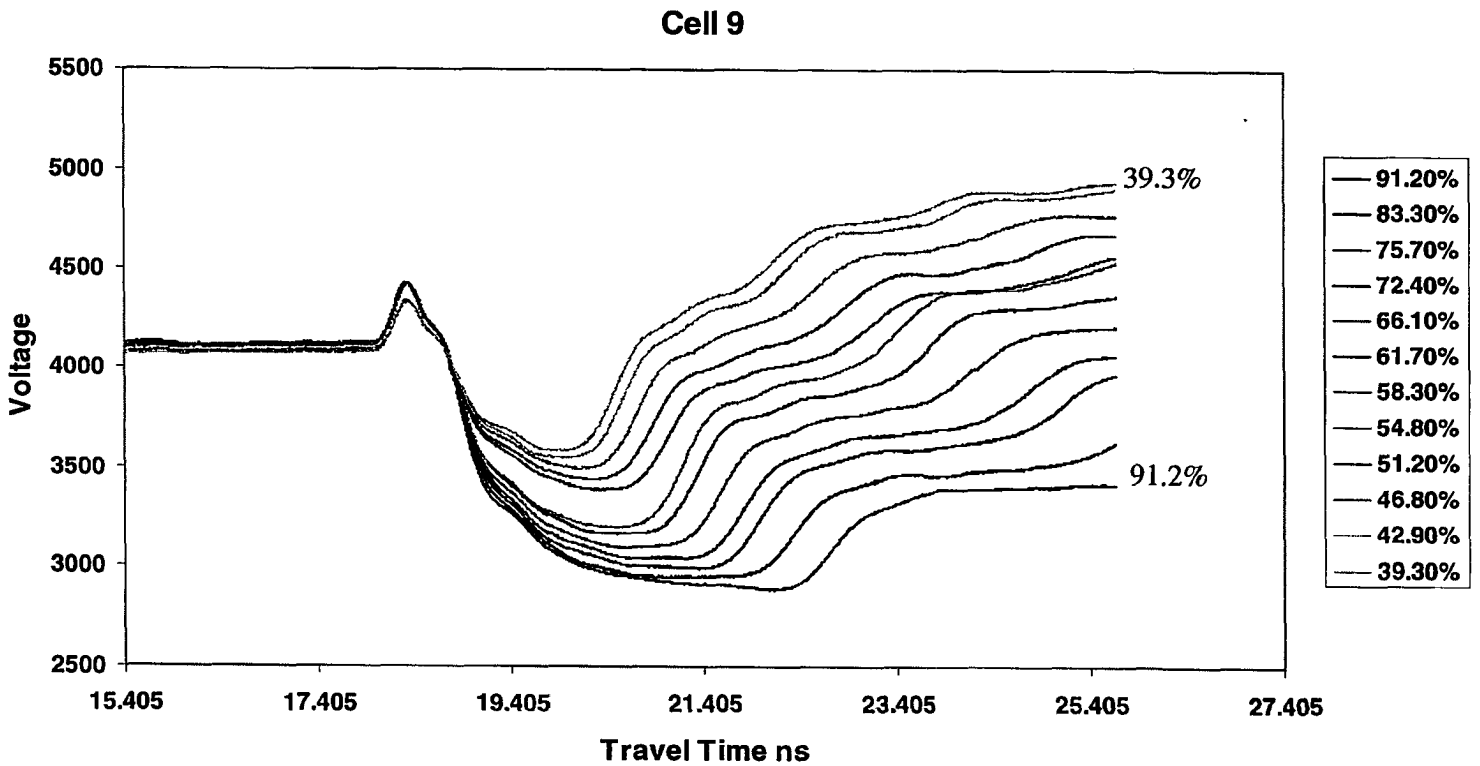

Figure A. 22: Waveforms for cell 9, bulk density 120 Kg/m^3

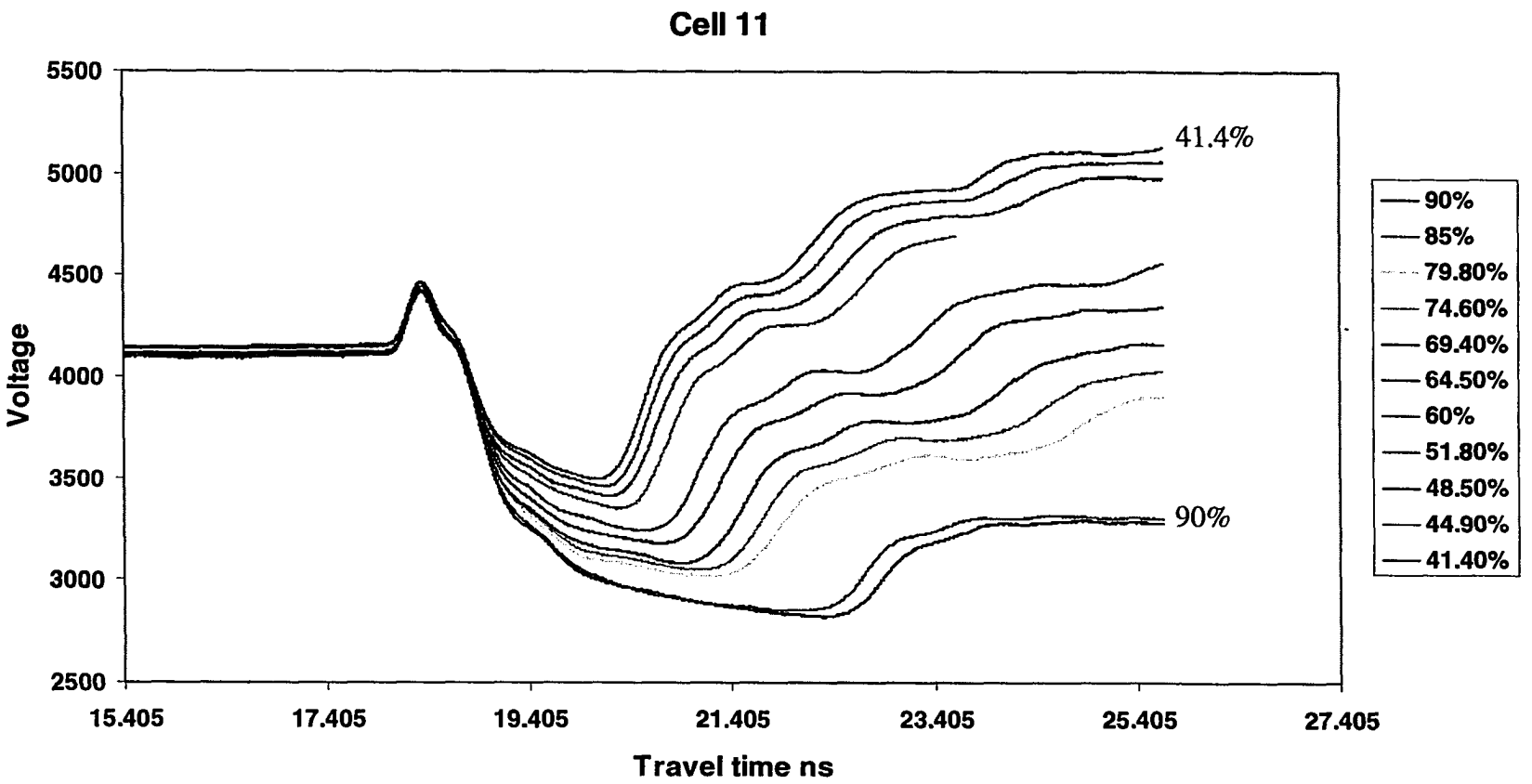

Figure A. 23: Waveforms for cell 11, bulk density 125 Kg/m^3

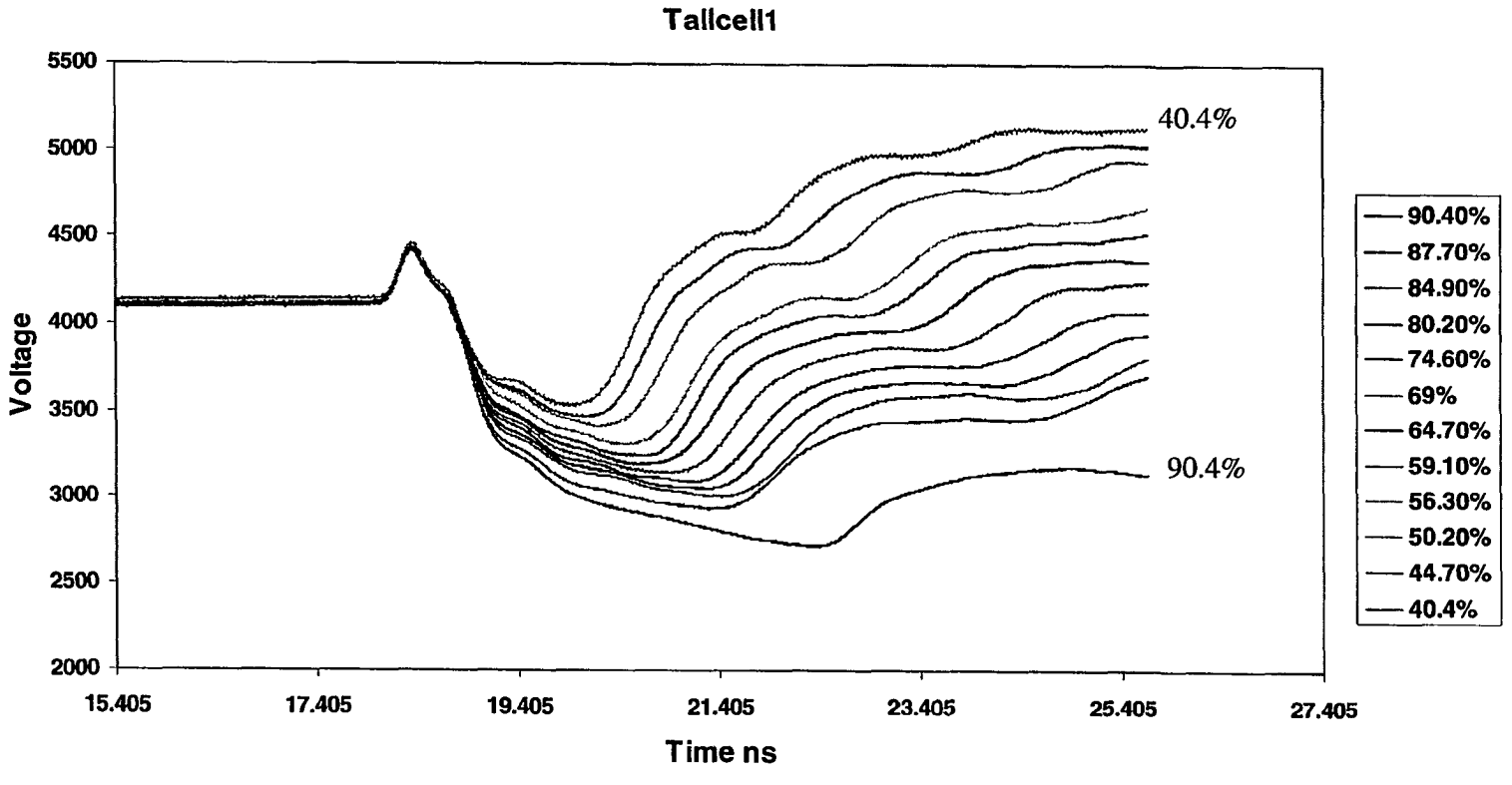

Figure A. 24: Waveforms for tall cell 1, bulk density 114 Kg/m^3

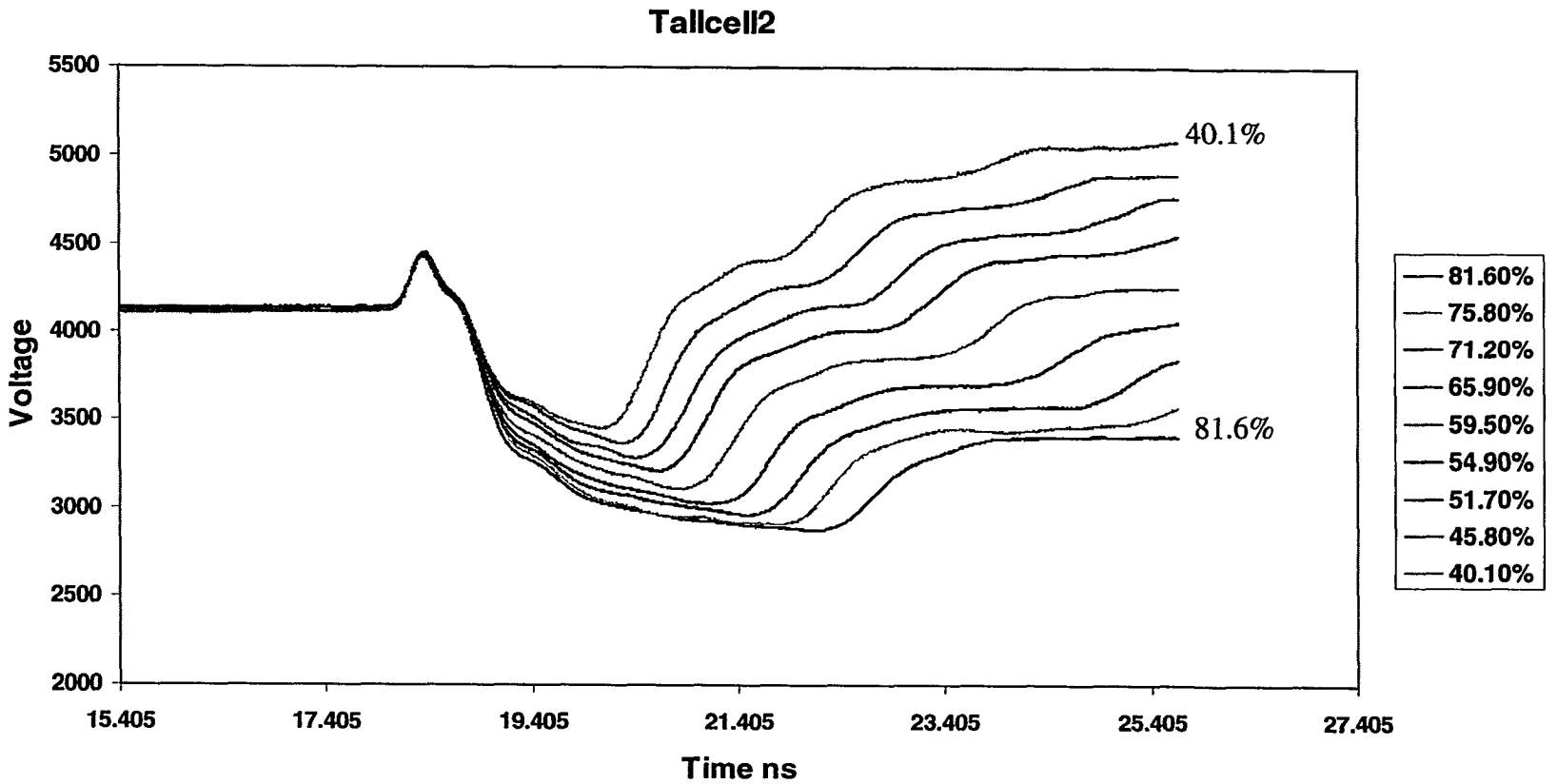

Figure A. 25: Waveforms for tall cell 2, bulk density 121Kg/m^3

APPENDIX B
DATA OBTAINED IN THE SIX PEAT COLUMNS DURING DRAINAGE

Experimental procedure

Presaturated peat was packed into six columns. Water contents were measured both by the vertical and horizontal TDR probes for the fours soil sections as illustrated in Figure 3.6 in section 3.6.1. Then the C-flex tubing connected to the drainage port of each column was lowered for several times to obtain a set of data of water content measured, the amount of water drained out of the column and suction applied to the peat. Gravimetric water contents were also determined at the end of the experiment.

Water contents measured by different methods were compared. In addition, drainage curves of the peat were obtained.

B 1: RAW DATA SETS

Table B.1: Drainage column data set #1: column 1

Column 1								
Height of peat packed cm:	49.5			Calculation of the dielectric constant of each soil section from directly measured travel times by the vertical probe:				
Internal diameter of column cm:	16.2							
	Soil section				Soil section	Δt ns measured	Δt ns in each soil section	Ka of each section
Volume of packed peat(cm^3):	1	2987.2233		Saturated	1	3.73	3.78	61.163
	2	2678.2002			2	6.86	3.13	52.173
	3	2678.2002			3	10.1	3.24	55.904
	4	1854.1386			4	12.72	2.62	56.036
	Total:	10197.7623		1 drain	1	2.25	2.25	21.671
					2	5.52	3.27	56.944
Dry bulk density (kg/m^3):	1	103.90921			3	8.9	3.38	60.84
	2	99.320432			4	11.43	2.53	57.608
	3	103.98775		2 drain	1	1.94	1.94	16.1105
	4	128.14576			2	4.48	2.54	34.358
	Ave.	107.13135			3	7.78	3.3	57.994
					4	10.32	2.54	58.064
Amount of water in peat at the end g:	1	1127.1		3 drain	1	1.66	1.66	11.796
	2	981.1			2	3.59	1.93	19.837
	3	1161.1			3	6.64	3.05	49.540
	4	1297.2			4	9.25	2.61	61.309
	Total:	4566.5		4 drain	1	1.46	1.46	9.125
					2	3.02	1.56	12.96
Volumetric water content at the end:	1	0.3773069			3	5.64	2.62	36.556
	2	0.3663281			4	7.89	2.25	45.563
	3	0.4335374						

			4	0.6996241		5 drain	1	1.39	1.39	8.271
			Ave.	0.4477943			2	2.91	1.52	12.304
							3	4.59	1.68	15.031
Total amount of water in peat at saturation g:				8382			4	6.35	1.76	27.878

	Horizontal		Vertical measured		Vertical sectional		Water collected	Water in peat	Actual θv	Weight of column g	suction cm H_2O
	K_a	Θ_h	Ka	Θ_v	Ka	Θ_v'					
Saturated											
1	59.4	0.865	63.5	0.881	61.163	0.871					0
2	55.9	0.848	57	0.853	52.173	0.830					
3	55.9	0.848	58.9	0.861	55.904	0.848					
4	56	0.849	58.3	0.859	56.036	0.849					
Ave.		0.853		0.859		0.850		8382	0.822	19385	
1st drain											
1	23.8	0.629	21.8	0.606	21.671	0.605					
2	57.6	0.856	36.3	0.737	56.944	0.853					
3	59.7	0.865	43.3	0.782	60.84	0.870					
4	57.9	0.857	45.1	0.793	57.608	0.856					
Ave.		0.792		0.793		0.785	643.1	7738.9	0.759	18745	12.7
2nd drain											
1	13.3	0.480	15.8	0.524	16.111	0.529					
2	43	0.781	23.8	0.629	34.358	0.723					
3	58.6	0.860	33.2	0.714	57.994	0.857					
4	55.8	0.848	39	0.756	58.064	0.858					
Ave.		0.725		0.756		0.726	660	7078.9	0.694	18085	21.3
3rd drain											
1	12.7	0.468	11.8	0.449	11.796	0.449					
2	20.3	0.588	15.3	0.515	19.837	0.582					
3	56.7	0.852	24.1	0.632	49.540	0.817					
4	54.4	0.841	31.7	0.702	61.309	0.872					
Ave.		0.668		0.702		0.657	650.7	6428.2	0.630	17430	29
4th drain											
1	10.3	0.414	9.2	0.385	9.125	0.383					

2	14.2	0.496	10.8	0.426	12.96	0.473					
3	28.2	0.672	17.4	0.548	36.556	0.739					
4	55.6	0.847	22.4	0.613	45.561	0.796					
Ave.		0.582		0.613		0.575	656.1	5772.1	0.566	16775	36.8
5th drain											
1	10	0.406	8.3	0.358	8.271	0.358		0.377			
2	13.3	0.479	10.1	0.409	12.304	0.460		0.366			
3	15.8	0.524	11.6	0.444	15.031	0.511		0.434			
4	24.1	0.632	14.5	0.502	27.878	0.669		0.700			
Ave.		0.497		0.502		0.481	1205.6	4566.5	0.448	15555	59
				Total water collected:			3815.5				
							Total weight loss of the column:			3830	

Table B.2: Drainage column data set #2: column 2

Column 2								
Height of peat packed cm:	50			Calculation of the dielectric constant of each soil section from directly measured travel times by the vertical probe:				
Internal diameter of column cm:	16.2				Soil section	Δt measured	Δt in each soil section	Ka of each section
	Soil section			Saturated	1	3.48	3.78	61.16319
Volume of packed peat(cm^3):	1	2987.223			2	6.66	3.18	53.85302
	2	2678.2			3	9.79	3.13	52.17284
	3	2678.2			4	12.41	2.62	56.03592
	4	1957.146		1 drain	1	2.3	2.3	22.64447
	Total:	10300.77			2	5.34	3.04	49.21562
Dry bulk density (kg/m^3):	1	99.62429			3	8.56	3.22	55.21633
	2	107.4976			4	11.1	2.54	58.0644
	3	113.0237		2 drain	1	1.96	1.96	16.44442
	4	111.8465			2	4.32	2.36	29.66059
	Ave.	107.4774			3	7.49	3.17	53.51485
Amount of water in peat at the end g:	1	1058			4	9.94	2.45	54.0225
	2	1100.2		3 drain	1	1.79	1.79	13.71553
	3	1226.1			2	3.56	1.77	16.68408
	4	1113.8			3	6.44	2.88	44.17136
	Total:	4498.1			4	8.75	2.31	48.0249
Water content at the end:	1	0.354175		4 drain	1	1.58	1.58	10.68614
	2	0.410798			2	3.34	1.76	16.49609
	3	0.457807			3	5.53	2.19	25.54136
	4	0.569094			4	7.78	2.25	45.5625
	Ave.	0.569094		5 drain	1	1.37	1.37	8.034293
Total amount of water in peat at saturation g:		8181.5			2	2.82	1.45	11.19675
					3	4.54	1.72	15.75479
					4	6.03	1.49	22.1395

	Horizontal		Vertical measured		Vertical sectional		water collected	water in peat	Actual Θ_v	Weight of column g	Suction cm H_2O
	Ka	Θ_h	Ka	Θ_v	K_a	Θ_v'					
saturated											
1	53	0.834374	51.9	0.82899	61.16319	0.871147					
2	56.6	0.851244	52.6	0.832429	53.85302	0.838473					
3	55.1	0.844349	52.5	0.831941	52.17284	0.830336					
4	55.2	0.844814	53.2	0.835341	56.03592	0.848672					
Ave.		0.843337		0.835341		0.847771		8181.5	0.794261	19315	0
1st drain											
1	18	0.557158	22.6	0.615578	22.64447	0.616082					
2	55.5	0.846206	33.8	0.718902	49.21562	0.815357					
3	54.4	0.841067	40.1	0.762776	55.21633	0.84489					
4	56.2	0.849423	42.6	0.778301	58.0644	0.857801					
Ave.		0.761657		0.778301		0.77331	654.5	7527	0.730722	18655	17.4
2nd drain											
1	14.5	0.501654	16.3	0.531692	16.44442	0.533957					
2	28.6	0.67602	22.2	0.610994	29.66059	0.685367					
3	54.5	0.841538	30.8	0.695043	53.51485	0.836856					
4	57	0.853051	36.3	0.73722	54.0225	0.839279					
Ave.		0.702124		0.73722		0.710088	620	6907	0.670532	18035	28.5
3rd drain											
1	10.9	0.428395	13.8	0.488952	13.71553	0.487376					
2	17.2	0.545488	15	0.510356	16.68408	0.537671					
3	52.9	0.833889	22.8	0.617839	44.17136	0.787599					
4	56.7	0.851697	27.5	0.665952	48.0249	0.80907					
Ave.		0.644695		0.665952		0.639633	664.3	6242.7	0.606042	17370	33.3
4th drain											
1	9.5	0.393107	10.6	0.421231	10.68614	0.423309					
2	15.5	0.518774	13.2	0.477542	16.49609	0.534762					
3	20.7	0.593035	16.8	0.539448	25.54136	0.646985					
4	57.2	0.85395	21.8	0.606326	45.5625	0.795559					
Ave.		0.565322		0.606326		0.58117	715.9	5526.8	0.536542	16655	41.2

5th drain											
1	10.4	0.416342	8.1	0.352182	8.034293	0.350091			0.354175		
2	13.3	0.479479	9.4	0.39039	11.19675	0.43529			0.410798		
3	13.3	0.479479	11.3	0.437647	15.75479	0.522959			0.457807		
4	16.3	0.531692	13.3	0.479479	22.1395	0.610293			0.569094		
Ave.		0.47109		0.479479		0.466627	1028.7	4498.1	0.436676	15620	59
				Total water collected g:			3683.4				
							Total weight loss g:			3695	

Table B.3: Drainage column data set #3: column 3

Column 3							
Height of peat packed cm:		50		Calculation of the dielectric constant of each soil section from directely measured travel times by the vertical probe:			
Internal diameter of column cm:		16.2					
	Soil section				Soil section	Δt measured ns	Δt in each soil section ns
Volume of packed peat(cm^3):	1	2987.223		Saturated	3.78	3.78	61.16319
	2	2678.2			6.95	3.17	53.51485
	3	2678.2			10.24	3.29	57.64314
	4	1957.146			12.66	2.42	58.40177
	Ave.	10300.77		1 drain	2.54	1.75	13.10939
Dry bulk density (kg/m^3):	1	97.2475			5.75	3.21	54.87391
	2	106.1907			9	3.25	56.25
	3	124.4866			11.26	2.26	50.93452
	4	111.0801		2 drain	1.78	1.78	13.56271
	Ave.	109.2831			4.65	2.87	43.86515
Amount of water in peat at the end g:	1	1021			7.82	3.17	53.51485
	2	1063.1			10.15	2.33	54.13861
	3	1360.9		3 drain	1.65	1.69	12.22587

	4	1038.6		3.63	1.98	20.87787
	Total:	4483.6		6.47	2.84	42.9529
				8.61	2.14	45.66914
Water content at the end:	1	0.341789	**4 drain**	1.37	1.37	8.034293
	2	0.396946		3.05	1.68	15.03053
	3	0.50814		5.22	2.17	25.07698
	4	0.530671		7.3	2.08	43.14416
	Ave.	0.435268	**5 drain**	1.36	1.36	7.917432
Total amount of water in peat at saturation g:		8326.9		2.94	1.58	13.29444
				5.02	2.08	23.04
				7.09	2.07	42.7303
			6 drain	1.31	1.31	7.345969
				2.84	1.53	12.46633
				4.49	1.65	14.49852
				5.92	1.43	20.39235

	Horizontal		Vertical measured		Vertical sectional		Water Collected g	Water in peat g	Actual θ_v	Weight of column g	Suction cm H_2O
	Ka	Θ_h	Ka	Θ_v	K_a	Θ_v'					
saturated											
1	57.5	0.855293	61.2	0.871302	61.16319	0.871147					
2	58.6	0.860158	57.5	0.855293	53.51485	0.836856					
3	57.2	0.85395	57.3	0.854399	57.64314	0.855931					
4	58.4	0.85928	57.6	0.855739	58.40177	0.859288					
Ave.		0.856966	57.6			0.856022		8326.9	0.808376	19445	0
1st drain											
1	20.2	0.586759	27.6	0.666883	13.10939	0.475774					
2	59.4	0.863638	39.4	0.758256	54.87391	0.843293					
3	57.1	0.853501	44.3	0.788346	56.25	0.849651					
4	57.1	0.853501	45.6	0.79577	50.93452	0.82417					
Ave.		0.778782	45.6			0.734732	623.2	7703.7	0.747876	18820	13.4
2nd drain											
1	14.9	0.508639	13.6	0.485205	13.56271	0.4845					

2	47.7	0.807328	25.8	0.649571	43.86515	0.785814					
3	59	0.861904	33.5	0.716614	53.51485	0.836856					
4	59	0.861904	37	0.742123	54.13861	0.83983					
Ave.		0.745267	37			0.721967	637.5	7066.2	0.685988	18175	21
3rd drain											
1	12.7	0.467629	11.7	0.446576	12.22587	0.457862					
2	18	0.557158	15.6	0.520424	20.87787	0.595232					
3	58.5	0.859719	22.9	0.618963	42.9529	0.780419					
4	58.5	0.859719	26.7	0.658373	45.66914	0.796159					
Ave.		0.667347	26.7			0.641719	622	6444.2	0.625604	17550	29.3
4th drain											
1	11.6	0.444373	8	0.348993	8.034293	0.350091					
2	13.4	0.481402	11	0.43074	15.03053	0.510878					
3	24.7	0.638386	15	0.510356	25.07698	0.642275					
4	58.3	0.85884	21.5	0.602769	43.14416	0.781559					
Ave.		0.583193	21.5			0.549842	644.9	5799.3	0.562997	16905	37.7
5th drain											
1	10.2	0.411357	7.9	0.345764	7.917432	0.346329					
2	12	0.453076	10.4	0.416342	13.29444	0.479372					
3	19	0.571037	13.8	0.488952	23.04	0.620527					
4	57.3	0.854399	18.3	0.561402	42.7303	0.779085					
Ave.		0.547899	18.3			0.534435	614.6	5184.7	0.503331	16285	45
6th drain											
1	9.8	0.401088	7.4	0.32898	7.345969	0.327099			0.341789		
2	11.2	0.435365	9.6	0.395795	12.46633	0.462862			0.396946		
3	15.5	0.518774	11.1	0.433063	14.49852	0.501628			0.50814		
4	18.2	0.559995	12.8	0.469643	20.39235	0.589192			0.530671		
Ave.		0.47079	12.8			0.457572	701.1	4483.6	0.435268	15565	59
				Total water collected g:			3843.3				
									Total weight loss g:	3880	

Table B.4: Drainage column data set #4: column 4

Column 4		
Height of peat packed cm:	50	
Internal diameter of column cm:	16.2	
	Soil section	
Volume of packed peat(cm^3):	1	2987.2233
	2	2678.2002
	3	2678.2002
	4	1957.1463
	Ave.	10300.77
Dry bulk density (kg/m^3):	1	97.046645
	2	97.528183
	3	110.26061
	4	105.40857
	Ave.	102.19624
Amount of water in peat at the end g:	1	1017
	2	977.1
	3	1193.7
	4	1019.2
	Total:	4207
Water content at the end:	1	0.3404499
	2	0.3648346
	3	0.4457098
	4	0.5207582
	Ave.	0.4084161
Total amount of water in peat at saturation g:		8118.1

Calculation of the dielectric constant of each soil section from directly measured travel times by the vertical probe:

	Soil section	**Δt measured ns**	**Δt in each soil section ns**	**K_a of each section**
Saturated	1	3.78	3.78	61.16319
	2	7.26	3.48	64.49325
	3	10.7	3.44	63.01917
	4	13.49	2.79	70.0569
1 drain	1	2.6	2.6	28.93698
	2	5.85	3.25	56.25
	3	9.41	3.56	67.49254
	4	11.71	2.3	52.75346
2 drain	1	1.87	1.87	14.96889
	2	4.59	2.72	39.39976
	3	8	3.41	61.92479
	4	10.43	2.43	58.88543
3 drain	1	1.78	1.78	13.56271
	2	4.03	2.25	26.96006
	3	7.2	3.17	53.51485
	4	9.63	2.43	58.88543
4 drain	1	1.5	1.5	9.631391
	2	3.11	1.61	13.80408
	3	6.03	2.92	45.40686
	4	8.27	2.24	50.03701
5 drain	1	1.48	1.48	9.376266
	2	2.97	1.49	11.82302
	3	5.1	2.13	24.16101
	4	7.21	2.11	44.39767

						6 drain	1	1.32	1.32	7.458549
							2	2.66	1.34	9.562367
							3	4.24	1.58	13.29444
							4	6.06	1.82	33.03224

	Horizontal		Vertical measured		Vertical sectional		Water collected	Water in peat	Actual θv	Weight of column g	Suction cm H2O
	K_a	Θ_h	K_a	Θ_v	K_a	Θ_v'					
saturated											
1	64.8	0.885974	61.1	0.8708818	61.163187	0.871147					
2	61.2	0.871302	62.5	0.8766973	64.493254	0.884756					
3	62	0.874635	63.4	0.8803674	63.019172	0.878821					
4	63.5	0.880772	65.4	0.8883401	70.0569	0.905997					
Ave.		0.878223	65.4	0.8883401		0.883302		8118.1	0.788106	19485	0
1st drain											
1	24.5	0.636299	28.8	0.6778084	28.93698	0.679026					
2	60.5	0.868349	40.7	0.7665888	56.25	0.849651					
3	62.6	0.877108	48.5	0.8115974	67.492544	0.896425					
4	62.3	0.875874	50.3	0.8209519	52.753463	0.833177					
Ave.		0.804762	50.3	0.8209519		0.809201	619.6	7498.5	0.727955	18865	13.3
2nd drain											
1	17.4	0.548456	15	0.5103565	14.968894	0.509824					
2	41.1	0.769099	25.1	0.6425102	39.399763	0.758254					
3	61.5	0.872557	35	0.7278578	61.924793	0.874324					
4	61.4	0.872139	39.9	0.7614928	58.885429	0.861405					
Ave.		0.751589	39.9	0.7614928		0.735986	615.7	6882.8	0.668183	18245	22
3rd drain											
1	13.7	0.487086	13.6	0.4852049	13.562711	0.4845					
2	18.4	0.5628	19.3	0.575059	26.960059	0.660861					
3	62.5	0.876697	28.4	0.6742181	53.514852	0.836856					
4	62.4	0.876286	34	0.7204167	58.885429	0.861405					
Ave.		0.682019	34	0.7204167		0.693578	637	6245.8	0.606343	17605	29.3
4th drain											
1	12.8	0.469643	9.6	0.3957946	9.6313912	0.396633					

2	14.9	0.508639	11.5	0.4421505	13.804083	0.489028					
3	30.5	0.69253	20	0.5842045	45.406864	0.794681					
4	62.6	0.877108	21.1	0.5979484	45.1584	0.793272					
Ave.		0.615151	21.1	0.5979484		0.59951	658.3	5587.5	0.542435	16970	36
5th drain											
1	11.4	0.439909	9.4	0.3903902	9.3762663	0.389741					
2	13	0.473623	10.5	0.418798	11.823018	0.449261					
3	16.7	0.537915	14.2	0.4962872	24.161006	0.632723					
4	62.2	0.875462	19	0.5710375	44.397673	0.788911					
Ave.		0.556911	19	0.5710375		0.544234	679.6	4907.9	0.47646	16365	42.2
6th drain											
1	10.7	0.423642	7.4	0.3289799	7.4585493	0.331003			0.34045		
2	11.8	0.448761	8.4	0.3615171	9.5623669	0.394786			0.364835		
3	14.2	0.496287	9.9	0.4036937	13.294438	0.479372			0.44571		
4	29.8	0.68657	13.5	0.4833104	29.8116	0.68667			0.520758		
		0.499017		0.4833104		0.453739	700.9	4207	0.408416	15730	50.3
				Total water collected g:			3911.1				
								Total weight loss g:		3755	

Table B.5: Drainage column data set #5: Column 5

Column5							
Height of peat packed cm:	50			Calculation of the dielectric constant of each soil section from directly measured travel times by the vertical probe:			
Internal diameter of column cm:	16.2						
	Soil section				Soil section	Δt measured ns	Δt in each soil section ns	Ka of each section
Volume of packed peat(cm^3):	1	2987.223						
	2	2678.2		Saturated	1	3.63	3.63	56.40528
	3	2678.2			2	6.77	3.14	52.50675
	4	1957.146			3	10.16	3.39	61.20053
	Total:	10300.77			4	12.33	2.17	46.95856
				1 drain	1	2.69	2.6	28.93698
Dry bulk density (kg/m^3):	1	95.47328			2	5.76	3.07	50.19178
	2	107.2735			3	9.07	3.31	58.34609
	3	100.8513			4	11.32	2.25	50.48476
	4	104.3356		2 drain	1	1.76	1.87	14.96889
	Ave.	101.6235			2	4.71	2.95	46.34467
Amount of water in peat at the end g:	1	956.2			3	7.74	3.03	48.89237
	2	926.4			4	10.27	2.53	63.83169
	3	1108.6		3 drain	1	1.65	1.78	13.56271
	4	1139			2	3.75	2.1	23.48521
	Total:	4130.2			3	6.98	3.23	55.55982
					4	9.15	2.17	46.95856
Water content at the end:	1	0.320097		4 drain	1	1.59	1.5	9.631391
	2	0.345904			2	3.09	1.5	11.98225
	3	0.413935			3	5.57	2.48	32.75361
	4	0.58197			4	7.85	2.28	51.84
	Ave.			5 drain	1	1.51	1.48	9.376266
Total amount of water in peat at saturation g:		8337.4			2	2.84	1.33	9.420178
					3	4.64	1.8	17.25444
					4	6.61	1.97	38.7015

						6 drain	1	1.31	1.32	7.458549	
							2	2.55	1.24	8.188402	
							3	4.23	1.68	15.03053	
							4	5.82	1.59	25.21097	

	Horizontal		Vertical measured		Vertical sectional		water collected	water in peat	Actual θv	weight of column g	suction cm H2O
	K_a	Θ_h	K_a	Θ_v	K_a	Θ_v'					
Saturated											
1	49.9	0.818902	56.8	0.852149	56.40528	0.850359					
2	58.3	0.85884	54.5	0.841538	52.50675	0.831974					
3	53.2	0.835341	56.6	0.851244	61.20053	0.871304					
4	54	0.839172	53.6	0.837264	46.95856	0.803306					
Ave.		0.837411		0.837264		0.842084		8337.4	0.809396	19335	0
1st drain											
1	20.9	0.595504	31	0.696705	28.93698	0.679026					
2	58.8	0.861032	39.4	0.758256	50.19178	0.820399					
3	58.2	0.858399	45.1	0.79294	58.34609	0.859043					
4	58.6	0.860158	46.1	0.79857	50.48476	0.821893					
Ave.		0.783178		0.79857		0.789732	633	7704.4	0.747944	18695	12
2nd drain											
1	15.4	0.517112	13.2	0.477542	14.96889	0.509824					
2	56.9	0.852601	26.4	0.655473	46.34467	0.799929					
3	56.4	0.850335	32.8	0.711193	48.89237	0.813666					
4	58.4	0.85928	37.2	0.743506	63.83169	0.882109					
Ave.		0.755989	39.9	0.743506		0.734984	738.1	6966.3	0.676289	17950	20.5
3rd drain											
1	12.4	0.461493	11.6	0.444373	13.56271	0.4845					
2	17.5	0.549927	16.7	0.537915	23.48521	0.62544					
3	58.9	0.861468	26.7	0.658373	55.55982	0.846482					
4	58.8	0.861032	30.1	0.689142	46.95856	0.803306					
Ave.		0.664392	34	0.689142		0.675833	701.1	6265.2	0.608226	17250	28
4th drain											

1	11.4	0.439909	10.8	0.426029	9.631391	0.396633					
2	14.8	0.506911	11.4	0.439909	11.98225	0.452696					
3	30.8	0.695043	17	0.542486	32.75361	0.71083					
4	58.3	0.85884	22.1	0.609835	51.84	0.828693					
Ave.		0.603261	21.1	0.609835		0.574992	704.5	5560.7	0.539833	16545	36.5
5th drain											
1	9.2	0.38487	9.5	0.393107	9.376266	0.389741					
2	11.3	0.437647	9.6	0.395795	9.420178	0.390941					
3	13.6	0.485205	11.8	0.448761	17.25444	0.546299					
4	57	0.853051	15.7	0.522065	38.7015	0.753664					
Ave.		0.513633	19	0.522065		0.499904	754.9	4805.8	0.466548	15790	47.3
6th drain											
1	9.3	0.387645	7.7	0.339181	7.458549	0.331003			0.320097		
2	11.1	0.433063	7.7	0.339181	8.188402	0.354968			0.345904		
3	12.6	0.4656	9.8	0.401088	15.03053	0.510878			0.413935		
4	20	0.584204	12.2	0.457319	25.21097	0.643643			0.58197		
		0.457068		0.457319		0.443403	675.6	4130.2	0.40096	15105	59
				Total water collected g:			4207.2				
							Total weight loss g:			4230	

Table B.6: Drainage column data set #6: Column 6

Column 6								
Height of peat packed cm:	50.5			**Calculation of the dielectric constant of each soil section from directly measured travel times by the vertical probe:**				
Internal diameter of column cm:	16.2				**Soil section**	**Δt Measured ns**	**Δt in each soil section ns**	**Ka of each section**
	Soil section			**Saturated**	1	3.78	3.78	61.16319
Volume of packed peat(cm^3):	1	2987.223			2	7.26	3.48	64.49325
	2	2678.2			3	10.7	3.44	63.01917
	3	2678.2			4	13.49	2.79	70.0569
	4	2060.154		**1 drain**	1	2.6	2.6	28.93698
	Ave.	10403.78			2	5.85	3.25	56.25
Dry bulk density (kg/m^3):	1	96.1428			3	9.41	3.56	67.49254
	2	101.6354			4	11.71	2.3	52.75346
	3	107.7589		**2 drain**	1	1.87	1.87	14.96889
	4	123.2432			2	4.59	2.72	39.39976
	Ave.	105.9135			3	8	3.41	61.92479
Amount of water in peat at the end g:	1	974.8			4	10.43	2.43	58.88543
	2	1066.3		**3 drain**	1	1.78	1.78	13.56271
	3	1330.5			2	4.03	2.25	26.96006
	4	1485			3	7.2	3.17	53.51485
	Total:	4856.6			4	9.63	2.43	58.88543
Water content at the end:	1	0.326323		**4 drain**	1	1.5	1.5	9.631391
	2	0.398141			2	3.11	1.61	13.80408
	3	0.496789			3	6.03	2.92	45.40686
	4	0.72082			4	8.27	2.24	50.03701
	Ave.	0.466811		**5 drain**	1	1.48	1.48	9.376266
Total amount of water in peat at saturation g:		8560.9			2	2.97	1.49	11.82302
					3	5.1	2.13	24.16101
					4	7.21	2.11	44.39767

						6 drain	1	1.32	1.32	7.458549	
							2	2.66	1.34	9.562367	
							3	4.24	1.58	13.29444	
							4	6.06	1.82	33.03224	
Horizontal			Vertical measured		Vertical sectional		Water collected	Water in peat	Actual Θ_v	Weight of column g	Suction cm H2O
	Ka	Θ_h	Ka	Θ_v	Ka	Θ_v'					
Saturated											
1	53.2	0.835341	58.5	0.859719	61.16319	0.871147					
2	58.8	0.861032	55.2	0.844814	64.49325	0.884756					
3	55.1	0.844349	55.9	0.848049	63.01917	0.878821					
4	55.2	0.844814	58.3	0.85884	70.0569	0.905997					
Ave.		0.846149		0.85884		0.883527		8560.9	0.822865	19700	0
1st drain											
1	23.8	0.628858	29.6	0.684842	28.93698	0.679026					
2	59.7	0.864932	38.9	0.754977	56.25	0.849651					
3	58.4	0.85928	44.4	0.788925	67.49254	0.896425					
4	64	0.882785	47.2	0.804623	52.75346	0.833177					
Ave.		0.799229		0.804623		0.809438	657.3	7903.6	0.759686	19015	12.6
2nd drain											
1	17.3	0.546976	16.1	0.528523	14.96889	0.509824					
2	53.8	0.83822	26.7	0.658373	39.39976	0.758254					
3	56.9	0.852601	34.6	0.724907	61.92479	0.874324					
4	63.3	0.879962	39.5	0.758906	58.88543	0.861405					
Ave.		0.766563		0.758906		0.737228	691.9	7211.7	0.693181	18325	21.5
3rd drain											
1	11.7	0.446576	11.2	0.435365	13.56271	0.4845					
2	20.3	0.588026	15.5	0.518774	26.96006	0.660861					
3	58.1	0.857958	26	0.651553	53.51485	0.836856					
4	63.5	0.880772	33.6	0.717379	58.88543	0.861405					
average		0.674869		0.717379		0.69524	681.4	6530.3	0.627685	17640	29.4
4th drain											

1	10.8	0.426029	10.1	0.408828	9.631391	0.396633					
2	13.9	0.490806	12.6	0.4656	13.80408	0.489028					
3	21.8	0.606326	18.9	0.569683	45.40686	0.794681					
4	65.2	0.887554	24.5	0.636299	45.1584	0.793272					
Ave.		0.580509		0.636299		0.601428	732.5	5797.8	0.557278	16905	38.5
5th drain											
1	10.7	0.423642	8.4	0.361517	9.376266	0.389741					
2	13	0.473623	9.7	0.398455	11.82302	0.449261					
3	15.5	0.518774	12.3	0.459414	24.16101	0.632723					
4	46.5	0.800787	17.2	0.545488	44.39767	0.788911					
Ave.		0.53568		0.545488		0.546656	611.6	5186.2	0.498492	16295	48.6
6th drain											
1	9.4	0.39039	6.2	0.283562	7.458549	0.331003			0.326323		
2	10.9	0.428395	8	0.348993	9.562367	0.394786			0.398141		
3	12	0.453076	10.2	0.411357	13.29444	0.479372			0.496789		
4	28	0.670577	14.2	0.496287	29.8116	0.68667			0.72082		
		0.471793		0.496287		0.456046	329.6	4856.6	0.466811	15965	59
				Total water collected g:			3704.3				
							Total weight loss g:			3735	

B 2: WATER CONTENT PROFILES WITH DEPTH FOR COLUMNS 3, 5, 6 MEASURED BY THE HORIZONTAL AND VERTICAL TDR PROBES

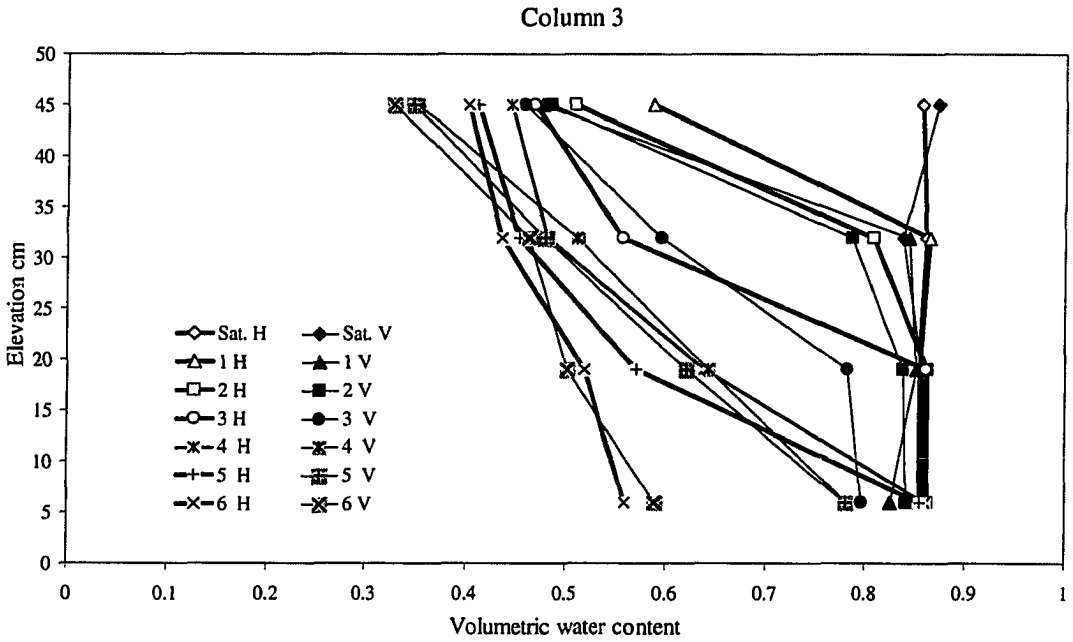

Figure B.1: Water content profiles with depth in column 3

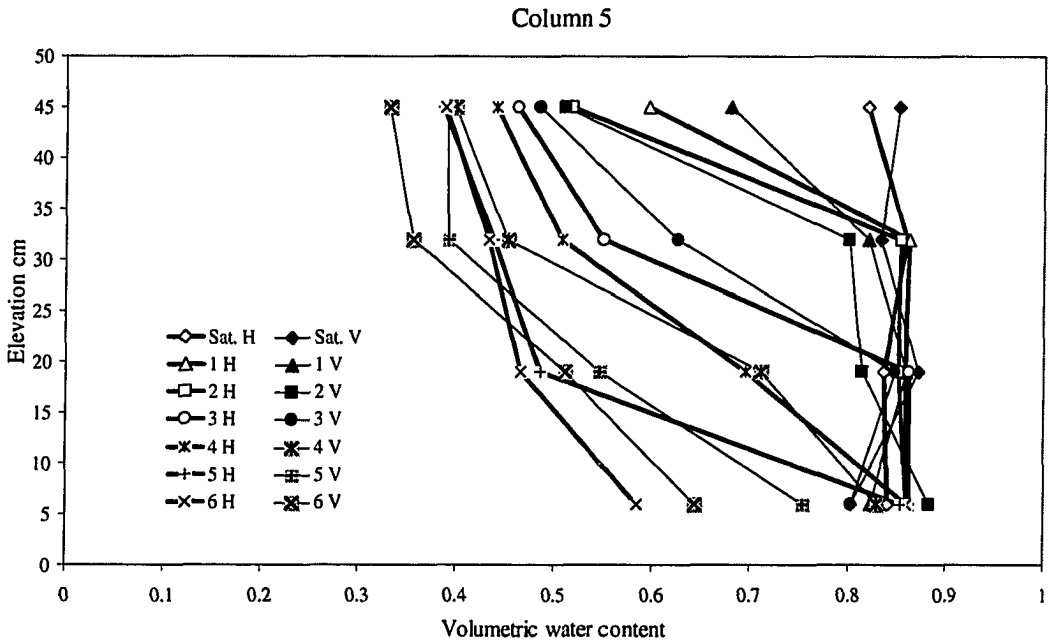

Figure B.2: Water content profiles with depth in column 5

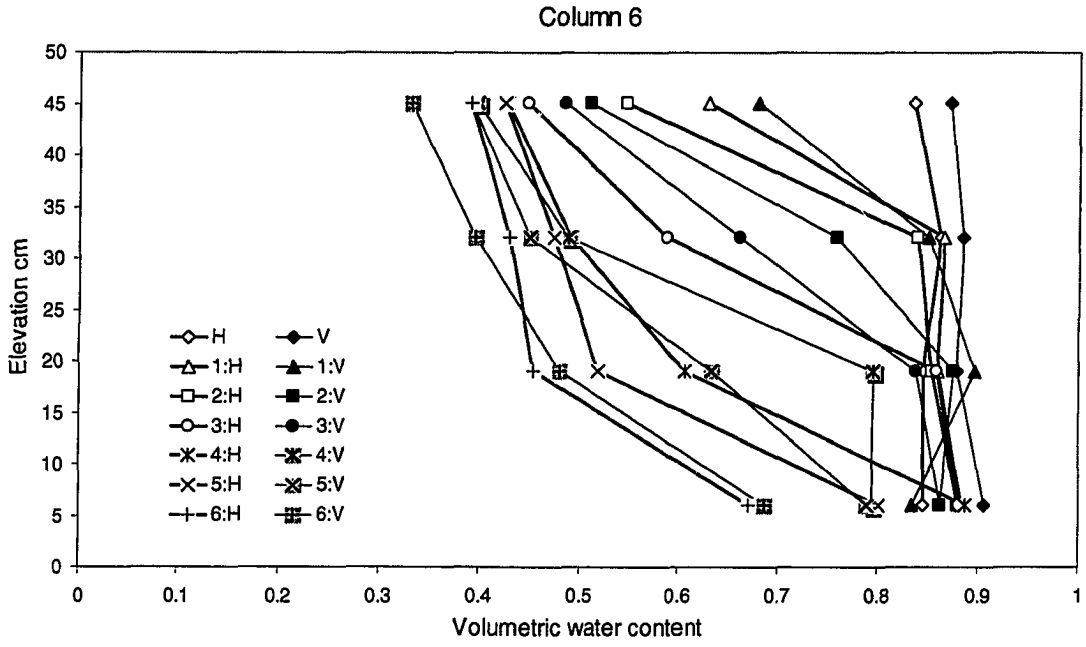

Figure B.3: Water content profiles with depth in column 6

B3: DESCRIPTIVE STATISTICS AND PAIRED T-TEST RESULTS FOR COMPARISON OF WATER CONTENTS MEASURED BY DIFFERENT METHODS

Table B. 7: Comparison of water contents measured by the vertical probe (Θ_v) and the horizontal probe (Θ_h)

Descriptive statistics of Θ_h-Θ_v	
	Θ_h-Θ_v
Mean	0.0064
Standard Error	0.0037
Median	0.0114
Mode	0.0244
Standard Deviation	0.047
Sample Variance	0.0022
Kurtosis	1.2196
Skewness	-0.5651
Range	0.2993
Minimum	-0.1884
Maximum	0.111
Sum	1.0309
Count	160

t-Test: Paired Two Sample for Means		
	Θ_h	Θ_v
Mean	0.6849	0.678
Variance	0.0331	0.034
Observations	160	160
Pearson Correlation	0.9669	
Hypothesized Mean Difference	0	
df	159	
t Stat	1.7343	
P(T<=t) one-tail	0.0424	
t Critical one-tail	1.6545	
P(T<=t) two-tail	0.0848	
t Critical two-tail	1.975	

Table B.8: Comparison of the vertical probe water content (Θ_v) with the gravimetric (Θ_g)

Descriptive statistics of Θ_v- Θ_g	
	Θ_v- Θ_g
Mean	0.0411
Standard Error	0.0038
Median	0.0421
Mode	#N/A
Standard Deviation	0.0241
Sample Variance	0.0006
Kurtosis	0.7026
Skewness	-0.213
Range	0.1084
Minimum	-0.013
Maximum	0.0952
Sum	1.6436
Count	40

t-Test: Paired Two Sample for Means		
	Θ_v	Θ_g
Mean	0.665	0.6239
Variance	0.0184	0.0166
Observations	40	40
Pearson Correlation	0.9848	
Hypothesized Mean Difference	0	
df	39	
t Stat	10.796	
P(T<=t) one-tail	1E-13	
t Critical one-tail	1.6849	
P(T<=t) two-tail	3E-13	
t Critical two-tail	2.0227	

Table B. 9: Comparison of the horizontal probe water content (Θ_h) with the gravimetric (Θ_g)

Descriptive statistics of $\Theta_h - \Theta_g$	
	$\Theta_h - \Theta_g$
Mean	0.04693
Standard Error	0.00344
Median	0.04064
Mode	#N/A
Standard Deviation	0.02174
Sample Variance	0.00047
Kurtosis	-0.61535
Skewness	0.49267
Range	0.08562
Minimum	0.00498
Maximum	0.0906
Sum	1.87703
Count	40

t-Test: Paired Two Sample for Means		
	Θ_h	Θ_g
Mean	0.67084	0.62391
Variance	0.01673	0.01657
Observations	40	40
Pearson Correlation	0.98582	
Hypothesized Mean Difference	0	
df	39	
t Stat	13.6518	
P(T<=t) one-tail	9.7E-17	
t Critical one-tail	1.68488	
P(T<=t) two-tail	1.9E-16	
t Critical two-tail	2.02269	

Table B. 10: Comparison of TDR measured water contents (Θ_T) with the gravimetric (Θ_g)

Descriptive statistics of $\Theta_T - \Theta_g$	
	$\Theta_T - \Theta_g$
Mean	0.044
Standard Error	0.0026
Median	0.0418
Mode	#N/A
Standard Deviation	0.023
Sample Variance	0.0005
Kurtosis	0.2894
Skewness	0.0437
Range	0.1084
Minimum	-0.013
Maximum	0.0952
Sum	3.5206
Count	80

t-Test: Paired Two Sample for Means		
	Θ_T	Θ_g
Mean	0.6679	0.6239
Variance	0.0174	0.0164
Observations	80	80
Pearson Correlation	0.9848	
Hypothesized Mean Difference	0	
df	79	
t Stat	17.13	
P(T<=t) one-tail	1E-28	
t Critical one-tail	1.6644	
P(T<=t) two-tail	3E-28	
t Critical two-tail	1.9905	

Table B. 11: Comparison of TDR measured water contents (Θ_T) with the gravimetric (Θ_g) in individual soil sections at the end of the experiments

Descriptive statistics of $\Theta_T - \Theta_g$	
	$\Theta_T - \Theta_g$
Mean	0.036165
Standard Error	0.007324
Median	0.034968
Mode	#N/A
Standard Deviation	0.025372
Sample Variance	0.000644
Kurtosis	1.600552
Skewness	0.240882
Range	0.101367
Minimum	-0.01077
Maximum	0.090601
Sum	0.433981
Count	12

t-Test: Paired Two Sample for Means		
	Θ_T	Θ_g
Mean	0.46882	0.4327
Variance	0.000292	0.0005
Observations	12	12
Pearson Correlation	0.244451	
Hypothesized Mean Difference	0	
df	11	
t Stat	4.937793	
P(T<=t) one-tail	0.000222	
t Critical one-tail	1.795884	
P(T<=t) two-tail	0.000444	
t Critical two-tail	2.200986	

B 4: DRAINAGE CURVES OBTAINED IN SIX COLUMNS

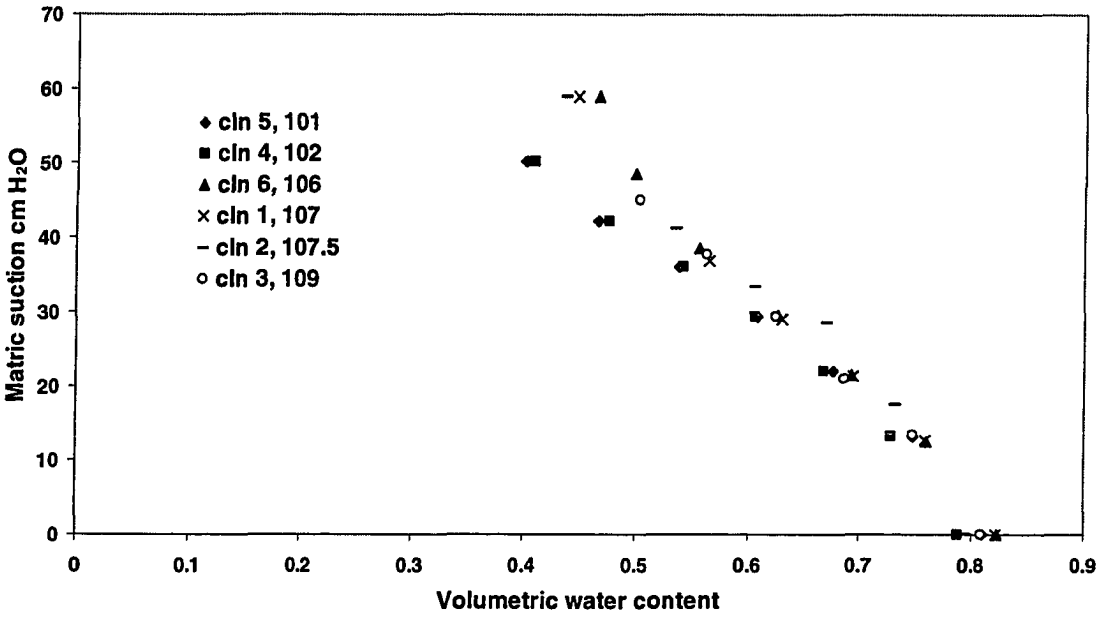

Figure B.4: Drainage curves obtained in six columns of various bulk densities (101-109 Kg/m^3)

APPENDIX C
DATA OBTAINED IN THE TWO COLUMNS DURING A CLOGGING PROCESS

Experimental Procedure

Column A and B were packed with saturated peat, gravity drained and pulsed with high organic loading twice a day. Water contents in the four soil sections of each column at saturation, after gravity drainage and at various times during the clogging process were monitored by both the horizontal and vertical TDR probes. At the end of the experiment, each column was dismantled into 8 soils sections to obtain the gravimetric water content in each section. The illustration of horizontal and vertical probe locations and column dismantlement were illustrated in Figure 3.6 and Figure 3. 7 in sections 3.6.1 and 3.8.

C 1: RAW DATA

Table C.1: Raw data obtained in column A during the clogging process

Column A		
Height of peat packed cm:		51
Internal diameter of column cm:		16.2
Volume of packed peat(cm^3):		
Soil sections	1	2987
	2	2678
	3	2678
	4	2163
	Total:	10301

Dismantlement of the column at the end									TDR measured water content	
Soil section	Tray only g	Tray + wet peat g	Tray + dry peat g	Dry peat g	Water in g	Section volume cm^3	Bulk D. Kg/m^3	Water content	Horizontal	Vertical
1	39.1	775	168.2	129.1	606.8	824.062	156.663	0.736		
2	39.5	1107.3	229.5	190	877.8	1648.123	115.283	0.533	0.627	0.704
3	39.1	769	169.6	130.5	599.4	1030.077	126.690	0.582		
4	39.1	1176	243.3	204.2	932.7	1648.123	123.899	0.566	0.599	0.620
5	39.2	827	176.3	137.1	650.7	1030.077	133.097	0.632		
6	39.1	1219.4	239.9	200.8	979.5	1648.123	121.836	0.594	0.711	
7	39.1	756.6	153.6	114.5	603	1030.077	111.157	0.585		
8	39.1	1406.2	237.9	198.8	1168.3	1442.108	137.854	0.810	0.772	
			Sum:	1305	6418.2	10300.770				
					Average :		126.690	0.623		

Elevation cm	Horizontal		Vertical measured		Vertical sectional					
	K_a	Θ_h	K_a	Θ_v	K_a	Θ_v'	Weight of column g	Weight change g	Water in column g	Gravimetric W. content
Saturated, Aug. 09, 2004										
45	58.2	0.858	59.6	0.865	59.556	0.864				
32	57	0.853	52.8	0.833	46.031	0.798				
19	53.5	0.837	57.1	0.854	49.540	0.817				
6	56.1	0.849	56.2	0.849	56.036	0.849				
	Ave.	0.850		0.849		0.832	19465		8328.2	0.809
After gravity drainage, Aug. 10, 2004, Weight										
45	12.2	0.457	14.7	0.505	14.650	0.504				
32	15.3	0.515	14.2	0.496	13.804	0.489				
19	14.7	0.505	15.3	0.515	17.640	0.552				
6	34.2	0.722	17.6	0.551	29.160	0.681				
	Ave.	0.539		0.551		0.549	16250	-3215	5113.2	0.496
Before second pause of water in the afternoon, Aug. 11										
45	12.7	0.468	13	0.474	12.960	0.473				
32	14.3	0.498	14.2	0.496	15.572	0.520				
19	15.1	0.512	15.4	0.517	18.226	0.560				
6	24.5	0.636	18.2	0.560	26.744	0.659				
	Ave.	0.521		0.560		0.545	16025	-225	4888.2	0.475
Started pause with organic feed from Aug. 13										
Aug. 18										
45	11.9	0.451	13.7	0.487	13.716	0.487				
32	13.2	0.478	14.6	0.503	15.755	0.523				
19	15.5	0.519	15.3	0.515	16.684	0.538				
6	25.1	0.643	18.7	0.567	30.093	0.689				
	Ave.	0.514		0.567		0.551	16140	115	5003.2	0.486
Aug. 23										

45	12.2	0.457	15.7	0.522	15.616	0.521				
32	14.4	0.500	15	0.510	14.323	0.499				
19	17.3	0.547	16.4	0.533	19.632	0.579				
6	29.3	0.682	17.5	0.550	15.546	0.520				
	Ave.	0.537		0.550		0.530	16255	115	5118.2	0.497
Aug. 27										
45	16.7	0.538	17.8	0.554	17.814	0.554				
32	15.4	0.517	18.7	0.567	19.837	0.582				
19	19.3	0.575	18	0.557	16.309	0.532				
6	24.7	0.638	19.7	0.580	23.040	0.621				
	Ave.	0.563		0.580		0.569				
Sept. 02										
45	19	0.571	25.8	0.650	25.905	0.651				
32	19.1	0.572	20.1	0.585	19.141	0.573				
19	21.6	0.604	21.1	0.598	23.485	0.625				
6	27	0.661	23	0.620	25.864	0.650				
	Ave.	0.598		0.620		0.624	16515	260	5378.2	0.522
Sept. 12										
45	23	0.620								
32	19.4	0.576								
19	24.5	0.636								
6	33.2	0.714								
		0.632					16845	330	5708.2	0.554
Sept. 16										
45	21.9	0.608	29.3	0.682	29.384	0.683				
32	20.8	0.594	20.6	0.592	19.581	0.579				
19	25.3	0.645	22.9	0.619	27.927	0.670				
6	35	0.728	25	0.641	41.327	0.771				
	Ave.	0.638		0.641		0.671	17015	170	5878.2	0.571
Sept. 22										
45	23.4	0.625								
32	22.8	0.618								
19	26.9	0.660								
6	35.5	0.731								

	Ave.	0.654								
Sept.23										
45	23.6	0.627	28.4	0.674	28.494	0.675				
32	23.8	0.629	20.8	0.594	15.210	0.514				
19	26.6	0.657	22.7	0.617	26.960	0.661				
6	34.7	0.726	26.7	0.658	32.653	0.710				
	Ave.	0.655		0.658		0.638	17100	85	5963.2	0.579
Oct. 05										
45	24.3	0.634								
32	22.9	0.619								
19	29.5	0.684								
6	36.8	0.741								0.000
	Ave.	0.665					17295	195	6158.2	0.598
Oct.6										
45	26.1	0.653	31.5	0.701	31.670	0.702				
32	22.2	0.611	28.7	0.677	25.775	0.649				
19	30.7	0.694								
6	35.2	0.729								
	Ave.	0.668					17315	20	6178.2	0.600
Oct.11										
45	26.6	0.657								
32	23.2	0.622								
19	27.4	0.665								
6	37.8	0.748								
	Ave.	0.669					17320	5	6183.2	0.600
Oct.27										
45	25.2	0.644								
32	23.9	0.630								
19	27.4	0.665								
6	40.2	0.763								
	Ave.	0.670								
Nov. 04										
45	25.5	0.647								
32	26	0.652								

19	34	0.720								
6	43	0.781								
	Ave.	0.694					17575	255	6438.2	0.625
Nov. 17										
45	23.6	0.627	31.9	0.704	31.903	0.704				
32	21.2	0.599	30.3	0.691	23.040	0.621				
19	32.8	0.711								
6	41.6	0.772								
	Ave.	0.671					17555	-20	6418.2	0.623

Table C.2: Raw data obtained in column B during the clogging process

Column B		
Height of peat packed:		51
Internal diameter of column:		16.2
Volume of packed peat(cm^3):		
Soil sections	1	2472.185
	2	2678.2
	3	2678.2
	4	2163.162
		9991.747

Dismantlement at the end of the experiment									**TDR measured water content**	
Sections	**Tray only**	**Tray + wet peat**	**Tray + dry peat**	**Dry peat**	**Water in**	**Section volume**	**Bulk D.**	**Water content**	**H**	**V**
1	39	403.3	101.4	62.4	301.9	412.0308	151.445	0.733		0.812
2	39.5	1271.5	243.5	204	1028	1648.123	123.777	0.624	0.656	0.635
3	39.1	743.5	163	123.9	580.5	1030.077	120.282	0.564		

4	39.1	1145.5	236.7	197.6	908.8	1648.123	119.894	0.551	0.637	
5	39.1	686.6	152.3	113.2	534.3	1030.077	109.895	0.519		
6	39	1310.1	259.3	220.3	1050.8	1648.123	133.667	0.638	0.672	
7	39.1	900.6	173.5	134.4	727.1	1030.077	130.476	0.706		
8	39.2	1471.2	246.3	207.1	1224.9	1545.116	134.035	0.793	0.739	
				Sum:	6356.3	9991.747				
						Average:	126.394	0.636		

Elevation Cm	**Horizontal**		**Vertical measured**		**Vertical sectional**					
	K_a	**Θ_h**	**K_a**	**Θ_v**	**K_a**	**Θ_v'**	**Weight of column g**	**Weight change g**	**Water in column g**	**Gravimetric water content**
Saturated, Aug. 09, 2004										
45	50.7	0.822985	61.9	0.874221	61.81213	0.873856				
32	44.6	0.790078	54.2	0.840121	46.34467	0.799929				
19	43.8	0.785432	52.1	0.829977	47.92899	0.808557				
6	46.8	0.802438	51.5	0.827004	44.69878	0.790646				
		0.800795		0.827004		0.821236	19240		8021.3	0.802793
After gravity drainage, Aug. 10, 2004										
	Ka	Θv	Ka	Θv	Ka	Θv				
45	10.1	0.408828	11.3	0.437647	11.37317	0.439304				
32	12.4	0.461493	12.8	0.469643	14.49852	0.501628				
19	15.1	0.512062	14.6	0.503418	18.82225	0.568625				
6	29.4	0.683101	16.7	0.827004	27.14958	0.66266				
		0.505035		0.827004		0.534139	16065	-3175	4846.3	0.48503
Before second pause of water in the afternoon, Aug. 11, 2004										
	Ka	Θv	Ka	Θv	Ka	Θv				
45	11.3	0.437647	10.7	0.423642	10.68614	0.423309				
32	11.7	0.446576	12.2	0.457319	14.14917	0.495367				
19	14.1	0.494473	14.6	0.503418	20.25	0.587393				
6	30.4	0.691687	17.7	0.552844	21.95592	0.608156				

		0.506711		0.552844		0.521559	16025	-40	4806.3	0.481027
Started pulsing with organic feed from Aug. 13										
Aug. 18										
	K_a	Θ_h	K_a	Θ_v	K_a	Θ_v				
45	12.7	0.467629	14.3	0.498089	14.33536	0.498723				
32	11.9	0.450927	14.2	0.496287	14.14917	0.495367				
19	15.3	0.51544	16	0.526924	20.25	0.587393				
6	24.4	0.635249	19.9	0.582918	31.36	0.699668				
	Ave.	0.510069		0.582918		0.561841	16180	155	4961.3	0.49654
Aug. 23										
45	15.3	0.51544	16.7	0.537915	16.61265	0.536569				
32	14.1	0.494473	17.1	0.543991	17.64	0.551972				
19	17.3	0.546976	17.2	0.545488	17.44669	0.549144				
6	28.7	0.676915	20.8	0.594272	27.93878	0.670015				
	Ave.	0.551379		0.594272		0.571175	16325	145	5106.3	0.511052
Aug. 27										
45	20.7	0.593035	19.8	0.581625	19.78716	0.581458				
32	17.3	0.546976	19.5	0.577705	19.22485	0.574058				
19	17.1	0.543991	19.1	0.572385	18.42391	0.563134				
6	26.1	0.652539	21.4	0.601572	24.1502	0.632608				
	Ave.	0.581044		0.601572		0.585432				
Sept. 2										
45	20.8	0.594272	28.3	0.673313	28.27306	0.673068				
32	19.7	0.580325	23.7	0.627777	19.22485	0.574058				
19	23	0.620081	24.5	0.636299	26.01	0.651652				
6	27.5	0.665952	26.7	0.658373	27.63755	0.667232				
	Ave.	0.612053		0.658373		0.64117	16730	405	5511.3	0.551585
Sept. 12										
45	24.8	0.639424								
32	21.7	0.605146								
19	24.6	0.637345								

6	29.3	0.682227					17115	385	5896.3	0.590117
	Ave.	0.638969								
Sept. 16										
45	25.3	0.644547	29.5	0.683973	29.60861	0.684916				
32	21.2	0.599162	27.1	0.66219	24.61686	0.637521				
19	28.3	0.673313	27.8	0.668737	31.44621	0.700373				
6	31.8	0.703245	30.9	0.695875	31.68082	0.702281				
	Ave.	0.652396		0.695875		0.68035	17015	-100	5796.3	0.580109
Sept. 22										
45	24.5	0.636299								
32	21.1	0.597948								
19	28.2	0.672404								
6	34.8	0.726387								
	Ave.	0.654274					17015	0	5796.3	0.580109
Sept. 23										
45	27.3	0.664078	29	0.679585	29.16	0.680997				
32	21.6	0.60396	22.1	0.609835	15.39053	0.516954				
19	26.6	0.65741	24.6	0.637345	30.41947	0.691852				
6	37.5	0.745568	27.6	0.666883	34.64163	0.725216				
		0.663832		0.666883		0.651053	17390	375	6171.3	0.61764
Oct. 05										
45	29.6	0.684842								
32	23.9	0.629935								
19	27.7	0.667812								
6	38.9	0.754977								
	Ave.	0.680944					17585	195	6366.3	0.637156
Oct.06										
45	30.4	0.691687	32.5	0.708834	32.60804	0.709686				
32	23.1	0.621195								
19	25.4	0.64556								
6	39.8	0.760849								
	Ave.	0.6762					17595	10	6376.3	0.638157
Oct.27										
45	30.7	0.694208								

32	24.1	0.632074								
19	25.6	0.647573								
6	36.8	0.740731								
	Ave.	0.676061								
Nov. 29										
50										
49			49	0.81423	48.65063	0.812393				
45	26.5	0.656443	33.2	0.714305	24.33778	0.634594				
32	24.6	0.637345								
19	28.2	0.672404								
6	36.5	0.73863								
	Ave.	0.672564					17575	-20	6356.3	0.636155

C 2: WATER CONTENT PROFILES WITH DEPTH FOR COLUMN A WITH CLOGGING

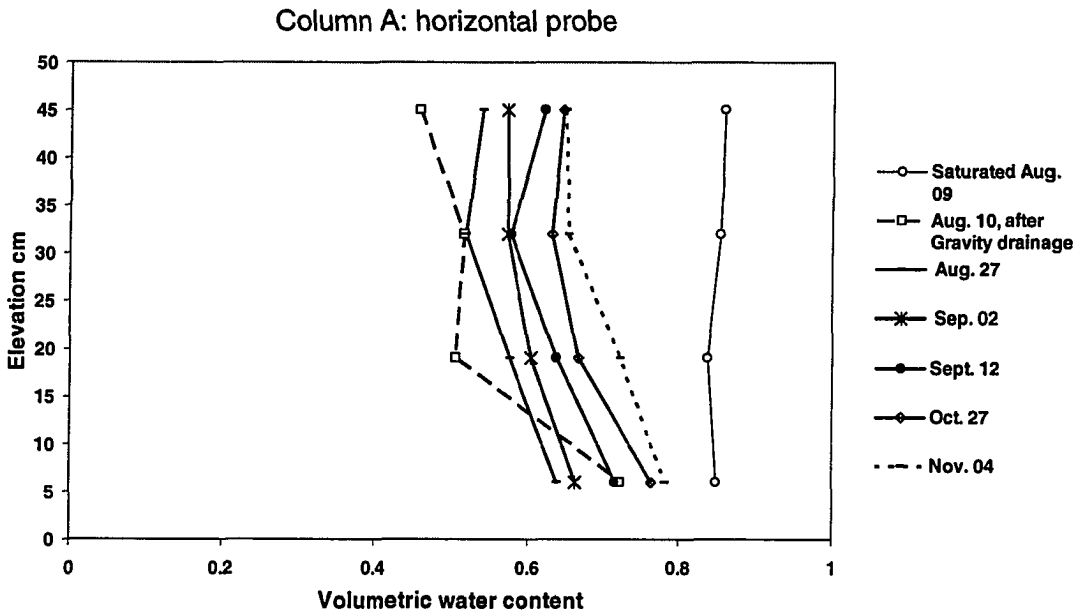

Figure C.1: Water content profiles in column A determined by the horizontal probe

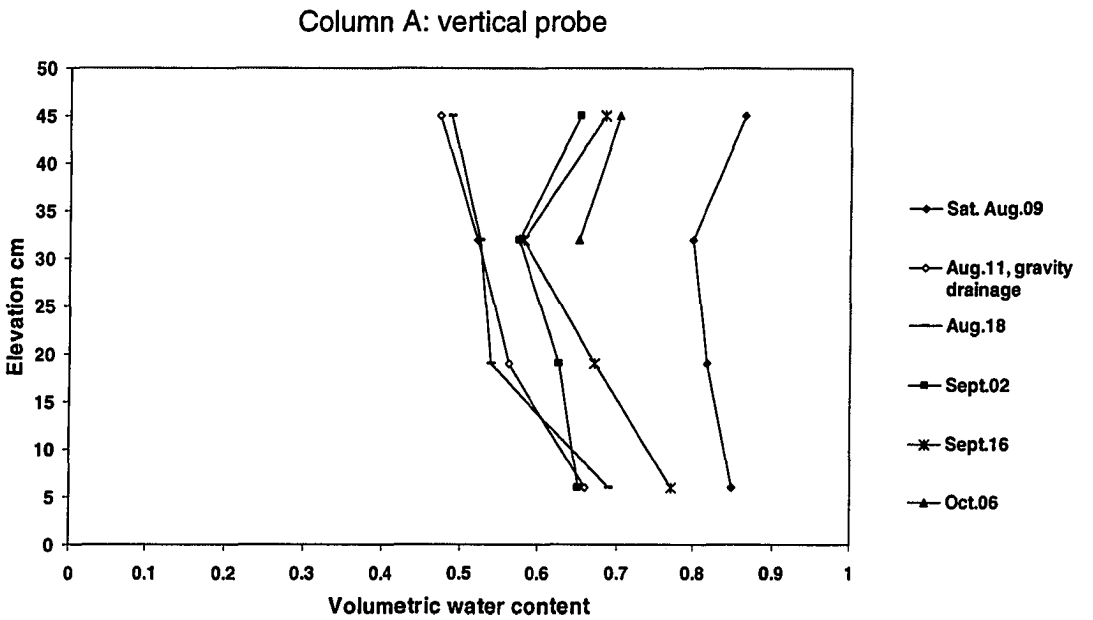

Figure C.2: Water content profiles in column A determined by the vertical probe

C 3: WATER CONTENT PROFILES AT THE END OF THE EXPERIMENT IN COLUMN A AND B DETERMINED BY TDR AND THE GRAVIMETRIC METHOD

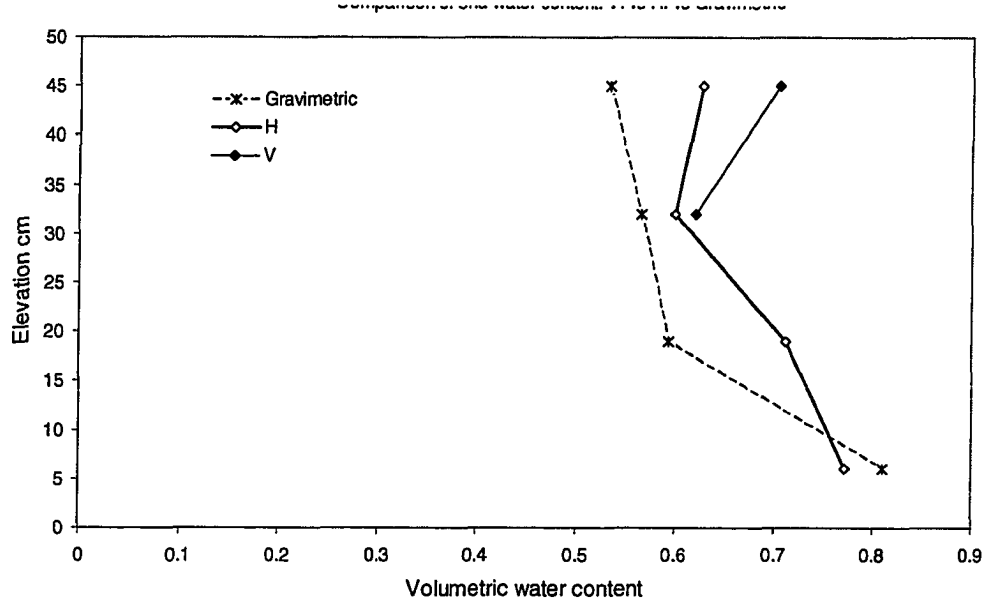

Figure C. 3: Water content profiles determined by the horizontal (H) and vertical (V) TDR probes and the gravimetric method in column A

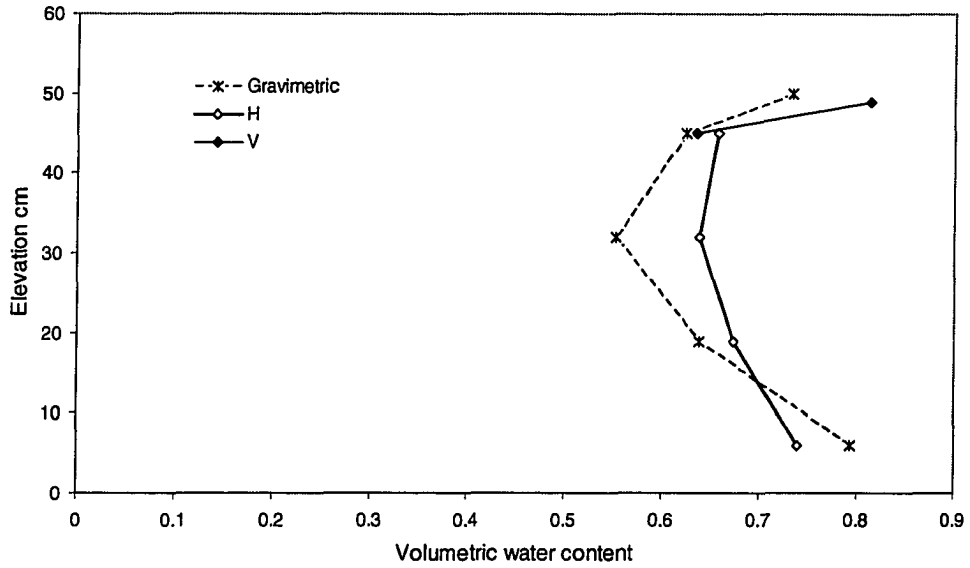

Figure C.4: Water content profiles determined by the horizontal (H) and vertical (V) TDR probes and the gravimetric method in column B

C3: DESCRIPTIVE STATISTICS AND PAIRED T-TEST RESULTS FOR COMPARISON OF WATER CONTENTS MEASURED BY DIFFERENT METHODS

Table C. 3: Comparison of water contents measured by the vertical probe (Θ_v) and the horizontal probe (Θ_h) in the clogging columns

Descriptive statistics results of Θ_v-Θ_h	
	Θ_v-Θ_h
Mean	0.0122
Standard Error	0.0055
Median	0.0214
Mode	#N/A
Standard Deviation	0.0485
Sample Variance	0.0024
Kurtosis	2.6621
Skewness	-1.371
Range	0.2556
Minimum	-0.163
Maximum	0.0929
Sum	0.9495
Count	78

t-Test: Paired Two Sample for Means	α=0.01		α=0.05	
	Θ_v	Θ_h	Θ_v	Θ_h
Mean	0.6204	0.6082	0.6204	0.6082
Variance	0.0111	0.012	0.0111	0.012
Observations	78	78	78	78
Pearson Correlation	0.8991		0.8991	
Hypothesized Mean Difference	0		0	
df	77		77	
t Stat	2.2172		2.2172	
P(T<=t) one-tail	0.0148		0.0148	
t Critical one-tail	2.3758		1.6649	
P(T<=t) two-tail	0.0296		0.0296	
t Critical two-tail	2.6412		1.9913	

Table C. 4: Comparison of water contents measured by the vertical probe (Θ_v) and the gravimetric method (Θ_g) in the clogging columns

Descriptive statistics results of Θ_v-Θ_g	
Θ_v-Θ_g	
Mean	0.0607
Standard Error	0.0072
Median	0.0601
Mode	#N/A
Standard Deviation	0.0281
Sample Variance	0.0008
Kurtosis	-1.124
Skewness	0.1543
Range	0.0834
Minimum	0.0184
Maximum	0.1019
Sum	0.9104
Count	15

t-Test: Paired Two Sample for Means α=0.05		
	Θ_v	Θ_g
Mean	0.6249	0.5642
Variance	0.0096	0.0115
Observations	15	15
Pearson Correlation	0.9667	
Hypothesized Mean Difference	0	
df	14	
t Stat	8.3781	
P(T<=t) one-tail	4E-07	
t Critical one-tail	1.7613	
P(T<=t) two-tail	8E-07	
t Critical two-tail	2.1448	

Table C. 5: Comparison of water contents measured by the horizontal probe (Θ_h) and the gravimetric method (Θ_g) in the clogging columns

Descriptive statistics results of Θ_h-Θ_g	
	Θ_h-Θ_g
Mean	0.0502
Standard Error	0.004
Median	0.0472
Mode	#N/A
Standard Deviation	0.0212
Sample Variance	0.0004
Kurtosis	-0.254
Skewness	-0.552
Range	0.0799
Minimum	-0.002
Maximum	0.0779
Sum	1.4062
Count	28

t-Test: Paired Two Sample for Means α=0.05		
	Θ_h	Θ_g
Mean	0.6298	0.5795
Variance	0.0071	0.0069
Observations	28	28
Pearson Correlation	0.9681	
Hypothesized Mean Difference	0	
df	27	
t Stat	12.529	
P(T<=t) one-tail	5E-13	
t Critical one-tail	1.7033	
P(T<=t) two-tail	9E-13	
t Critical two-tail	2.0518	

Table C. 6: Comparison of water contents measured by the horizontal probe (Θ_T) and the gravimetric method (Θ_g) in the clogging columns

Descriptive statistics results of Θ_T-Θ_g	
	Θ_T-Θ_g
Mean	0.0539
Standard Error	0.0037
Median	0.0491
Mode	#N/A
Standard Deviation	0.024
Sample Variance	0.0006
Kurtosis	-0.286
Skewness	0.0093
Range	0.1039
Minimum	-0.002
Maximum	0.1019
Sum	2.3166
Count	43

t-Test: Paired Two Sample for Means α=0.05		
	Θ_T	Θ_g
Mean	0.6281	0.5742
Variance	0.0078	0.0084
Observations	43	43
Pearson Correlation	0.9649	
Hypothesized Mean Difference	0	
df	42	
t Stat	14.706	
P(T<=t) one-tail	2E-18	
t Critical one-tail	1.682	
P(T<=t) two-tail	4E-18	
t Critical two-tail	2.018082	

C 4: TDR WAVEFORMS AT DIDFFERENT PROBE LOCATIONS DURING CLOGGING IN THE TWO COLUMNS

**The waveforms at saturation are bolded. Others started from the waveform after gravity drainage to those at difference stages of clogging with time.*

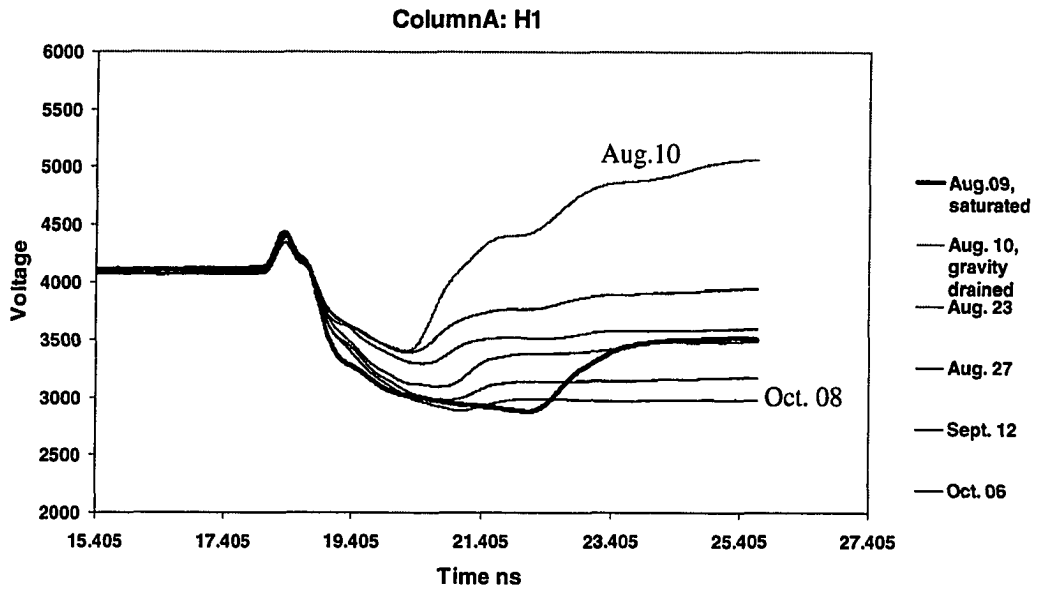

Figure C. 5: Waveforms with clogging in column A: the top horizontal probe

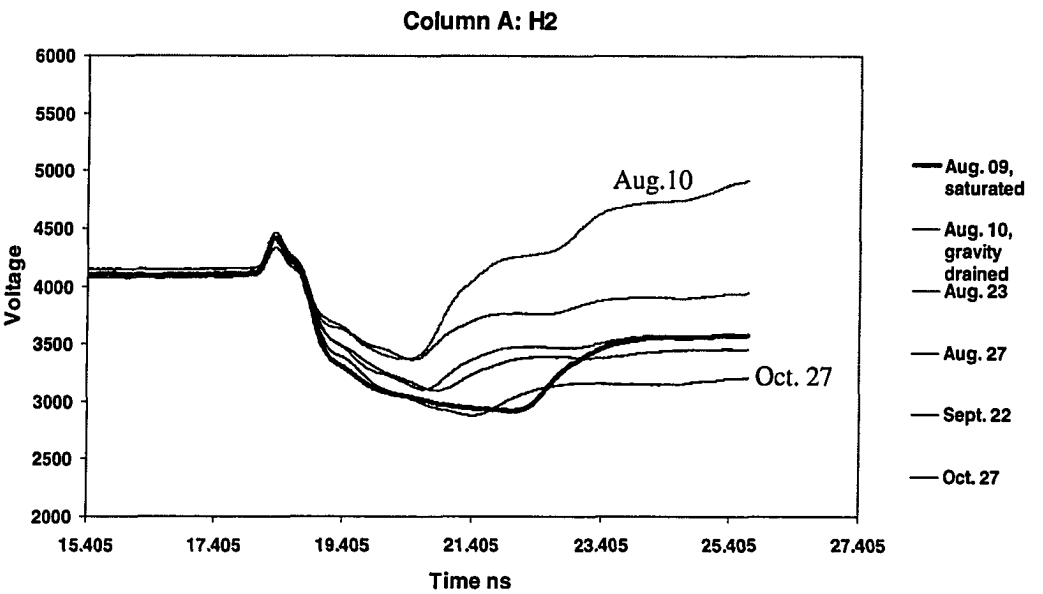

Figure C. 6: Waveforms with clogging taken by the second horizontal probe (from the top) in column A

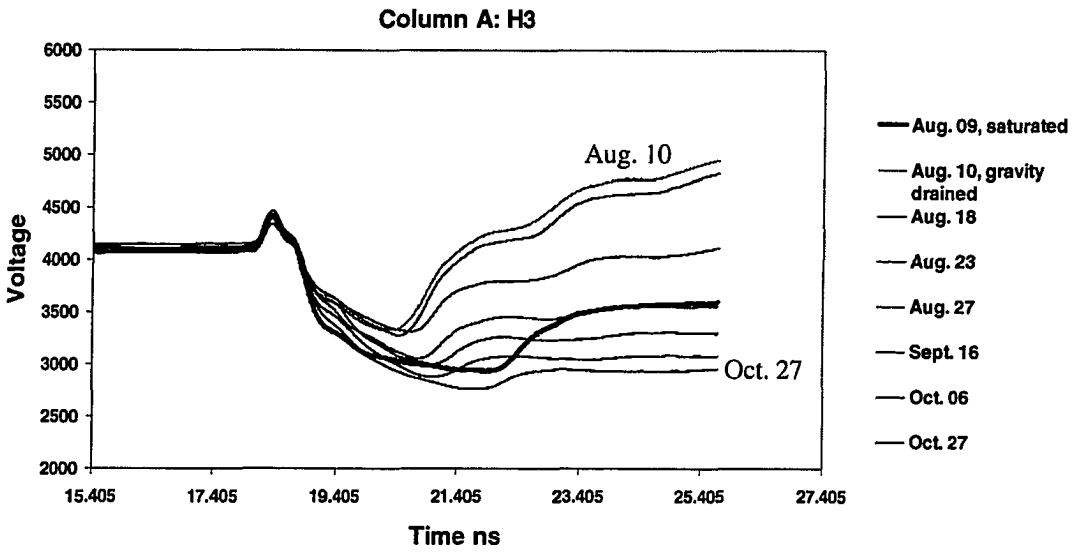

Figure C. 7: Waveforms with clogging taken with the third horizontal probe (from the top) in column A

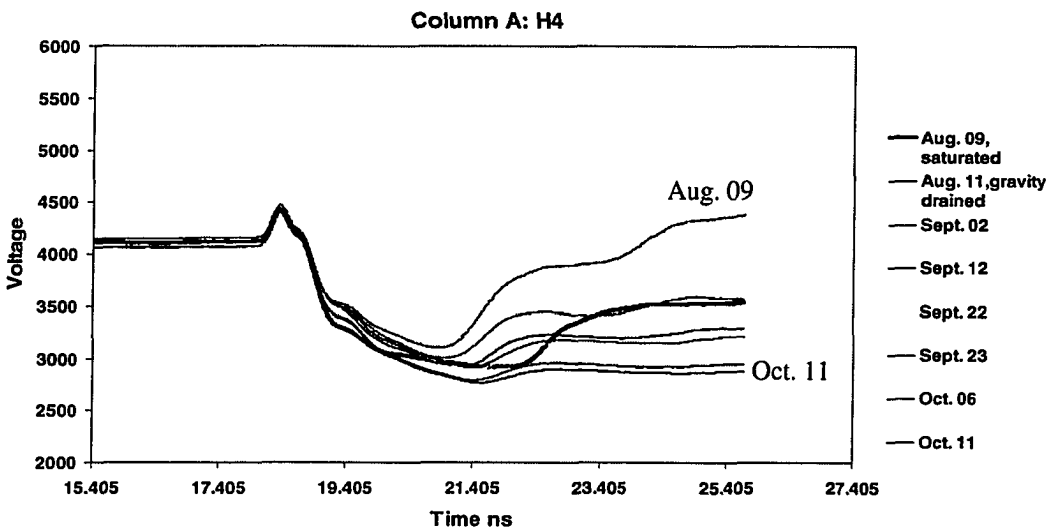

Figure C. 8: Waveforms with clogging taken with the bottom horizontal probe in column A

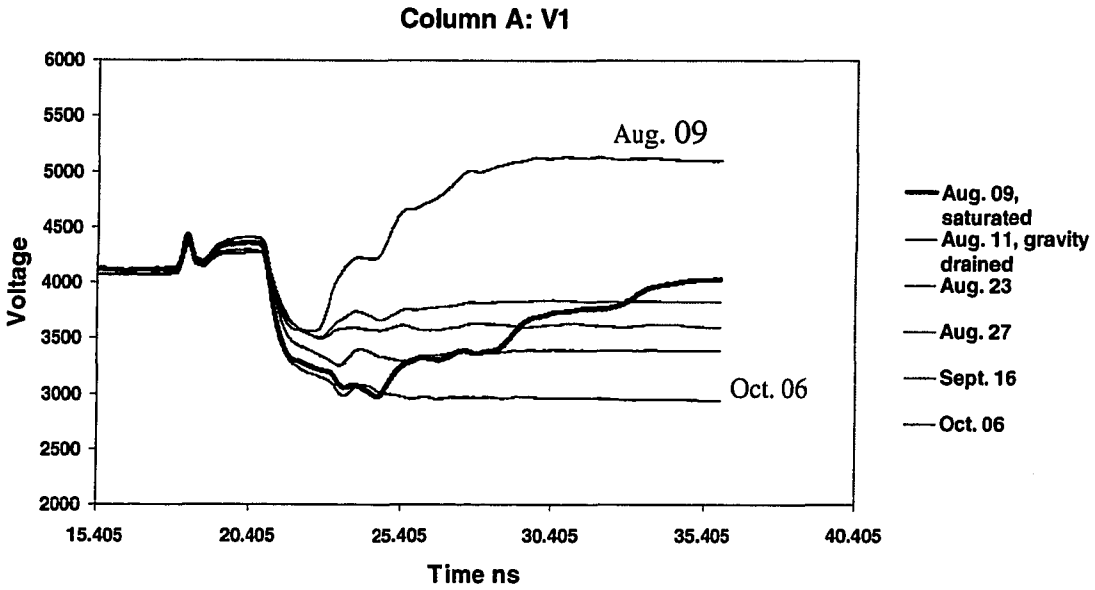

Figure C. 9: Waveforms with clogging taken with the 14.5 cm vertical probe in column A

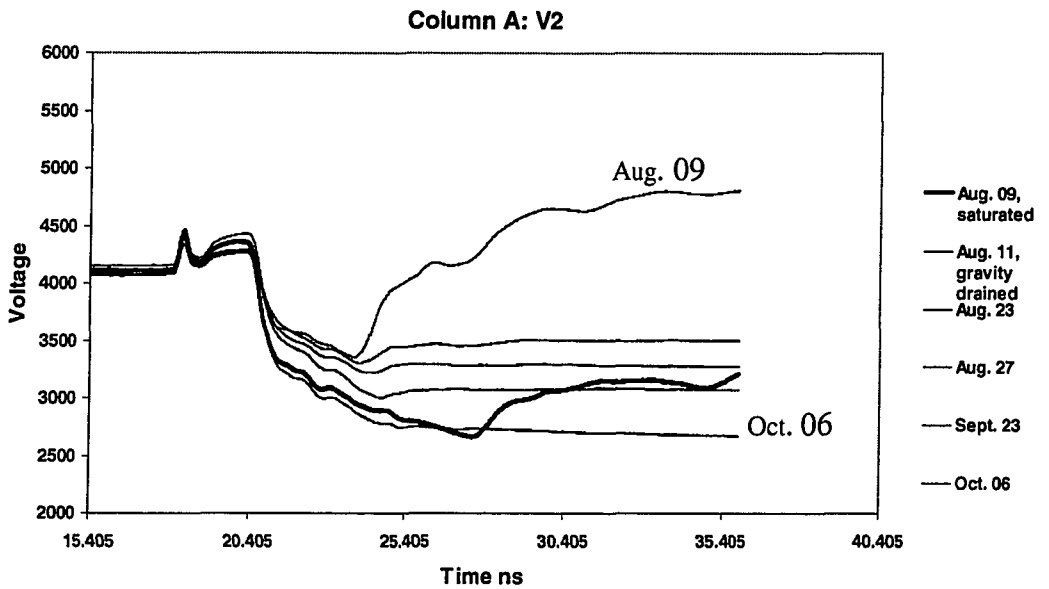

Figure C. 10: Waveforms with clogging taken with the 27.5 cm vertical probe in column A

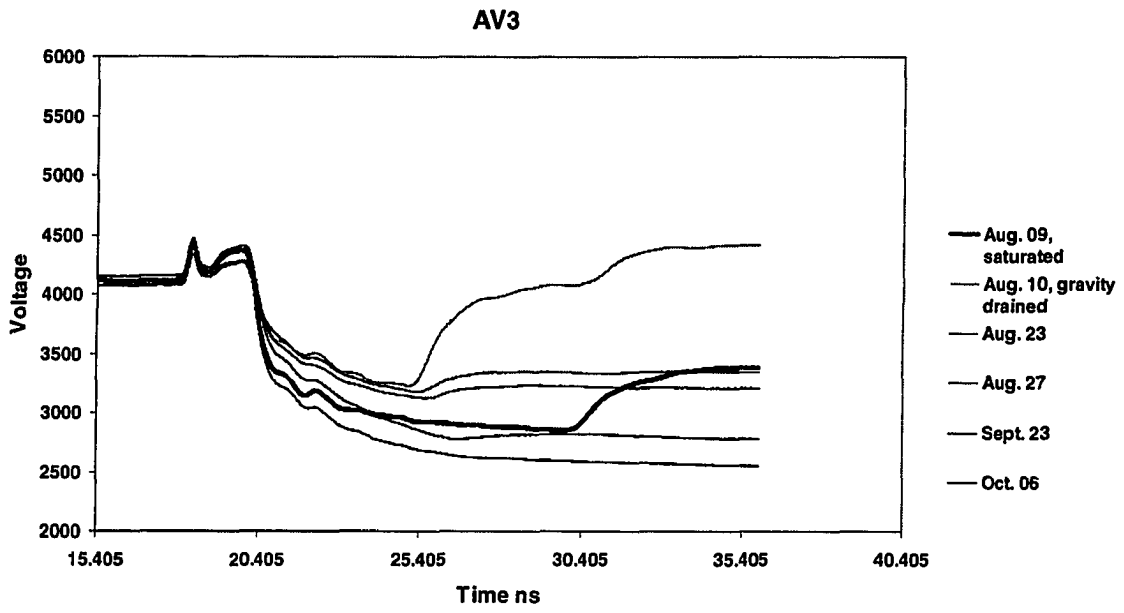

Figure C. 11: Waveforms with clogging taken with the 40.5 cm vertical probe in column A

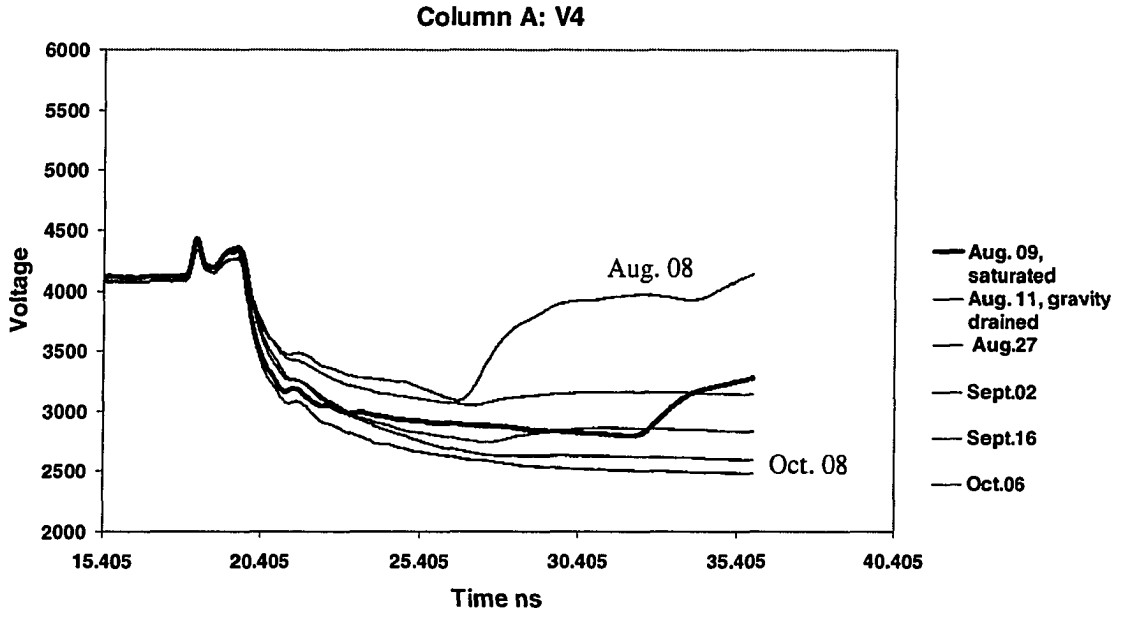

Figure C. 12: Waveforms with clogging taken with the 49.5 cm vertical probe in column A

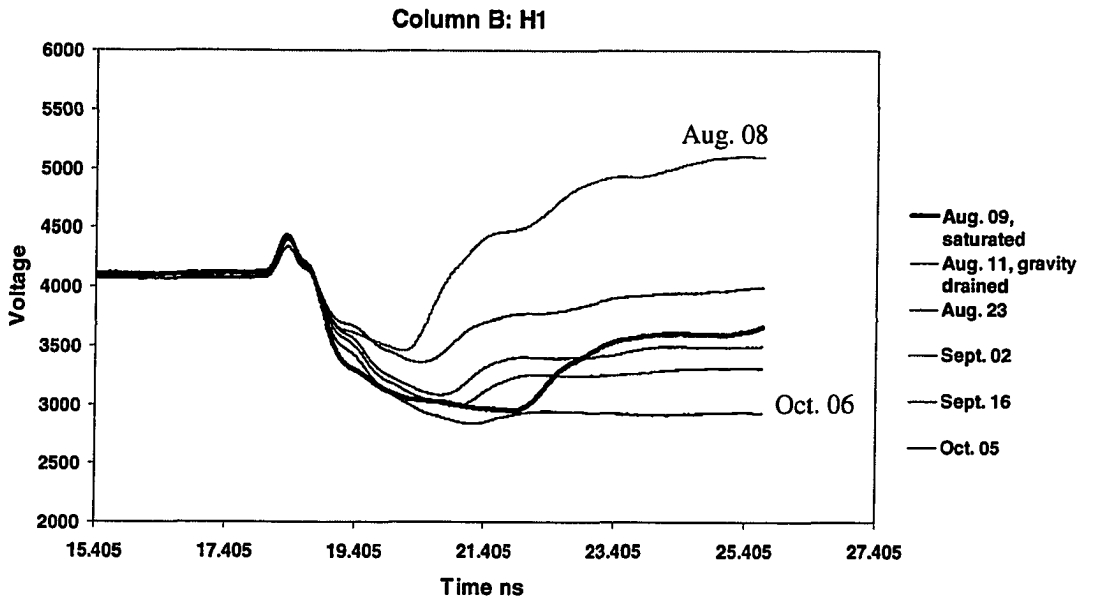

Figure C. 13: Waveforms with clogging taken with the top horizontal probe in column B

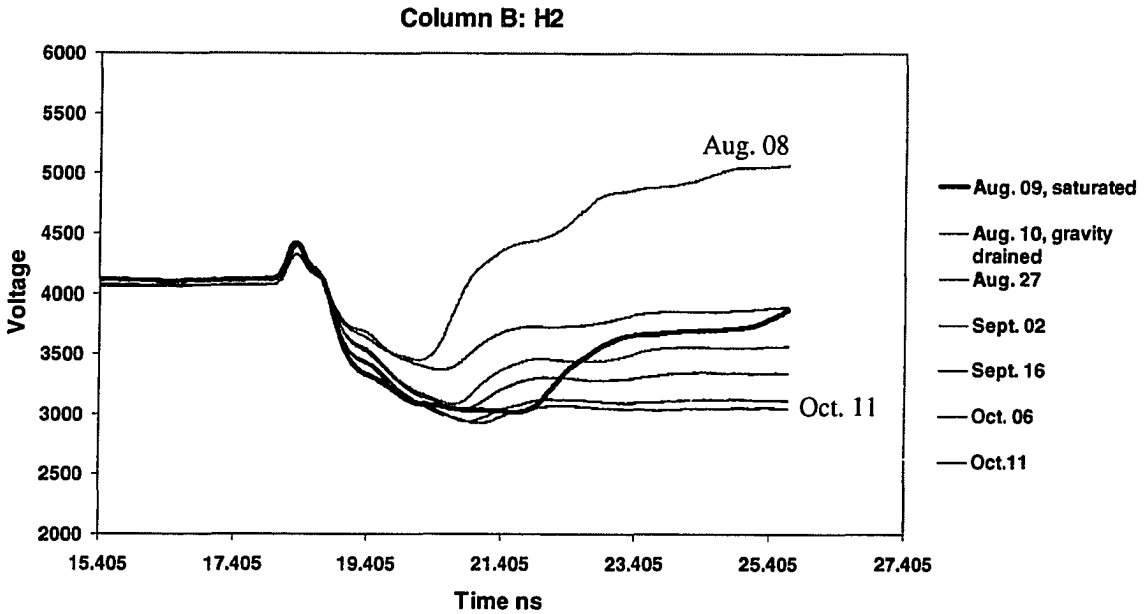

Figure C. 14: Waveforms with clogging taken with the second horizontal probe (from the top) in column B

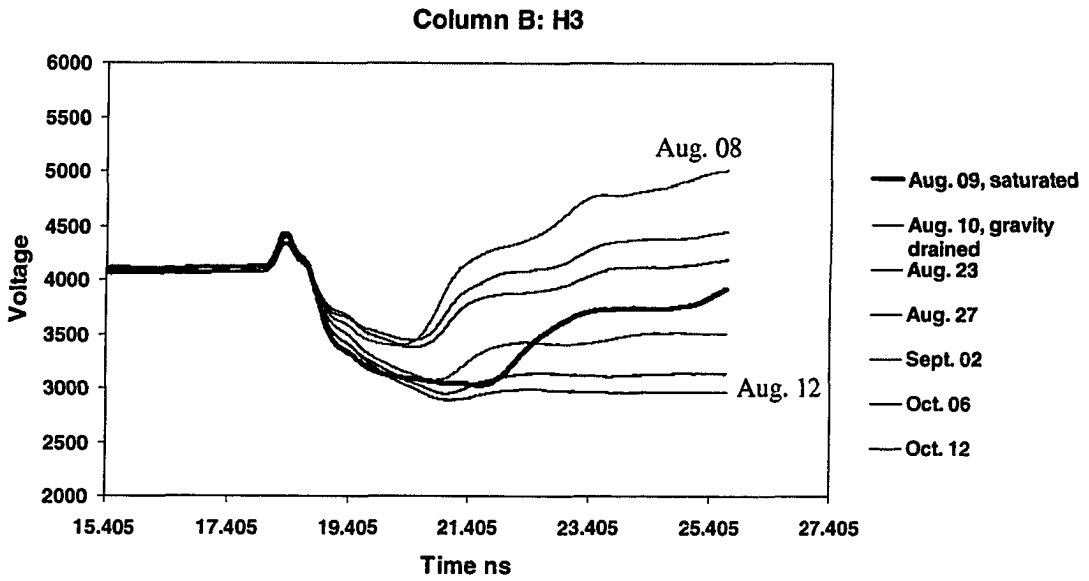

Figure C. 15: Waveforms with clogging taken with the third horizontal probe (from the top) in column B

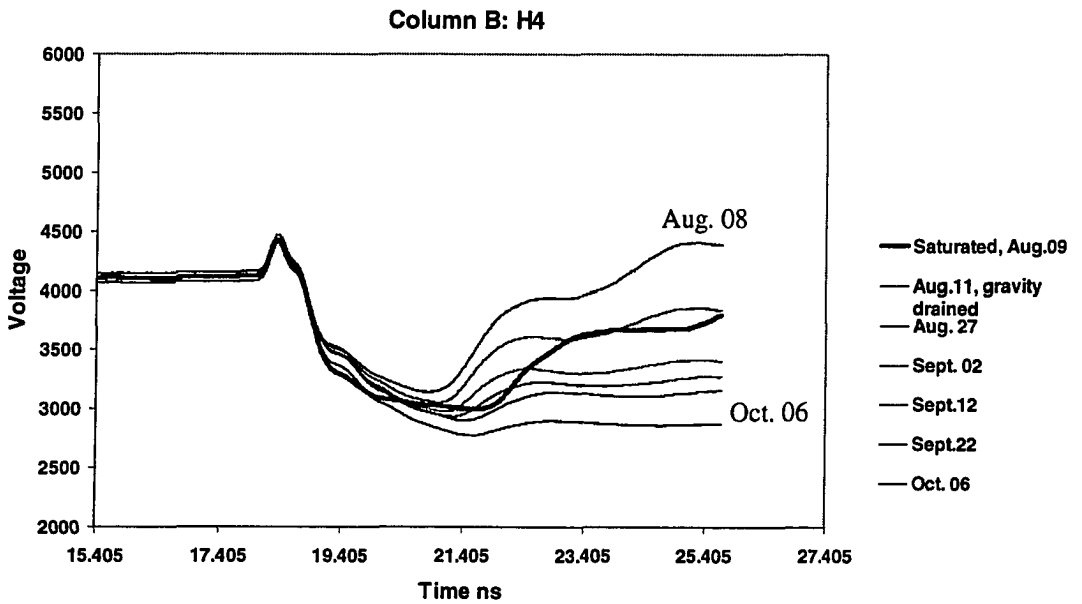

Figure C. 16: Waveforms with clogging taken with the bottom horizontal probe in column B

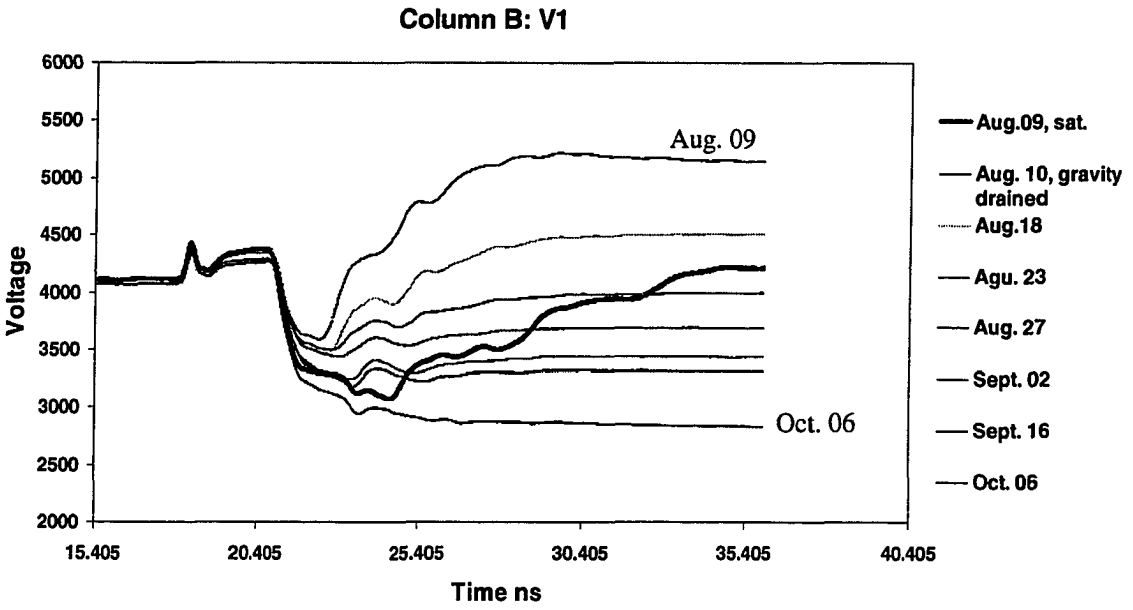

Figure C. 17: Waveforms with clogging taken with the 14.5 cm vertical probe in column B

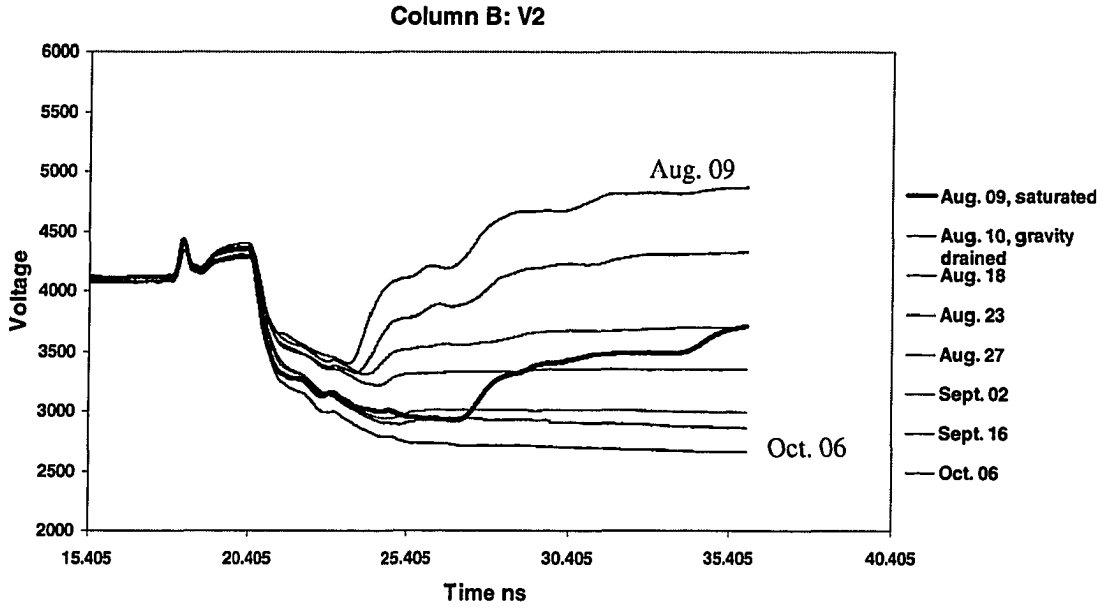

Figure C. 18: Waveforms with clogging taken with the 27.5 cm vertical probe in column B

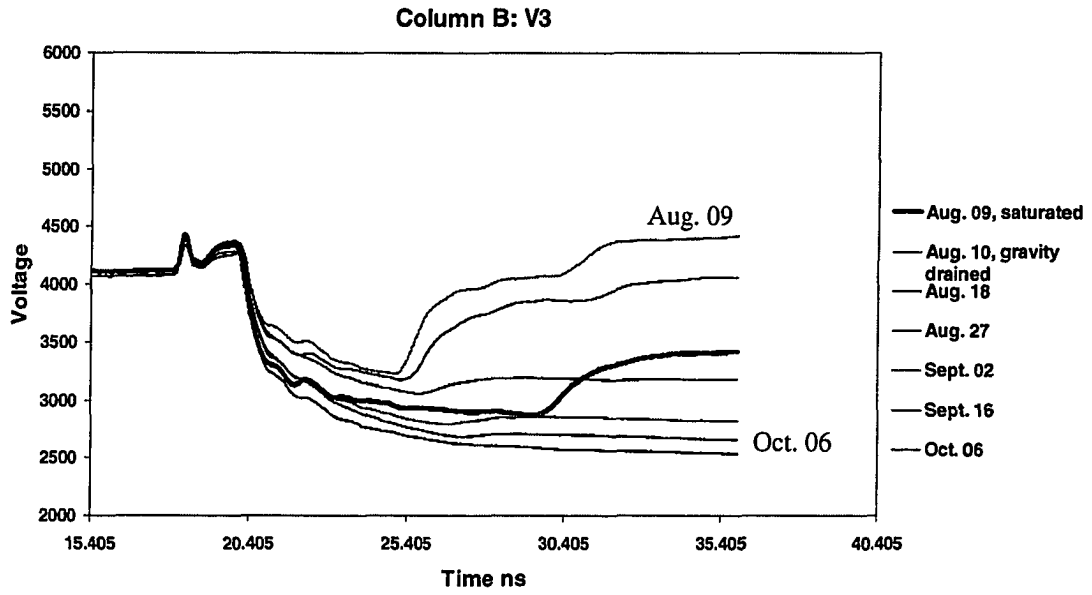

Figure C. 19: Waveforms with clogging taken with the 40.5 cm vertical probe in column B

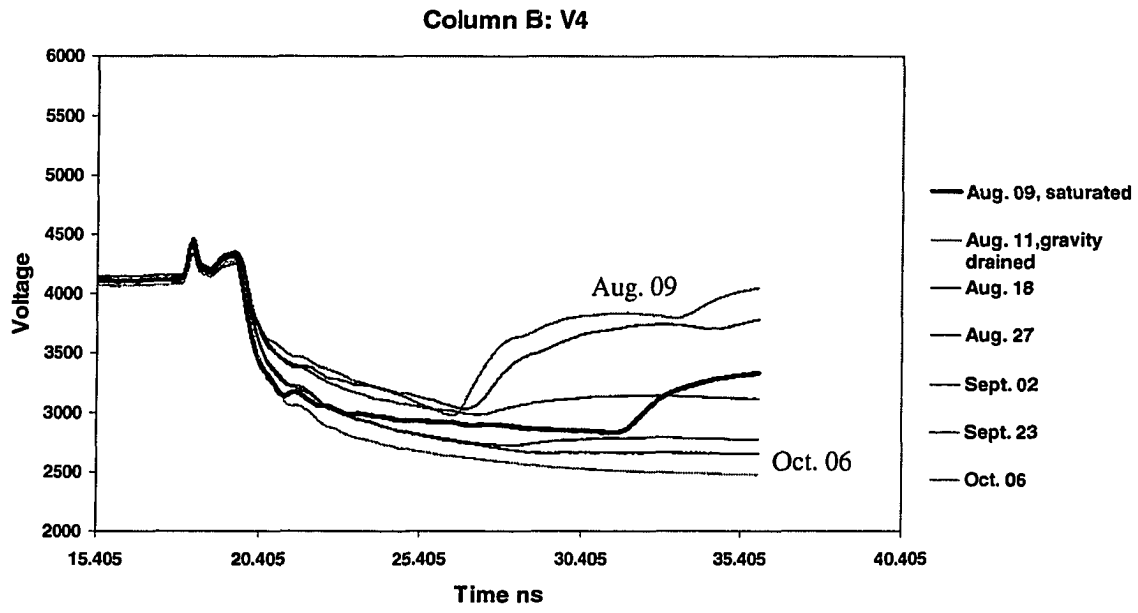

Figure C. 20: Waveforms with clogging taken with the 48.5 cm vertical probe in column B